THE ROLE OF NOVEL ROCK1/2 INHIBITORS IN CORONARY CIRCULATION & MYOCARDIAL REPERFUSION/INJURY

Thesis submitted for the degree of Doctor of Philosophy (PhD) in Cardiovascular Sciences (2019-2024)

University College London, UK

Submitted by Dr Lucie Elizabeth Pearce

BMBS, BMedSci, MRCP

Institute of Cardiovascular Science

The Hatter Cardiovascular Institute

University College London

67 Chenies Mews

London

WC1E 6HX

2nd April 2024

DECLARATION

I, Lucie Elizabeth Pearce, confirm that the work presented in this thesis is my own. Information used from other sources is referenced in this thesis and publication rights have been granted where necessary.

FUNDING & AWARDS

This research was supported by a Clinical Fellowship from the UCL/Wellington Hospital between Oct 2019-Feb 2022. In February 2022 I was awarded a British Heart Foundation Clinical fellowship (CRT) for the remainder of this work. In October 2022 I received an International Travel Award from the American Heart Association to present a selection of this work at the AHA Annual Scientific Sessions in Chicago.

ABSTRACT

INTRODUCTION: ROCK1/2 (Rho kinases 1 and 2) are important intracellular kinases which regulate apoptosis, vascular smooth muscle contraction and organisation of the cytoskeleton (Shimokawa et al., 2016). Fasudil (a ROCK1 and 2 inhibitor) is cardioprotective in vivo during myocardial ischaemia/reperfusion (I/R). The drug has been used in clinical practice to treat vasospasm in subarachnoid haemorrhage (Satoh et al., 2014). However, it is not established whether ROCK1 or ROCK2 is cardioprotective. Vasospasm is a known pathology of ischaemic microvascular obstruction (MVO). At present there are no gold standard therapies for MVO, despite its poor prognosis (Niccoli et al., 2016). This thesis aims to investigate the role of the ROCK2 isoform in myocardial and coronary circulation protection.

AIMS: To investigate i) the expression of ROCK2 mRNA in the heart and its role in myocardial I/R using selective ROCK2 inhibitors and genetically modified mice, ii) the role of ROCK2 inhibitors as vasodilators and therefore potential MVO drugs.

METHODS: An RNAscope assay quantified ROCK1/2 expression in whole rat hearts. Vascular myography studies were performed to investigate arterial response to ROCKi. Male Sprague Dawley rats (250-350g) underwent I/R by LAD ligation for 30/180-minutes. 15-minutes prior to reperfusion either selective ROCK2 inhibitor or DMSO control were administered I.P. Hearts were stained with TTC to measure IS% and Thioflavin S to measure MVO%. ROCK2 (+/-) C57B6/J mice were subject to 30/120 minutes of I/R using transient LAD infarction.

RESULTS: ROCK2 mRNA expression was greater than ROCK1 mRNA expression in whole hearts and coronary vasculature ($p=0.003$, $p=0.03$).10mg/kg Fasudil (ROCK1/2 inhibitor) reduced infarct size in vivo (34.5±5.7 vs 55.8±4.7,$p=0.02$, $n=6$), however 100mg/kg of the selective ROCK2 inhibitor, KD025, did not (43.7±5.5 vs 48.3±4.9, $p=0.87$, $n=8$). KD025 did not demonstrate vasodilatory potential ex vivo. Following I/R, no significant difference in IS% was observed between genotypes in mice (ROCK2+/- 34.4±4.5 vs WT 37.6±6.6, $p=0.70$, $n=6$). 100mg/kg KD025 (ROCK2i) reduced MVO% in vivo (21.8±2.5 vs 32.2±1.8, $p=0.04$, $n=8$) as did Fasudil 3mg/kg (19.2±4.1 vs 32.2±1.8,$p=0.01$, $n=6$).

CONCLUSION: Inhibition of both ROCK1 and 2 with Fasudil was cardioprotective, however selective ROCK2 inhibition and ROCK2 KO did not reduce IS%. This suggests that the ROCK1 isoform may be more important in myocardial protection.

IMPACT STATEMENT

Although primary percutaneous intervention (PPCI) remains a lifesaving therapy for patients with ST elevation myocardial infarction (STEMI), a number of patients still develop heart failure and require prolonged admission to hospital (Niccoli et al., 2019). The field of cardioprotection aims to investigate novel therapies to complement PPCI and improve mortality outcomes (Davidson, Ferdinandy, et al., 2019). Such new therapies can involve medications or be non-pharmacological and are usually considered at the time of emergency admission to hospital in the cardiac catheter laboratory. Research into cardioprotection, benefits clinical Cardiologists and patients alike, by improving treatment outcomes, reducing recovery times, and making the admissions process more efficient.

This thesis has explored the use of Rho kinase (ROCK) inhibitors in cardioprotection and microvascular obstruction (MVO). Many ROCK inhibitors are available on the market and have undergone phase II and phase III clinical trials for other non-cardiac conditions e.g. KD025 (ROCK2 inhibitor) (Cutler et al., 2021). It is therefore of benefit to re-purpose these medications and this is cost-effective.

In particular, the Interventional Cardiology world has identified a clear need for new therapies in coronary MVO post-STEMI (de Waha et al., 2017), (Niccoli et al., 2016). This is not cured by PPCI, and often requires further imaging after discharge from hospital. Moreover, it is a leading cause of refractory angina (Bodi et al., 2023). Whilst many translational researchers have aimed to improve outcomes with regards to infarction size, not as many studies have addressed this important issue concerning MVO and myocardial haemorrhage. Those clinical trials that have investigated this, yielded mixed results (Nazir et al., 2016).

This thesis has aimed to address this, by re-purposing at least one available ROCK inhibitor, given that these drugs are also known to relieve vasospasm (Satoh et al., 2014). Finally, it is hoped that improvements in MVO could, not only bring new original research publications, but could also improve both the Doctor and patient experience. The work from this thesis has been presented at both National and International conferences, which suggests that there is a current appetite for ongoing research into this topic.

STATEMENT OF CONTRIBUTIONS

EXPERIMENTAL TECHNIQUES PERFORMED INDEPENDENTLY BY DR LUCIE PEARCE

1. RNAscope for mRNA expression
2. Immunohistochemistry (IHC) for protein expression
3. Western Blotting for protein expression
4. DNA PCR for genotyping
5. Aortic ring myography in rats (ex vivo vascular studies)
6. M-mode echocardiography in rats
7. Breeding and maintenance of ROCK2 KO animals

Myocardial ischaemia/reperfusion experiments in vivo were performed with the expert assistance of Dr David He and Dr Liyana Yusof.

Contents

INDEX OF FIGURES

CHAPTER ONE: GENERAL INTRODUCTION

1.1 *:* PAST AND PRESENT CONCEPTS IN CARDIOPROTECTION

i) Background

We have entered a new era of cardioprotection, where coronary circulation Ischaemia-reperfusion injury (I/R) is an emerging target for novel therapies (Hausenloy, Chilian, et al., 2019), (Heusch, 2016). Although primary percutaneous coronary intervention (PPCI) vastly improves survival during ST elevation myocardial infarction (STEMI) (Niccoli et al., 2019), a significant proportion of patients still develop injury because of reperfusion, namely heart failure (cell death), arrhythmias, myocardial stunning and microvascular obstruction (MVO) (Konijnenberg et al., 2020). Importantly, MVO results in regions of “no reflow” (NRF) in the myocardium (Kloner et al., 1974) and is therefore considered to be a lethal form of reperfusion injury (Hausenloy & Yellon, 2016), (Yellon & Hausenloy, 2007). This is important, as the extent of microvascular damage has independent prognostic value, compared to measures of infarct size (Borlotti et al., 2019), (de Waha et al., 2017), (Stiermaier et al., 2017). MVO is a complex syndrome of pathologies occurring within the coronary circulation and capillaries and it is likely that a new multi-factorial, therapeutic approach is warranted (Davidson et al., 2019).

Unfortunately, few therapeutic agents have demonstrated coronary vascular protection in large scale clinical trials (McCartney et al., 2020), (Nazir et al., 2016) suggesting that there is a pressing need for new drug development. Post myocardial infarction NRF is not a new concept, and is one of the four key mechanisms comprising myocardial injury, including myocardial stunning, reperfusion arrhythmia and lethal reperfusion injury (Yellon & Hausenloy, 2007). It is important to consider how a new era in cardioprotection has evolved, by revisiting these original concepts.

ii) Lethal reperfusion injury

Lethal reperfusion injury was first described in the 1960's when it was noted that independent cardiomyocyte death could occur during the reperfusion phase of revascularisation (Jennings et al., 1960). Yellon and colleagues completed further extensive investigations to conclude, that whilst reperfusion with PPCI+/- thrombolysis does reduce myocardial infarction size by approximately 40%, there remains a residual infarcted area that was otherwise viable, despite adequate reperfusion (Yellon & Hausenloy, 2007). Reperfusion injury occurs when flow is restored to infarcted myocardium, bringing a flurry of toxins, immune cells and waste products, (generated during a period of sustained hypoxia) (Hausenloy & Yellon, 2016). This is detrimental to the cardiomyocyte, and induces structural damage secondary to sudden pH restoration, intra-cellular calcium over-load (which contributes to opening of the mitochondrial permeability transition pore, MPTP), and myofibril hyper contracture (fig.1) (Yellon & Hausenloy, 2007), (Heusch, 2020). Upon reperfusion, the mitochondria undergo a process known as reenergization, leading to succinate accumulation and the production of harmful reactive oxygen species (ROS) (Hausenloy & Yellon, 2016), (Chouchani et al., 2014).

Elevated levels of ROS induce dysfunction of the cardiomyocyte sarcoplasmic reticulum and reduce the amount of available nitric oxide (NO). They are therefore an important source of damage during reperfusion (Yellon

& Hausenloy, 2007), (Toldo et al., 2018). At lower levels however, ROS can be cardioprotective (Heusch et al.,2008).

Disruption to Na-H+ and Na-Ca^{2+} ion exchange systems, also leads to alterations in mitochondrial dynamics, and contributes to calcium overload (Hausenloy & Yellon, 2013). Davidson et al have recently published an extensive review of key mitochondrial dependent mechanisms which occur in I/R, including changes to the homeostasis of mitochondrial fission and fusion (Sean M. Davidson et al., 2020).

This 'first phase' of lethal cardiomyocyte reperfusion injury, is amplified by neutrophils and immune cells, which infiltrate the infarct zone in response to danger associated molecular proteins, (DAMPS) (Prabhu & Frangogiannis, 2016). DAMPS such as fragments of RNA, mitochondrial DNA and extracellular histones, ATP, heat shock proteins (HSP), and high mobility group box 1 (HMGB1), are released directly from necrotic cells and macrophages (Prabhu & Frangogiannis, 2016), (Shah et al., 2022), (Zuurbier et al., 2019). Each DAMP binds to specific receptors within the cardiomyocyte known as toll-like receptors (TLR) e.g., TLR4, or receptors for advanced glycation end-products (RAGE). DAMPS can also activate a highly potent inflammatory molecule known as the NLRP3 inflammasome in a process known as pyroptosis, (discussed below) (Prabhu & Frangogiannis, 2016). Moreover, extracellular histones have been shown for the first time, to initiate a DAMP-like response in absence of the TLR4 pathway (Shah et al., 2022)

Targeting the inflammatory phase of myocardial I/R has gained much interest over the last decade, especially as it is known to persist into the hours and

days following infarction (Hausenloy & Yellon, 2013). In preclinical studies, inhibiting neutrophils, monocyte infiltration and the actions of cardiac fibroblasts have all had positive effects on myocardial infarction outcomes (Andreadou et al., 2019). Notable clinical trials of anti-inflammatory therapies during myocardial infarction have included the use of cyclosporine before PPCI during STEMI, in the CIRCUS trial (Cung et al., 2015), and post myocardial infarction colchicine in the COLCOT trial (Tardif et al., 2019). Cyclosporine is thought to inhibit the actions of cyclophilin D, a protein which facilitates the opening of the MPTP (Sean M. Davidson et al., 2020). However, despite large study numbers, (*n=791*) cyclosporine failed to improve mortality and heart failure outcomes (Cung et al., 2015). Blockade of interleukin-1 during myocardial infarction has also received much attention, and a recent pooled analysis of the three clinical trials (VCUART1-3) has demonstrated that Anakinra (an IL-1 inhibitor) reduces heart failure incidence, in addition to reducing c-reactive protein (CRP) (Abbate et al., 2022). Immune modulating therapies are not without side-effects, and maybe associated with an increase in serious infections, and damage to the humoral immune system (Newby, 2019). Other strategies have therefore sought to target other components in the process of cell death, rather than the immune cells themselves.

iii) Cell death & destruction

There are many forms of cell death which contribute to myocardial I/R injury including, necrosis, necroptosis, and pyroptosis (inflammatory cell death)

(Sean M. Davidson et al., 2020), (Lodrini & Goumans, 2021). It is now understood that necrosis and necroptosis play a significant role in cardiomyocyte death, with contributions from pyroptosis (S. M. Davidson et al., 2020). The role of apoptosis in cardiomyocyte death is more controversial, with more evidence suggesting that this process occurs during reperfusion rather than ischaemia (Krijnen et al., 2002). Apoptosis is distinct to the other forms of cell death and comprises caspase 3/9 activation, the development of TUNEL positive nuclei and mitochondrial outer membrane permeabilization (MOMP) (S. M. Davidson et al., 2020). Apoptosis is inhibited by upregulation of the JAK-STAT and PI3K/AKT pathways (Krijnen et al., 2002). This process may be more important several weeks after LAD infarction, and at the border zone of the infarct (Lodrini & Goumans, 2021). Necroptosis is a form of caspase independent cardiomyocyte cell death which can lead to abnormal ventricular remodelling and the development of heart failure (S. M. Davidson et al., 2020). As with other forms of cardiac cell death, there is opening of the MPTP and cellular rupture, however this is likely also driven by receptor-interacting serine/threonine-protein kinase 1 and 3, (RIP1/3) and phosphorylated mixed lineage kinase domain-like pseudo kinase (MLKL) (S. M. Davidson et al., 2020), (Lodrini & Goumans, 2021) The combination of RIP1/3 and MLKL as a linked molecule, is collectively known as the ‘necroptosome’ which induces cellular damage by formation of the MLKL pore and impaired Ca2+/Na exchange (Heusch, 2020), (Seo et al., 2021).

In contrast, pyroptosis is a form of inflammatory cell death which is closely linked to formation of the NLRP3 mediated 'inflammasome' molecule (Toldo et al., 2018),(Zuurbier et al., 2019), (Rauf et al., 2019). NLRP3 can both sense 'danger' related signals via its NOD-like receptors, and function as an instigator of inflammation (Zuurbier et al., 2019). This complex molecule activates caspase-1, and the formation of Gasdermin -D (GSDM-D) pores on the cell membrane. GSDM-D stimulates the secretion of important proinflammatory cytokines, inducing cell lysis and inflammation (Prabhu & Frangogiannis, 2016). Pyroptosis is triggered by other inflammatory molecules such as high mobility group box-1 (HMGB1), activation of toll like receptors (TLRs) and other DAMPS and is therefore a key initiator of the cytokine cascade (Sean M. Davidson et al., 2020), (Rauf et al., 2019), (Yellon et al., 2023). There is evidence that targeting multiple processes of cell death can have an additive effect of cardioprotection (Davidson, Ferdinandy, et al., 2019), (Heusch, 2020).

When isolated guinea pig hearts underwent treatment with dual necroptosis and apoptosis inhibitors during myocardial I/R, there was greater protection observed compared to single agent therapy alone (Koshinuma et al., 2014). Combination therapies in cardioprotection have previously involved the activation of specific intra-cellular signalling pathways, capable of reducing programmed cell death (Davidson, Ferdinandy, et al., 2019). These important '*pro-survival*' pathways are known to attenuate lethal reperfusion injury and include the reperfusion injury salvage kinase (RISK) pathway (Yellon et al., 2023), (Rossello & Yellon, 2018), the survivor activating factor

enhancement pathway (SAFE) (Lacerda et al., 2009) (Lecour, 2009) and their downstream targets, such as PKC (protein kinase C) (Heusch et al., 2008).

iv) Novel pathways in cardioprotection

RISK was first described in the early 2000's by Yellon and colleagues, following the observations that protein kinases including PI3K (phosphoinositide 3-kinase), MEK (mitogen activated protein kinase), ERK (extracellular signal related kinase), and PKC (protein kinase C), have important actions in cell survival (Yellon et al., 2023). PI3K, triggers the phosphorylation of AKT which is linked to mitochondrial protection and the inhibition of the MPTP opening (Sean M. Davidson et al., 2020), (Yellon et al., 2023), (Heusch, 2015), possibly by regulation of the enzyme glycogen synthase kinase - 3β (GSK-3β) (Comità et al., 2021). Endothelial PI3K also promotes the bioavailability of nitric oxide (NO) by the increased phosphorylation of endothelial nitric oxide synthase (eNOS) at SER1177 (Sata & Nagai, 2002). Survival kinases such as PI3K are activated via growth factors such as urocortin, insulin, various cytokines and autocoids such as adenosine and bradykinin (Heusch, 2015). Yellon et colleagues have recently summarised an extensive list of cardioprotective strategies which target the RISK pathway and PI3K/AKT (Yellon et al., 2023), including both pharmacological approaches and mechanical means of cardioprotection such as ischaemic preconditioning (IPC) and remote ischaemic conditioning (RIC) (Yellon et al., 2023).

IPC is a phenomenon which is observed when animal hearts are subjected to short periods of sequential, but non-lethal ischaemia, prior to larger myocardial infarction (Yellon et al., 1998). Prior IPC reduces the final infarct size, activates the RISK pathway, and generates low levels of ROS which enable conditioning (Heusch, 2015). Whilst some cardioprotective drugs are already well established in clinical practice for conditions such as diabetes and atherosclerosis (GLP-1 agonists and atorvastatin respectively) (Basalay et al., 2016), (Bell & Yellon, 2003), both IPC and RIC have proved more difficult to translate to clinical practice (Hausenloy & Bøtker, 2019), (Hausenloy, Kharbanda, et al., 2019), (Pearce et al., 2021). One explanation for this maybe that the patients who participated in the CONDI-2-ERIC-PPCI trial, (RIC during ST-elevation MI and prior to reperfusion) may have belonged to a lower risk cohort who received timely revascularisation, thus limiting the need for further myocardial protection (Hausenloy & Bøtker, 2019), (Heusch & Gersh, 2020). RIC is now being investigated in high-risk patients to ascertain whether this low cost, non- interventional technique can still be of benefit (Lukhna et al., 2023). However, IPC remains a gold-standard control in pre-clinical models of myocardial infarction (Hausenloy & Yellon, 2016).

Recent, important advances, have been made by directly activating the molecule PI3K (of which there is more than one isoform, including α, β and γ) (Sata & Nagai, 2002), (Gong et al., 2023). Whilst the α isoform is most closely correlated with cardioprotection in rodents (Rossello & Yellon, 2018), the novel compound 1938 (recently identified as a fast-acting agonist of

PI3Kα and published in Nature© Journal) has demonstrated the ability to reduce infarct size following myocardial I/R in vivo, by phosphorylation of AKT (Gong et al., 2023). This compound has also been used in studies of neuroprotection, to stimulate the re-growth of muscular neuronal fibres and to induce cell proliferation (Gong et al., 2023). 1938 as a direct RISK pathway activator, is a promising new avenue in cardioprotection, and warrants further study (Yellon et al., 2023)

The survival activating factor enhancement pathway (SAFE) is a second important pro-survival kinase pathway, of which the transcription factors STAT3 and JAK play a pivotal role (Lecour, 2009). The actions of JAK/STAT are not exclusive to cardioprotection, and this complex also has an important role in cytokine secretion (Prabhu & Frangogiannis, 2016). There is some overlap of the RISK and SAFE pathways, considering that ERK and MAPK may also phosphorylate STAT3 (Lecour, 2009). In terms of its cardioprotective role, JAK/STAT evokes mitochondrial protection during I/R by reducing the opening of the MPTP (Lecour, 2009). Many activators of SAFE have been identified, including tumour necrosis factor alpha, (TNF-α), insulin, interleukin10 (IL-10) and sphingosine-1-phosphate (Heusch, 2015). Insulin analogues (known to activate PI3K and RISK) therefore, have the potential to activate multiple cardioprotective pathways. Despite this, providing insulin as background therapy during myocardial infarction does not significantly mitigate immediate major adverse cardiovascular effects (MACE) in large scale clinical trials (Selker et al., 2012). Insulin does however improve survival outcomes and reduce heart failure hospitalisation rates after

1-year, as was observed in a follow-up study of the IMMEDIATE trial (Selker et al., 2014).

The ‘additive’ theory of in vivo cardioprotection, hypothesises that activation of the RISK pathway, in combination with newer anti-inflammatory drugs, may lead to better clinical translation (Davidson, Ferdinandy, et al., 2019), (He et al., 2020). As the SAFE pathway is also a distinct target, future therapies may aim to therefore activate RISK, SAFE and prevent pyroptosis in combination (Davidson, Ferdinandy, et al., 2019). Combination therapies are currently mainstay in other research areas such as stem cell survival (Chen et al., 2021). Chen et al have recently demonstrated that a cocktail (known as CEPT) containing Emricasan (pan-caspase inhibitor), Chroman 1 (a potent rho kinase inhibitor), polyamines and trans-ISRIB (inhibited stress response inhibitor) greatly enhances stem cell survival in vitro. These survival benefits were also observed in CEPT treated cardiomyocytes (Chen et al., 2021). Whilst Emricasan is known to reduce pyroptosis and inflammatory cell death (Stoess et al., 2023), Rho Kinase inhibitors such as Chroman 1 (ROCK inhibitors) activate the RISK pathway and augment NO levels in vivo (Huang et al., 2018a). It is yet to be established whether CEPT confers myocardial protection in vivo.

With regards to the above additive theory of cardioprotection, Cohen et al propose that this is to only beneficial where two distinct mechanisms of cardioprotection can be identified. Therefore, mechanisms which exclusively target the RISK pathway in combination, e.g. agonists of PI3K and

preconditioning, are not likely to provide protection and be clinically translatable (Cohen & Downey, 2017).

v) Reperfusion arrhythmia & myocardial stunning

Many traditional cardioprotective interventions are designed to primarily inhibit the opening of the MPTP, as this is an irreversible step in the cell death process (Hausenloy & Yellon, 2013). By contrast, myocardial stunning and reperfusion arrhythmia may be thought of as reversible processes, and in the case of reperfusion arrhythmia, can be managed with appropriate pharmacotherapy (Hausenloy & Yellon, 2016). Commonly used agents in the treatment of reperfusion arrhythmias include beta-blockers, amiodarone and calcium channel blockers, however cautious selection is required when there is concurrent haemodynamic disturbance (Niccoli et al., 2019). Reperfusion arrhythmia refers to the electrophysiological disturbances observed in both humans and animals at the onset of reperfusion, with most arrhythmias being ventricular in origin (Taggart & Yellon, 2002). Ventricular fibrillation can be instantly fatal, whereas other slower idioventricular rhythms may be sustained for longer periods of time (Bhar-Amato et al., 2017). At a cellular level, this phenomena arises due to likely damage from ROS, and changes to myocyte membrane potential, with subsequent disturbances to calcium, potassium and sodium homeostasis (Kloner, 1993). Vascular smooth muscle cell (VSMC) contraction and vasospasm is also a potential cause of sudden reperfusion induced cardiac arrhythmia (Kloner, 1993). The development of

reperfusion arrhythmias provides a physiological marker of appropriate injury in preclinical studies of I/R, whereas the relative importance of these events in the clinical domain, is more controversial (Lie, 1993).

Myocardial stunning is considered by many to represent a sub-lethal form of ischaemia/reperfusion injury and is the result of ROS inhibiting cardiomyocyte contractile function, and calcium overload causing disturbances to ventricular excitation-coupling and contraction (Bolli, 1990). Stunning results in temporary reduction to left ventricular contractility and so jeopardises ejection fraction leading to heart failure. This is associated with brief periods of ischaemia and is fully reversible given that the underlying myocardium is viable (Heusch, 2021). Heusch et al also describe myocardial stunning to be least associated with clinical haemodynamic compromise compared to other kinds of ischaemia/reperfusion injury (Heusch, 2021). The older more historical concepts of myocardial stunning and hibernation have recently been called into clinical question, following large-scale clinical trials such as the REVIVED trial (Perera et al., 2022). This randomised control trial (RCT) of 700 patients, found that revascularisation of ischaemic but viable myocardium, did not result in improved heart failure outcomes compared to medical therapy.

This possibly challenges the traditionally held opinion that viable myocardium (hibernating) is sub-lethal and entirely reversible with PCI (Perera et al., 2022), (Perera et al., 2023). It must be stated that the above trial related, to chronically ischaemic myocardium and is not applicable to acute STEMI.

vi) Summary – an overview of reperfusion injury

To summarise, myocardial I/R is comprised of cell death, reperfusion arrhythmia, myocardial stunning and no-reflow Figure 1. All except the latter concept, have been considered in this introduction section 1.1. Section 1.2 will be dedicated to the pathophysiology of no reflow and microvascular obstruction (MVO), which is a key focus of this thesis. It has been considered that cell death is traditionally felt to be the most integral (and potentially the most modifiable) aspect of I/R. This section has discussed that necrosis, necroptosis, pyroptosis and apoptosis are some of the key processes involved in cell death. Many of these mechanisms rely on both mitochondrial dependent and independent pathways (S. M. Davidson et al., 2020) Traditionally, pathways such as RISK and SAFE have been fundamental targets in cardioprotection (Rossello & Yellon, 2018), (Lecour, 2009) however new frontiers in pharmacotherapy include the combination of treatments, including those which target the above pathways, and anti-inflammatory therapies (Davidson, Ferdinandy, et al., 2019). 1938 is a novel compound which has demonstrated cardioprotective properties in vivo, via direct activation of PI3Kα (Gong et al., 2023). Further research is awaited with regards to this promising RISK pathway activator (Yellon et al., 2023).

Several prominent authors have hypothesised that early reperfusion injury within the coronary vasculature (secondary to microvascular obstruction

(MVO), vasospasm and immune cell plugging, amongst other processes) maybe a key event in the development of myocardial damage, and that this may occur earlier in the sequence of injury than originally thought (Heusch, 2019), (Hausenloy, Chilian, et al., 2019). The pathophysiology and treatment of MVO will next be considered in more depth in section 1.2.

Figure 1 Key components of lethal myocardial ischaemia/reperfusion injury. Myocardial infarction and occlusion of the culprit vessel is associated with myocardial ischaemia, generation of ROS and calcium overload. The MPTP opens and there is cell death. Reperfusion arrhythmias and myocardial stunning are reversible changes, whereas opening of the MPTP is irreversible. Vascular injury is a key contributor to regions of myocardium which do not reperfuse, (regions of 'no reflow'). Acute vascular injury leads to chronic microvascular injury which carries a poor prognosis (Heusch, 2016), (Yellon & Hausenloy, 2007), (Yellon et al., 2023).

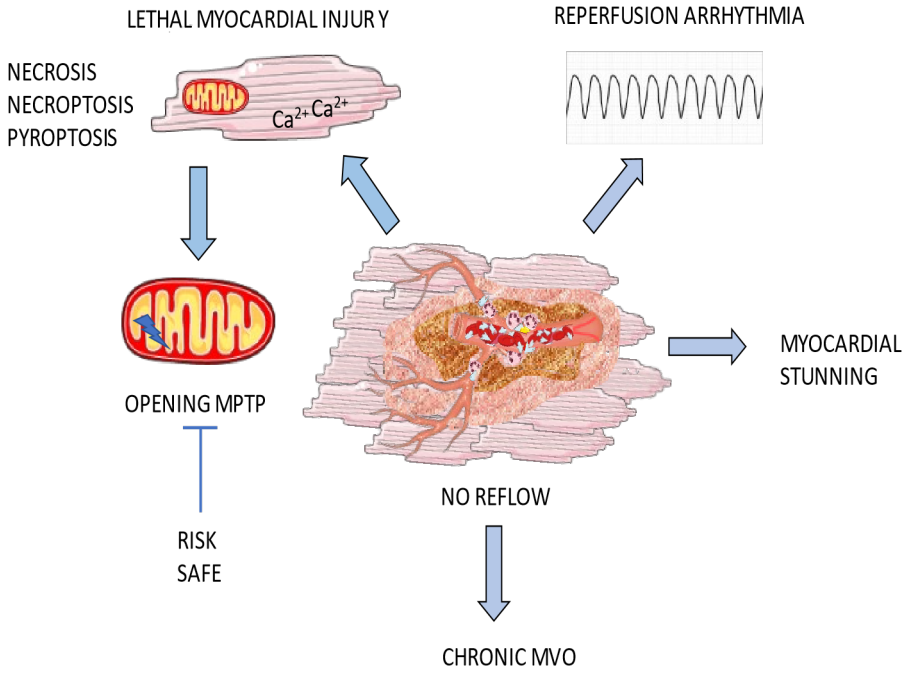

1.2– THE PATHOPHYSIOLOGY AND TREATMENT OF MVO

i) Defining coronary circulation injury

Section 1.1 has established that ‘no re-flow’ is a key concept in myocardial ischaemia/reperfusion injury (Heusch, 2016), (Hausenloy & Yellon, 2016). However, it is important to be precise with terminology, to avoid confusion. Myocardial ‘no reflow’ (NRF) describes the reperfusion failure of distinct areas of myocardium, despite successful restoration of flow in the infarct related artery (Kloner et al., 2018), (Niccoli et al., 2016). This is observed in 20-60% of patients during STEMI (Hausenloy, Chilian, et al., 2019). Myocardial NRF may occur due to continued obstruction of the smaller vessels of the coronary circulation such as capillaries and smaller arterioles (MVO) or, because of inflammatory injury to these small vessels, termed microvascular injury (MVI) (Reffelmann & Kloner, 2006). Whilst often used interchangeably, in the past few years, ‘MVO’ has been adopted as the main term denoting microvascular damage following myocardial infarction (Niccoli et al., 2016). Table 1 summarises these commonly used abbreviations, including some relevant clinical terms. MVO is most often confused with angiographic NRF (A-NRF). This refers to the acute vessel closure (AVC) of a culprit artery after PPCI, observed by a sudden reduction in coronary flow on fluoroscopy, which is a medical emergency (Reffelmann & Kloner, 2006). A precursor to this is known as ‘slow flow’ (Niccoli et al., 2016). Despite obvious differences in A-NRF and MVO, they exist on the same continuum of

coronary vascular injury and may occur because of the same underlying pathologies (Heusch, 2019), (Giannini et al., 2018). Important features of MVO include obstruction due to micro-emboli, erythrocytes and immune-platelet complexes, structural changes (such as endothelial blebbing and alterations to endothelial membrane permeability), and compression of small vessels caused by vascular smooth muscle cell (VSMC) vasospasm, myocardial oedema (causing external compression) and pericyte constriction (Reffelmann & Kloner, 2006),(Sanjiv Kaul et al., 2023), (Bonfig, Soukup, Shah, Olet, et al., 2022), (Kloner et al., 2017) (fig.2). Individual susceptibility, such as genetic predisposition to vasospasm, can also increase small vessel obstruction (Hubert et al., 2020). This section aims to describe this complex syndrome of events in further detail and consider their translational relevance.

ii) Plaque rupture and myocardial infarction

Myocardial infarction occurs via either plaque erosion or spontaneous plaque rupture, within a culprit coronary artery (the latter being more commonly associated with ST elevation MI (STEMI) in 75% of patients) (Kanwar et al., 2016). The origins of such a sudden atherothrombotic event, can be explained by the prior development of atherosclerotic plaque in the coronary circulation (Palasubramaniam et al., 2019). Atherosclerosis begins with an increase in circulating levels of low-density lipoproteins (LDLs) (Falk, 2006). LDLs are prone to induce inflammation in regions of coronary arteries which are more vulnerable to plaque, such as areas of the vessel wall which

are prone to shear stress or structural bifurcation (Bentzon et al., 2014). An increase in lipoprotein deposition, inflammation, and foam cell involvement, causes coronary artery VSMC proliferation and remodelling of the tunica media (Palasubramaniam et al., 2019). A fibrous cap forms, with an underlying lipid rich core, which is prone to rupture at a crucial moment of instability (Palasubramaniam et al., 2019), (Bentzon et al., 2014). There is variation in individuals between the development of unstable coronary plaques, and this does not explain all STEMIs, including those which are caused by thrombus alone (Niccoli et al., 2019). However, immune mediated injury is thought to accelerate plaque instability, via inflammatory molecules such as CCL2, and the switching of macrophages to an M1 subtype (Palasubramaniam et al., 2019).

During myocardial infarction sudden rupture of a vulnerable plaque, exposes the lipogenic core to the blood stream triggering a cascade of pro-thrombotic events which culminates in the formation of an obstructive thrombus, total occlusion, and ST-elevation (Niccoli et al., 2019), (Frangogiannis, 2015). Von Willebrand's Factor and thrombin contribute to clotting, platelet adhesion and activation (Bentzon et al., 2014). Complete or near-complete obstruction of the vessel lumen renders the myocardium in the area at risk (AAR), ischaemic. Section 1.1 has described the damage to the myocardium during I/R fuelled by DAMPS and cytokines. Spontaneous plaque rupture is, however, also the beginnings of post-STEMI MVO (Davidson, Andreadou, Garcia-Dorado, et al., 2019), (Reffelmann & Kloner, 2002).

Table 1- Commonly used abbreviations in studies of MVO. Adapted from (Niccoli et al., 2016), (Reffelmann & Kloner, 2006), (Heusch, 2019).

ABBRIEVIATION	MEANING	APPLICATION
1. NRF	No reflow	Refers to areas of myocardium which do not re-perfuse following successful revascularisation by PPCI or thrombolysis
2. MVO	Microvascular Obstruction	The physical obstruction of resistance vessels and capillaries by immune cells, red cells, vasospasm, and micro emboli
3. MVI	Microvascular Injury	Like MVO, however, refers more specifically to inflammation without physical obstruction
4. A-NRF	Angiographic NRF	Visual reduction in epicardial coronary artery flow during coronary angiography. Can result in AVC
5. AVC	Acute vessel closure	Occurs secondary due to A-NRF. An epicardial coronary vessel closes completely either due to complex spasm, injury due to PPCI or thrombus burden
6. AAR	Area at risk	The area which could theoretically become infarcted during regional ischaemia or myocardial infarction
7. MSI	Myocardial Salvage Index	A measure of reperfusion success. Assessed by cardiac MRI. The MSI is the area between the necrotic zone and the AAR
8. CMR	Cardiac magnetic resonance imaging	Specialised MRI imaging for the heart which is gold standard in diagnosis of MVO and MSI

iii) Microvascular injury during ischaemia

Prior to the PPCI era, Robert Kloner performed experiments in canines, to investigate the effects of acute myocardial infarction on MVO (Kloner et al., 1974). Dogs were subjected to varying amounts of ischaemia following LAD ligation, (40 minutes or 90 minutes) followed by reperfusion of up to 20 minutes. An endothelial tracer known as Thioflavin S, (which is seen to fluoresce under UV light) was administered systemically prior to sacrifice of the animals, after the release of a coronary artery ligation (Kloner et al., 1974). Kloner subsequently studied the ultrastructural changes observed under electron microscopy in a demarcated region of 'no re-flow'; defined as the region of myocardium where no ultra fluorescence was observed after reperfusion (Kloner et al., 1974). Endothelial changes observed during ischaemia, included the formation of large tissue blebs and amorphous bodies, which were seen to obscure capillary lumens and impede microvascular flow. Meanwhile in reperfusion, other changes were observed including microvascular clumping of erythrocytes and 'occasional' thrombi (Kloner et al., 1974). This work has formed the basis of what is known today about the structural microvasculature changes involved in NRF, including the distinction between pathological changes in ischaemia and reperfusion (Kloner et al., 1974).

Specific to the ischaemia phase, there are formation of 'in-situ thrombi' which occur due to intra-vascular stasis (Sezer et al., 2018). 50 years later, the role

of micro-emboli in post-infarct MVO remains controversial (Kleinbongard & Heusch, 2022), (Coffey & Adamson, 2021) and the limited evidence for thrombolytics in clinical trials will be considered below in section vii). Endothelial swelling during ischaemia induces damage to the endothelial glycocalyx, causing changes in membrane permeability which contributes to capillary haemorrhage (Figure 2). Intra-myocardial haemorrhage because of vascular reperfusion injury is a poor prognostic sign, and often signals irreversible endothelial damage (Reffelmann & Kloner, 2002).

Myocardial oedema, which is known to be a phenomenon of ischaemic injury, may also cause external compression of the microvasculature leading to obstruction and a reduction in blood flow (Niccoli et al., 2016), (Bonfig, Soukup, Shah, Olet, et al., 2022). Furthermore, these microcirculation ischaemic changes, as described by Kloner and colleagues (Kloner et al., 1974), were noted to be proportional to the duration and extent of hypoxia (Niccoli et al., 2016).

iv) Microvascular injury during reperfusion

Neutrophils and NETs

Kloner's original work demonstrated that the greatest extent of microvascular damage during STEMI occurs during reperfusion (Niccoli et al., 2016), (Sezer et al., 2018). Moreover, the zone of MVO, can expand for up to 8 hours following the onset of this phase (Hausenloy, Chilian, et al., 2019). Upon

reperfusion, there is an initial period of hyperaemia, followed by a sudden return of blood flow, to parts of the microvascular network (Niccoli et al., 2016). Within the regions of NRF or slow flow, there is a large extent of capillary damage secondary to immune cell plugging, inflammation, further structural damage and an increase in vasoconstriction caused by inflammatory mediators such as endothelin-1 (ET1) and thromboxane (Figure 2) (Niccoli et al., 2016), (Sezer et al., 2018). Platelets and neutrophils are likely to be some of the first cell types to contribute to significant MVO (Sezer et al., 2018). Moreover, neutrophils and platelets may form complexes and migrate through the endothelium together causing obstruction (Reffelmann & Kloner, 2006), (Ziegler et al., 2019). Neutrophils are attracted to regions of endothelial dysfunction in the microvasculature where there has been damage to the protective glycocalyx, and subsequent upregulation of P-selectin and ICAM-1 (Niccoli et al., 2016), (Brandt et al., 2021). High mobility group box-1 (HMGB1) has also been identified as an important source of vascular neutrophil and immune cell recruitment, especially given its role as a DAMP like molecule.

HMGB1 can bind to either toll-like receptors (TLRs), or RAGE receptors, (receptor for advanced glycation end products) to encourage endothelial cytokine secretion (IL-6 and tumour necrosis factor alpha (TNF-α)), which then recruits further immune cells (Prabhu & Frangogiannis, 2016). Platelet derived micro-particles also secrete HMGB1 (Zhao et al., 2023). In a study of 44 STEMI patients, HMGB1 was found to be upregulated in platelets from the infarct related artery, of those patients with angiographic NRF (A-NRF) (Zhao

et al., 2023). In addition to the above, neutrophil extracellular traps, (NETs) which are novel inflammatory molecules, may also contribute to small vessel obstruction (Rada, 2019). Neutrophils attached to activated endothelium produce increased NAPDH and ROS, promoting the release and explosion of extracellular 'NETs'; an obstructive meshwork of neutrophil chromatins, granular components, histones and myeloperoxidase (MPO) (Zdanyte et al., 2023). These NETs and intracellular waste products can cause obstruction in situ or migrate downstream to the small resistance vessels and contribute to I/R injury (Bonaventura et al., 2020).

The role of monocytes and monocyte/platelet aggregates

Mononuclear leucocytes such as monocytes and macrophages have an important role in inflammation and myocardial reperfusion injury. In addition, increased white cell count is an adverse prognostic marker in patients with acute myocardial infarction (Dutta & Nahrendorf, 2015), (Peet et al., 2020) . Monocytes and macrophages are recruited to the infarction zone in two distinct waves and secrete fibronectin, thus having a key role in myocardial repair (Dutta & Nahrendorf, 2015). Ly-6c 'high' monocytes are a more inflammatory subtype of monocytes and are associated with the secretion of pro-inflammatory cytokines such as TNF-α and IL-1β. Whereas, Ly-6C 'low' monocytes may have a role in repair from inflammation (Peet et al., 2020). During myocardial infarction, there is an overall increase in adrenergic signalling, which stimulates secretion of hematopoietic stem cells from the bone marrow (under influence from hormones such as CXCL2) leading to

secretion of monocytes (Dutta & Nahrendorf, 2015). These differentiate via capillaries into the infarct zone and become macrophages. The role of inflammatory processes such as the above in myocardial reperfusion injury is well reported, and has been discussed elsewhere in this thesis (Prabhu & Frangogiannis, 2016), (Zuurbier et al., 2019).

In addition to the role of mononuclear leucocytes in myocardial inflammation, several authors have suggested a role for monocytes as contributing factors to the vascular no reflow phenomenon (Niccoli et al., 2016), (Rezkalla et al., 2017). Notably, this is distinct from the role of neutrophils and NETS (other leukocytes causing capillary obstruction) as described in the section above, and by Robert Kloner, in his original no reflow work in canines (Kloner et al., 1974). In an important literature review by Niccoli et al, it is suggested that cardiac monocytes in the infarct zone may alter the ratio of superoxide: nitric oxide, therefore altering coronary circulation vasodilatory reserve (Niccoli et al., 2016). Similarly, Rezkalla et al suggest that monocytes/macrophages can lead to microvascular plugging in the same manner as neutrophils and NETs (Rezkalla et al., 2017). Several important monocyte ratios have also been explored in relation to the development of no reflow. Balta et al, investigated the role of monocyte to HDL-C ratio in a cohort of 600 PPCI patients undergoing treatment for STEMI (Balta et al., 2016). In the study there was noted to be a greater incidence of monocytes found in patients with no reflow. The authors postulated that this was likely secondary to the integral role of monocytes in atherosclerosis and plaque rupture (Balta et al., 2016). Therefore, monocytes may play a role in plaque instability associated with no reflow in humans, but potentially not in animal ligature models (which

do often not involve atheroma unless this is related to a specific genotype). These findings by Balta et al, were further corroborated in a study by Wang et al, which demonstrated that monocyte counts were elevated overall in acute STEMI patients with angiographic no reflow (Wang et al., 2016). The predictors and experimental biomarkers under investigation for MVO, are discussed elsewhere in this chapter.

The role of platelets in no reflow will also be considered separately, however, it is important to mention here that specifically, platelet-monocyte aggregates during acute myocardial infarction have also been associated with microvascular obstruction (Mavroudis et al., 2011), (Rolling et al., 2023). Platelet-monocyte aggregates (MPA) are known to be pro-inflammatory and form as a result of increased P-Selectin markers on platelets, and CD40 ligands, tissue factor (TF) on monocytes (Rolling et al., 2023). The baseline level of MPA in the general population is estimated to be around 5-20%, however this increases significantly in atheroma, acute myocardial infarction and microvascular obstruction (Dong et al., 2015), (Furman et al., 2001), (Mavroudis et al., 2011). Similarly to NETs, MPAs likely provide mechanical obstruction during acute MVO, and are involved in the cytokine cascade (considered below) (Rolling et al., 2023).

Inflammation & reactive oxygen species (ROS)

During myocardial infarction, cytokines and inflammation promote endothelial membrane leakage, and capillary haemorrhage via interruptions to VE

Cadherin and gap junctions, (Figure 2) (Reffelmann & Kloner, 2006). Pyroptosis in endothelial cells, and the production of the NLRP3 inflammasome, further heightens vascular inflammation and microvascular damage (Heusch, 2019). Sun et al recently demonstrated in mice, and in in vitro studies using cardiac microvascular cells, (CMECs) that caspase-4 mediated pyroptosis is important in MVO (Sun et al., 2021). Despite these findings there is, perhaps, less of a role for cell death in MVO overall, and rather it is the inflammatory based changes to vascular physiology and structural integrity, which are most deleterious (Reffelmann & Kloner, 2006). The TLR/MyD88/NF-κβ pathway of inflammation has been implicated in micro-emboli related MVO, in rats (Su et al., 2018). These inflammatory changes were reversed by administration of nicorandil, a dual NO donor and K_{ATP} channel opener (Su et al., 2018). ROS molecules generated by endothelial cells, as well as neutrophils, can precipitate MVO by inducing changes in mitochondrial dynamics and inducing apoptosis. H_20_2 in small amounts, may be cardioprotective as it encourages mild vasodilation, however in larger amounts this is harmful and pro-apoptotic (Shaw et al., 2021). Kloner's group investigated the role of an antioxidant administered to rats undergoing LAD infarction (Dai et al., 2022). Compound OP113 both encouraged mitochondrial protection and was found to reduce the area of NRF%. However, it is unclear how much of this effect was secondary to accompanying cardiomyocyte protection and a reduction in infarct size % (Dai et al., 2022).

Other anti-inflammatory agents and peptides which have been found to limit

MVO in animal models have included imatinib, (a tyrosine kinase inhibitor) (Konijnenberg et al., 2023) and the GI hormone relaxin (Gao et al., 2019), (which may have both vasodilatory and anti-inflammatory actions, and is thus cardioprotective). Increased levels of inflammation within the coronary circulation evoke a pro-thrombotic state, which contributes to the development of micro-emboli.

Micro-emboli

Coronary plaque rupture and upregulation of the coagulation cascade secondary to thrombin has previously been described. The resulting microembolization is often a consequence of iatrogenic injury to the epicardial coronary artery, during PPCI as the index lesion is crossed (Kleinbongard & Heusch, 2022). Fragments of atherothrombotic plaque are dislodged by instrumentation, along with other vascular debris, which leads to downstream propagation of clotting products (Niccoli et al., 2016). Angiographically visible thrombi are reported in approximately 11-15% of patients (Sezer et al., 2018). MVO occurs in animal models of myocardial infarction (ligature models), in the absence of plaque rupture and thrombus, suggesting that the primary plaque is not the sole origin of downstream thrombi (Kloner et al., 2018). Moreover, micro-infarcts, (forming islands of necrosis and apoptosis) can occur in myocardial territory not supplied by the infarct related artery (Kleinbongard & Heusch, 2022). The mixed results of clinical trials of thrombolysis in myocardial infarction and MVO, (considered

in section vii), have re-affirmed the hypothesis that MVO must encompass more than simply distal emboli (Coffey & Adamson, 2021), (McCartney et al., 2020). Kleinbongonard et al describe the limitations of investigating coronary micro-emboli (CME) in animal models (Kleinbongard & Heusch, 2022). Specialised micro-spheres have been used in pigs to simulate thrombus fragmentation; however, this method does not accurately induce the native clotting cascade, and hence this method is less translational (Su et al., 2019).

Platelets and Vasospasm

Activated and aggregated platelets, (mediated via Glycoprotein IIb/IIIa) are known to contribute to small vessel obstruction in the coronary circulation (Heusch, 2019), (Ziegler et al., 2019). In an original study by Golino et al in 1987, New Zealand rabbits with hypercholesterolaemia, had pronounced areas of MVO following myocardial infarction, which could be abrogated by anti-platelet serum (APS) (Golino et al., 1987). APS also reduced myocardial infarct size (Golino et al., 1987). Anti-platelets are now the mainstay of treatment for STEMI alongside PPCI, however this has not entirely solved the problem of MVO (Coffey & Adamson, 2021). There are many available antiplatelets licensed for clinical practice, however pre-clinical studies can still provide important insights into the roles of platelets during myocardial infarction. Hjortbak et al administered different anti-platelet agents to male Sprague Dawley rats undergoing in vivo LAD ligation and found that only ticagrelor was able to diminish infarct size (Hjortbak et al., 2021). Comparable

results were not observed with clopidogrel and prasugrel. Kleinbongard et al have proposed that these results may be secondary to the ability of ticagrelor to influence adenosine mediated vasodilation (Kleinbongard et al., 2021).

Preclinical science has acknowledged the existence of a '*platelet paradox.'* This is the concept that whilst platelets contribute to clotting, inflammation, and platelet–leucocyte complexes, they may also be cardioprotective (Kleinbongard et al., 2021). Davidson et al reported that platelets can release cardioprotective substances during I/R such as stromal derived factor (SDF1α), (which activates the pro-survival RISK and SAFE pathways) and protective exosomes (Davidson, Andreadou, Barile, et al., 2019). Both activated platelets and fragments of the original coronary plaque rupture, may secrete vasoconstrictors such as tissue factor (TF), thromboxane (TXA_2), and histamine (5-HT) (Reffelmann & Kloner, 2002). In addition to promoting vasospasm, these substances also encourage activation of the coagulation cascade and micro-emboli propagation (Kleinbongard & Heusch, 2022). Platelet derived micro-particles also secrete HMGB1 (Zhao et al., 2023). In a study of 44 STEMI patients, HMGB1 was found to be upregulated in platelets from the infarct related artery, of patients with angiographic NRF (A-NRF) (Zhao et al., 2023). Niccoli et al, who have extensively reviewed the topic of STEMI associated MVO (Niccoli et al., 2016), suggest that endothelin-1 (ET1) is the most important vasoconstrictor involved in this phenomenon.

Endothelin-1

Endothelin-1 type A receptors are expressed on both endothelial cells and VSMCs and have an integral role in mediating VSMC via g-protein coupled mechanisms such as the RhoA- Rho Kinase pathway (Hubert et al., 2020), (Tona et al., 2023). The Rho kinase pathway of VSMC will be discussed in greater detail in section 1.3. Tona et al, recently investigated a link between MVO and ET-1 A receptor seropositivity in 50 STEMI patients (Tona et al., 2023). MVO was found to have occurred in 48% of patients, with a significantly higher number displaying ET-1A seropositivity (Tona et al., 2023), leading to the investigators to conclude that preventing ET-1 mediated constriction may be a future target in MVO therapy. Furthermore, in 2012, a small RCT of n=57 STEMI patients, demonstrated that pharmacological ET-1A blockade, was safe and associated with improvements in myocardial perfusion and IS% (Adlbrecht et al., 2012) . Endothelial and VSMCs may not be the only cell types central to microvascular spasm; the role of other VSMC-like cells, such as pericytes, are now being explored closely (O'Farrell et al., 2017).

Pericytes

Following the investigation of I/R in the brain, pericytes have been identified as an important source of MVO and vasoconstriction (Kloner et al., 2018). There are many notable parallels between NRF which occurs due to stroke,

and that which occurs due to myocardial infarction. There are similar predisposing factors, pathological changes and anti-platelet treatments recommended in both conditions (Kloner et al., 2018). Whilst NRF in the heart may lead to adverse remodelling and heart failure, NRF in the brain may result in longer term changes in cerebral perfusion and cognitive function (Uemura et al., 2020). Pericytes are VSMC-like cells that are poorly understood compared to other cell types, despite their abundance in the heart. These mural cells are responsible for capillary bed blood flow regulation and are found encasing capillaries at regular intervals (Sanjiv Kaul et al., 2023). Pericyte intervals correspond well with regions of capillary obstruction and MVO in animal models, when this is visualised under electron microscopy (O'Farrell et al., 2017).

There has been much less research into the physiology of pericyte constriction compared to VSMCs, but recent studies have suggested that pericytes enable capillary constriction via changes to intracellular Ca^{2+} currents and the G protein coupled receptor GPR39 (Methner et al., 2021). When GPR39 is knocked out in animal models of myocardial infarction, there are significantly smaller zones of MVO and infarct size observed (Methner et al., 2021). As pericytes are phenotypically like VSMC, (other mural cells), they have been difficult to isolate in pure form in animal models (Avolio et al., 2023), which may offer an explanation as to why research is limited. Pericytes are known to constrict the capillary bed during both ischaemia, and reperfusion, which can lead to irreversible vascular change (Sanjiv Kaul et al., 2023), (O'Farrell et al., 2017).

O’Farrell et al successfully administered adenosine to rats undergoing myocardial infarction to reduce pericyte constriction, thus providing an important mechanistic insight into pericyte mediated mechanisms of contraction (O'Farrell et al., 2017). The authors concluded that pericyte constriction is a major contributor to ischaemic MVO and induces approximately 40% capillary obstruction despite adequate reperfusion. Moreover, in the O’Farrell study, neutrophils (as stained with ICAM-1 or neutrophil elastase) were not felt to significantly contribute towards capillary obstruction, which is contrary to the traditionally held opinion that immune cells are important aggravators of MVO (Reffelmann & Kloner, 2006), (O'Farrell et al., 2017). Whilst the understanding of cellular specific changes is important during MVO, the coronary circulation is a dynamic organ, and its physiology must be considered.

v) Coronary physiology during ischaemia

The coronary circulation is a highly specialised and complex network of arteries, veins and capillaries with different properties and functions (Sezer et al., 2018). As part of normal homeostasis, the coronary circulation adjusts to changes in myocardial oxygen demand via a process known as autoregulation (Goodwill et al., 2017). Autoregulation allows the maintenance of adequate coronary blood flow (CBF) between coronary perfusion pressures of 40130mmHg (Johnson et al., 2021). This is achieved by changes to resistance vessel lumen diameter (i.e., vasoconstriction and

vasodilation) using a combination of endothelial, neurohumoral, metabolic and myogenic mechanisms (Brandt et al., 2021). Coronary pre -arterioles (100-500μM) and arterioles (10-100μM) as the main resistance vessels, are subject to greater changes in myogenic tone, whereas smaller capillaries (<10μM) contain few VSMC and are more sensitive to changes in the levels of metabolic mediators such as reactive oxygen species, adenosine and ATP (Brandt et al., 2021). Neurohumoral factors include the influence of the autonomic nervous system and neurotransmitters such as acetylcholine (Ach) and noradrenaline (NE) (Brandt et al., 2021). Overall, vagal tone is thought to contribute less to coronary autoregulation, however coronary resistance vessel response to Ach is species dependent (Brandt et al., 2021).

When there is an increase in myocardial oxygen demand, during normal exercise, the sympathetic nervous system (SNS) induces vasodilation of the coronary conduit vessels and larger arteries via stimulation of alpha-adrenergic receptors, to allow CBF to be maintained (Goodwill et al., 2017). Whilst this response predominates during exercise, the resistance arterioles enhance blood flow further, via alterations in the balance of alpha and beta mediated adrenergic stimulation (vasoconstriction and vasodilation respectively) (Brandt et al., 2021), (Goodwill et al., 2017). During total epicardial coronary occlusion, perfusion pressure rapidly drops across the network and there is no flow (Sezer et al., 2018). There may be an initial compensatory vasodilation in the coronary arterioles, possibly mediated by an increase in pC02, adenosine, and increased SNS activity (Sanjiv Kaul et al., 2023). This is likely to occur early in ischaemia, as with prolonged hypoxia

these adaptive responses are lost (Sezer et al., 2018). In humans, individual responses may also differ depending on prior remodelling of the coronary circulation, absence of pre-conditioning, diabetes, the formation of collaterals and underlying genetic factors (Brandt et al., 2021).

Endothelial factors such as nitric oxide (NO), prostacyclin, (PGI2), endothelin-1 (ET-1) and endothelium derived hyper-polarising factor (EDHF) are also important in coronary circulation autoregulation (Johnson et al., 2021), especially during reperfusion in the smaller arterioles and capillaries. Whilst there is vasodilation of the coronary arterioles during ischaemia, the pericytes constrict to induce contraction of the capillary bed. Conversely, when coronary perfusion pressure rises above the window of autoregulation, there is constriction of the arterioles, but a dilation of the capillary bed regulated by pericytes (S. Kaul et al., 2023).

In reperfusion, homeostasis is more difficult to maintain leading to loss of vasodilatory reserve in the resistance vessels and irreversible pericyte damage (Goodwill et al., 2017). It is according to this rationale that vasodilators have traditionally been administered during STEMI (Sezer et al., 2018). Figure 2 summarises the pathological changes that are described in sections a-e.

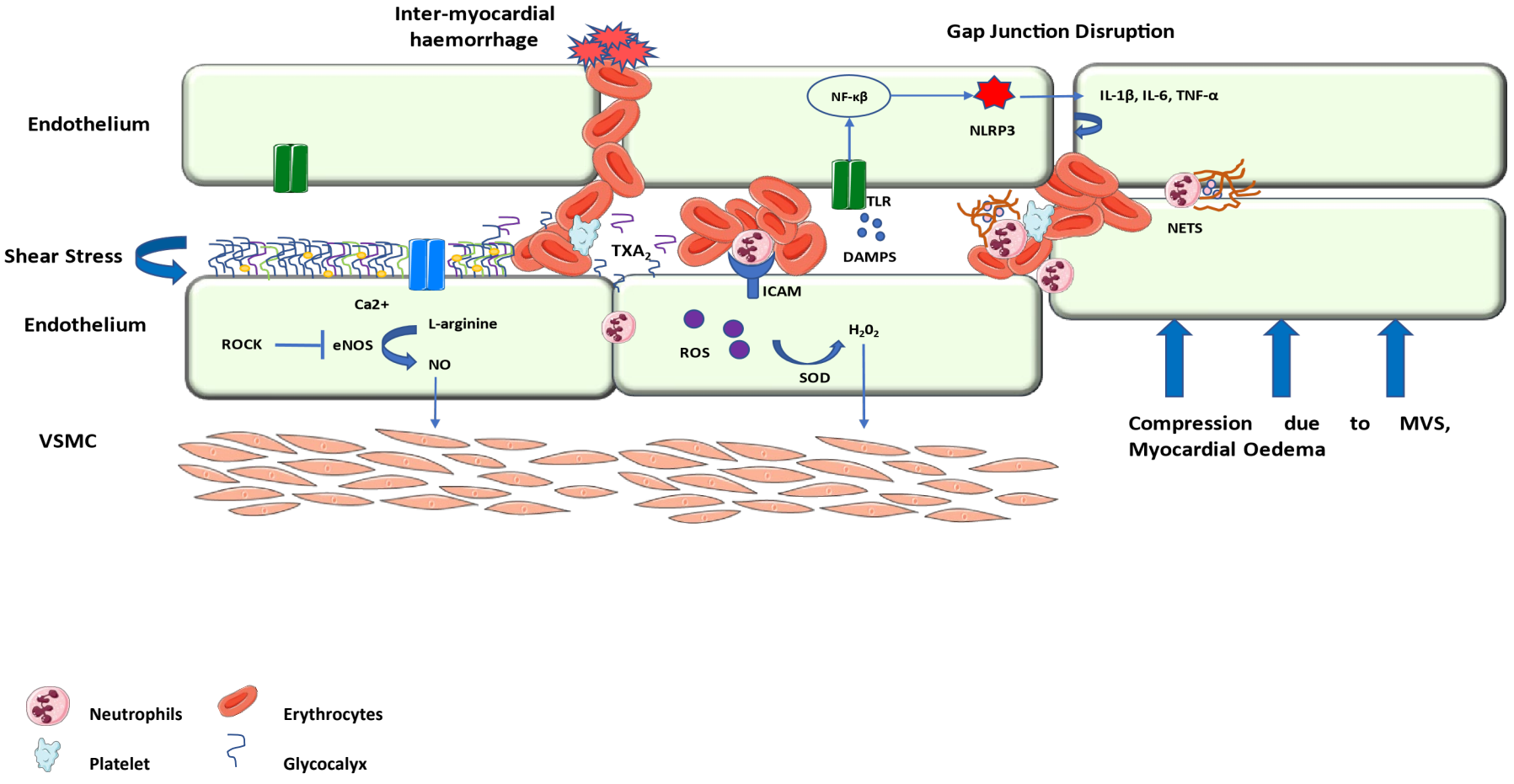
Inter-myocardial haemorrhage
Gap Junction Disruption
Endothelium
NF-κβ
NLRP3
IL-1β, IL-6, TNF-α
TLR
DAMPS
NETS
Shear Stress
TXA2
ICAM
Ca2+
Endothelium
ROCK
eNOS
L-arginine
NO
ROS
H2O2
SOD
VSMC
Compression due to MVS, Myocardial Oedema
Neutrophils
Erythrocytes
Platelet
Glycocalyx

Figure 2The pathophysiology of MVO in the coronary circulation. MVO is a phenomenon of downstream small vessel red cell clumping, leucocyte-platelet complexes, immune cell infiltration and external compression secondary to oedematous myocardium. Vasospasm is induced by endothelial dysfunction and the production of ET-1, TXA2 and a reduction in NO. Free radicals and generation of ROS species also contribute to MVO. Endothelial pyroptosis induced by DAMPS and activation of TLR's leads to activation of the NLRP3 inflammasome and the generation of pro-inflammatory cytokines. Neutrophils rupture to release NETs and DNA products into the extracellular space, which combine with other immune cells creating further obstruction. Inflammation is a pro-thrombotic state and increases the likelihood of clot formation. ROCK – Rho kinase, eNOS – endothelial nitric oxide synthetase, TXA2 – thromboxane A2, 5-HT – serotonin, ET-1 – endothelin 1, ATII – angiotensin II, MVS – microvascular spasm, ROS – reactive oxygen species, SOD - superoxide dismutase, H202 – hydrogen peroxide, PGI2 – prostacyclin, DAMPs – danger associated molecular proteins, TLR – toll like receptors, TNF – α – tumour necrosis factor alpha. Original illustration inspired by (Reffelmann & Kloner, 2006)

VI) The importance of prognosis in MVO

The urgent need to develop new treatments for STEMI related MVO, relates to its poor prognosis. This is particularly relevant considering that the incidence of acute MVO during STEMI is approximately 5-60%, depending on which imaging modality is used to estimate this (Niccoli et al., 2016), (Durante et al., 2017). The most accurate prognostic information has been derived from several important analyses of cardiac MRI (CMR) studies of STEMI, using both early and late gadolinium enhancement techniques (EGE/LGE) (de Waha et al., 2017), (Durante et al., 2017), (Wu et al., 1998) and MRI remains the gold standard in MVO detection (Niccoli et al., 2016). From the results of these trials, it is apparent that the presence of MVO post STEMI, is closely correlated with mortality (*fig.3*) (de Waha et al., 2017), event free survival (Durante et al., 2017), adverse LV remodelling and heart failure (Wu et al., 1998). Importantly, this remains the case when data is adjusted for infarct size (de Waha et al., 2017). De Waha et al performed an important analysis of seven large randomised controlled trials (RCTs) of STEMI and MVO outcomes, (n=1688).

Figure 3 shows that a graded response was present between the extent of MVO present on CMR, and MACE, (major adverse cardiovascular events) (de Waha et al., 2017). Findings of Intra-myocardial haemorrhage (IMH) on CMR, (T2 weighted) may be associated with an even worse prognosis, and the development of worsening heart failure compared with MVO alone (Berry & Ibanez, 2022), (Carrick et al., 2016). From a pathological

perspective, IMH may correlate closely with the necrotic infarct zone, harbouring more cell death, immune cells, and inflammatory molecules such as cytokines (Bochaton et al., 2021). In a prospective study of STEMI patients by Carrick et al, IMH was seen to occur less frequently but occurred later in the time course compared to MVO, and in some cases persisted even after MVO had resolved (Carrick et al., 2016).

Considering MVO, it has been hypothesised that improved knowledge of predictive factors, and advancing diagnostic techniques may be most beneficial in improving outcomes, i.e., an approach which favours prevention over cure (Niccoli et al., 2016). Over the past 5-years, there has been the increasing recognition that predictive factors for MVO may be gender specific, e.g., MVO with unobstructed coronary arteries (MINOCA) may be more common in women, due to differences in coronary anatomy and vasoreactivity. Women have a greater in-hospital mortality around the time of STEMI, but this may be related to older age at presentation (Reynolds et al., 2022).

Predictive factors of STEMI related reperfusion failure can be further divided into angiographic, pre-hospital factors, biochemical markers, and demographic features. To date, excluding troponin T, (which is used as a marker of myocardial damage) there is no one specific biomarker of microvascular damage used in clinical practice (Niccoli et al., 2016). Angiographic features such as pre-procedural high TIMI (thrombolysis in myocardial infarction) flow score, length of culprit lesion, LAD culprit vessel

and high thrombus burden are all associated with incomplete restoration of coronary flow (Niccoli et al., 2016), (Kirma et al., 2008), (Stajic et al., 2022).

Demographic features such as the presence of diabetes, smoking and advancing age >65 are also associated with worsening MVO or angiographic NRF (A-NRF)(de Waha et al., 2017), (Durante et al., 2017), (Stajic et al., 2022), whereas ischaemia time, symptom to balloon time (SBT) and circadian rhythms are time dependent factors which predict suboptimal reperfusion (Bonfig, Soukup, Shah, Davidson, et al., 2022), (Redfors et al., 2021). In the Durante et al study, LVEF% at presentation, and the presence of IMH were also predictive of both MVO and A-NRF (Durante et al., 2017). Other markers of more general endothelial dysfunction such as VEGF (vascular endothelial growth factor) are described as being predictive of reperfusion failure (Garcia et al., 2019).

In a large, multi-centre study of STEMI patients, (PREGICA, *n=147*) both troponin and higher VEGF-A levels in plasma were independently associated with CMR MVO, and this effect was observed in patients with TIMI 3 flow, (i.e. MVO but no A- NRF) (Garcia et al., 2019). Other experimental inflammatory biomarkers of interest have included soluble growth stimulation expressed gene 2 protein (ssT2) (Søndergaard et al., 2023), (Zhang et al., 2022) , TXA2 (thromboxane A2) (Niccoli et al., 2008), lymphocyte to monocyte ratio (Kurtul et al., 2015) and perilipin 2 (Russo et al., 2021). Of note, the intra-cellular protein Rho Kinase (ROCK), (which can influence coronary VSMC vasoreactivity) is upregulated during STEMI but has not been investigated as a specific marker of MVO (Li et al., 2016).

Where MVO cannot be prevented or predicted prior to myocardial infarction, intervention with pharmacotherapies before PPCI may be required (Niccoli et al., 2016). There has been a recent move to assessing acute MVO during STEMI, using invasive measures (Niccoli et al., 2016). As the microcirculation cannot be imaged directly, indirect measurements of resistance and flow must be obtained using parameters such as IMR, (index of microcirculatory resistance), RRR, (resistive reserve ratio) (De Maria et al., 2019), (Maznyczka et al., 2020) and thermodilution techniques (Maznyczka et al., 2021) . The intricacies of these techniques are outside the scope of this thesis; however, it is important to be aware of these emerging imaging modalities when considering the results of clinical trials, as below.

Figure 3 The effects of worsening MVO on MACE outcomes. – In a large, pooled analysis of 7 STEMI RCT's (n=1688), extent of MVO on CMR was directly proportional to all-cause mortality (%) and heart failure hospitalisation (%), and inversely proportional to the time to first event (p<0.001). From De Waha et al with publisher permission granted for use (de Waha et al., 2017).

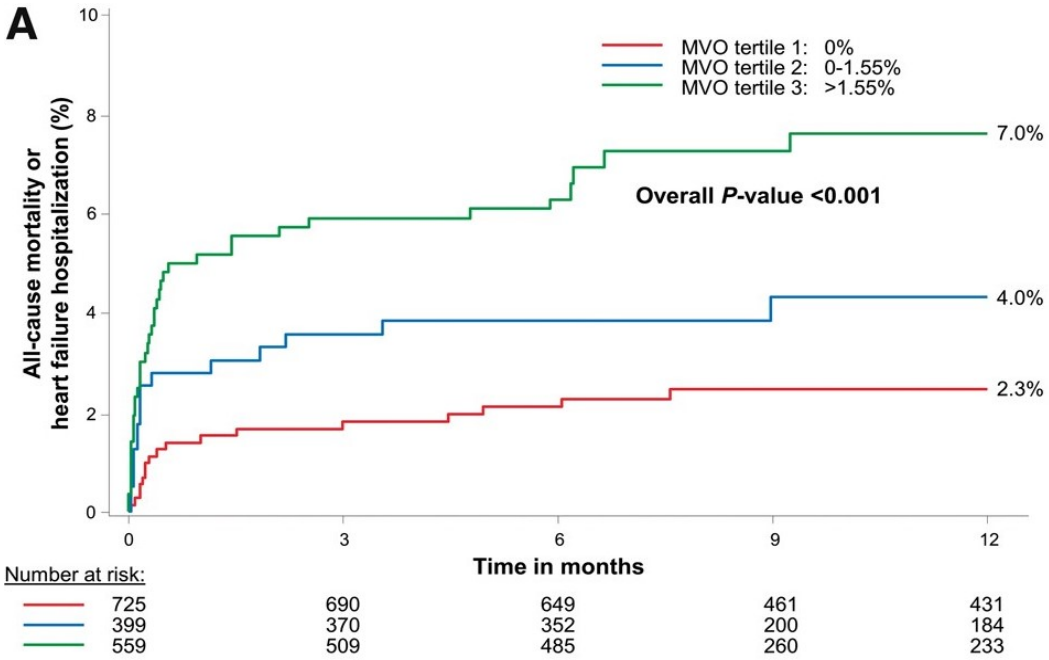

VII) Treatment of MVO – an overview clinical trials 2018-23

Emerging themes

A detailed review article by Heusch et al, entitled 'Coronary microvascular obstruction: a new frontier in cardioprotection' previously provided a detailed meta-analysis of clinical trials in interventions for MVO (2012-2019) in context of STEMI (Heusch, 2019). In 2019, there were few positive clinical trials which had improved CMR outcomes for MVO, especially when considering IS% as the primary outcome and MVO% as the secondary outcome (Heusch, 2019). At the time of Heusch's publication, a large clinical trial by Ibanez et al (METOCARD-CNIC) had previously demonstrated positive outcomes following the administration of IV metoprolol during STEMI. IV metoprolol was associated with both improvements in IS% and myocardial salvage index (MSI%) on CMR (Ibanez et al., 2013).

Heusch's group have recently undertaken preclinical studies in swine to argue that metoprolol may be less cardioprotective than previously thought, demonstrating that it is associated with an increase and not a reduction, in %NRF when administered in vivo (Kleinbongard et al., 2023). Whilst these two studies are not directly comparable, this may throw some doubt onto the consistency of the use of beta-blockers acutely, in the prevention of MVO. Many clinicians may also have concerns regarding the safety of routine metoprolol during STEMI, due to the potential for negative inotropic effects and AV block in inferior infarction (Rezkalla et al., 2017).

At the time of Heusch's previous review, two important large scale clinical trials had considered the benefits of adenosine and nitrate derivatives for STEMI related MVO; RE-OPEN AMI (2013) and REFLO STEMI (2016) (Nazir et al., 2016), (Heusch, 2019), (Niccoli et al., 2013). Unfortunately, these studies provided conflicting results, at a time when both therapeutic agents were used in the cardiac catheterisation lab as a treatment for A-NRF. In RE-OPEN AMI, intra-coronary adenosine significantly improved both ST-elevation resolution and TIMI flow following thrombus aspiration, (both markers of A-NRF), whereas sodium nitroprusside did not (Niccoli et al., 2013). There were no significant differences in MACE outcomes observed between treatment groups. Conversely, several years later in the REFLO-STEMI trial, concerns over the effectiveness and even safety, of intracoronary adenosine were raised by Nazir et al (Nazir et al., 2016). In the trial, not only were there no significant improvements in STEMI related MVO outcomes following the administration of intracoronary adenosine, but this was associated with both an increase in MACE outcomes and a deterioration in LVEF%.

These findings were interpreted as a potential harm signal and recommendations were made that adenosine should no longer be considered in clinical practice (Nazir et al., 2016). As adenosine functions as a VSMC dilator, induces hyperaemia and increases coronary vasodilatory reserve, it was hypothesised that it potentially worsens reperfusion injury by over-dilating the resistance vessels, leading to a sudden and uncontrolled increase in CBF (Nazir et al., 2016). Despite these

results, several recent important review articles of MVO do not discount adenosine as a potential treatment option (Rezkalla et al., 2017), (De Marco et al., 2022). The clinical trials which have contributed to this decision will be considered in more detail in the next paragraph.

A PUBMED/MEDLINE indexed search was performed on 1st August 2023 for the terms STEMI, STEMI+MVO and STEMI+NRF. This search identified 39 randomised controlled trials (RCTs) with MVO related outcomes between 2018-2023 (5-year period). Proof of concept trials, and trials without a control arm were discounted, as were study population sizes of less than *n=50* patients. Sub studies of >50 patients from original RCT's meeting the above criteria were included. The remaining *n=23* studies are displayed in figure 4, and arranged according to whether the tested intervention was pharmacological, device related or preconditioning related, and whether these trials were positive. Positive trials for the purpose of this analysis were considered as showing either: - an improvement of perfusion-based MVO outcomes by an appropriate imaging modality e.g., CMR, or an improvement of angiography-based outcomes and NRF e.g., TIMI flow, corrected TIMI frame count (cTFC) or myocardial blush grade (MBG).

Using these definitions a total of 57% of trials had at least one positive MVO or NRF outcome (García-Méndez et al., 2018), (Feng et al., 2019), (Naghshtabrizi et al., 2020), (Broch et al., 2021), (Qian et al., 2022), (Sadeghian et al., 2022), (Qian et al., 2023), (Pelliccia et al., 2021), (Aguiar et al., 2020), (Scarsini et al., 2022), (Nepper-Christensen et al., 2022), (Ma et al., 2022), (Traverse et al., 2019) 39% were neutral for any MVO or NRF

outcome (Wang et al., 2019), (McCartney et al., 2020), (Stähli et al., 2022), (Hosseini et al., 2022), (Kakavand et al., 2023), (Freund et al., 2019), (Kim et al., 2022), (García Del Blanco et al., 2021), (Francis et al., 2021) and 2 trials were negative and associated with increased harm (Soylu et al., 2018), (Figure 4).

Figure 4. *Randomised controlled trials STEMI related MVO 2018-23*

SUMMARY RCTS 2018-23, n>50

PHARMACOTHERAPY

Garcia-Mendez et al, 2018, n=103	Atorvastatin prior to PPCI
Wang et al, 2019, n=185	Recombinant BNP
McCartney et al, 2019, T-TIME, n=440, update 2020	Low-dose IC alteplase thrombolysis
Feng et al, 2019, n=170	IV Nicorandil after thrombus aspiration
Naghshtabrizi et al, 2020, n=104	IC Adenosine
Broch et al, 2021, ASSAIL-MI, n=199	Tocilizumab (IL-6 inhibition)
Qian et al, 2022. CHANGE TRIAL, n=238	IV Nicorandil
Stahli et al, 2022, CLEVER-ACS, n=150	Everolimus (mTOR inhibitor)
Hosseini et al, 2022, n= 451, Pod CAST-PCI	Colchicine
Sadeghian et al, 2022, n=228	IC Adenosine
Qian et al, 2023, n=173	Oral Trimetazidine
Pelliccia et al, 2021, DISSOLUTION, n=95	Low Dose IC thrombolysis
Kakavand, 2023, PENTOS-PCI, n=161	IV Pentoxifylline

DEVICE RELATED THERAPY

Soylu et al, 2018, n=124	Post dilation NC balloon after PPCI
Freund et al, 2019, n=144	Manual thrombus aspiration
Aguiar et al, 2020, MRUSMI sub study n= 100	Sono thrombolysis
Scarsini et al, 2022, OX-AMI sub-study, n=108	PISCO device

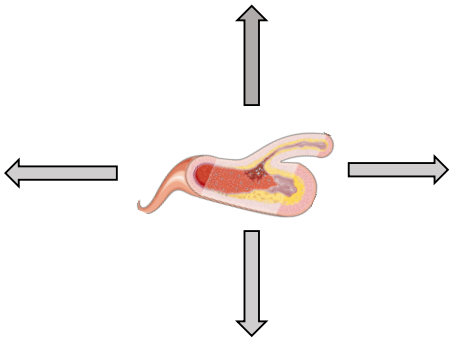

Nepper-Christensen,2022 DANAMI-3-DEFER update, n=1205	Deferred PCI
Kim et al, 2022, n=72	Direct stenting
Ma et al, 2022, n=120	Prolonged balloon inflation

DEVICE RELATED THERAPY

PRECONDITIONING RELATED THERAPY

Traverse et al, 2019, n=122	Ischaemic PostC
Garcia del Blanco, 2021, COMBAT-MI, n=378	RIC and/or Exenatide
Francis et al, 2021, CONDI-2/ERIC-PPCI CMR sub study, n=169	RIC

KEY

- POSITIVE: TRIAL SIGNIFICANTLY REDUCED INCIDENCE OR EXTENT OF MVO OR NRF
- NEUTRAL: NO SIGNIFICANT DIFFERENCE IN MVO OR NRF OUTCOMES
- NEGATIVE: TRIAL CAUSED HARM OR INCREASE IN MVO OR NRF OUTCOMES

Pharmacological agents

Most interventions were pharmacological, (Figure 4). In response to the previous findings of REFLO-STEMI and RE-OPEN AMI (Nazir et al., 2016), (Niccoli et al., 2013), two further studies have explored the effects of intra-coronary (IC adenosine) on A-NRF (Naghshtabrizi et al., 2020), (Sadeghian et al., 2022). Naghshtabrizi et al, found that a bolus of IC adenosine before and after PPCI, was associated with improvements in TIMI flow from 0 to 3 compared to placebo, (p=0.002) however there were no significant improvements in secondary outcomes such as MACE and cardiac arrhythmias (Naghshtabrizi et al., 2020). Unlike REFLO-STEMI there were no harmful events identified following the use of adenosine (Nazir et al., 2016). In a second study (Sadeghian et al., 2022) IC adenosine was administered prior to PPCI only, in a cohort of STEMI patients at an Iranian Heart Centre. Similarly significant outcomes were observed for improvement of TIMI flow and corrected TIMI frame count (cTF), but no other secondary outcomes were analysed.

Other vasodilators and anti-anginal drugs such as IV nicorandil and trimetazidine have been investigated by the same group, and investigators of the recent CHANGE trial (Qian et al., 2022), (Qian et al., 2023). The CHANGE trial compared IV nicorandil vs placebo in a STEMI cohort of n=238 patients, and is one of few recent trials to report positive results across a range of outcomes, including a reduction in infarct size (IS%), reduction in incidence of MVO%, improvement in LVEF% and improvement in A-NRF (Qian et al., 2022). Nicorandil is a well-

established anti-anginal drug with dual properties both as a K_{ATP} channel opener and NO donor, resulting in coronary arterial vasodilation (Pearce et al., 2023). The CHANGE trial is evidence that vasodilators can mitigate MVO and suggests that they do not necessarily worsen I/R injury (Qian et al., 2022). Further large-scale trials are required to explore the effects of Nicorandil during STEMI on both infarct size, A-NRF/MVO and MACE outcomes.

Similarly, Nicorandil has been shown to improve MVO outcomes compared to placebo in patients undergoing thrombectomy for heavy thrombus burden (Feng et al., 2019). This should be interpreted with some caution however, as manual thrombus aspiration, is not advised routinely in A-NRF (following the results of both historical (Jolly et al., 2015) and more recent clinical trials (Freund et al., 2019)). In the previous TOTAL trial, (a large cohort of 10,732 STEMI patients) manual thrombus aspiration did not significantly improve coronary flow and moreover, was associated with increased cerebral vascular events at 30-days (Jolly et al., 2015). Thrombolytic agents such as alteplase have equally had limited success in improving MVO outcomes (McCartney et al., 2020).

The T-TIME trial was a prospective study of n=440 STEMI patients receiving either alteplase (thrombolysis) 20mg vs placebo or a 10mg lower dose of alteplase (McCartney et al., 2020). Not only did alteplase not significantly improve MVO outcomes, a sub-analysis in patients with an ischaemic time >4hours demonstrated that there was a dose dependent

increase in MVO and intra-myocardial haemorrhage, and the intervention was therefore associated with significant harm (McCartney et al., 2020). Since the trial there has been a move away from testing IC lytic therapy, however intravenous GPIIb/IIIa agents are still indicated at operator discretion for heavily thrombotic occlusions (Collet et al., 2021). Since the outcomes of both the CIRCUS and COLCOT trials were revealed (investigating the benefits of anti-inflammatory agents in myocardial infarction) there has been increasing interest in suppressing inflammation in MVO. In addition, the recent COVID-19 pandemic has highlighted the novel role of immune suppression, in certain high-risk patients (Group, 2022). AMI associated with COVID-19 has been observed to be both more thrombotic and inflammatory in origin (Fanaroff et al., 2021).

Since 2018, there have been three key trials of immune suppressants in STEMI related MVO, including IL-6 suppression with Tocilizumab (Broch et al., 2021), the use of an mTOR inhibitor, (mammalian target of rapamycin) (Stähli et al., 2022) and trial of oral colchicine in the PodCAST-PCI trial (Hosseini et al., 2022). Of these interventions, the use of Tocilizumab in the ASSAIL-MI trial, (a biological agent and IL-6 inhibitor, used in the treatment of rheumatoid arthritis) was associated with the most positive MVO outcomes (Broch et al., 2021). ASSAIL-MI was an RCT conducted at three large PPCI centres in Norway where, n=199 patients were randomised to receive either pre-PPCI Tocilizumab infusion or placebo. In the study IL-6 suppression was associated with an improvement in myocardial salvage index (MSI) and extent of MVO%, but not a reduction in final infarct size.

CRP levels during index hospital admission were found to be significantly lower (Broch et al., 2021).

Conversely, in a larger trial of STEMI patients receiving oral colchicine before and after PPCI (n=451), treatment was not associated with benefits in any outcome, including reduction in A-NRF, vascular inflammatory markers such as P-selectin and CRP, and MACE (Hosseini et al., 2022). This is disappointing given that COLCOT reported a reduction in the risk of MACE in patients with recent AMI (Tardif et al., 2019), however it did not measure MVO outcomes, hence the two trials are not directly comparable (Tardif et al., 2019). It is also quite likely that colchicine via an oral route, is not adequate to prevent immediate A-NRF as suggested by the investigators of the Hosseini et al trial (Hosseini et al., 2022). Given that the original COLCOT trial reported an increase in the incidence of severe pneumonia due to innate immune suppression (Tardif et al., 2019), it is important to note that none of the recent trials of anti-inflammatories described, raised infection related safety concerns following short term administration (Broch et al., 2021), (Stähli et al., 2022), (Hosseini et al., 2022).

Device related interventions & ischaemic conditioning

There have been more trials of pharmacological therapies than device related interventions in the treatment of A-NRF and MVO (Figure 4). This does not include PPCI itself, which has revolutionized treatment of STEMI and grossly improved mortality rates (Niccoli et al., 2019). The limited

success, and associated risks of manual thrombectomy have previously been discussed (Freund et al., 2019), (Jolly et al., 2015). Other novel PPCI strategies analysed have included direct stenting, (without prior balloon pre-dilation which can dislodge thrombi), changes to balloon inflations and the deferral of PCI to a later stage after successful balloon reperfusion (Ma et al., 2022), (Kim et al., 2022), (Soylu et al., 2018).

One of the larger trials to investigate delayed stenting in STEMI was the DANAMI-3-DEFER trial and associated 2022 update, (the latter considered in this analysis) (Nepper-Christensen et al., 2022), (Kelbæk et al., 2016; Lønborg et al., 2017). These trials were in response to an earlier trial in 2014 called DEFER-MI (Carrick et al., 2014), which demonstrated a benefit in A-NRF following delayed stenting. A previous 2017 sub-analysis of DANAMI-3DEFER enrolled n=510 patients and included CMR data to extend outcomes to MSI and MVO. Unfortunately, direct stenting did not significantly improve either of these parameters in the study (Lønborg et al., 2017). Fig.4 includes a summary of the recent 2022 update of the DANAMI-3-DEFER trial, where n=1205 patients underwent either immediate PCI or delayed stenting by 24 hours after restoration of TIMI2/3 flow, followed by systemic bivalirudin, (direct thrombin inhibitor) or GPIIb/IIIa (Lønborg et al., 2017). Of note there was a greater proportion of patients in the treatment group who received GPIIb/IIIa, which is an important limitation. The updated sub-analysis found a significant benefit in A-NRF outcomes and observed reduced distal embolization (assessed angiographically), especially in high-risk patients >65 years (Nepper-Christensen et al., 2022).

Similarly, other interventions associated with improved outcomes have included micro-bubble catheter directed thrombolysis, (Sono thrombolysis) and use of the PISCO device (pressure-controlled intermittent coronary sinus occlusion) (Aguiar et al., 2020), (Scarsini et al., 2022).

PISCO was investigated as an intervention by the investigators of the large OX-AMI registry (Scarsini et al., 2022). This involves the angiographic placement of a catheter directed balloon into the coronary sinus, which then undergoes cyclical inflations and deflations, to a maximum pressure of >800mmHg for twenty minutes, to provide intermittent increases in coronary sinus pressure, and increase blood flow to the ischaemic area (Scarsini et al., 2022). The results of this small trial, (n=108 patients) demonstrated that use of the PISCO device significantly improved %MVO on CMR in both anterior and inferior STEMI. In addition, use of PISCO was associated with improvement in IS% at 6 months (Scarsini et al., 2022). The study is one of the few studies analysed to provide complex parameters of microcirculatory function during angiography, (IMR and RRR) in addition to CMR and follow-up parameters. The results of the larger PISCO-AMI trial are currently awaited, (NCT03625869).

The concept of intermittent coronary sinus occlusion bears some similarity to the concept of ischaemic pre-conditioning (IPC). First discovered in animal models of myocardial infarction, this is a phenomenon where intermittent and sub- lethal ischemia and reperfusion protects the myocardium from subsequent lethal/reperfusion injury. (Yellon et al., 1998). Although gold standard in animal models of cardioprotection, there has been difficulty translating this into humans, leading to much discussion

surrounding the most important mechanisms involved, e.g., whether IPC evokes changes to coronary pressure and flow, humoral factors, neural or metabolite mediated pathways (Yellon et al., 1998). IPC can also be performed via a distant delivery site in a process known as remote ischaemic conditioning (RIC). This involves placing a tourniquet or blood pressure cuff around a remote limb to occlude blood flow temporarily and sequentially (Yellon et al., 1998). In animal models RIC reduces infarct size in myocardial infarction, but these beneficial effects have only been demonstrated in proof-of-concept studies but not in large RCT's. With respect to the latter, RIC has been investigated as a potential intervention for MVO (Figure 4) as part of a separate sub-analysis of the large multi-centre CONDI2/ERIC PPCI trial, however there were no significant differences in MVO outcomes observed following sequential 5-minute inflations (4-cycles) to a total pressure of 200mHg, prior to PPCI (Francis et al., 2021). Section 1.1 has detailed the plans to conduct further trials of RIC in high-risk STEMI patients (Lukhna et al., 2023).

VIII) Summary – Future perspectives for MVO therapy

Ischaemic MVO is a multi-factorial phenomenon and likely requires more than one treatment strategy (Reffelmann & Kloner, 2006). Originally described as one of the key concepts in ischaemia/reperfusion injury, there is now an emerging school of thought that 'no reflow' and MVO, require independent attention (Davidson, Andreadou, Garcia-Dorado, et al., 2019), (Heusch, 2019), (Wu et al., 1998). Whilst micro-emboli were first thought to

be the most significant contributing factor, there has been a move away from this concept (Coffey & Adamson, 2021), to consider previously overlooked pathologies such as inflammation and pericyte constriction (Sanjiv Kaul et al., 2023), (O'Farrell et al., 2017). Although the overall prognosis of myocardial infarction has improved drastically since the introduction of PPCI (Niccoli et al., 2019), MVO still creates significant prognostic concern, especially in the additional presence of intra-myocardial haemorrhage (Berry & Ibanez, 2022). Both are associated with long term adverse effects such as pathological left ventricular remodelling (de Waha et al., 2017). A recent analysis of clinical trials 2018-23 (Figure 4), has demonstrated mixed efficacy of treatment options for MVO. This analysis has considered any positive MVO or NRF outcome, however very few treatments demonstrated a combined improvement in infarct size, MVO and long-term outcomes, which Heusch identifies as an important future aim (Heusch, 2019). One such exception is the drug Nicorandil, which has demonstrated improvements across multiple categories in the recent CHANGE trial (Qian et al., 2022). Nicorandil is clinically safe and would need to only be re-fashioned from its current purpose as an anti-anginal drug. Despite this, Nicorandil is a vasodilator and there is only limited evidence in preclinical studies for its anti-inflammatory mechanisms of action (Su et al., 2018) .

Rho kinase inhibitors (ROCKi) as vasodilators, have received little consideration in acute coronary MVO, yet they have been considered as therapeutic in cerebral vasospasm secondary to sub-arachnoid

haemorrhage (Tanaka et al., 2005) and cerebral infarction (Lee et al., 2014). ROCKi are versatile drugs with potential actions in vasodilation (Otsuka et al., 2008), inflammation (H. Liu et al., 2022), and reduction of atheroma (Matsumoto et al., 2013). The role of rho kinase in the heart and coronary circulation, will be considered next.

1.3 THE ROLE OF RHO KINASE IN THE HEART

i) Introduction

Rho kinase (ROCK) is an important intracellular protein kinase (serine/threonine), with a molecular weight of 160kDa. Since ROCK was discovered over twenty years ago, more is understood of its wide range of actions within different cell types (Loirand et al., 2006), (Nakagawa et al., 1996), (Shimokawa et al., 2016), (Riento & Ridley, 2003). ROCK is an effector of multiple cellular signalling processes, including VSMC contraction, actin filament assembly, (and assembly of the cytoskeleton), nitric oxide metabolism (via eNOS) (Shimokawa & Rashid, 2007) and apoptosis (Shi et al., 2011) . It is an integral component of homeostasis at the vascular endothelial/VSMC junction (Alvarez-Santos et al., 2020), and has over 30 different downstream substrates (Loirand, 2015). ROCK is activated upstream, by the small G protein coupled molecule RhoA (Nakagawa et al., 1996), in a self-regulating process involving conversion of GDP to GTP by GTPase (Loirand et al., 2006). ROCK can also be activated directly by LPS (arachidonic acid), and by a self-regulating mechanism involving auto phosphorylation (Loirand, 2015), (Noma et al., 2006).

The RhoA/ROCK pathway is stimulated by VSMC agonists, including angiotensin II (ATII), 5-HT, endothelin-1 (ET-1), and norepinephrine (NE) (Shimokawa et al., 2016). Activation of G-protein coupled receptors by these agonists leads to VSMC contraction and calcium sensitisation (Wang

et al., 2009). ROCK plays a role within the endothelium in mechano-sensing of turbulent flow, and coupling changes to NO metabolism, (ROCK inhibits eNOS and reduces available NO). It may also have a role in endothelial insulin receptor signalling and promoting inflammatory pathways (Shimokawa et al., 2016).

Due to its wide range of downstream functions, ROCK is pathological in many cardiovascular disorders including ischaemic heart disease (IHD) (Huang et al., 2018a), atherosclerosis (Matsumoto et al., 2004), atrial fibrillation (Chen et al., 2018), heart failure (Do e et al., 2013), (Ocaranza et al., 2011), hypertension (Tsai et al., 2017), vasospastic angina (Masumoto et al., 2002) and pulmonary hypertension (Loirand et al., 2006). In the last few years, it has also been recognised as a contributor of inflammation in non-cardiac disorders such as graft vs host disease, (a multi-organ complication of bone marrow transplant) (Cutler et al., 2021). There are two isoforms of ROCK: ROCK1 and ROCK2. These isoforms share a 92% genetic identity (Shi et al., 2011) and are located on chromosome 18 and 2 respectively (Loirand et al., 2006).

As ROCK2 resides within the cell cytoplasm, this was the first isoform to be discovered, whereas ROCK1 is thought to be located closer to the endothelial cell layer (Loirand, 2015). Few isoform-specific substrates have been identified; therefore, it is challenging to separate activity of ROCK1 from ROCK2 entirely. Moreover, documentation of isoform specific ROCK expression is variable in the literature (Hartmann et al., 2015). ROCK2 is the predominant isoform in the heart, and VSMC, whereas ROCK1 is

expressed the liver, lungs, spleen, and immune cells (Loirand, 2015). ROCK2 -/- deficient mice do not survive, and ROCK1 -/- deficient mice are born with eyelids open (Loirand et al., 2006). Heterozygous ROCK1 or ROCK2 mice can be used to investigate isoform specific effects, as can ROCK inhibitors (ROCKi), which have been in development since the 1990's and were first pioneered in the treatment of post sub-arachnoid haemorrhage vasospasm and glaucoma (Noma et al., 2006). There are now over 170 available ROCKi on the market, all with varying potency and selectivity for ROCK1/2. The following sections will consider in further detail, the role of ROCK in VSMC contraction, and cardiovascular disorders relevant to ischaemia- reperfusion.

ii) ROCK regulates VSMC contraction

VSMC contraction is a complex process which is governed by multiple pathways, all converging to promote the phosphorylation of myosin light chain kinase (MLC20), actin polymerisation and vascular contraction (Touyz et al., 2018). It is an agonist mediated process, which is also under neurohumoral control (Touyz et al., 2018). Firstly, an increase in Ca2+ ion concentration activates calcium dependent pathways such as the calcium-calmodulin complex, and G-protein coupled receptor (GQ11) increases in IP3 and protein kinase C (PKC). Ca2+-calmodulin activates myosin light chain kinase (MLCK), an enzyme which encourages the phosphorylation of MLC20 and subsequent contraction. Simultaneously, there is a calcium independent pathway of VSMC contraction which is regulated by ROCK

(Wettschureck & Offermanns, 2002). Like the calcium dependent pathway, this is stimulated by the agonists angiotensin II (ATII), 5-HT, endothelin-1 (ET-1), thromboxane A2, (TXA2) and norepinephrine (NE), via the small G-protein coupled molecule (G12/13), RhoA (Shimokawa et al., 2016). Activated ROCK, induces VSMC contraction via the phosphorylation of myosin light chain kinase (MLC) and the inhibition of myosin light chain phosphatase, (MLCP) (Figure 5). ROCK inhibits MLCP by interrupting the usual binding of this protein to MLC20 (Touyz et al., 2018). Two intermediary proteins are also able to regulate the ROCK/MLCP pathway including ZIPK and CPII7 (Hartmann et al., 2015). MLCP activity is regulated at the myosin binding sub-unit 'MYPT1', which contains ROCK specific binding sites such as Ser507/Thr853 (Alvarez-Santos et al., 2020), whereas MLC is also phosphorylated by other protein kinases and is not ROCK specific (Alvarez-Santos et al., 2020). For this reason, MYPT1 is most often relied upon as a measure of downstream ROCK activity, but even this is not completely exclusive to ROCK (Loirand, 2015).

As part of in vitro investigations, Wang et al suggested that ROCK2 is the most important isoform in VSMC contraction (Wang et al., 2009). It was proposed that whilst both isoforms initiate contraction, only ROCK2 binds to MYPT1 directly (Wang et al., 2009). Similarly, endothelin-1 dependent constriction of murine mesenteric arteries has been shown to be ROCK2 dependent, and can be inhibited by the selective ROCK2 inhibitor, KD025 (Björling et al., 2018). In the same study, a greater expression of ROCK2 in mesenteric arteries was noted with advancing age, leading to the authors

to conclude that disorders such as chronic hypertension may be mediated by the ROCK2 isoform, over ROCK1 (Björling et al., 2018). Loirand et al state that ROCK must be upregulated for ROCKi to have blood pressure lowering effects, i.e. they are ineffective in absence of disease pathology (Loirand, 2015). The ROCK pathway of VSMC may be more pronounced in those with vascular disease, due to an increase in abnormal G-proteins or 'GEFs.' This occurs secondary to an increase in sodium concentration and chronic secretion of ATII (Kawarazaki & Fujita, 2021). In this setting Rho dependent vasoconstriction is especially associated with activity of G12/13, rather than Gq11 (Kawarazaki & Fujita, 2021) Conversely, patients with Gittleman's disease, (salt-wasting) have deficient amounts of ROCK, which leads to normotension in the presence of persistently high ATII levels (Kawarazaki & Fujita, 2021), (Calò et al., 2005). The significant role of ROCK in VSMC contraction and calcium sensitization has led to much interest in its role in hypertension and arterial remodelling. This research is relevant to the coronary circulation as many patients with ischaemic heart disease, have undergone vascular remodelling secondary to hypertension.

iii) ROCK and endothelial barrier function

ROCK is a major regulator of eNOS metabolism and reduces production of NO by endothelial cells (Noma et al., 2006). ROCK inhibitors therefore encourage vasodilation two-fold; firstly, via reducing VSMC contraction, and by increasing the production of AKT and NO (Shimokawa & Rashid, 2007). The effects of activated ROCK on endothelial membrane permeability, may

be relevant to NRF and the development of IMH (Figure 2). The control of endothelial membrane permeability is complex, and endothelial cells are initially resistant to damage during the ischaemia phase of I/R (Hausenloy, Chilian, et al., 2019). During reperfusion, cytokines and changes to calcium homeostasis cause the endothelium to become activated and adhesion molecules to appear, (ICAM1). Some of the protective function of the glycocalyx is lost, and gap junctions emerge, increasing membrane permeability and facilitating capillary haemorrhage (Hausenloy, Chilian, et al., 2019), (Heusch, 2019), (Hubert et al., 2020). Other inflammatory molecules such as VEGF, MPO and endothelial NLRP3 also contribute to changes in permeability (Hausenloy, Chilian, et al., 2019).

Several studies have implicated ROCK in increasing endothelial membrane permeability, in different diseases (Huang et al., 2011), (Lee et al., 2020). The mechanisms by which ROCK enhances permeability, are not well understood, however VSMC contraction may prompt the development of gap junctions by the movement of F-actin fibres (van Nieuw Amerongen et al., 2007) (Figure 5). Others have postulated that ROCK interacts with VE-cadherin molecules and occludins to directly facilitate an increase in permeability (Grothaus et al., 2018). Despite these sources suggesting that ROCK is deleterious to endothelial membrane function, a small amount of basal ROCK activity is required to maintain homeostasis (Loirand, 2015). Further research is needed to investigate the role of ROCK in coronary/microvascular barrier function.

Figure 5 Agonist induced pathway of ROCK dependent VSMC contraction. G proteins activate RhoA, which activates ROCK. ROCK inhibits MLCP and so promotes the phosphorylated form of MLC, leading to contraction. This pathway is distinct to the calcium dependent pathway of VSMC contraction and so provides calcium sensitisation. Movement of F-actin fibres during VSMC results in the development of GAP junctions and increases endothelial barrier permeability. ROCK inhibits eNOS and reduces the amount of available NO. Original drawing based on the concepts from (Kawarazaki & Fujita, 2021), (Touyz et al., 2018), (Shimokawa et al., 2016)

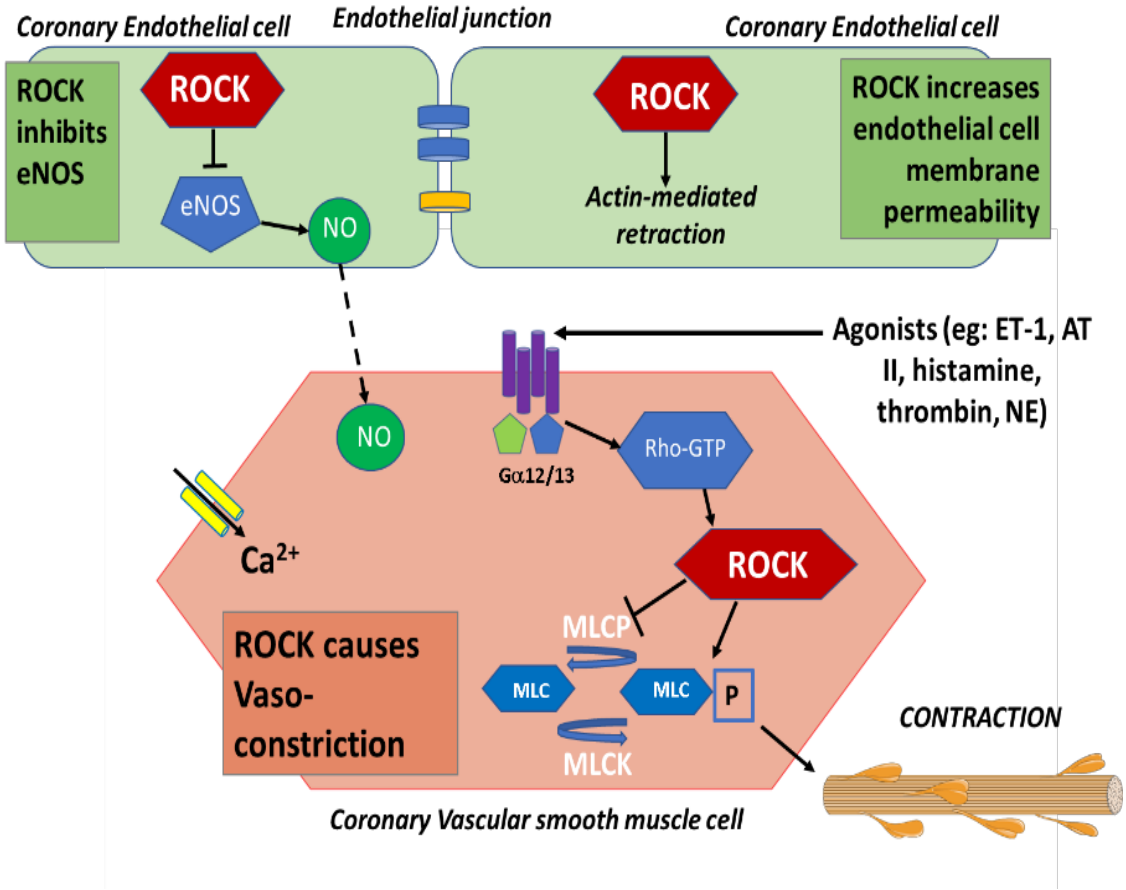

iv) ROCK inhibitors in studies of Cardioprotection

Many new ROCK inhibitors (ROCKi) have entered the clinical arena since Fasudil (isoquinolone derivative, HA-1077) was discovered in 1995 (Feng et al., 2016). ROCKi were first licenced for the treatment of cerebral vasospasm (Satoh et al., 2014), but now have applications in the treatment of glaucoma, asthma, cancer, kidney disease, pulmonary fibrosis and degenerative neurological conditions (Feng et al., 2016), (Knipe et al., 2015), (Loirand et al., 2006), (Shimokawa & Rashid, 2007). Fasudil is the most tested ROCKi in preclinical studies. The drug is readily accessible, but is associated with a greater systemic side-effects, (such as hypotension) compared to other newer ROCKi (Feng et al., 2016). For this reason, the therapeutic window of Fasudil is narrow, unless the drug is applied topically, or is chemically modified so that its active metabolites do not remain in the systemic circulation, ('soft-ROCK') inhibition (Defert & Boland, 2017). Substitution with hydroxyfasudil, the active metabolite of Fasudil, may minimise any unwanted off-target effects (Shimokawa & Rashid, 2007) However, both compounds still have affinity for other protein kinases such as protein kinase C (PKC). Fasudil is also known to have a calcium channel blocking effect (Liu et al., 2020).

Selective ROCK2 inhibitors, such as KD025, (SLX-2119) appear promising in the treatment of non-cardiac disorders such as psoriasis (Yoon et al., 2020), (Zanin-Zhorov et al., 2017) and GVHD (Cutler et al., 2021). KD025

has 200-fold higher selectivity toward ROCK2 (IC_{50} 105 nmol/L) compared with ROCK1 (IC_{50} 24 μmol/L). (Lee et al., 2014) .

In human studies, ROCKi have been tested in cardiovascular disorders such as vasospastic angina (Masumoto et al., 2002), (Shimokawa et al., 2002), PCI induced coronary injury (Kikuchi et al., 2019) and ischaemic stroke (Shibuya et al., 2005). A small retrospective study, *n=36* using Fasudil in the treatment of reduced coronary flow post PCI, (including routine procedures) was promising, however significant hypotension complicated a proportion of cases, and patients required inotropic support (Kikuchi et al., 2019). Trial participants were treated with intra-coronary Fasudil where slow-flow/no-reflow was resistant to initial intra-coronary nitrate administration. The most common aetiology observed was micro-emboli (69%), followed by vessel spasm (22%) and iatrogenic coronary dissection (8%). Fasudil significantly improved TMI flow in treated patients, ($p<0.05$) (Kikuchi et al., 2019). To date, no other clinical studies have investigated ROCKi in the specific management of STEMI related MVO.

Huang et al (Huang et al., 2018a), provide a comprehensive meta-analysis of 19 pre-clinical studies of myocardial I/R, where the ROCKi Fasudil has been used as a therapeutic intervention (*n=400*). With respect to this analysis, Fasudil treated animals showed reduced infarct size (IS%), improved LV function, a reduction in troponin levels and improved survival (*p<0.05*). Mechanisms of cardioprotection discussed were coronary vasodilation mediated by increased levels of NO, attenuation of apoptosis (caspase 3 mediated) and a reduction in oxidative stress (OS) associated

compounds (Huang et al., 2018a). Fasudil at doses of 10mg/kg was most frequently used, both in vivo and ex vivo. Further to this meta-analysis (Huang et al., 2018a), another study investigated Fasudil, (3-10mg/kg) in a rodent model of chronic myocardial infarction (Zhou & Ma, 2020). The ROCK inhibitor Fasudil was administered for 4-weeks prior to the induction of I/R, and outcomes were measured 4-weeks following myocardial ischaemia. There was a significant increase in ROCK1 & 2 expression reported, (by real-time PCR) and ROCK activity, (measured using levels of P-MYPT1) was increased in control animals. In the Fasudil treated group, there was a significant reduction in IS%, improved left ventricular ejection fraction (LVEF%), reduced levels of SOD1/2, (superoxide dismutase), caspase-3 and caspase 9, (apoptosis) (Zhou & Ma, 2020).

Similarly, Y-27632 (a potent ROCK1/2 inhibitor) significantly attenuated myocardial I/R in male Wistar rats, following LAD ligation and reperfusion for 5 days (Dong et al., 2019). Treatment with Y-27632 (5mg/kg) significantly reduced IS%, improved ST-segment elevation, and diminished levels of the pro-inflammatory cytokines (IL-6, TNF-αand IL-1β) ($p<0.05$). In control animals, I/R significantly increased myocardial expression of RhoA and ROCK1 from baseline, (which was attenuated by prolonged treatment with Y27632). I/R also increased phosphorylation of ERK 1/2 which is associated with ROCK activity (Dong et al., 2019; Feng et al., 2016). In animal studies of cardioprotection to date, ROCK1/ROCK2 inhibitors have been investigated, however, KD025, (a ROCK2i) has not been evaluated in myocardial I/R, although it has been investigated in cerebral I/R (Lee et al., 2014). KD025 significantly reduced cerebral infarct volume in mice, (pre-

treated PO 2 -days, 100-300mg/kg). Effects were sustained for 6hrs after I/R, suggesting that there was a large therapeutic window. Moreover, KD025 was well haemodynamically tolerated (Lee et al., 2014).

In vascular models, Yada et al (Yada et al., 2005) were amongst the first to demonstrate that hydroxyfasudil significantly attenuates 5-HT induced constriction of epicardial coronary and resistance vessels, in canines. Administration of hydroxyfasudil significantly improved coronary and microvascular blood flow in a dose dependent manner, ($p<0.05$) (Yada et al., 2005). In pre-clinical studies, ROCKi have also been studied in vascular models of in-stent restenosis and neo-intimal formation (Hsiao et al., 2016). Fasudil at doses 30mg/day significantly reduced in-stent restenosis of the carotid artery, following balloon angioplasty in a porcine model (Hsiao et al., 2016). Statins, (HMG-CoA reductase inhibitors) are understood to act synergistically with ROCKi to inhibit RhoA/ROCK activation and reduce the development of atherosclerosis (Matsumoto et al., 2013), (Rikitake & Liao, 2005). ROCKi demonstrate a multitude of vascular protective actions including vasodilatation, angiogenesis, reduced in-stent restenosis/atheroma formation and reduced vascular inflammation (Hsiao et al., 2016), (Shimokawa & Rashid, 2007), (Yada et al., 2005).

v) Summary – Is ROCK inhibition a potential target for coronary no reflow?

In summary the role of ROCK is well established in the heart, especially with regards to VSMC and hypertension (Noma et al., 2006), (Shimokawa et al., 2016). Moreover, the non-selective ROCKi Fasudil, has been well researched in preclinical studies of ischaemia/reperfusion (with regards to myocardial protection) (Huang et al., 2018a). Fasudil however, is a low potency drug with a side-effect profile that may not be desirable in STEMI patients (Kikuchi et al., 2019). Whilst Fasudil is protective in animal models, there have been no largescale clinical trials of ROCK inhibitors during STEMI. The theoretical benefits of this might be a combination of vasodilation, and reduction in inflammation and apoptosis, which may be of benefit in the NRF phenomenon. NRF is mentioned here, and not MVO, as ROCKi may have the potential to mediate both processes on this continuum of vascular injury.

Selective ROCK2 inhibitors are newer drugs and have shown better side effect profiles in complex patients such as those with GVHD (Cutler et al., 2021). As ROCK2 is implicated in VSMC contraction (Wang et al., 2009) then ROCK2 specific inhibition may be a novel future target in cardiovascular protection.

CHAPTER 2: GENERAL HYPOTHESES

The research that is undertaken is based upon the following hypotheses: Each chapter that follows outlines individual experimental objectives: -

1. ROCK 1/2 isoforms are expressed in rat myocardium and coronary circulation

2. VSMC agonists such as ET-1 will induce vasoconstriction of rat aortic rings

3. ROCK inhibitors including selective ROCK2 inhibitors will alleviate agonist mediated arterial vasoconstriction (e.g. PE, ET-1)

4. As vasospasm is a known feature of myocardial I/R injury and no reflow, selective ROCK2 inhibitors will be cardioprotective with respect to i) Infarct size% and ii) MVO%

CHAPTER 3: ROCK2 mRNA IS EXPRESSED IN HEALTHY RAT HEART & CORONARY VASCULATURE

3.1: BACKGROUND

i) Introduction

The two main ROCK isoforms, (ROCK1 and ROCK2) were first identified in 1996, following original research by Nakagawa et al (Nakagawa et al., 1996). Prior to this, there was much uncertainty surrounding different ROCK forms and downstream substrates. The above investigators performed experiments using a human platelet probe for ROCK (human P160) to screen mouse DNA libraries for different genetic sequences (Nakagawa et al., 1996). Review articles which describe ROCK expression as '*ubiquitous*' (Loirand et al., 2006), (Shimokawa & Rashid, 2007) are sourcing the work of this original paper (Nakagawa et al., 1996). Where ROCK1 was identified as abundantly expressed in all tissues studied, ROCK2 was found to be expressed more specifically in the brain, heart, lung, skeletal muscle, and placenta. ROCK2 was not noted to be highly expressed in liver or kidney (Nakagawa et al., 1996). Most of the literature refers to ROCK1 and ROCK2 as 'isoforms' of rho kinase (Loirand, 2015), (Shimokawa et al., 2016). They are protein isoforms in a functional sense, but not strictly genetic isoforms, as they reside at different loci (homologs) (Julian & Olson, 2014). Since the original Nakagawa work (Nakagawa et al., 1996), there have been very few studies of ROCK expression in healthy hearts and vasculature, despite much interest regarding the role of ROCK in the cardiovascular system and improving genetic techniques (Lu & Thum, 2019).

ii) ROCK1/2 molecular structure

Figure 6 demonstrates the similarities in the genetic structure of ROCK1 (Ch18) and ROCK2 (Ch2). The ROCK molecule is made up of three main regions including a kinase domain (N-terminal responsible for catalytic activity), a coiled-coiled domain (containing the rho binding domain for RhoGTP) and a cysteine rich domain (which may be involved in a kinase autoinhibitory loop) (Loirand, 2015). The isoforms are 90% homologous at the kinase binding domain and share an overall 65% genetic identity (Loirand, 2015). Most diversity exists at the cysteine rich domain (containing pleckstrin homology) (Julian & Olson, 2014). The kinase binding domain bares most similarity to other kinases such as those regulated by CD42 (and not RhoA) i.e. myotonic dystrophy related kinase (MRCK) (Julian & Olson, 2014). Chapter 1 has discussed the agonist-based activation of ROCK, including direct activation by LPS (Loirand, 2015), and by RhoA and RhoC at the Rho binding domain (Julian & Olson, 2014).

ROCK1 is activated via an additional auto-regulatory mechanism by cleavage of the C-terminal (caspase-3 mediated), and similarly for ROCK2 via granzyme B (Matoba et al., 2020). This occurs in relation to apoptosis, as activation results in uncontrolled VSMC contraction, and contraction of the cytoskeleton, which enables formation of cellular blebs and apoptotic bodies (rho independent mechanism) (Loirand, 2015), (Julian & Olson, 2014). RhoE is another small GTP binding molecule which can deactivate ROCK1 in the kinase binding domain and reduce stress fibre assembly

(Julian & Olson, 2014). There are therefore multiple mechanisms involved in the autoregulation of ROCK1 and ROCK2, some common to both proteins and others, more

isoform specific (Loirand, 2015).

Figure 6The molecular structure of ROCK1 and ROCK2 which share a 65% overall identity. ROCK1 resides on Ch18 whereas ROCK2 is found on Ch2. KD – kinase domain, C-C – coiled coiled domain, RBD – rho binding domain, PH – pleckstrin homology on the cysteine rich domain. Original image based on illustrations of ROCK isoforms from (Loirand, 2015), (Koch et al., 2018)

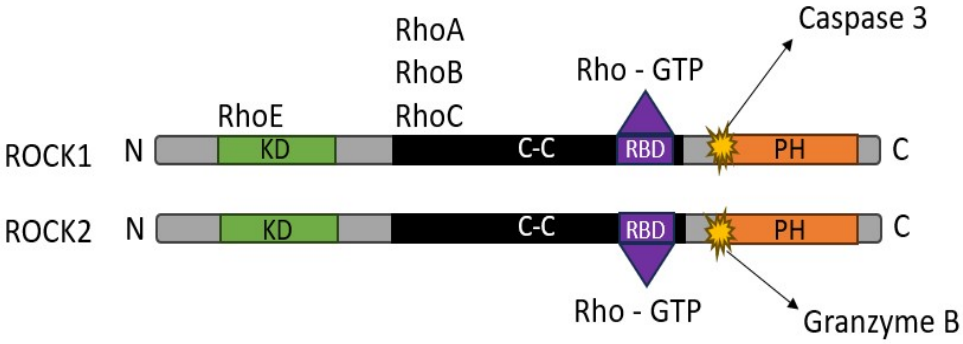

iii) ROCK1/2 isoform expression in studies of the heart

Several studies have examined ROCK1/2 protein expression in diabetic hearts using immunohistochemistry (IHC) and Western Blotting techniques (Pearson et al., 2013), (Waddingham et al., 2015). Both Pearson et al, and Waddington et al demonstrated only modest ROCK1/2 protein expression using IHC in control rat hearts. Although non-significant, there was a trend to greater ROCK2 protein expression at baseline in control animals (compared to ROCK1). In both studies, there were no significant differences in ROCK1 vs ROCK2 protein expression in diabetic animals, however a trend towards greater ROCK2 protein expression was observed (Pearson et al., 2013), (Waddingham et al., 2015). In addition, Wang et al demonstrated that both ROCK1&2 proteins are expressed in rat aortic VSMC, as part of a pivotal paper which concluded that ROCK2 is the most important isoform in VSMC contraction (Wang et al., 2009). The pathway in which ROCK2 binds to MYPT1 to phosphorylate MLC20, has been discussed in section 1.3.

Such is the importance of ROCK2 in the vasculature, that pathological polymorphisms have now been identified, such as those associated with aortic stiffening (Liao et al., 2015). Similarly, the ROCK2 isoform has been detected in vitro, in cultured coronary microvascular endothelial cells (CMECs) (Tiftik et al., 2008). In the latter experiments, CMEC cells were isolated and cultured from rat hearts perfused with Langendorff apparatus. Western blot analyses were performed to demonstrate a change in ROCK2

protein expression after 16 hours incubation with thrombin (agonist mediated pathway) (Tiftik et al., 2008).

It is important to distinguish between ROCK expression (mRNA or protein), and ROCK activity. Recent studies have detected significant changes to gene expression in the first 24 hours after myocardial infarction (Li et al., 2019) However, persistent upregulation of ROCK activity, can lead to eventual changes in gene transcription over time, and therefore changes to ROCK mRNA and protein expression. ROCK activity is best assessed by measuring changes to the phosphorylation of the proteins involved in downstream VSMC contraction such as MLC, MLCP and MYPT1 .However, in practice it is difficult to distinguish ROCK1 activity from ROCK2 activity, since both isoforms either directly or indirectly lead to phosphorylation of MLC20 (Loirand, 2015). Due to these complexities, most modern investigations have favoured haplosufficient genetic models to measure functional parameters in disease e.g., ROCK2 specific changes in pulmonary hypertension (Knipe et al., 2018).

In their paper demonstrating ROCK homology and function, Julian et al also describe the tissue specific expression of ROCK1/2, as defined by results from the TIGER database (tissue specific gene expression and regulation) (Julian & Olson, 2014). The TIGER database is a resource compiled by investigators at John Hopkins, first described in 2008, detailing human tissue specific profiles for >20,000 genes (Liu et al., 2008). An analysis of this database demonstrated a greater concentration of ROCK2 expression in the heart compared to ROCK1, this was also the case in brain tissue

(Julian & Olson, 2014). Since the early 2000's there have been advances in genetic techniques, and new single cell sequencing (ScRNA-seq) methods are considered the most accurate way of assessing gene expression in various cell types. These will be discussed below.

IV) ROCK1/2 expression in cardiovascular single cell sequencing databases (scRNA-seq)

RNA sequencing techniques (scRNA-seq) and proteomics have become novel techniques in enhancing the understanding of cardiac cell types in health and disease (Lu & Thum, 2019), (Miranda et al., 2023). There are now multiple databases containing results from scRNA-seq investigations in both human and animal hearts, which can be interrogated for any gene of choice (Tucker et al., 2020), (Chaffin et al., 2022). scRNA-seq is a complex technique which involves the digestion of the target organ with separation into its single cells/single cell nuclei components. Once single cells are captured, they must undergo reverse transcription and amplification to create RNA/DNA sequencing. These sequences are then matched to genetic information and compiled onto a database for each cell type (Paik et al., 2020). This is done on a large scale, with many databases acquiring genetic information from over 500,000 cells (Chaffin et al., 2022). As cardiomyocytes are relatively large compared to other cell types in the heart, a sequencing technique isolating single cell nuclei is often used in cardiac studies (snRNA-seq) (Paik et al., 2020).

In a recent dataset of over 600,000 nuclei from both healthy and failing human hearts, ROCK1 mRNA was expressed in 37% of normal hearts, and ROCK2 mRNA in 40% of normal hearts (Chaffin et al., 2022). Another database of post-natal mouse hearts demonstrated a greater number of pericyte/VSMC cells expressing ROCK2 in control mice (58%) vs % pericytes/VSMC cells from control mice expressing ROCK1 mRNA (50%) (Figure 7) (Hu et al., 2018).

Chapter 1 has discussed the potential importance of pericytes in MVO and the NRF phenomenon (O'Farrell et al., 2017). As 'VSMC- like' cells, it is not surprising perhaps, that ROCK has been linked to pericyte activity in the brain (Hartmann et al., 2021). In a study by Hartmann et al, pericyte constriction of brain capillary networks was found to be slower and more sustained, however this could be reversed by ROCK inhibition (Hartmann et al., 2021). Due to embryonic similarities, it is technically very challenging to differentiate pericytes from VSMC entirely (Sanjiv Kaul et al., 2023). In the same dataset demonstrated by Figure 7, there were notably, a large amount of lymphocytic endothelial cells expressing ROCK2 VS ROCK1 (Hu et al., 2018). Other datasets demonstrate that adipocytes express a substantial proportion of ROCK2 mRNA (Tucker et al., 2020). Single development of these databases, ROCK2 has been closely associated with adipogenesis (Wei et al., 2020) Whilst these techniques have provided robust quantifiable background information on the ROCK1/2 isoforms in the cells of the cardiovascular system, further studies are necessary to

visualise the localisation of ROCK1 and ROCK2 in the coronary circulation, and across different vessel types.

Figure 7. Dot plot from single nuclear RNA data base created by (Hu et al., 2018), The above database was interrogated for P10 (control) mice, (n=3, >12,000 nuclei) for ROCK1 and ROCK2 mRNAs across 14 cell type clusters. ROCK2 is notably present in pericytes and VSMC, and lymphocytic endothelial cells. ROCK1 is also present in pericytes and VSMC. Accessed at https://singlecell.broadinstitute.org/single_cell/study/SCP283.

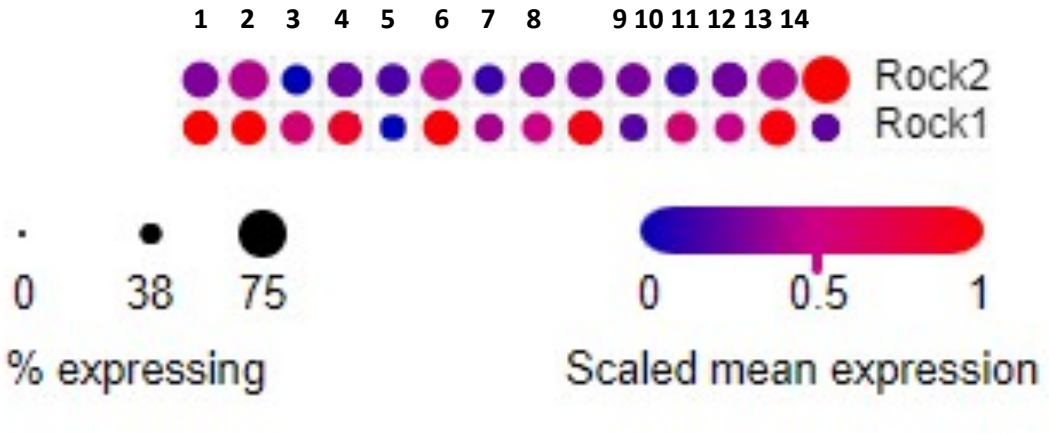

Key: 1- mature cardiomyocytes, 2 – pericytes/VSMC, 3-mature cardiomyocytes, 4 – endothelial cells, 5 – epithelial cells, 6 – developing cardiomyocytes, 7- fibroblasts, 8- endothelial cells, 9 – developing cardiomyocytes, 10-fibroblasts, 11- developing cardiomyocytes, 12 – BCs, 13 – pCM, 14 – lymphocytic endothelial cells. Scaled mean expression refers to expression relative to total expression of isoform in whole hearts.

Following these observations, experiments were designed to further investigate both ROCK protein and mRNA expression in rat hearts and coronary circulation. A set of immunohistochemistry experiments were devised to firstly, localise ROCK1/2 proteins to cardiac and coronary tissue, before considering other more complex quantitative genetic techniques.

3.2: ROCK1/2 PROTEIN LOCALISATION (IMMUNOHISTOCHEMISTRY)

i) Objectives

1. To develop an immunohistochemical staining technique for healthy rat hearts
2. To investigate the localisation of ROCK1/2 proteins in rat myocardium and coronary circulation

ii) Methods

Unless otherwise stated, methods for IHC were adapted from the following protocols (ABCAM), (Laboratories, 2022). With thanks to Miss Alice Baker (BSc student) for her help with slide preparation.

Animals

Adult male SD rats (Charles-River Laboratories) 250-300g were obtained from the central animal facility at University College London (UCL). Animal handling protocols were followed in accordance with ASPA 1986 and the UK Home Office. Experiments were conducted at the Hatter Cardiovascular Institute, University College London. Anaesthesia was undertaken with 60 mg/kg sodium pentobarbitone via intraperitoneal injection and 1000 units/ml heparin for anti-coagulation. A thoracotomy was performed to remove the heart under full surgical sedation, (confirmed by absence pedal reflexes) and this was flushed thoroughly with a syringe of H_20 to remove

erythrocytes and blood components. n=4 animals were sacrificed for these experiments.

Sectioning

Irrigated, whole heart samples were placed in 10% neutral buffered formalin for 24hrs and then transferred to 70% ethanol solution. Samples were immediately transferred to the Department of Neuro-histopathology at Queen's square, University College London, for paraffin fixation and sectioning. Slides containing tissue sections (5μM thickness) were returned to the Hatter Cardiovascular Institute.

Day one

Deparaffinization

Heart sections were rehydrated with xylene and decreasing concentrations of ethanol according to the protocol in Table 2. IHC deparaffinisation protocol, adapted from ABCAM guide to IHC-P(ABCAM), (25 minutes). Care was taken to keep slides immersed in H_20 prior to antigen retrieval, to avoid the tissue drying out.

Antigen retrieval

Heat induced antigen retrieval was performed to break methylene bridges and reveal antigenic binding sites. Sections were immersed in sodium citrate buffer (10mM, 0.05% tween 20, pH 6.0), and placed in an 850W scientific microwave on high heat for 3 minutes to achieve a temperature of 95^0C. This temperature was maintained for a further 15 minutes on a low/medium heat setting. Temperature was measured with a thermometer at regular intervals to ensure it did not exceed this target.

Table 2. IHC deparaffinisation protocol, adapted from ABCAM guide to IHC-P(ABCAM)

i)	**Xylene**	6 minutes
ii)	**Xylene: 100% Ethanol**	3 minutes
iii)	**100% Ethanol**	6 minutes
iv)	**70% Ethanol**	3 minutes
v)	**50% Ethanol**	3 minutes
vi)	**Tap H_20**	4 minutes

Immunohistochemical staining

Immunohistochemical staining was conducted with the VECTASTAIN© horseradish peroxidase ABC kit, (Vector laboratories) which uses an avidin/biotin binding complex to bind to an appropriate primary antibody. The VECTASTAIN© kit uses horseradish peroxidase (HRP) for further staining and DAB chromogen (3,3'-Di amino benzidine) to produce a brown pigment in target antigen regions. Sections were quenched with 3% hydrogen peroxide solution for 5 minutes at room temperature, to remove endogenous peroxidase activity. Due to a high amount of background staining in heart specimens, (

Figure 8. Optimisation of myocardial tissue sections for background staining was required (panel A) when sections were incubated with 5 minutes of 3% hydrogen peroxide. 30 minutes of 3% hydrogen peroxide improved

background staining but caused tissue damage (panel B). Panel C is a negative control (DAB chromogen + haematoxylin only) quenched in BLOXHALL© solution for 10 minutes, which effectively removed all background staining. All images 10X magnification.) optimisation steps were performed to evaluate different incubation periods for hydrogen peroxide, (5-30 minutes). Background staining could not be abolished without visible tissue detachment. Modifications were made to switch to a 'BLOXHALL'© endogenous blocking solution (Vector Laboratories), which is a dual peroxidase and phosphatase inactivator. In the final protocol, samples were incubated in BLOXHALL© for 10 minutes, prior to primary antibody application.

Slides were washed with PBS (10mM sodium phosphate, pH7.5, 0.9% saline) for 5 minutes and then blocked in normal goat serum solution for 20 minutes, to prevent non-specific binding. This was prepared according to the VectaStain© kit instructions as 3 drops, (150µl of normal serum) in 10mls of PBS buffer. Primary rabbit anti-ROCK1 and 2 antibodies, (ABCAM 97592 and 228000) and primary rabbit alpha smooth muscle actin (α-SMA) antibodies (ABCAM 124964), were prepared according to manufacturer's instructions in normal goat serum. An optimisation panel was performed for varying concentrations of ROCK1/2 primary antibodies, (1:500 – 1: 100) (Figure 9). Final concentrations of 1:100 were used for all three primary antibodies. Sections were incubated in primary antibody at 4^0c overnight.

Day two

The following day, slides were washed once with PBS for 5 minutes and incubated for 30 minutes with diluted biotinylated secondary antibody. After

a further 5-minute PBS wash, slides were incubated for 30 minutes with prepared VECTASTAIN© Elite ABC Reagent. The PBS wash was repeated and DAB chromogen, (ImmPACT© DAB substrate kit, Vector laboratories) was applied for 4-minutes. Slides were rinsed in H_20 for 5-minutes and immersed in haematoxylin for 4 minutes, to counterstain the cell nuclei purple. Dehydration protocol was performed in the reverse order to table.2 (i.e., steps vi-i) and slides were mounted with non -organic mounting media and allowed to dry overnight. Finally, slides were visualised under the light microscope.

For each animal, a negative control slide was included, (DAB chromogen and counterstaining only). A second slide was stained only with secondary antibody, DAB, and haematoxylin, to control for non-specific secondary antibody binding. Anti- α smooth muscle actin antibody was used as a positive marker of the tunica media layer of coronary vasculature, to enable further localisation of ROCK isoforms to the coronary circulation. In these set of experiments a separate primary antibody (not relevant to these studies) was not utilised (Figure 9). However, this could be considered in future work, as evidence of a primary antibody positive control.

iii) Results

α – Smooth muscle actin protein was expressed in the coronary vasculature (Figure 10 panel B, C). Both ROCK1 and ROCK2 proteins were localised to myocardium, however only ROCK2 protein was observed clearly in the tunica media of coronary vasculature (Figure 11, panel D, E).

Figure 8. Optimisation of myocardial tissue sections for background staining was required (panel A) when sections were incubated with 5 minutes of 3% hydrogen peroxide. 30 minutes of 3% hydrogen peroxide improved background staining but caused tissue damage (panel B). Panel C is a negative control (DAB chromogen + haematoxylin only) quenched in BLOXHALL© solution for 10 minutes, which effectively removed all background staining. All images 10X magnification.

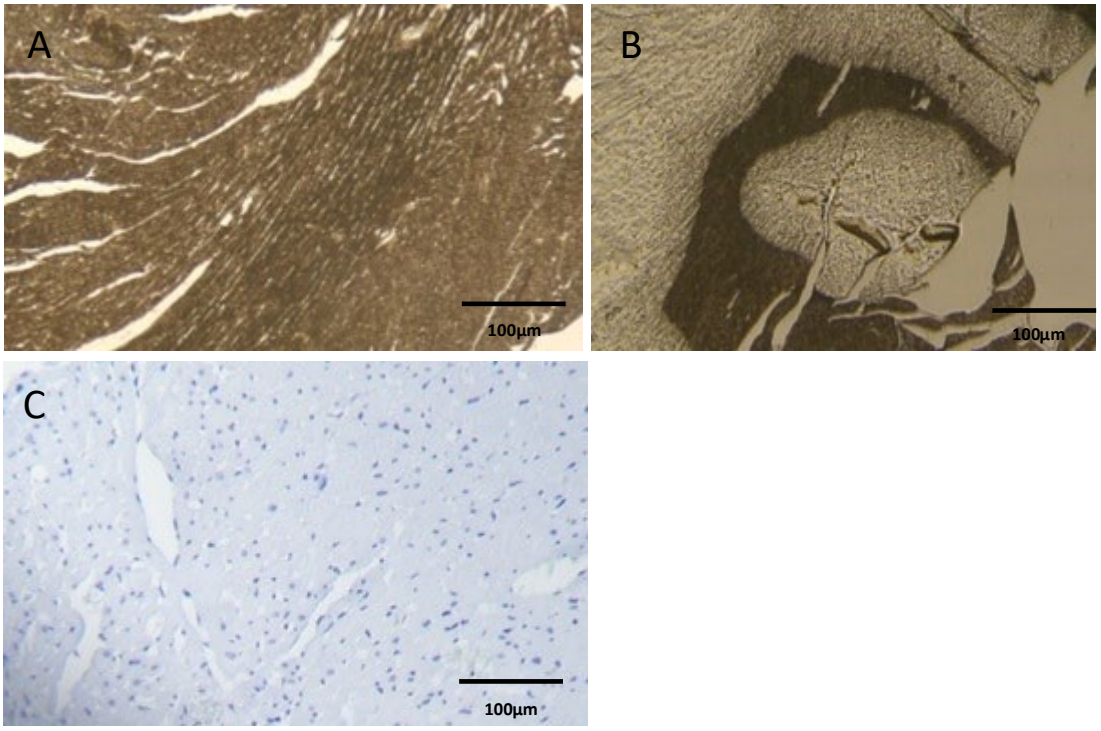

Figure 9. Antibody optimisation panel for three concentrations of ROCK1 and 2 primary antibodies (1:500, 1:200, 1:100). Antibodies were diluted accordingly in normal goat serum. Left to right: - Control panel (C) was stained with secondary antibody and DAB chromogen only, R1 – ROCK1 1:500, 1:200, 1:100, R2 – ROCK2 1:500, 1:200, 1:100.

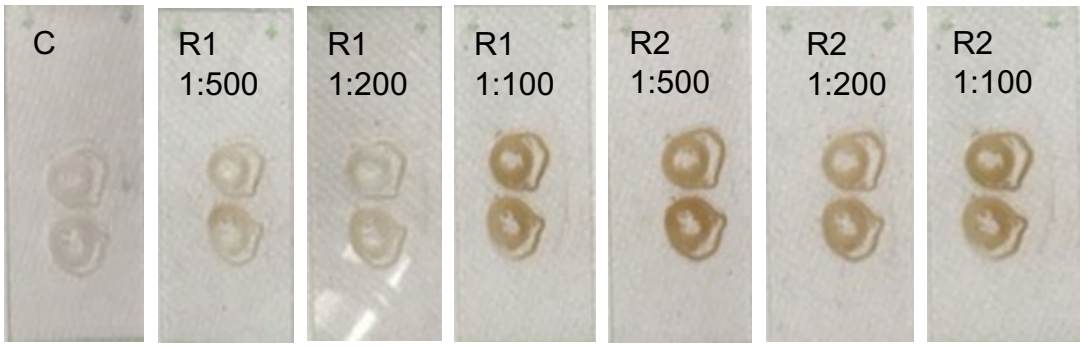

Figure 10- α-SMA expression in rat myocardium and coronary vasculature. Left to right, panel A is a primary antibody control at 20X magnification (secondary antibody, DAB chromogen and haematoxylin

applied). Panel B (10X), and panel C (40X) demonstrate coronary vessel tunica media (VSMC layer) stained with α-SMA antibody. V – vessel.

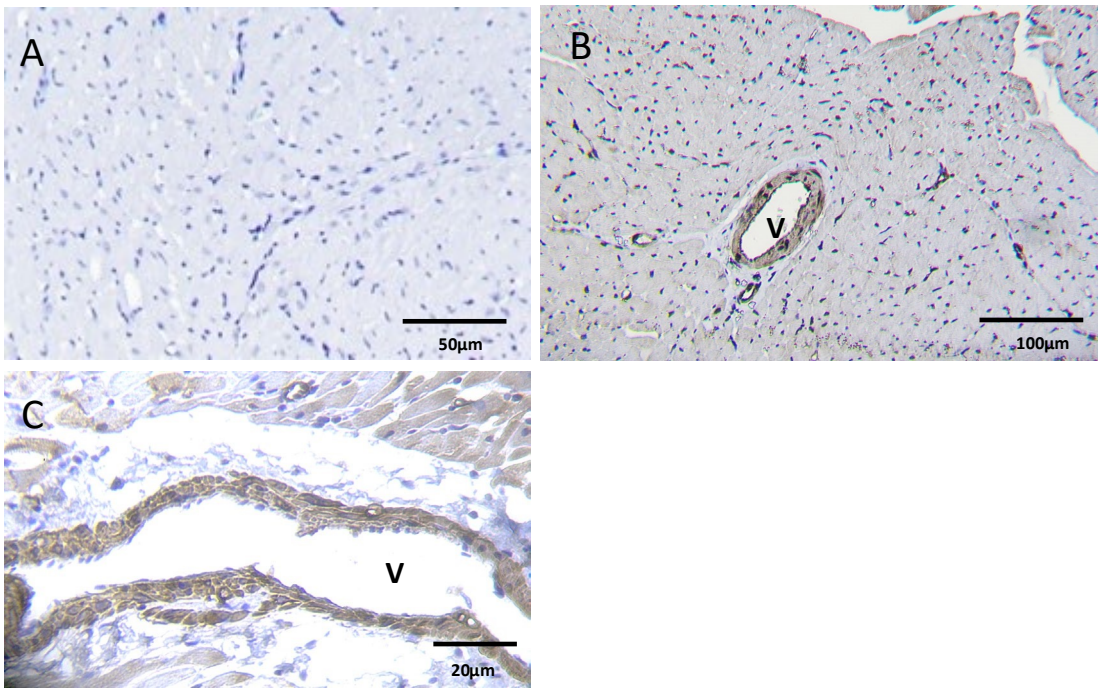

IV) Conclusions

In this initial set of qualitative experiments, the ROCK1 isoform protein was localised to healthy rat myocardium, but not the coronary vasculature, whereas the ROCK2 isoform protein was clearly localised to both healthy rat myocardium and the coronary vasculature. A more detailed and quantifiable, method of ROCK1/2 expression was next sought. An RNAscope© assay was selected to investigate ROCK1 and ROCK2 mRNA expression in healthy heart tissue.

Figure 11- ROCK1 &2 protein expression in rat myocardium and coronary vasculature. Left to right, panel A (10X) demonstrates a section stained with ROCK1 1:100 and is a view of myocardium. Panel B (20X) is also stained with ROCK1 1:100, and demonstrates a larger vessel seen in cross section with no visible ROCK1 staining. Below: - Panel C (20X) shows a section stained with ROCK2 1:100 and is a view of myocardium, panel D (20X) demonstrates a vessel in cross section and is stained with ROCK2 1:100.

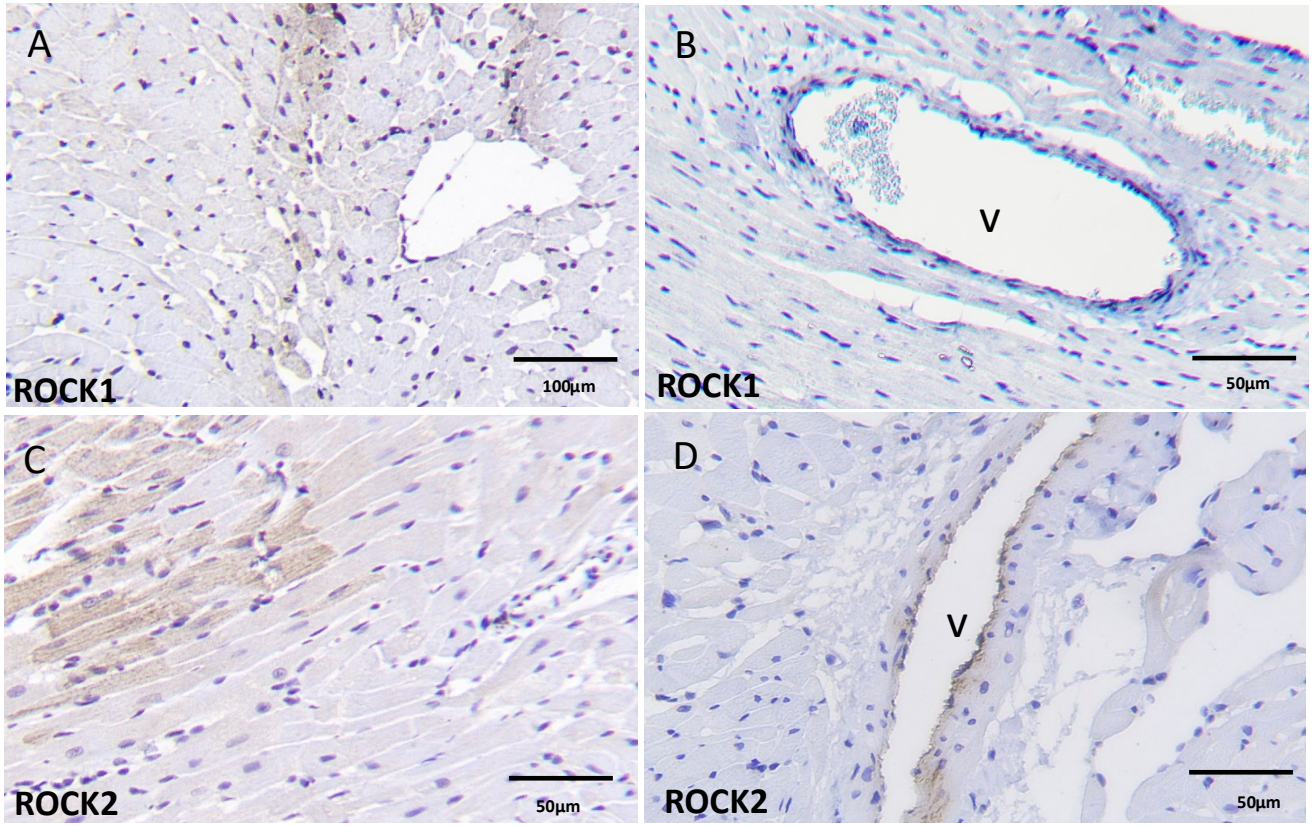

3.3: ROCK1/2 mRNA EXPRESSION (RNAscope© assay)

i) Objectives

1. To use an RNAscope© technique to visualise ROCK1/2 mRNA expression in healthy rat hearts and coronary vasculature
2. To quantify ROCK1, ROCK2 mRNA expression within the coronary vasculature using a quantifiable method of mRNA detection

ii) Methods

All methods for the RNAscope© assay were obtained from ACD Bio (Bio, 2022), unless otherwise specified. Many thanks to Dr Alhanoof Almalki for her practical advice regarding this technique. Animal sacrifice and preparation were as detailed in section 3.2. All reagents were supplied by ACD Bio unless otherwise stated. Paraffin embedded whole heart 5 μM sections from 3.2b) were used for these experiments (n=4).

Probe design

The target mRNAs were identified as ROCK1, ROCK2 and Transgelin (TAGLN or SM22α), which is a marker of differentiated VSMCs. Target probes were designed by the genetics team at ACD Bio, with accompanying control probes for cardiac and vascular tissue. Probes were designed carefully to not cross detect each ROCK isoform.

RNAscope © fluorescent multiplex assay

The RNAscope multiplex fluorescent assay is a novel technique which uses an in-situ method of hybridization (ISH) to visualise multiple RNA targets in the same sample. Specialised gene specific probes are designed to target mRNAs of interest. Probes are hybridized to their target mRNAs, and this genetic sequence is then amplified and assigned to one of three channels (C1,2,3). Different fluorophores are assigned to each channel, creating a distinct fluorescent signal which is visible under the confocal microscope.

It can be considered that using the above assay provides an unbiased approach to mRNA quantification, as it relies less heavily on user interpretation of transcripts.

Day one

Deparaffinization

Slides were carefully placed in a rack and baked in a dry oven for a period of 1 hour, to preheat. Deparaffinization was performed with serial agitations of xylene (200mls for 5 minutes x2) followed by 100% alcohol (200mls for 2 minutes x2). Care was taken not to fully submerge samples in solution and damage mRNA. Slides were carefully removed from the rack and allowed to air dry on absorbent paper.

Quenching

Dry, deparaffinized slides were quenched with 5-8 drops of RNAscope© hydrogen peroxide solution and incubated at room temperature for 10

minutes. Quenching removes background staining and endogenous peroxidase activity.

Target retrieval

A method of manual target retrieval was performed to reveal RNA binding sites (Figure 12). 300mls of RNAscope© target retrieval reagent was prepared by adding 30mls of 10x target retrieval reagent to 270mls of distilled water. This was added to a beaker covered with tin foil, and mixed and heated on a hot plate to 95^0C. The slide rack was slowly submerged into the beaker and left for 15 minutes (standard protocol). Care was taken to ensure that the solution did not exceed 95^0c, nor overboil. After 15 minutes slides were transferred to distilled water and agitated for 2 minutes. Finally, samples were washed in 100% alcohol for 2 minutes and allowed to dry fully at room temperature. A hydrophobic pen was used to carefully trace around the tissue, to form a hydrophobic barrier. Specimens were left overnight at room temperature.

Day 2

Protease plus application

At the beginning of day 2, the dry oven was turned on to 40 degrees to preheat RNA probes and reagents for the upcoming RNAscope© assay. A protease plus solution was applied to each slide to cover each section. Slides were then placed facing upwards into a hybridization oven at 40^0C for 30 minutes (standard protocol).

Figure 12: - Apparatus used during manual target retrieval for RNAscope technique

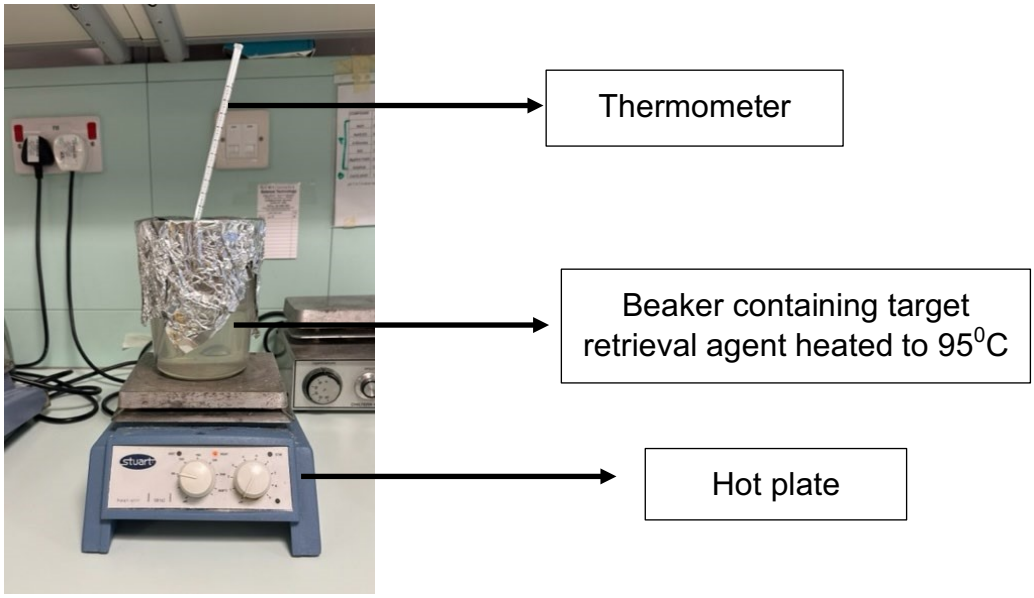

RNAscope© assay

Excess liquid was removed from slides and probe mix was applied to fully cover each heart section. For n=1, a total of four slides were used, including one slide for positive and negative control probes, and two slides each containing 3 target probes, (ROCK1, ROCK2 and Transgelin (TAGLN, VSMC). All target probes were prepared to a final concentration of 1:50. Channel 1 corresponded to ROCK1 probe, Channel 2 corresponded to TAGLN probe (VSMC) and channel 3, to the ROCK2 probe. Positive and negative control probes were prepared and applied separately to control slides. After applying the probes, slides were inserted into the hybridization oven at 40^{0}c for 2 hours, and then removed from the oven and washed in pre-prepared wash buffer, for 2 minutes at room temperature. The slides then underwent signal amplification (Table 3). Sections were covered in amplification solution,

washed in pre-prepared wash buffer, and then returned to the hybridization oven. This process was repeated three times.

Fluorophore application

Fluorophores are fluorescent labels which are assigned to each hybridization channel to produce a distinct excitation, emission wavelength and corresponding fluorescent colour, when visualised under laser microscopy. Opal© dyes 520, 570 and 690 were purchased from Akoya Biosciences and reconstituted in 75µL of DMSO according to manufacturer's instructions, (these solutions must be protected from the light to avoid decomposition). Each fluorophore was applied to the slides individually following the addition of a paired RNAscope© multiplex fluorescent solution (HRP) to bind to the amplified probe signals. This process was repeated for each channel sequentially on the same slide (Table 4).

Counterstaining & DAPI

Excess liquid was removed from the slides and 4 drops of DAPI (6-diamidino2-phenylindole) were added to each section to stain cell nuclei (30 seconds incubation time). Slides were mounted with 1-2 drops of Prolong© Gold Antifade Mountant, and a glass coverslip was applied. Slides were stored in a darkened room overnight to dry.

Table 3 RNAscope Hybridization amplification steps

STEP	SOLUTION	INCUBATION
AMPLIFICATION 1	Amp1	30 min, 40^0c
WASH	2x Wash buffer	2 min, room temperature
AMPLIFICATION 2	Amp2	30 min, 40^0c
WASH	2x Wash buffer	2 min, room temperature
AMPLIFICATION 3	Amp3	15 min, 40^0c
WASH	2x Wash buffer	2 min, room temperature

Table 4.Fluorophore application steps (multiplex protocol). C1 – green, C2 – red, C3 – clear (assigned purple)

STEP	SOLUTION	INCUBATION
C1 SIGNAL (ROCK1)	HRP-C1	15 min, 40^{0}c
WASH	2x Wash buffer	2 min, room temperature
FLUOROPHORE C1	Opal dye 520	30 min, 40^{0}c
WASH	2x Wash buffer	2 min, room temperature
BLOCKING	HRP BLOCKER	15 min, 40^{0}c
WASH	2x Wash buffer	2 min, room temperature
C2 SIGNAL (SM22α)	HRP-C2	15 min, 40^{0}c
WASH	2x Wash buffer	2 min, room temperature
FLUOROPHORE C2	Opal dye 570	30 min, 40^{0}c
WASH	2x Wash buffer	2 min, room temperature
BLOCKING	HRP BLOCKER	15 min, 40^{0}c
WASH	2x Wash buffer	2 min, room temperature
C3 SIGNAL (ROCK2)	HRP-C3	15 min, 40^{0}c
WASH	2x Wash buffer	2 min, room temperature
FLUOROPHORE C3	Opal dye 690	30 min, 40^{0}c
WASH	2x Wash buffer	2 min, room temperature
BLOCKING	HRP BLOCKER	15 min, 40^{0}c
WASH	2x Wash buffer	2 min, room temperature

Day 3

Confocal microscopy

Slides were imaged with the Leica© microsystems confocal microscope and accompanying Leica© microsystems software. The confocal laser microscope uses point to point scanning, and short wavelength continuous wave (CW) lasers to create high-intensity excitation light and illuminate a sample stained with fluorophores (Elliott, 2020). Lasers must be programmed to detect various fluorophores which are recognisable by their specific excitation emissions detailed by the fluorophore manufacturer. For example, Opal dye 520 produces a green colour, Opal dye 570 (red) and Opal dye 690 is clear. 690 was assigned a purple colour by Leica© microsystems software. Excitation wavelengths were 494nm, 550nm and 676 nm, respectively.

Halo© analysis (quantification method)

HALO© software (Indica labs) is an artificial intelligence (AI) platform used to quantify gene expression and multiplex ISH, on a cell-to-cell basis. This platform has been used in published RNAscope© studies (Khatib et al., 2022) to quantify fluorescently labelled RNA probes, by producing an automated 'H+ score.' H+ score takes account of both the number of probes present per cell (RNA transcripts) and the intensity of each signal. This model was not previously set up at our laboratory and was installed with the help of Indica labs, software tutorials and guided remote sessions.

Channel assignment

Images were saved as individual channel files from Leica microsystems and imported into the Halo software platform. Once opened in HALO©, single channel images were fused together. For each sample of n=4, five different fields of view were obtained for each analysis. Firstly, each individual image was allocated four channels, corresponding to each probe of interest: - e.g. turquoise (DAPI), green (ROCK1), purple (ROCK2) and red (VSMC) (Figure 15).

Parameter setting (optimisation)

Prior to running an automated analysis, the assay must be validated by screening 5 fields of view and performing an auto-tuning optimisation process (Figure 13). This begins with a review of the sensitivity settings and minimum intensity thresholds for the DAPI probe (cell nuclei). Cell detection parameters utilized the HALO AI™ nuclear segmentation algorithm `AI Default' for the DAPI channel. Real time auto-tuning must be performed until HALO has correctly identified all cell nuclei present, this is important as RNA counts are analysed as a % of total cells. Next the auto-tuning process is performed for each probe and individual channel. For these analyses, the default settings for ROCK1/ROCK2 RNA minimum size and spot intensity thresholds were adhered to. This ensures that any fluorescent pigmentation identified on the screen corresponds correctly to one RNA transcript and that regions of autofluorescence are not included in the analysis. Once the validation slides have been completed then these settings are saved and applied to each analysis (Figure 13).

Figure 13.Image processing steps in HALO© software (L-R). The first image (L) demonstrates cell nuclei detection via DAPI (turquoise). In the middle image, an autotuning window is open to optimise the detection of all ROCK1, ROCK2 and VSMC FISH probes. The image on the right demonstrates the original fused image in the absence of DAPI channel and depicts a coronary vessel in cross section (red) surrounding by myocardium containing ROCK1 (green) and ROCK2 (purple), probes. Settings were programmed to detect mRNA within the whole cell.

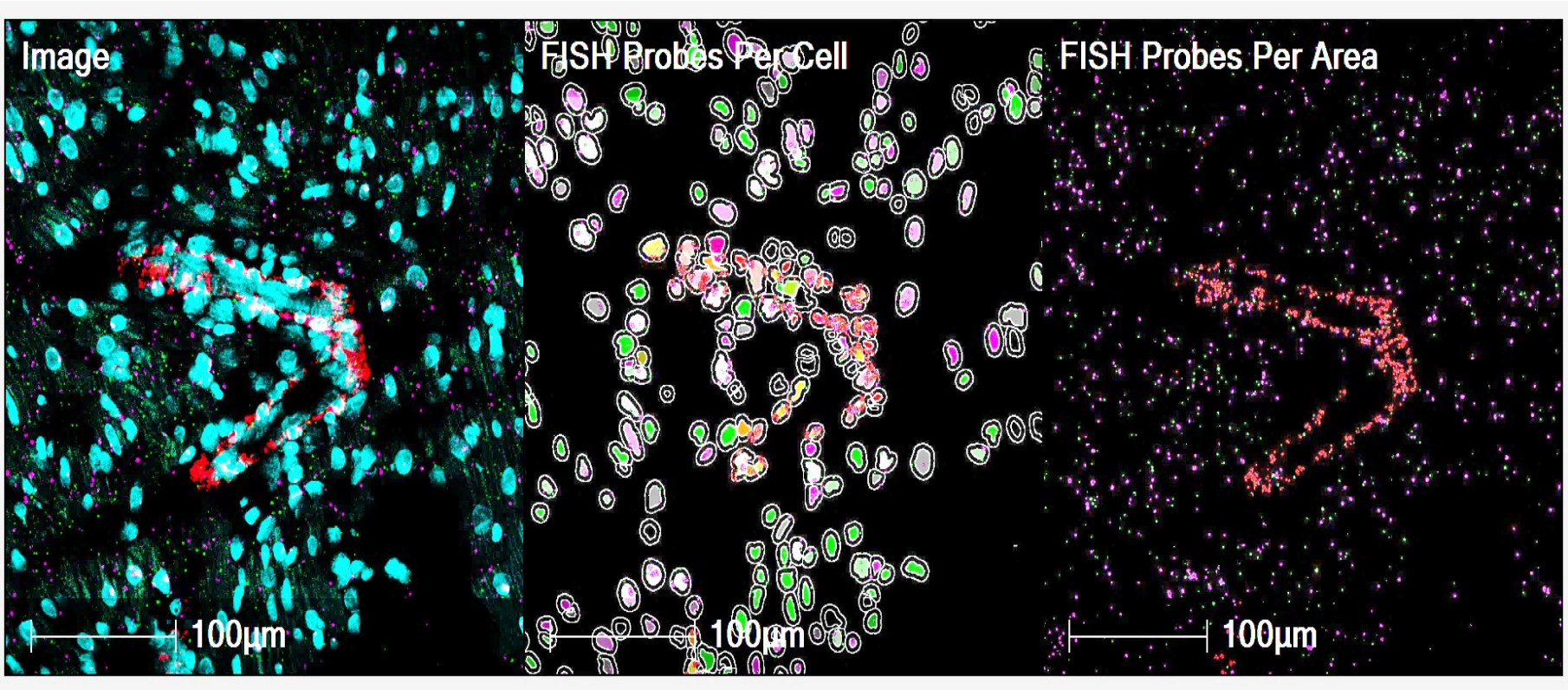

Outputs and quantification methods

Running a Halo© analysis produces multiple outputs including, total cell count, total probe dot count (RNA transcripts), average dots per cell, % positive cells for a single probe, % cells which are dual or triple probe positive, and a quantifiable H+ score from 0-400 for each probe of interest. There are two aspects in calculating the quantifiable H+ score. The first is the programme's ability to auto-detect signal intensity (based upon control minimum signal intensity) and dot size (again based upon controls). When these parameters have been standardised, Halo automatically counts RNA transcripts per cell and places them into one of 5 bins (Table 5). This is distinct from other semi quantifiable programmes, where the signal intensity is not considered and is not automatically calculated. Results can therefore be expressed as a standard semi-quantifiable score histogram or using the more comprehensive full H+ score.

Table 5 - HALO© scoring protocol based on number RNA transcripts per cell

BIN (SCORE)	CRITERA
0+	No staining or <1 dot per 10 cells
1+	1-3 dots per cell
2+	4-9 dots per cell
3+	10-15 dots per cell (<10% clusters)
4+	>15 dots per cell (>10% clusters)

All data was quantified according to ACD recommendations (Labs, 2022)

iii) Results - Qualitative analysis

Multiplex positive control probes confirmed the presence of detectable mRNA. The negative control probe confirmed no significant false positive staining or autofluorescence (Figure 14). On general inspection, the C2 probe (red, TAGLN) had successfully stained the tunica media of coronary vasculature (Figure 15, Figure 16). Figure 15 demonstrates that when ROCK1 and ROCK2 channels were viewed separately to DAPI and VSMC, there appeared to be a greater concentration of ROCK2 (purple) within the arterial vessel wall, compared to ROCK1 (green). Both ROCK2 and ROCK1 mRNA could be visualised in the myocardium.

Figure 14. RNA scope control panels. Panel A shows negative control slides with dapB probe (universal negative). Panel B demonstrates triplex positive control probes, (Polr2a – green, PPIB – red, UBC – purple). Image magnification 40X.

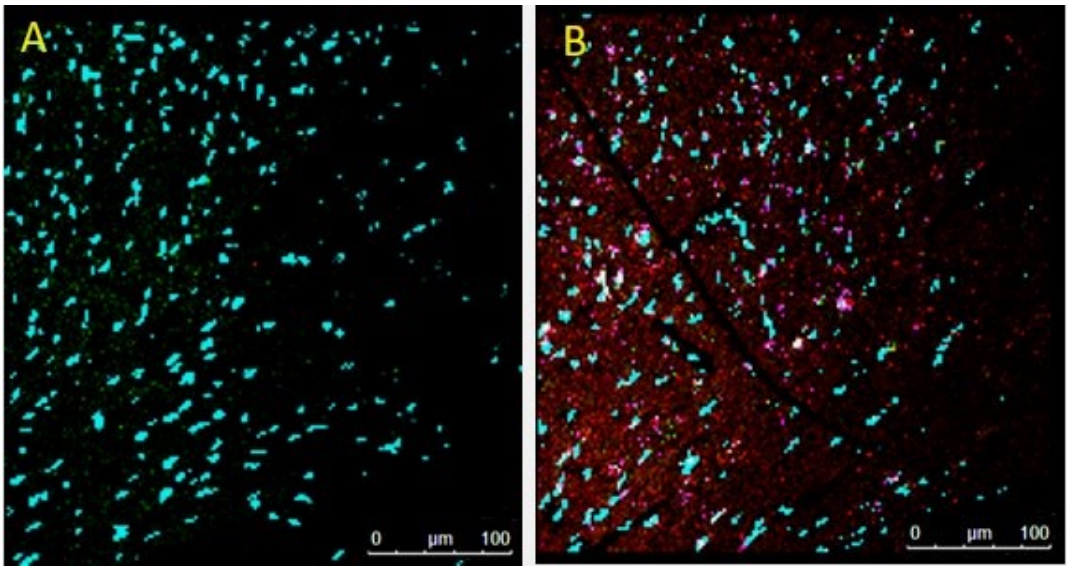

Figure 15. Single channel RNAscope analysis. Images were split across four channels, DAPI (turquoise), VSMC (red), ROCK1 (green) and ROCK2 (purple). A smaller coronary vessel is shown in cross section, with adjacent capillary. Image magnification 40X.

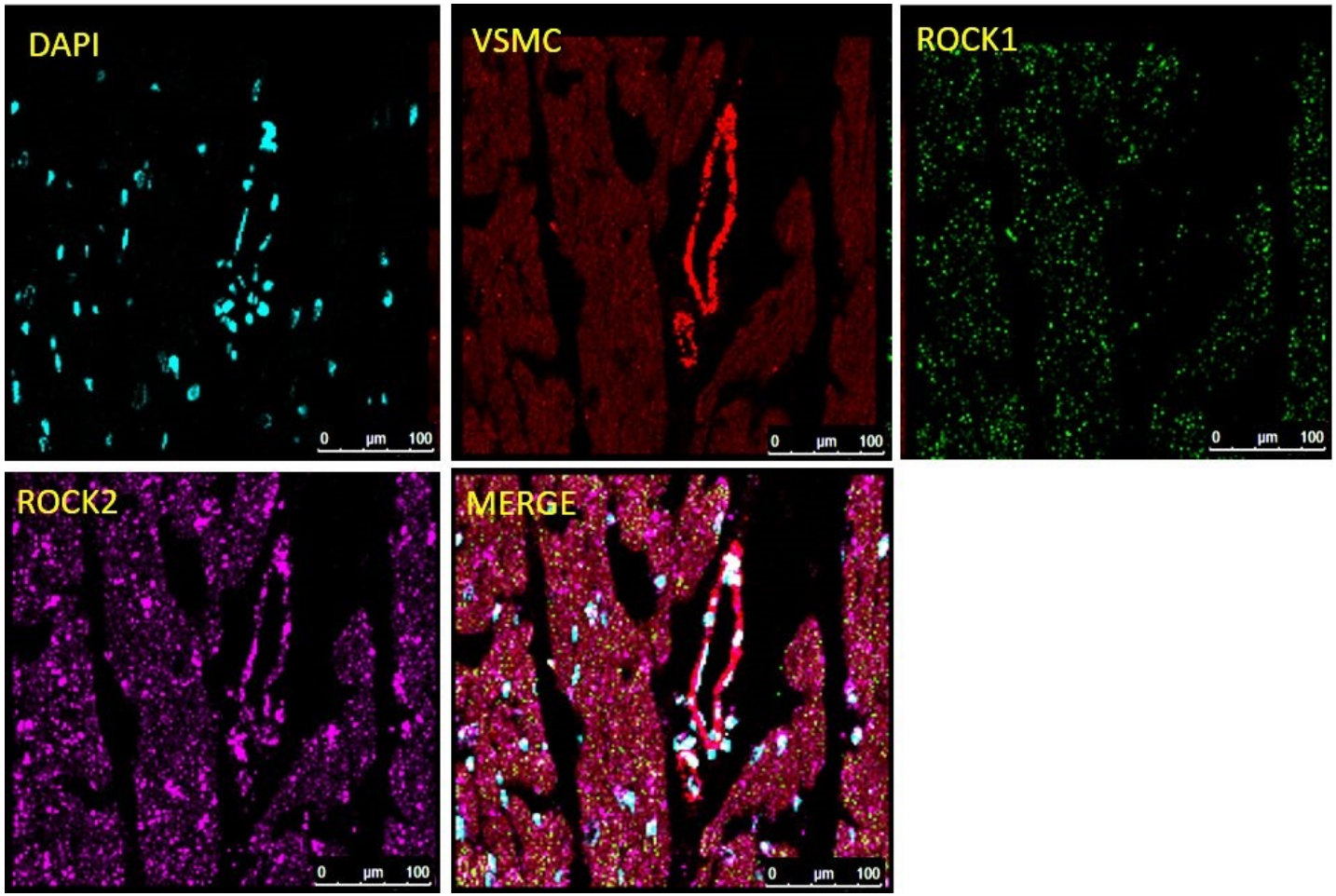

Figure 16. RNAscope imaging of whole hearts and coronary vessels. Panel A is a view of a large coronary arterial vessel stained for VSMC (red) and cell nuclei stained with DAPI (turquoise). Panel B shows the same field of view with visible ROCK1 (green) and ROCK2 (purple probes) present in the VSMC tunica media. The ROCK2 probe appears to have stained the tunica media and the ROCK1 appears to have stained the endothelium. V – vessel lumen, M – myocardium. Magnification 40X.

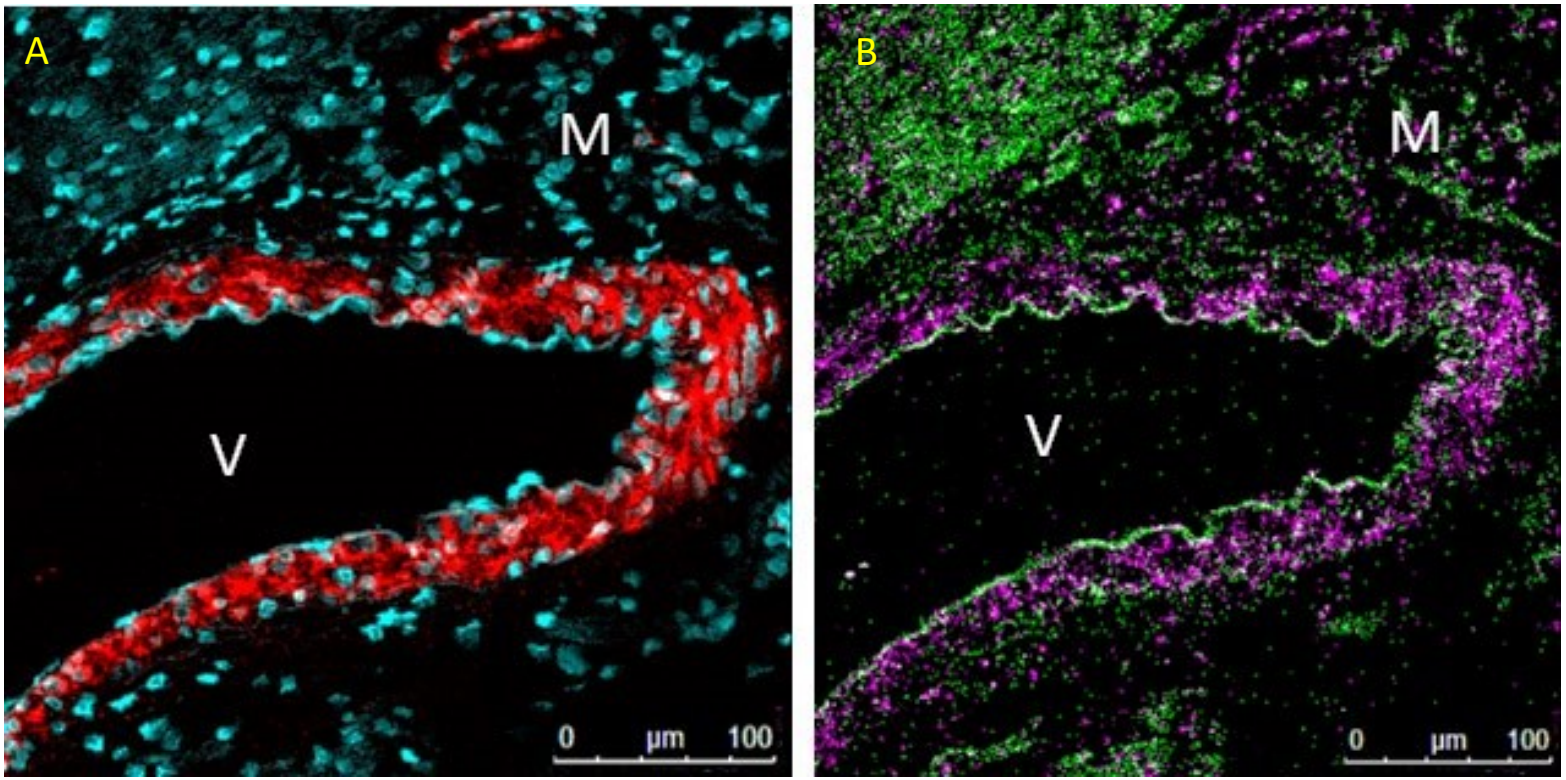

Quantitative analysis – whole hearts (n=4)

A quantitative analysis was performed, to measure ROCK1, and ROCK2 mRNA in whole heart sections. 20 images were analysed in total (n=4, each with 5 fields of view). % ROCK1 and % ROCK2 positive cells, and respective H+ scores were compared using a paired student's t-test (data passed normal distribution testing) (Table 6 & Figure 17). There was greater expression of ROCK2 vs ROCK1 mRNA in whole hearts as measured by both % cells positive and Halo© H+ score, (*p=0.0008, p=0.0032,* respectively.)

VSMC wall thickness (µm) (n=4)

A second analysis was performed to measure the wall thickness of the tunica media of the 18 coronary vessels seen across n=4 samples. Wall thickness was measured to scale, using a ruler tool across the widest part of the vessel wall (Figure 18a). Vessel wall thickness diameter ranged from 4-43µm. Figure 18 below (panel A) is a single channel image which, demonstrates one of the larger vessel's being measured to scale. The greatest number of vessels measured had a wall thickness of <10µm, however panel B demonstrates that a range of coronary vessel sizes were included in the analysis.

Table 6– HALO quantitative analysis of whole heart sections

CELLS (% WHOLE HEARTS)	n=1	n=2	n=3	n=4	MEAN ±SEM
% ROCK1 positive	45	55	51	39	48±-4
% ROCK1 0+	55	45	49	51	53±4
% ROCK1 1+	33	45	42	37	40±3
% ROCK1 2+	10	7	8	2	7±2
% ROCK1 3+	2	2	1	0	1±0
% ROCK1 4+	1*	0	0	0	0±0
ROCK1 H+ score	61	68	61	40	58±6
%ROCK2 positive	94	94	91	91	93±-1
%ROCK2 0+	6	6	8	9	7±1
%ROCK2 1+	9	31	32	29	25±5
%ROCK2 2+	29	43	38	40	37±3
%ROCK2 3+	20	9	10	14	13±2
%ROCK2 4+	37	10	11	8	16±7
ROCK2 H+ score	272	187	184	183	185±1
%VSMC positive	14	17	17	13	15±1
VSMC H+ score	41	54	54	35	46±5

Figure 17.The frequency and distribution of ROCK1 and ROCK2 isoforms in whole heart sections (panels A-D). Panel A compares % cells positive for ROCK1 and ROCK2 (p=0.0008), panels B and C are histograms demonstrating mRNA bin frequency in whole hearts. Panel D compares final Halo H+ scores for ROCK1 and ROCK2 (p=0.0032).

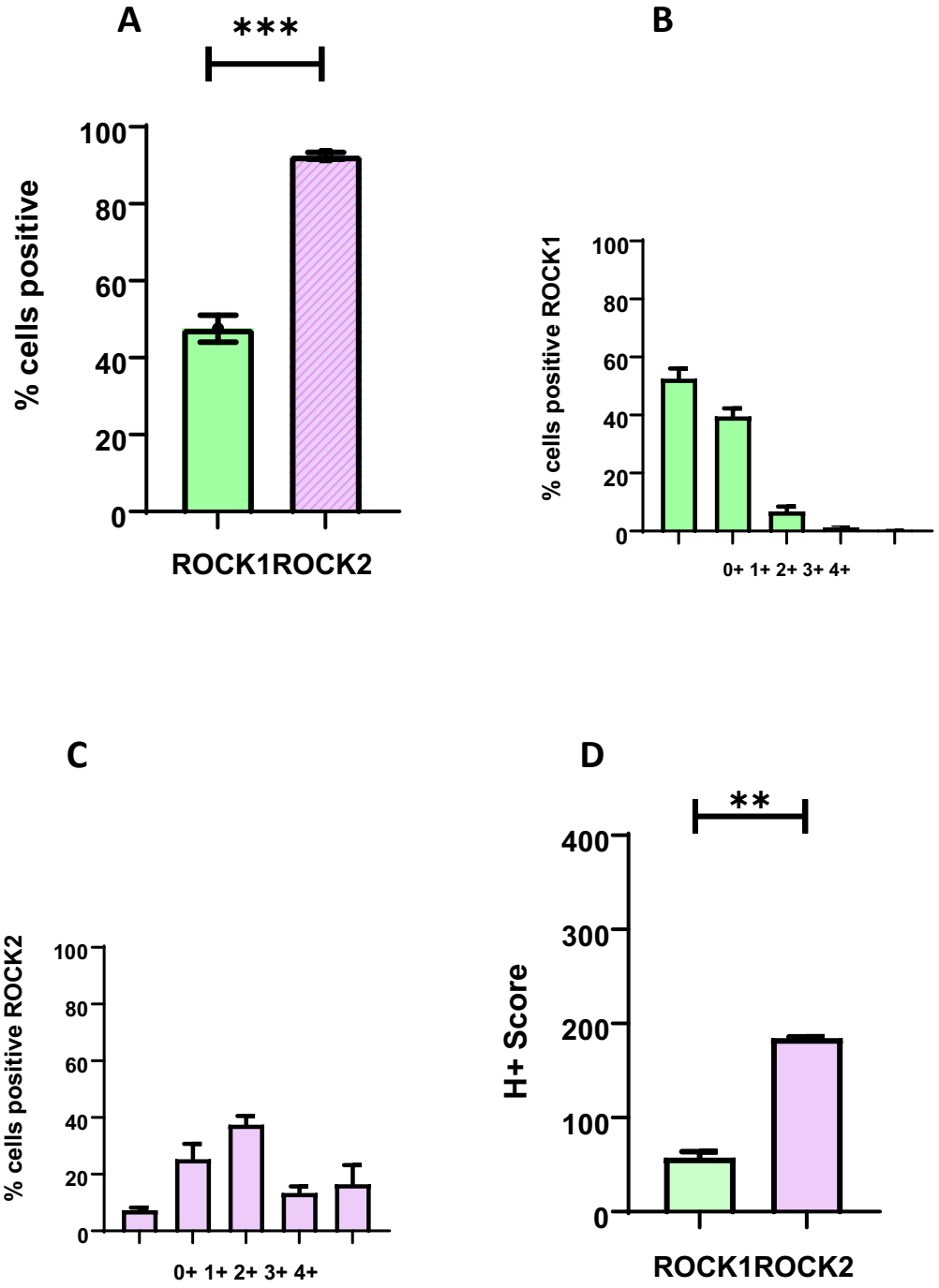

Figure 18: An analysis of coronary vessel wall thickness. Panel A demonstrates an arterial vessel, (red, TAGLN) measured by VSMC wall thickness (μm). Panel B: - a range of coronary vessels analysed from 4-43 (μm).

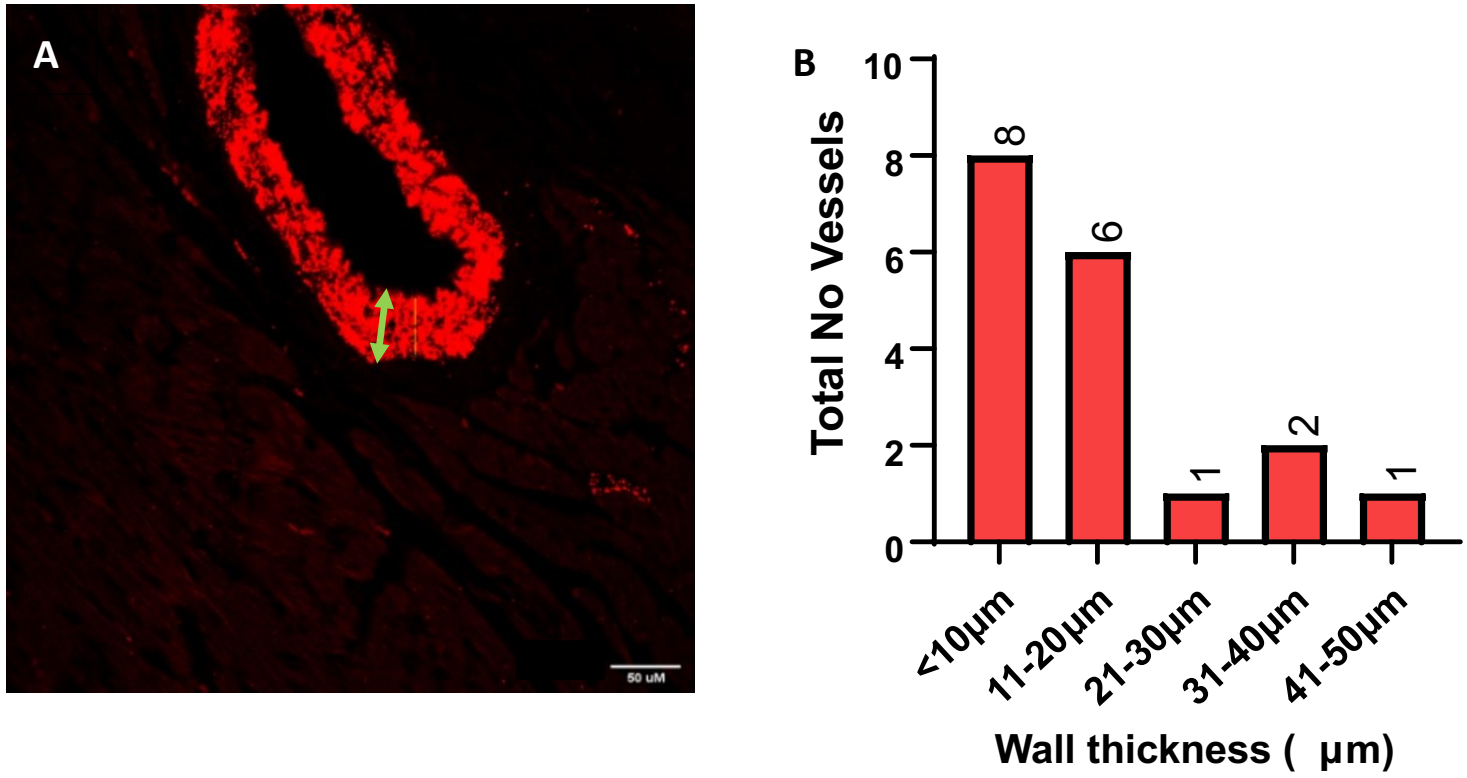

Co-expression of ROCK1/2 in VSMC

A sub-analysis was performed using VSMC areas only, depicted by VSMC probe positivity (vessels were traced around freehand and then automated analysis performed for these areas). There were a greater number of ROCK2 positive VSMC compared to ROCK1 positive VSMC, (*p=0.03*). The VSMC H+ score has a high SEM (Table 7, row 4), which can be explained by the fact that different sized coronary vessels were analysed in each field of view. To adjust for this, VSMC ROCK1 and ROCK2 H+ scores were normalised as a % of the total VSMC H+ score, for each field of view. VSMC ROCK2 H+ score was greater than VSMC ROCK1 H+ score (*p=0.03*). This suggests that there is a greater expression of ROCK2 mRNA in the tunica media of coronary vasculature, compared to ROCK1 (Figure 19). There was a greater ROCK2:ROCK1 ratio (1.9) in whole hearts, compared to a ROCK2:ROCK1 ratio of 1.3 in VSMC (*p=0.04*). Therefore, the relative proportion of ROCK1 was greater in VSMC compared to whole hearts (Figure 19c).

iv) Conclusions

This RNAscope analysis has demonstrated that both ROCK1 and ROCK2 mRNAs are expressed in healthy rat heart tissue and coronary vasculature VSMC. Both on qualitative inspection and quantitative analysis of 20 images (n=4) using the AI program HALO©, it has been demonstrated that there is greater expression of ROCK2 mRNA in both whole heart sections and VSMCs compared to ROCK1.

However, considering % cells positive, ROCK2:ROCK1 ratio is smaller in VSMC compared to whole hearts, indicating that there is a greater relative proportion of ROCK1 in VSMC compared to whole hearts.

Table 7– Co-expression of ROCK1/2 mRNA (as % of VSMC)

CELLS	n=1	n=2	n=3	n=4	MEAN±SEM
% VSMC ROCK1 positive	74	61	76	88	75±5
%VSMC ROCK2 positive	99	93	90	97	94±2
VSMC H+ score	319	280	275	327	300±13
VSMC ROCK1 H+ score (as % VSMC H+ score)	32	28	40	51	38±5
VSMC ROCK2 H+ score (as % VSMC H+ score)	102	68	64	82	79±9

Figure 19- ROCK1,2 mRNA expression in VSMC. Panel A demonstrates that there is a greater % of ROCK2 +ve VSMC compared to ROCK1 (p=0.03). Panel B – ROCK2 VSMC H+ score is greater than ROCK1 VSMC H+ score (p=0.03). Panel C – ROCK2:ROCK 1 ratio for % cells positive, is greater in whole hearts than in VSMC (p=0.04).

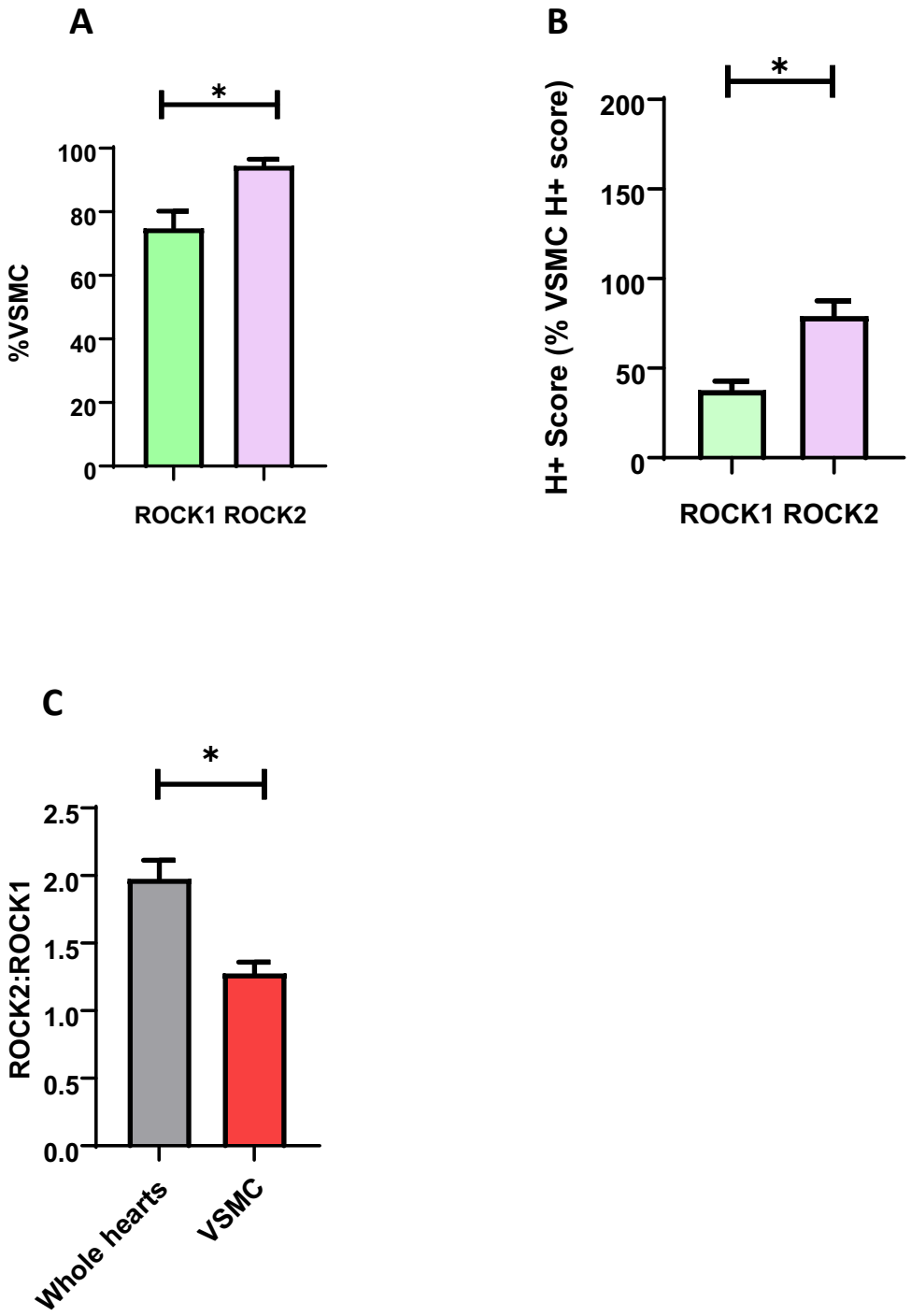

3.4 CHAPTER DISCUSSION

The findings that ROCK2 mRNA and protein are present in the heart and coronary vasculature, are supported by previous studies (as detected by Northern blotting and analysis of the TIGER genetic tissue database) (Nakagawa et al., 1996), (Julian & Olson, 2014). Moreover, the latter source as quoted by Julian et al, found that ROCK2 was increased compared to ROCK1 in cardiac tissue, in similar proportions to these results (Julian & Olson, 2014), (Liu et al., 2008). However, there appears to greater variation of results when considering ROCK1/2 RNA expression in the heart in ScRNA-Seq/SnRNA-Seq databases (Chaffin et al., 2022), (Hu et al., 2018). In the study by Chaffin et al(Chaffin et al., 2022) , ROCK isoform ratio appeared more balanced in human control hearts, however this technique investigated nuclear RNA, whereas ROCK2 mRNA may also reside in the cytoplasm, therefore potentially underestimating total ROCK2 expression (Julian & Olson, 2014), (Chaffin et al., 2022).

In a similar Sn-RNA-Seq study of murine hearts, a greater % of VSMC/Pericytes were found to express ROCK2 compared to ROCK1 (Figure 7) therefore it is likely that there is species dependent variation (Hu et al., 2018). The marker of VSMC for this work was TAGLN (αSMA-22). As TAGLN is also expressed by pericytes in scRNA-seq studies, it is possible that some pericytes have also been analysed by the VSMC probe (Hu et al., 2018). In practice it is difficult to find markers which separate VSMC from pericytes (Sanjiv Kaul et al., 2023). ROCK1/2 expression in pericytes is useful information however, given that pericytes

have a likely role in MVO and the NRF phenomenon (Sanjiv Kaul et al., 2023).

Figure 18 has demonstrated that 18 coronary vessels were identified in the RNAscope© experiments with a range of different wall thickness measurements. In practice, it is more challenging to identify these vessels, in the same way as the human coronary circulation, due to much less published literature on the wall diameter size of rodent coronary vasculature. Given the range expressed, it is likely that arterioles and resistance vessels were included in this analysis, in addition to some branch epicardial coronary vessels. It is also difficult to exclude larger coronary veins (containing a thin VSMC layer) from this analysis, however vessels were selected by the presence of an elastic lamina (Figure 16). A high-resolution 3D study of the coronary circulation in mice, demonstrated a comparable wall-thickness range of 13-37μm in the main coronary tree (Bonanno et al., 2015), however these measurements are likely to be smaller compared to rats. Wall thickness was chosen above vessel diameter, due to vessels fixed in cross-section which may have provided misleading measurements. However, in future work, vessel diameter would strengthen this analysis to correctly identify the subdivisions of the coronary tree.

Considering the VSMC-only analysis, ROCK1/2 H+ score was adjusted for total vascular H+ score for each sample n number. This should have normalised ROCK1/2 expression for different vessel sizes across the samples.

These results showed that ROCK2 remained the most abundant isoform in VSMC. Moreover, ROCK2 was observed visually in both smaller and larger coronary vessels whereas ROCK1 was not (Figure 15).

The IHC results have provided information regarding the localisation of ROCK1 and ROCK2 protein, however they have the limitations of qualitative results. RNAscope© was selected to provide a more advanced technique of ROCK1/2 mRNA expression, localised to VSMC, which was quantified using the AI program HALO©. This is a more robust method of quantifying RNA expression as it removes human error from RNA transcript counting and improves user bias. In addition, the technique can provide information on mRNA localisation and cellular co-expression. Multiplex technique is possible for more than one gene of interest, and the assay is highly sensitive and specific (Atout et al., 2022). Considering RNAscope© limitations, some of the optimisation processes are, however, still mildly subjective (e.g. probe/cell auto-tuning) and protocols must be kept constant across all samples to maintain uniformity. As ROCK2 has been localised to the heart and coronary circulation, it is therefore a potential target in cardioprotection and MVO.

As these experiments using RNAScope do not provide evidence for the role of ROCK activity in arterial vasospasm, this will be examined in the next chapter (4) by investigating the vasoactive properties of ROCK inhibitors.

CHAPTER 4: FASUDIL (A ROCK 1,2 INHIBITOR) INDUCES VASORELAXATION AND ATTENUATES MVO IN VIVO

4.1 : BACKGROUND

i) The evolution of ROCK inhibition – Fasudil (ROCK1 & 2 inhibitor)

Fasudil (manufactured as Fasudil Hydrochloride) was first produced in Japan in 1995 and used to treat the vasospasm associated with intra-cerebral haemorrhage (Feng et al., 2016), (Shimokawa et al., 2016). ROCKi were developed from a larger reservoir of protein kinase inhibitors which were first recognised by the Japanese scientist Hidaka in 1984 (Hidaka et al., 1984) . Japan is currently the only country which has licenced the ROCKi, Fasudil for cerebral vasospasm in humans (in addition to Ripasudil for glaucoma), (Liao et al., 2007). Despite a lack of licenced clinical applications outside of the preclinical research domain, Fasudil remains the ‘gold-standard’ in biochemical assessments of ROCK inhibition, both ex vivo and in vivo. Many author’s challenge this traditionally held status, as there are now over 170 ROCK inhibitors available on the market, with superior biochemical and pharmacological properties (Feng et al., 2016).

Nevertheless, Fasudil represents the most common starting point for many researchers in studies of ROCK inhibition, as the drug is well tested and readily available (Feng et al., 2016). It is particularly useful for investigating vasodilation in models of hypertension (Kawarazaki & Fujita, 2021), and other aetiologies where vasoconstriction and intimal

remodelling are problematic e.g., pulmonary hypertension (Abedi et al., 2023). Fasudil (compound 28/HA-1077) as described by Feng et al (Feng et al., 2016)) is an isoquinolone based derivative (fig.20) which is actively metabolised to another well-known ROCK inhibitor, known as hydroxyfasudil. Fasudil is both a ROCK1 and ROCK2 inhibitor with Ki of 0.33μM for ROCK1 and 1.9μM for ROCK2 (Feng et al., 2016), (Shimokawa et al., 2016), (Liao et al., 2007).

Fasudil is non-selective for ROCK and inhibits other protein kinases including protein kinase C (PKC), protein kinase A (PKA) and myosin light chain kinase (MLCK), it also a calcium channel antagonist (Feng et al., 2016), (Hidaka et al., 1984). The active metabolite of Fasudil, hydroxyfasudil, is also nonselective for ROCK1/2 (Liao et al., 2007). This variety of pharmacological actions is responsible for a wide range of side-effects, which include hypotension, deranged liver function and white cell depletion (Liao et al., 2007). Although hypotension was not significant in the original clinical study which investigated the effects of Fasudil in cerebral SAH, a smaller study in stable patients undergoing coronary intervention, demonstrated that patients receiving intra-coronary administration of the drug, subsequently required inotropic support (Kikuchi et al., 2019; Shibuya et al., 1990).

Because of the observations that poor ROCK selectivity is undesirable, researchers aimed to develop, firstly, selective ROCK inhibitors (without affinity for other PKC like targets) and then secondly, ROCK2 specific inhibitors (Lorenz et al., 2021). To achieve this, further research was required concerning the mechanism of action, of these drugs.

ii) Mechanism of ROCK inhibition

Feng et al report that most ROCKi are type I ATP competitive kinase inhibitors (Feng et al., 2016). These mechanistic insights were originally derived from the original protein kinase work by Hidaka et al (Hidaka et al., 1984). Kinase inhibitor type molecules were found to mimic adenine residues in the ATP binding region of the kinase, therefore directly competing with them and inhibiting the future transfer of Y-phosphate onto its serine/threonine targets (Lorenz et al., 2021). This process can be better visualised in studies of crystal formation (Lorenz et al., 2021). ROCK inhibitors bind to ATP binding sites on ROCK in the previously discussed kinase domain (depicted by figure 6). Original PKs were also vasodilators, due to their antagonism of calmodulin (involved in the calcium dependent pathway of VSMC contraction) (Liao et al., 2007). ROCK inhibitors such as Fasudil, are ATP competitors as per these original studies, and they subsequently prevent ROCK from phosphorylating SER/THR residues on the rho binding site (MYPT1) of the enzyme MLCP (Loirand, 2015).

As described previously in chapter 1, MLCP is part of the calcium independent pathway of VSMC contraction (thus helping to sensitize the calcium response), where MLCP leads to VSMC relaxation, unless this is inhibited by activated RhoA/ROCK. ROCK inhibitors, release this inhibition of relaxation by ROCK, therefore promoting the inactive form of MLC (the end effector of contraction in VSMC) and VSMC relaxation (see fig.5) (Shimokawa et al., 2016), (Kawarazaki & Fujita, 2021), (Loirand, 2015). ROCKi induced vasodilation is multi-factorial, as these drugs also prevent the inhibition of

eNOS (Shimokawa & Rashid, 2007), thus increasing NO levels. Increased NO levels leads to vasorelaxation by increasing amounts of cGMP within the VSMC. ROCKi therefore act on both the endothelium and the VSMC to induce vascular

protection (Liao et al., 2007).

Figure 20 The biochemical structure of Fasudil Hydrochloride (isoquinolone derivative). IC_{50} 1.9μM ROCK2. Re-drawn from (Feng et al., 2016).

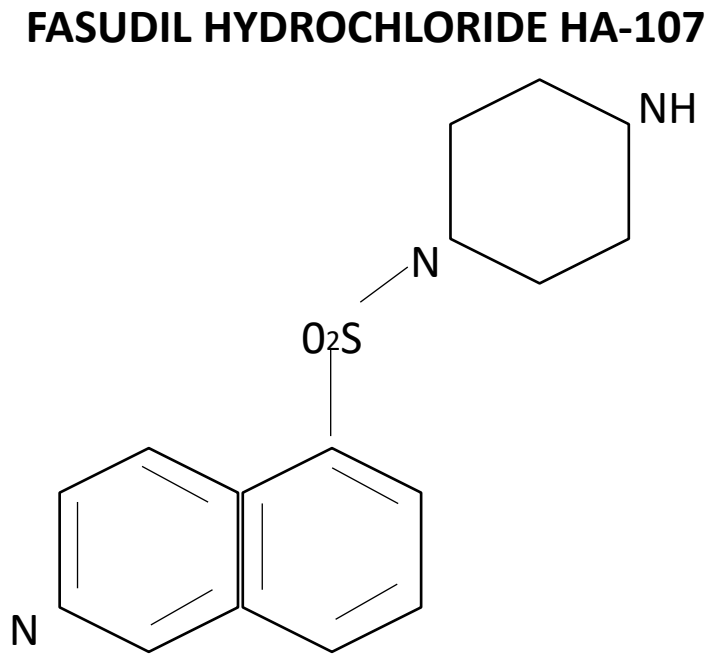

iii) Fasudil in preclinical models of Ischaemia/reperfusion

Fasudil has been tested in animal studies in a wide range of cardiovascular diseases including hypertension (Yuan et al., 2019), atherosclerosis (Matsumoto et al., 2013), heart failure (Santos et al., 2019) and ischaemia/reperfusion (Huang et al., 2018b). Chapter 1 has already discussed the important meta-analysis by Huang et al (Huang et al., 2018b), which analysed the effects of the drug (following myocardial ischaemia/reperfusion) in 19 pre-clinical studies, with total n=400 (Huang et al., 2018b). To recap, Fasudil administered prior to reperfusion, was associated with improvements in infarct size (Wu et al., 2014), cardiac enzymes (Jiang et al., 2013), (Zhang et al., 2018), and ST- elevation resolution (Huang et al., 2018b) in animals undergoing myocardial I/R. Both in vivo and ex vivo studies (Langendorff) were included in the paper, with the latter technique enabling the further analysis of coronary blood flow (CBF) (Huang et al., 2018b), (Hamid et al., 2007).

Huang et al concluded that the observed cardioprotection induced by Fasudil, may have been secondary to i) reduction of ROS and apoptosis, 2) an increase in NO mediated vasodilation and 3) upregulation of PI3K/AKT (i.e. The RISK pathway) (Huang et al., 2018b), (Wu et al., 2014), (Hamid et al., 2007). Moreover, the protective effects of Fasudil can be reversed by Wortmannin in another study (Hamid et al., 2007). A more recent study in 2022 by Gao et al (Gao et al., 2022) linked remote ischaemic conditioning (RIC) to the inhibition of ROCK, via autophagy and the upregulation of the RISK pathway. In this study, 60 male SD rats underwent myocardial ischaemia-

reperfusion and were treated with either Fasudil, RIC or combination therapy. There was no extra protection conferred from combination therapy (RIC + Fasudil), and treatments were individually attenuated by Wortmannin, an inhibitor of the RISK pathway. RIC was observed to reduce levels of the phosphor-MYPT1 protein, which is a downstream effector of ROCK (Gao et al., 2022).

In summary, the cardioprotective effects of Fasudil are well known, however the drug has not been well investigated with regards to post MI microvascular obstruction.

iv) Scope of this work

Before investigating the effects of Fasudil in an in vivo rat model of MVO/NRF, it was important to first investigate/confirm the vascular mechanism of the drug and its potential as a vasodilator, although as above, this is also well documented in the literature (Goel et al., 2007). Nevertheless, it was important to introduce two new experimental models (aortic ring tissue bath assay) and the thioflavin model of MVO assessment, before expanding investigations to more novel and selective ROCK2 inhibitors. Fasudil is therefore a useful positive control for these models.

It must be acknowledged that the aorta is a conduit vessel and responds in a different physiological manner to resistance vessels, such as coronary arterioles (Wenceslau et al., 2021). The next model to be introduced, was not

used as a surrogate for these vessels; however, it provides an insight into potential drug potency and mechanism of action.

4.2: FASUDIL INDUCES DOSE-DEPENDENT VASODILATION OF RAT AORTIC RINGS

i) Objectives

1) To investigate the vasoactive effects of Fasudil in rat aorta using a wire myography model.
2) If Fasudil is confirmed to be an arterial vasodilator, to proceed to investigate the potency and efficacy of the drug in rat aorta.

ii) Methods

With thanks to Dr Catherine Wilder and Miss Alex Jamieson for their helpful advice and guidance on setting up this model.

Animals

Animals were handled and anaesthetised according to section 3.1. Adult male Sprague-Dawley (SD) rats were selected for these experiments (250-300g). A thoracotomy was performed to remove the heart and ascending aorta under full surgical sedation as detailed previously in chapter 2, (confirmed by absence of pedal reflexes). The remaining thoracic aorta was carefully removed and placed into ice-cold Krebs-Ringer Solution (NaCl 118mM;

$CaCl_2H_20$ 2.5mM; Glucose D (+) 11.1mM; NaHC03 25mM; MgS04 1.2mM; KH_2P04 1.2mM; KCL 4.8mM). This buffer is specialised for vascular tissue.

Aortic ring tissue Preparation

The thoracic aorta was dissected whilst submerged in ice-cold Krebs-Ringer solution. Surrounding connective tissue was removed, with care not to damage the overlying endothelium of vessels. Once any residual blood and connective tissue were removed, the vessel was divided into 3mm sections and gently cut into rings.

Tissue bath apparatus (wire myography)

The water-bath apparatus (wire myography) for vascular tissue, was assembled as shown in figure 21, and as previously described in our laboratory (A Jamieson, 2018), (Wilder et al., 2018). Two reservoirs containing 2L Krebs-Ringer solution, were heated to 37 degrees and maintained via a (Radnoti©) heater pump. Buffer solution, which was heated from each reservoir, was supplied to 4 x 45ml water baths, via a 3-way tap system, so that a total of 4 rings could be investigated simultaneously. The Krebs-Ringer buffer was oxygenated with 95% 0_2; $C0_2$ throughout. Following the preparation of the aortic rings, oxygenated buffer was allowed to run through all 4 water baths before filling to a total volume of 45mls.

The aortic rings were mounted onto transducer wires, carefully separated, and submerged into the water bath. Transducers were connected to Lab Chart 7 Software to measure the change in force of the contraction of the rings, in millinewtons (mN) throughout. All four transducer wires were calibrated prior to the addition of vascular tissue. In addition to the resting tone of the vessel,

10mN of tension was added to each ring as passive stretch. This final starting force was then recorded as baseline. Following this, aortic rings were left to equilibrate in buffer for a period of 1 hour.

Figure 21 The aortic ring tissue bath assay apparatus. Two large reservoirs of Krebs-Ringer buffer solution are heated to 37 degrees and used to fill four individual 45ml water baths (left). Aortic rings are suspended in each water bath on two transducers which measure changes in forces of contraction (millinewtons) (right).

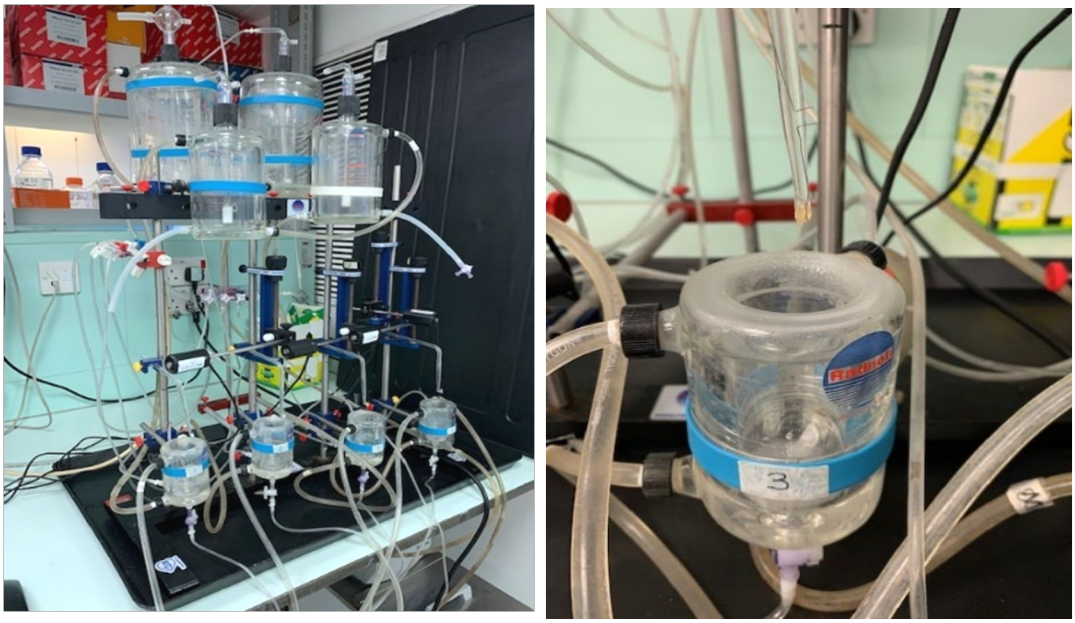

Baseline model (n=5)

For the basic wire myography model, rings were first treated with 60mM KCL to achieve maximum VSMC vasoconstriction (fig.22). High concentrations of KCL depolarize the VSMC membrane, and trigger activation of voltage-gated calcium channels and vasoconstriction (Wenceslau et al., 2021). After 40minutes KCL was washed out thoroughly and rings were pre-treated with 1μM phenylephrine (PE) to induce a second contraction. Phenylephrine is an alpha-adrenergic agonist and induces VSMC contraction via an agonist

induced pathway (Grimm et al., 2005). Rings that constricted to 70% of maximum KCL readings, were included in the analysis (Wilder et al., 2018), (A Jamieson, 2018). After 5 minutes, (or once contraction had plateaued) 10μM acetylcholine was added to each water bath to induce vasorelaxation and confirm endothelial function (A Jamieson, 2018), (Wilder et al., 2018). Ach induces endothelial dependent vasorelaxation by binding to muscarinic receptors on the endothelial membrane and increasing the amount of NO via increases in cGGMP (Kawarazaki & Fujita, 2021).

Figure 22 is a lab chart recording which demonstrates the changes in contraction and relaxation of a single aortic ring, over the time course of an experiment, and following the addition of KCL and PE agonists. % Relaxation to Ach was calculated by the formula as shown in Figure 23. Table 8 below, demonstrates the inclusion criteria for the basic aortic ring myography model, which would be adopted for future experiments. For this thesis, all aortic ring experiments were conducted in endothelial intact rings unless otherwise stated. Ach and PE were purchased from Sigma-Aldrich and diluted in H_20 to achieve the above desired concentrations.

Figure 22 Aortic ring myography vasoconstriction and vasorelaxation profile in a control aortic ring. A lab chart recording demonstrating experimental methods for the basic model of aortic ring myography. n=5 aortic rings were tested against the basic myography model to demonstrate that experimental standards could be met. The myography trace below begins after the addition 10mN of passive tension.

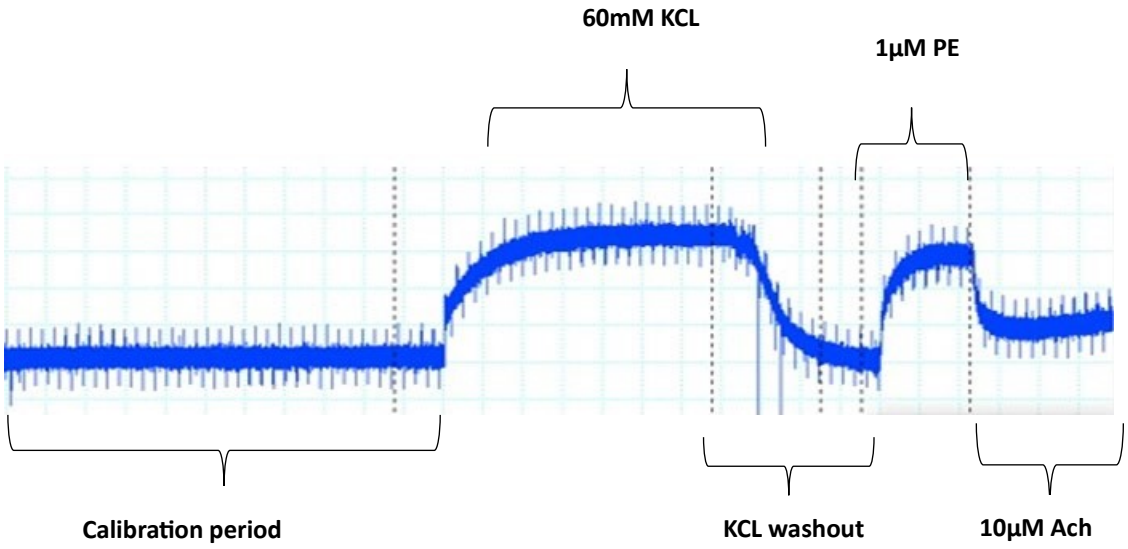

Mean PE response (% KCL): 95.9, mean Ach relaxation (%PE contraction): 86.4, for n=5

Table 8 Inclusion criteria for the basic aortic ring myography model.

DRUG	MINIMUM CHANGE
PE (1μM)	At least 70% of maximum KCL response
Ach (10μM)	% relaxation of at least 70% of PE contraction

Figure 23 Formula to calculate % relaxation of aortic rings to vasodilators including Acetyl choline: -

% Ach Relaxation = (PE peak – Ach min [Conc])/ (PE peak pre-constriction x 100)

Dose response experiments log [10^{-9}-10^{-5}]M, (n=5)

After establishing the basic model (figure 22), a further n=5 aortic rings were contracted with 1μM PE and treated with increasing concentrations of Ach log [10^{-9}-10^{-5}]M, to create a dose response curve. These experiments were repeated with two other vasodilators, sodium nitroprusside (SNP) log [10^{-9}-10^{5}]M and Fasudil hydrochloride log [10^{-9}-10^{-5}] M (the vasodilator of interest). Fasudil was purchased as Fasudil Hydrochloride (HA-1077) from MedChem Express and diluted in H_20 to achieve desired concentrations. SNP was purchased from Sigma-Aldrich and diluted in H_20 to achieve desired concentrations. Inclusion criteria were maintained for dose-response

experiments to confirm that vascular tissue was viable. Experimental protocol for SNP and Fasudil experiments is demonstrated below by Figure 24.

Figure 24 Protocol for dose-response experiments, Fasudil & SNP. Concentrations of both vasodilators log [10^{-9}-10^{-5}] M.

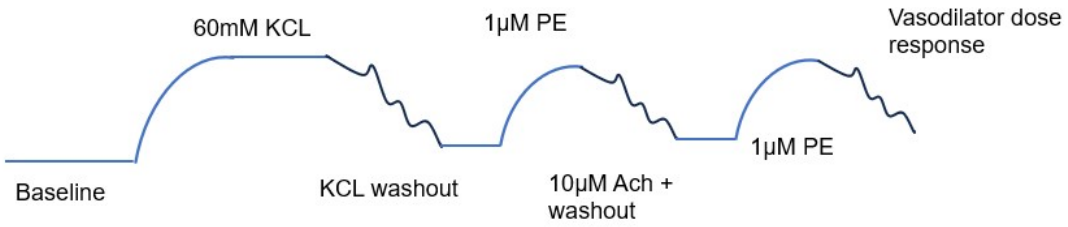

Fasudil mediated vasodilation in the presence of L-NAME or buffer control, (n=8)

L-NAME (NG-Nitro-L-Arginine Methyl Ester) is an eNOS inhibitor which limits NO mediated vasodilation when incubated with aortic rings (Haesen et al., 2020). To further investigate an endothelial independent mechanism of Fasudil induced vasodilation, rings from the same animal were pre-treated with either 1) 100µM L-NAME or 2) buffer vehicle, for 15-minutes directly after Ach washout equilibration (Figure 25). 1µM PE was then added as per usual protocol, followed by log [10^{-9}-$10^{-2.5}$]M Fasudil at 4-minute intervals. L-NAME was purchased from Sigma-Aldrich and diluted in H_20 to achieve desired concentration. Figure 26 is included to demonstrate the efficacy of L-NAME, i.e. that 100µM effectively inhibits Ach relaxation and inhibits endothelial function to a level appropriate for this work.

Figure 25 Experimental protocol for experiments described in f). The effects of L-NAME on Fasudil mediated vasodilation of aortic rings. Concentrations for Fasudil log [10^{-9}-$10^{-2.5}$] M.

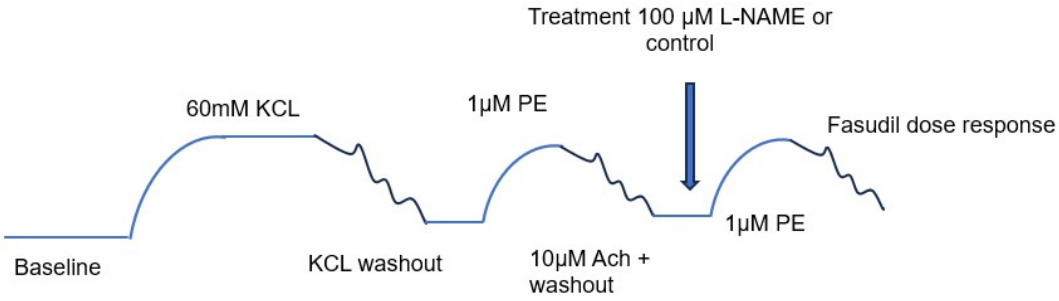

Statistical methods

Guidelines from the following vascular standards statement were adhered to when expressing results for statistical analysis (Wenceslau et al., 2021). Testing of vasodilators including Ach and ROCK inhibitors, are expressed as dose response curves, where X is increasing Log concentration of vasodilator dose, and Y is % relaxation. If data passed Log normality testing, non-logistic regression analysis was performed with a normalised 4-parameter curve fit generated by GraphPad Prism© Software and the $LogEC_{50}$ (concentration at which aortic rings were dilated to 50% of maximum) was automatically calculated.

Statistical power was determined by the following formula: - [sample size = $2\ SD^2\ (Z^{\alpha/2} + Z^{\beta})^2/d^2$], where SD = standard deviation, D= main effect size, and Z values which correspond to a type 1 error of 5% and 0.80 power. These

experiments were powered to 0.80, which required n=5 animal aortas per experiment, based on data from previous pilot experiments in our lab (A Jamieson, 2018).

Figure 26 The effects of 100μM L-NAME on endothelial function. L-NAME in the trace below prevents Ach mediated relaxation following 2nd PE contraction, (93% Ach relaxation following 1st addition of 10μM Ach and 1% relaxation following a 2nd challenge of Ach after rings were incubated with L-NAME). L-NAME is also shown to augment 2nd PE contraction %.

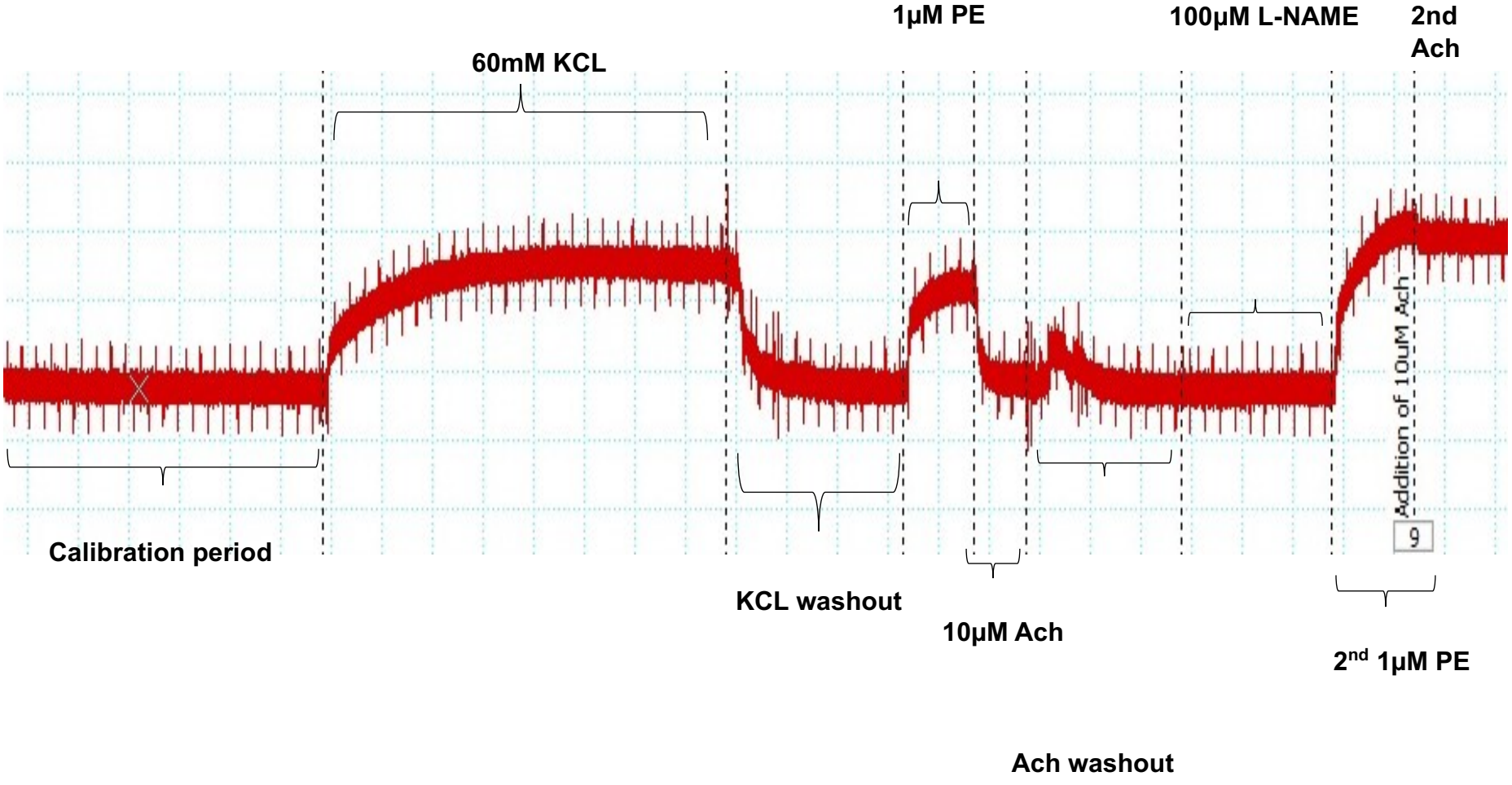

iii) Results

Dose response experiments

Ach dose response curves (n=5)

Mean % PE contraction (as % KCL) was 103.9, which exceeded the minimum inclusion threshold value of 70%. Ach at concentrations {10^{-9}-10^{-4}] induced dose dependent vasodilation of aortic rings to >70% (Figure 27). Best fit $LogEC_{50}$ was calculated to be -7.1, (R^2 for the model 0.9).

Fasudil vs SNP dose response curves log [10^{-9}-10^{-5}] (n=5)

Fasudil (ROCK1/2) inhibitor [10^{-9}-10^{-5}] induced dose dependent vasodilation of aortic rings (Figure 28). However, a more commonly used vasodilator sodium nitroprusside (SNP) was found to be more potent (curve shift to the left) (Figure 28). The E_{max} value for Fasudil was not reached at this dose range and therefore an accurate EC_{50} and non-linear regression model could not be established. Higher doses of Fasudil were planned for the next set of experiments to further determine this.

Fasudil dose response curves (L-NAME or control treated rings, n=8)

In a new set of experiments, aortic rings were treated with either L-NAME 100μM or equivalent volume of buffer control, prior to further PE contraction and Fasudil relaxation (protocol Figure 25). Fasudil was administered every 4minutes up to a concentration of 10^{-5} in n=5 aortic rings and up to $10^{-2.5}$ in a further n=3 rings (total n=8) to try to reach the true E_{max} of the curve which had not been obtained previously. $10^{-2.5}$ is 10mM Fasudil, which requires a large

quantity of drug and therefore it is not practical to perform many repetitions at this dose. Dose dependent vasodilation was observed in both treatment groups; however, the addition of L-NAME was seen to reduce the potency of Fasudil (Figure 29).

Figure 29 and Figure 30 demonstrate that whilst Fasudil was significantly less potent compared to other vasodilators, the drug efficacy (actual E_{max} value) was not significantly affected by the addition of L-NAME (inducing endothelial dysfunction). Fasudil therefore, at its Emax dose of $10^{-2.5}$ demonstrates endothelial independent vasodilation.

Figure 27 Acetyl choline mediated vasodilation, dose-response curve (n=5). A 4-parameter NLR curve was fitted to log transformed and normalised data. True E_{max} value is shown below for non-normalised data. R^2 for the curve fit 0.9.

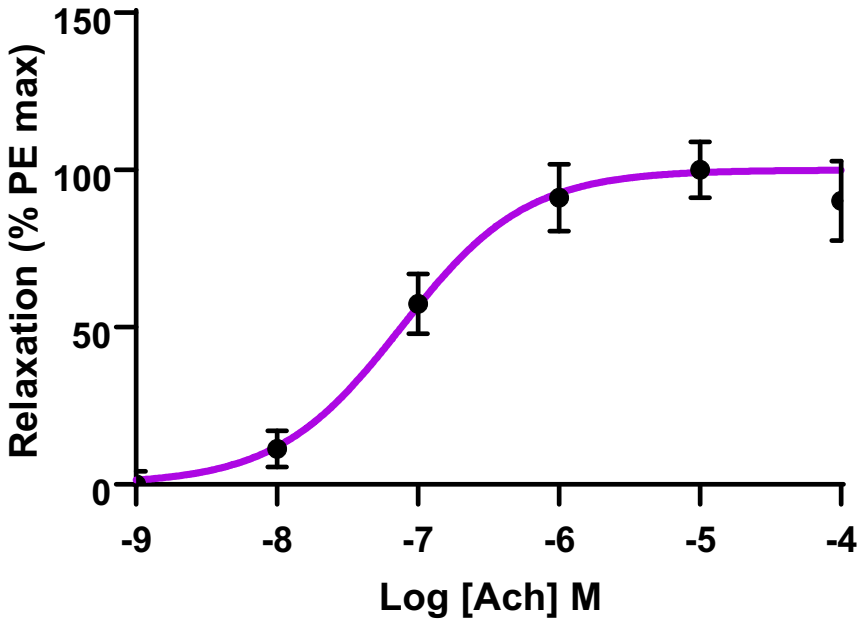

LOG [ACH] M	MEAN RELXATION (%)	SEM
10[-9]	0.0	4.2
10[-8]	11.3	5.8
10[-7]	57.4	9.5
10[-6]	91.1	10.7
10[-5]	100	8.9
10[-4]	90.2	12.7
Best fit $LogEC_{50}$	-7.1, R^2=0.9	
Emax	88.1	6.0

Figure 28 Dose response curves for Fasudil (blue) and SNP (green) in endothelial intact aortic rings (n=5). This figure represents log transformed and normalised data. Both drugs induced dose dependent vasodilation, however SNP was more potent as demonstrated by the curve shift to the left. E_{max} value is shown below for non-normalised data. An E_{max} value for Fasudil was not reached.

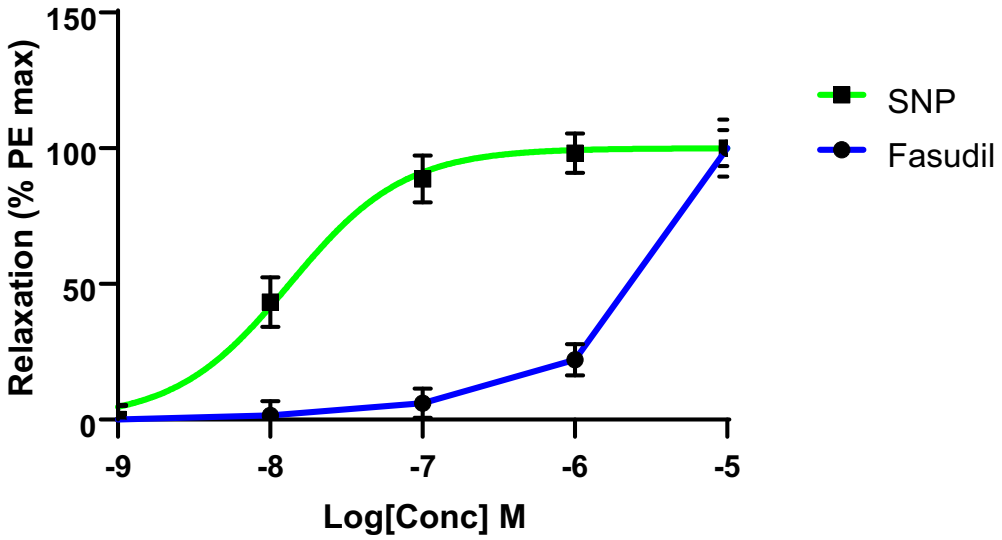

LOG [CONC] M	MEAN RELXATION (%) SNP ± SEM	MEAN RELAXATION (%) FAS ± SEM
10[-9]	0±5.4	0±5.1
10[-8]	43.3±9.2	1.5±5.3
10[-7]	88.7±8.7	6.0±5.4
10[-6]	98.2±7.3	22.1±5.9
10[-5]	100±6.7	100±10.5
Best fit LogEC$_{50}$	-7.9, R^2=0.9	
Emax	117.3±7.0	

Figure 29 Fasudil mediated vasodilation [10^{-9}-$10^{-2.5}$] in control or L-NAME pretreated aortic rings (n=8). This figure represents log transformed and normalised data to enable EC_{50} comparison. E_{max} value is given below for non-normalised data. A comparison of $LogEC_{50}$ values confirmed that one curve did not fit both datasets ($p<0.05$), and therefore $LogEC_{50}$ (potency) was significantly different between treatment groups.

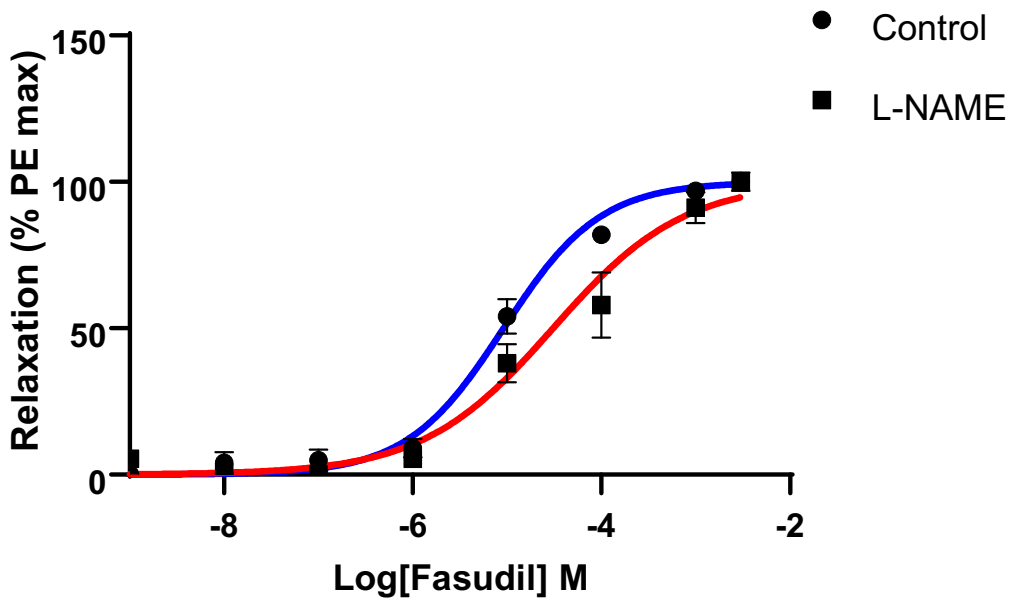

LOG [FAS] M	MEAN RELXATION (%) Fasudil +/- SEM	MEAN RELAXATION (%) Fasudil + L-NAME +/- SEM
10[-9]	0.0± 1.3	5.4±1.6
10[-8]	4.1±3.7	0.8±2.2
10[-7]	5.0±3/6	0.0±2.7
10[-6]	9.1±3.2	5.4±2.1
10[-5]	54.0±6.0	38.1±6.6
10(-4)	82.0±1.5	58.0±11.0
10(-3)	97.0±0.3	91/2±5.3
10(-2.5)	100.0±3.2	100.0±3.2
Best fit Log EC_{50}	-5.0, R^2=0.9	-4.5, R^2=0.9
Emax	103.3±0.8	102.7±3.5

Figure 30 A comparison of relative potencies for all vasodilators evaluated during these experiments, to demonstrate relative potencies. Comparison of all NLR models confirmed that one curve did not fit all datasets ($p<0.05$), and therefore $LogEC_{50}$ values were not shared between vasodilators.

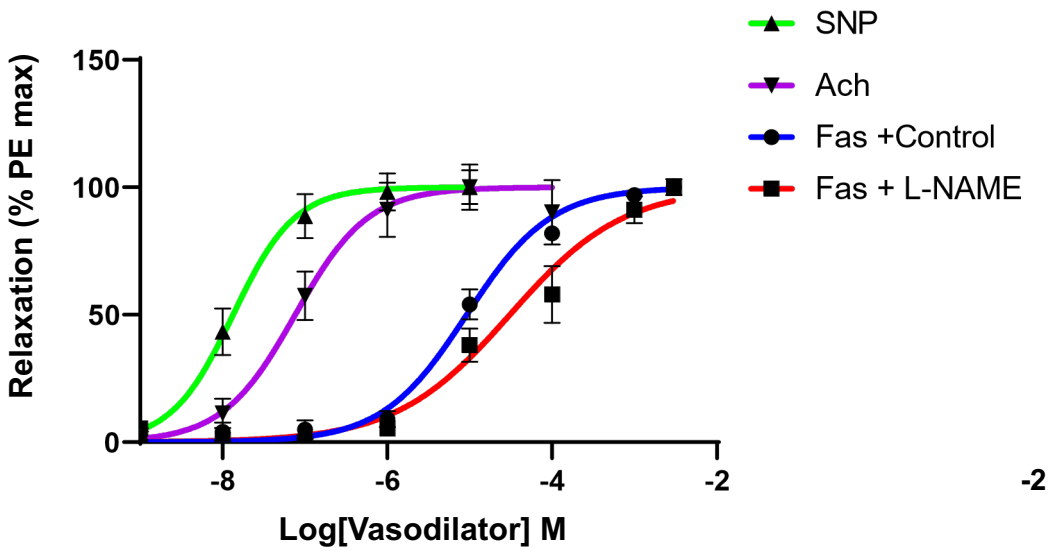

DRUG	SNP	Ach	Fasudil	Fasudil + L-NAME
BEST FIT $LogEC_{50}$	-7.9	-7.1	-5.0	-4.5

Figure 31 Comparison of actual E_{max} relaxation % values for aortic rings treated with Fasudil (103.3%) vs Fasudil + L-NAME (102.7%). There were no significant differences in drug efficacy observed at maximum treatment dose (p>0.05).

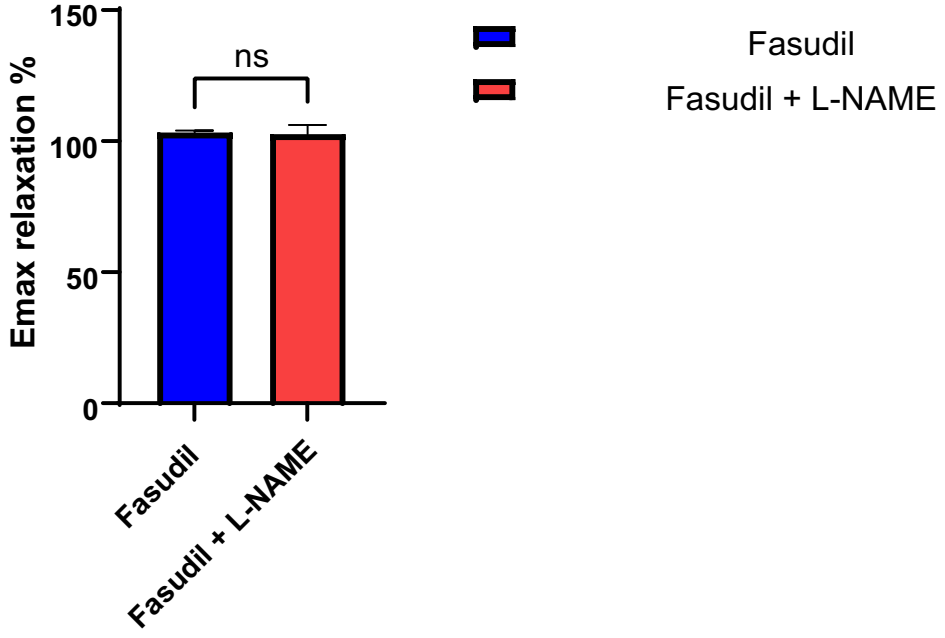

iv) Conclusions

Fasudil (a ROCK1,2 inhibitor) induces dose dependent vasodilation of aortic rings, however it is of lower potency compared to SNP and ACh, (other well-known vasodilators). Despite its lower potency, the efficacy of Fasudil is not significantly different compared to other vasodilators, and drug efficacy is not significantly affected by endothelial dysfunction and the presence of L-NAME. This may make it a useful drug in the study of myocardial infarction, where endothelial function compromised. Endothelial independent mechanisms (given these results) are further considered in the final chapter discussion.

In vivo studies were next performed to investigate the effects of Fasudil on infarct size (%) and MVO (%).

4.3: THE EFFECTS OF FASUDIL (10MG/KG) IN AN IN VIVO RAT MODEL OF MYOCARDIAL ISCHAEMIA/REPERFUSION

i) Objectives

1) To investigate the effects of Fasudil hydrochloride on myocardial infarction size (%) in an in vivo rat model of ischaemia/reperfusion (primary outcome)

2) To investigate the effects of Fasudil hydrochloride on MVO (%) in an in vivo rat model of myocardial infarction (secondary outcome)

ii) Methods

The in vivo experiments described in this section were performed by Dr David He. Experiments were designed and analysed by Dr Lucie Pearce.

Animals

Animals were handled according to section 3.1. Adult male Sprague-Dawley (SD) rats were selected for these experiments (250-350g). Anaesthesia was performed and maintained with 100mg/kg of phenobarbital, after which animals were intubated and ventilated with room air and oxygen.

In vivo model of myocardial ischaemia/reperfusion

Under anaesthesia, surgical thoracotomy was performed, and the left anterior descending coronary artery (LAD) was identified within the pericardium. This was ligated for 30 minutes, and myocardial ischaemia was confirmed by the presence of anterior ST-elevation. After 30 minutes of ischaemia, the LAD ligature was released, and the vessel was re-perfused for a period of 180 minutes. 15-minutes prior to the onset of reperfusion, either Fasudil 10mg/kg, or equivalent volume of DMSO (control), were injected via the I.P route (Figure 32). The haemodynamic status and blood pH of the animals was monitored continuously, via right carotid cannulation.

In accordance with previous in vivo no reflow models (Kloner et al., 1974), 4% Thioflavin S dye was administered at the end of reperfusion, into the systemic circulation, to measure MVO. Finally, the LAD vessel was re-occluded with the ligature, and Evans blue dye injected into the systemic circulation, to demonstrate the area at risk (AAR %). For analysis of the in vivo work, cardiac tissue was prepared into 2mm sections and stained with tetrazolium (TTC) to measure infarct size as a % of the AAR. Under UV light, regions not perfused by the Thioflavin S dye were quantified (%) and recorded as regions of NRF/MVO (Figure 33). % IS, MVO and IMH were all estimated for each section using the electronic software, Image J©. IMH was estimated visually following TTC staining from necrotic regions of myocardium (Figure 33). Fasudil was purchased as Fasudil hydrochloride from MedChem Express and diluted in dimethyl sulfoxide (DMSO) as per manufacturer's instructions.

Figure 32 Experimental protocol for in vivo myocardial ischaemia/reperfusion experiments, n=6. Animals underwent 30-minutes of LAD ischaemia followed by 180-minutes of reperfusion as per previous NRF protocols in the literature (Kloner et al., 2018)

Figure 33 Post experimental myocardial tissue sections stained with Thioflavin S and TTC demonstrating A) The fluorescence of Thioflavin under UV light in regions of re-flow and the dark regions of MVO/NRF B) TTC staining of the myocardial infarction zone and surrounding tissue necrosis used to estimate IMH% (intra-myocardial haemorrhage). TTC can also be used to identify IMH as dark red regions within the necrosis zone (Kumar et al., 2011)

A

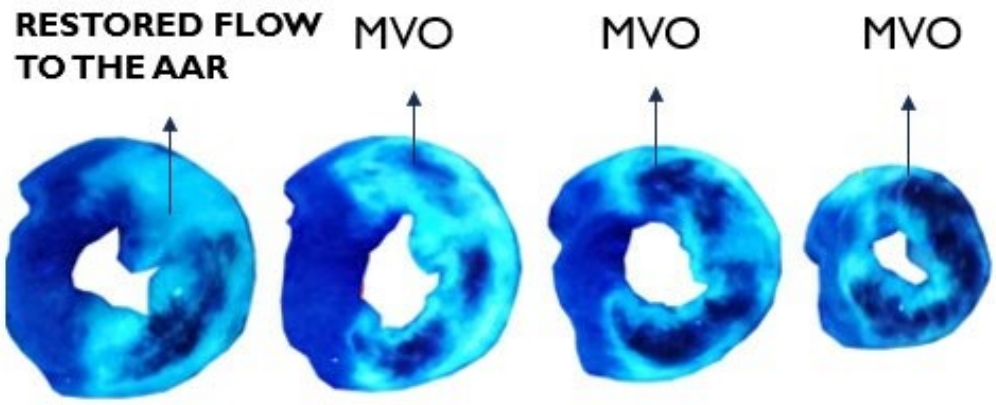

B

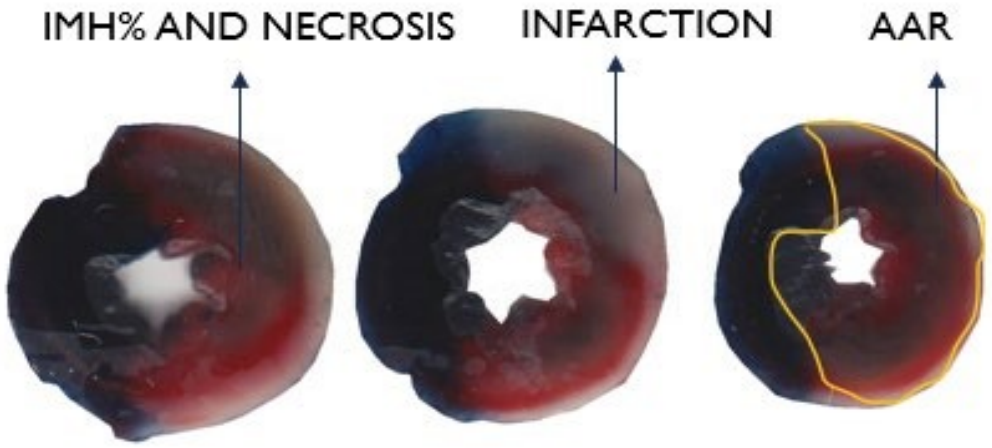

Statistics

Statistical power was determined by the following formula: - *[sample size = 2 SD^2 ($Z^{\alpha/2}$ + Z^{β})^2/d^2],* where SD = standard deviation, D= main effect size, and Z values which correspond to a type 1 error of 5% and 0.80 power. These experiments were powered to 0.80, which required *n=5* animals per experiment, based on data from previous in vivo ischaemia/reperfusion experiments in our lab (Rossello et al., 2017). Data was normality tested and then both groups were analysed with a student's T-test (if parametric) and one way analysis of variance (ANOVA) if >2 experimental groups. A simple linear regression model was used to investigate the correlation between IS% and MVO%, providing R^2 as a measure of correlation.

iii) Results

Fasudil (10mg/kg) injected prior to onset of reperfusion, significantly improved all outcome measures including IS%, MVO% and IMH% (Figure 34), whilst there were no significant differences observed between the AAR% in both groups (p=0.64, n=6). To further investigate the relationship between IS% and MVO%, a correlation analysis was performed using a simple linear regression model.

Figure 35 demonstrates a moderate positive correlation between IS% and MVO%, i.e., Increasing MVO% was associated with larger infarction size.

Fasudil 10mg/kg was associated with significant hypotension 15-minutes after i.p injection. Mean minimum MAP during this time point was 52mmHg (Table

9). Unfortunately, one animal did not survive this hypotensive crisis, and another animal survived, but required intensive oxygen resuscitation. There were no incidences of bradycardia except prior to arrest of one animal. Moreover, mean heart rate in the treatment group was significantly higher compared to vehicle, which was likely a compensatory response to hypotension (423.7 vs 397.8 bpm respectively, p=0.014). Table 9 and Table 10 below demonstrate the haemodynamic measurements for these sets of experiments.

Table 9 Mean arterial pressure (mmHg) during myocardial I/R experiments (n=6). Data provided for 1) Mean MAP throughout period 2) Mean minimum MAP value and 3) MAP range throughout period

MAP (mmHg)	DMSO VEHICLE	FASUDIL 10mg/kg	P VALUE
MEAN ± SEM	88.5±3.4	71.6±3.9	0.008**
MIN ± SEM	68.8±3.4	52.0±3.9	0.009**
MAP RANGE ± SEM	47.5±3.4	55±3.9	0.40

Table 10 Mean heart rate response (BPM) during myocardial I/R experiments (n=6). Data provided for 1) Mean HR throughout period 2) Mean minimum HR value and 3) HR range throughout period

HEART RATE (BPM)	DMSO VEHICLE	FASUDIL 10mg/kg	P VALUE
MEAN ± SEM	397.9±5.8	423.7±6.1	0.014*
MIN ± SEM	366.8±5.8	379.8±6.1	0.34
RANGE ± SEM	77.3±5.8	72.7±6.1	0.93

Figure 34 Fasudil at a dose of 10mg/kg significantly reduced IS%, MVO% and IMH% following myocardial I/R (p=0.02, p=0.01, p=0.02, n=6). There were no significant differences observed in the AAR% of both groups (panels A-D).

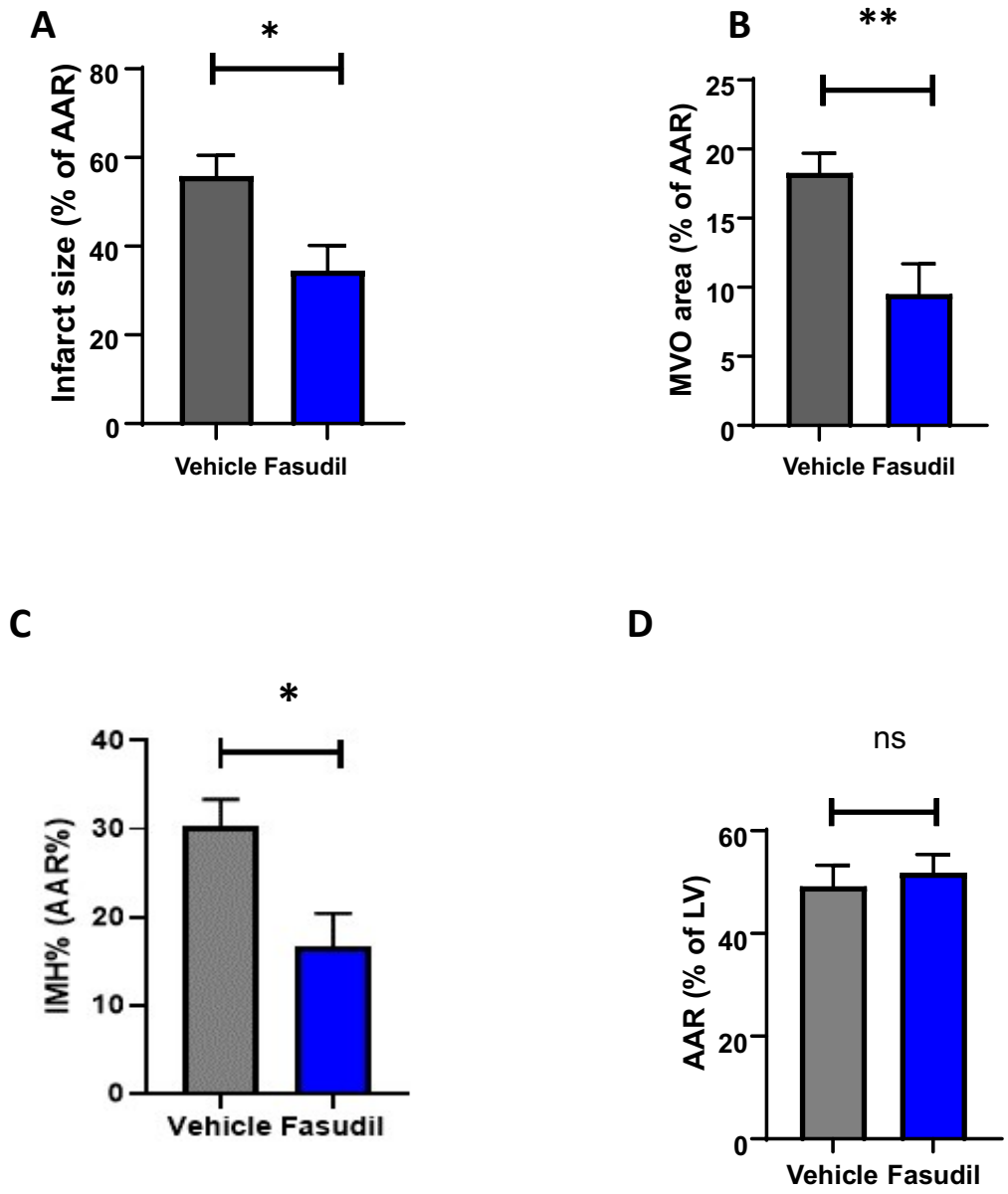

MEASURE ±SEM	DMSO VEHICLE	FASUDIL 10mg/kg	P VALUE
INFARCT SIZE (%)	55.8±4.7	34.5±5.7	0.02*
MVO (%)	18.3±1.4	9.5±2.2	0.01**
IMH (%)	30.4±2.3	16.7±3.7	0.02*
AAR (%)	49.1±4.1	51.7±3.6	0.64

Figure 35: A correlation analysis of IS% and MVO% variables. This figure demonstrates a moderate positive correlation between the two variables for this set of experiments (n=6).

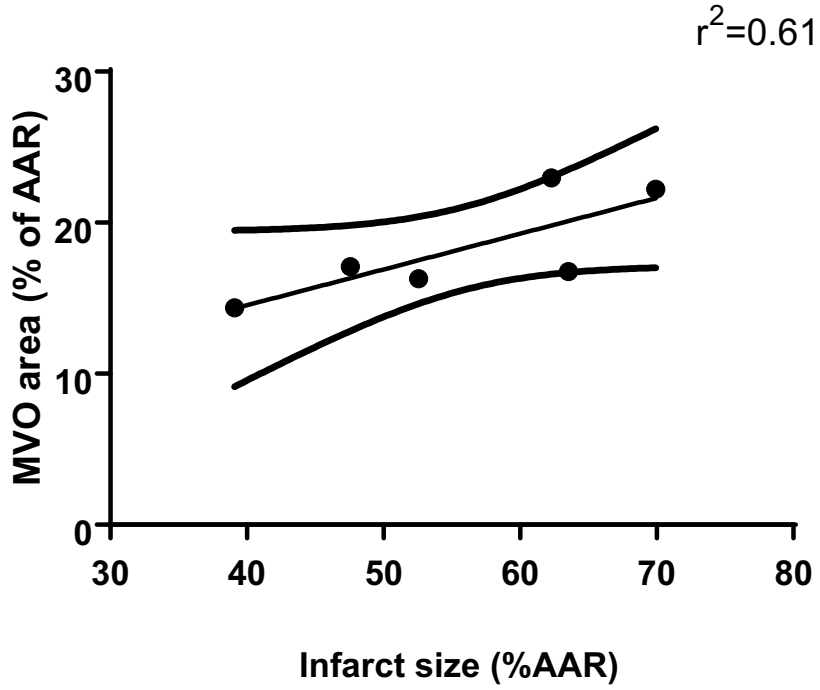

iv) Conclusions

In conclusion, Fasudil 10mg/kg has demonstrated cardioprotective effects in an in vivo rat model of myocardial ischaemia-reperfusion, however this dose is associated with significant hypotension, which may limit clinical translation. There is a moderate correlation between increasing IS% and MVO% observed, which makes it more challenging to separate these two variables when discussing cardioprotective effects, especially with respect to MVO. However, the in vivo model utilising Thioflavin S dye appears functional in these pilot experiments and would be suitable to use to further investigate the potential benefits of ROCK2 inhibitors during myocardial I/R.

4.4: CHAPTER DISCUSSION

i) The vasoactive properties of Fasudil

Fasudil at doses of [10^{-9}-$10^{-2.5}$] M demonstrated dose-dependent vasodilation of rat aortic rings, in a wire myography model. This is consistent with previous literature which has demonstrated that Fasudil is vasoactive, both in animal studies (Goel et al., 2007) and in humans with sub-arachnoid haemorrhage (Shibuya et al., 1990). These experiments have highlighted, that whilst Fasudil is able to induce vasorelaxation, the drug is of low potency compared to another commonly used vasodilator, SNP. Nitrate derivatives such as SNP, are currently used in clinical practice for the treatment of MVO (Niccoli et al., 2019), and so for the main hypothesis to be upheld, the effects of Fasudil need to be comparable to alternatives which are currently available and known to be well-tolerated. The low potency of Fasudil does not make this drug an ideal candidate as a NRF drug, as the therapeutic doses required are likely to induce significant hypotension (and off target effects due to multiple kinase inhibition and calcium antagonism), which is undesirable in unwell patients with myocardial infarction. These observations are reinforced by the previously discussed small clinical study of Fasudil during PCI in the Cath lab, where further inotropic support was required for patients receiving the drug (Kikuchi et al., 2019).

One strength of Fasudil as a ROCK1,2 inhibitor is its mechanism of action. This chapter has demonstrated that in high doses, Fasudil may

act directly on the VMSC of arteries to induce vasodilation, independently of other NO based endothelial mechanisms. This may be of benefit when there is endothelial dysfunction in myocardial infarction leading to post-STEMI MVO. This can be deduced, given that the compound L-NAME (an eNOS inhibitor) did not significantly affect the Emax relaxation value of Fasudil (Figure 31), therefore providing evidence of the uncoupling of eNOS from actin changes. These experiments did not, however, account for other mechanisms of vasodilation, such as those which are prostaglandin mediated. This could be explored in future work. Therefore, it is only possible to say that Fasudil acts independently of eNOS at maximum relaxation.

It must also be affirmed that the relaxation responses of the aorta, may not be reflective of physiology in different vessels such as the mesenteries and larger arterioles (Wenceslau et al., 2021). One suggestion to overcome a potentially profound hypotensive response in humans, may be to alter the route of administration of Fasudil e.g. to use an oral preparation. This may not be practical however in unwell patients with myocardial infarction, and the drug may not reach therapeutic concentration in the time frame necessary to take effect.

ii) Fasudil in an in vivo model of ischaemia/reperfusion

Consistent with the literature review, Fasudil was cardioprotective in vivo and attenuated IS%, MVO% and a measure of IMH% (Huang et al., 2018b).

Significant hypotension has already been discussed with suggestions to mitigate this. From a cardioprotection perspective, these results are promising and have achieved statistical significance at n=6 in all three outcomes, as is suggested to be gold standard by Heusch et al in preclinical experiments of MVO% (Heusch, 2019). Mechanisms of Fasudil mediated cardioprotection are well-documented in the literature, and so it is possible that protection has occurred secondary to upregulation of the RISK pathway, and a reduction in apoptosis, although this has not been proven in these pilot experiments (Wu et al., 2014), (Hamid et al., 2007). It could be suggested that VSMC relaxation may have been the mechanism behind an improvement in MVO, as has been demonstrated ex vivo in the aorta. Another plausible reason for an improvement in MVO may have been an improvement in infarct size, as evidenced by the positive correlation between the two variables. This is not surprising given that many predictive models of MVO list ischaemia time as a prognostic factor, and ischaemia time is closely related to infarct size (Niccoli et al., 2019).

Once the wire myography model and in vivo model of Thioflavin S (MVO%) had been established, and anticipated results with Fasudil had been achieved, it was decided to test the newer selective ROCK2 inhibitors, as these have not yet been examined in the heart, and moreover the side effect profile may be considered as more suitable. The selective ROCK2 inhibitor KD025 is licenced in humans for graft vs host disease (GVHD, an inflammatory haematological condition) and was well tolerated in previous large-scale clinical trials (Cutler et al., 2021). Therefore, the next chapter will describe the effects of selective ROCK2 inhibition on IS% and MVO%.

CHAPTER 5: THE EFFECTS OF SELECTIVE ROCK2 INHIBITION WITH KD025 ON ARTERIAL VASOSPASM AND CARDIOPROTECTION IN VIVO

5.1 : BACKGROUND

i) KD025 - a new selective ROCK2 inhibitor

The selective ROCK2 inhibitor, KD025 (SLX-2119) was introduced to the pharmaceutical market in 2021 as Belumosudil ©, by Kadmon Biotech (Ali & Ilyas, 2022). ROCK2 inhibitors such as KD025 evolved from other ROCKi as early as 2006, to reduce the hypotensive side-effects associated with ROCK1 inhibition (Feng et al., 2016). KD025 is a yellow powder with a molecular weight of 548.62g/mol and it is completely insoluble in water. Unlike Fasudil it is formed from an indoline scaffold (Figure 36) and must be dissolved completely in DMSO before use (Shah & Savjani, 2016). The IC_{50} of KD025 is estimated to be around 102nm for ROCK2, and 24μM for ROCK1, and it is deemed to be 200x more selective for ROCK2 over ROCK1 (Fu et al., 2023). ROCK2 inhibitors compete with ATP to prevent the phosphorylation of MYPT1 (myosin binding subunit of MLCP) by SER/THR residues, in the same manner as Fasudil. The exact mechanism by which ROCK2 inhibitors such as KD025, selectively inhibit ROCK2 is unclear, however one possibility is that changes to a phosphomimic residue enable this selectivity (Shah & Savjani, 2016). KD025 has not yet been investigated in studies of myocardial ischaemia/reperfusion but was found

to significantly limit cerebral ischaemia/reperfusion injury in the previously discussed animal study by Lee et al (Lee et al., 2014).

Belumosudil© has become perhaps most well-known since becoming licenced by the MRHA in 2021 for treatment of graft vs host disease (GVHD) – a complex inflammatory haematological condition which induces multi-organ damage post allogenic bone marrow transplantation (Cutler et al., 2021). GVHD is associated with a high mortality in transplant patients (who are often unwell with multiple co-morbidities) (Cutler et al., 2021). The ROCKstar trial has been, to date, the largest clinical trial of a ROCK2 inhibitor (*n=132*), and it is from this study, that researchers have gained a greater insight into the pharmacology and mechanism of the actions of KD025 (Cutler et al., 2021). Before discussing some of the more important implications of the ROCKstar trial in more detail below, Figure 37 summarises the other conditions in which KD025 has been studied, in both clinical trials and animal models. KD025 was chosen for its potential anti-inflammatory actions in ROCKstar, which includes the regulation of IL-17, IL-21, T-helper cells, and the regulation of JAK3/STAT5 (Ali & Ilyas, 2022). It is these proposed anti-inflammatory actions which are felt to also benefit the skin disorder psoriasis, and other auto-immune disorders such as systemic sclerosis (Zanin-Zhorov et al., 2017), (Gumkowska-Sroka et al., 2023). Any drug which could reduce pulmonary hypertension would also be of benefit in scleroderma and this is a known class effect of ROCK inhibitors (Abedi et al., 2023). ROCK2 inhibitors have also been studied as anti-fibrotic drugs in the management of idiopathic pulmonary fibrosis in in vivo models and phase II clinical trials (NCT05570058) (Gambardella et al.,

2022). Fu et al, who have worked in re-fashioning KD025 at a molecular level to improve its selectivity, hypothesise that ROCK2 inhibitors have anti-fibrotic properties as they can suppress collagen remodelling and α-SMA in models of chronic disease (Fu et al., 2023). ROCK2 inhibitors as a class of drug have also been shown to limit liver fibrosis (Zanin-Zhorov et al., 2023). In theory, KD025 should have vasodilatory properties – as ROCKi prevent MYPT1 and MLC2 related VSMC of arteries (Liao et al., 2007). However, at the time of writing this has not been directly investigated in the same way as ROCK1 inhibitors such as Fasudil (Shimokawa et al., 2016).

Figure 36. The molecular structure of KD025 ($C_{26}H_{24}N_6O_2$). Figure re-drawn from image published by Fu et al (Fu et al., 2023).

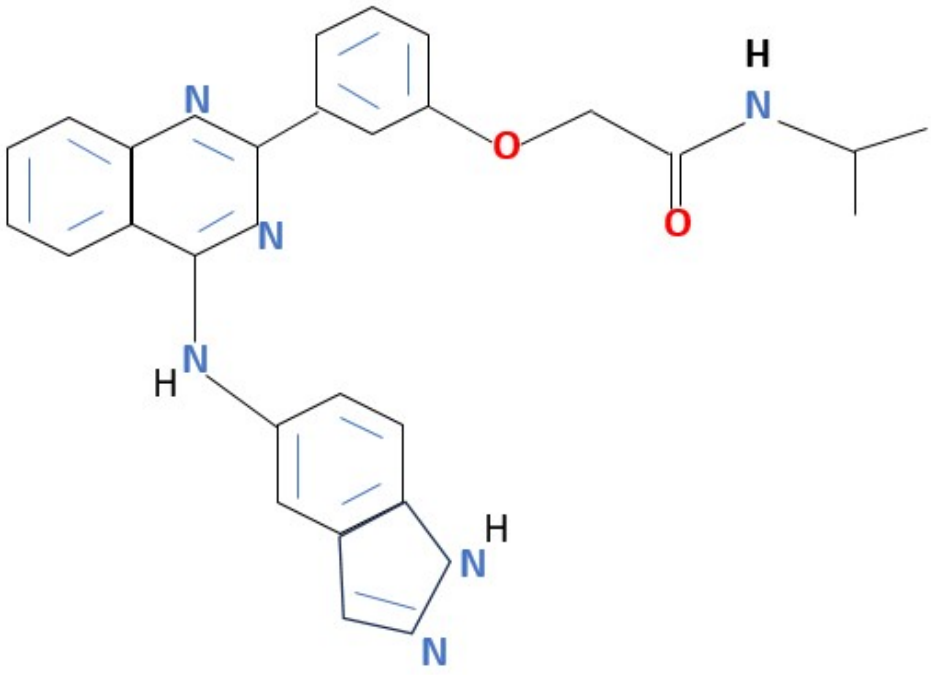

ii) Insights from the ROCKstar trial

The ROCKstar trial (Cutler et al., 2021) was a multi-centre phase II randomised control trial, which was published in 2021, whilst these PhD experiments were ongoing. Although KD025 was investigated as an anti-inflammatory therapy in the trial, the results have provided an insight into the pharmacodynamics of the drug, mechanism of action, and clinical safety profile. KD025 when administered via the oral route at doses of 200mg/kg daily or twice daily, was found to be clinically safe in patients with GVHD, who had failed at least two lines of systemic therapy, including dexamethasone (Ali & Ilyas, 2022), (Cutler et al., 2021). Participants in the trial received KD025 for a mean period of 14 months (*n=132*). The primary endpoint was overall organ response from failure (related to increased T-cell activity which defines the GVHD disorder) (Cutler et al., 2021). Common organs affected in this condition are the skin, liver, lungs, and the eyes, however cardiac GVHD is rare (Dogan et al., 2013), and was not therefore considered as a trial outcome.

From reported pre-clinical studies by the Kadmon Group, KD025 was found to be associated with foetal abnormalities in pregnancy and affected male fertility in a reversible manner. It was therefore not deemed to be suitable in patients of childbearing age (Przepiorka et al., 2022). This is not unusual for anti-inflammatory therapies e.g., methotrexate used in the treatment of rheumatoid arthritis is a well-known teratogen (Perry, 1983). In the trial, 12% of patients discontinued the drug because of adverse effects and one patient had a fatal adverse reaction secondary to nausea and vomiting, leading to multi-organ failure (Cutler et al., 2021), (Przepiorka et al., 2022).

Mild side effects included nausea, vomiting and headache, shortness of breath and deranged liver function tests (Cutler et al., 2021). 6% of patients developed hypertension, which might be considered surprising given that ROCK inhibitors generally lower blood pressure as a drug class (Liao et al., 2007). Some patients developed neutropenia and pneumonia because of immunosuppression with KD025, however this was felt to reside within the confines of what is expected for immunotherapy (Cutler et al., 2021). The anti-inflammatory actions of KD025, including the downregulation of STAT3 and upregulation of STAT5 (in addition to the former T cell related changes described) were first proven in murine studies of animals undergoing transplantation (Flynn et al., 2016) (Figure 37). In these pre-clinical studies, transplanted mice received 150mg/kg po of KD025 for 30-days after GVHD had been established. The authors performed PK studies for the oral route of administration, which demonstrated adequate blood serum concentration of the drug 1 hour after PO administration in doses >100mg/kg (Flynn et al., 2016).

ii) KD025 – Pharmacokinetics

As a newer ROCK inhibitor, there is significantly less research published with regards to dose regimes of KD025 in studies of cardio protection. The oral route of administration is more challenging for studies of acute myocardial infarction unless rapid absorption is achieved. The main dilemma that cardiologists face, is that it is not possible to predict who is going to present with a STEMI, which does not allow for extended periods of pre-medication. The oral half-life of KD025 has been estimated to be 19

hours (Przepiorka et al., 2022) in clinical studies, and therefore a steady state is required for the drug to be effective. Interestingly Lee et al (Lee et al., 2014) in their preclinical investigations of KD025 in cerebral ischaemia, also selected the PO route of drug administration. It has already been discussed previously that KD025 100200mg/kg PO of 5 days was found to reduce stroke volume in mice and improve neurological outcomes (Lee et al., 2014). PK studies for the PO route of administration for doses of 100-200mg/kg, demonstrated peak plasma and tissue (cerebral) uptake between 2-4 hours after ingestion (Lee et al., 2014) and the authors did not observe significant hypotension with therapeutic effect. Peak plasma concentrations reached at any dose, were 9μg/ml (Lee et al., 2014). Yoon et al are potentially the only investigators to have performed PK studies following IV administration of KD025, in rats (Yoon et al., 2020). In this study, intravenous administration achieved peak plasma levels of approximately 5μg/ml after injection of 2mg/kg KD025 (Yoon et al., 2020), which was achieved at less than 5 minutes.

In the only study of KD025 in a model of chronic cardiac fibrosis (published in 2022), transverse aortic constriction (TAC) mice injected intra-peritoneally with 50mg/kg/day of KD025 for a period of 4-weeks, demonstrated significantly less cardiac fibrosis compared to TAC mice receiving vehicle alone (Q. Liu et al., 2022). Liu et al demonstrated that ROCK2 inhibition in the heart was associated with improved left ventricular function, reduced markers of myocardial fibrosis including α-SMA, fibronectin 1 (FN1), periostin (POSTn) and reduced tumour growth factor beta-1 (TGF-β1) (Q.

Liu et al., 2022). ROCK2 inhibitor associated reduction in TGF-β1 and α-SMA is consistent with other investigations of ROCK2 inhibitors functioning as anti-fibrotics (Nagai et al., 2019; Shah & Savjani, 2016). Figure 37 below summarises the novel actions of KD025 and ROCK2 inhibition in the studies discussed.

Figure 37 The mechanisms of action of the ROCK2 inhibitor KD025 in disease pathology. The drug has become most well-known for its clinical applications as an anti-inflammatory drug in GVHD. Original artwork inspired by (Cutler et al., 2021), (Flynn et al., 2016),(Fu et al., 2023), (Q. Liu et al., 2022), (Lee et al., 2014).

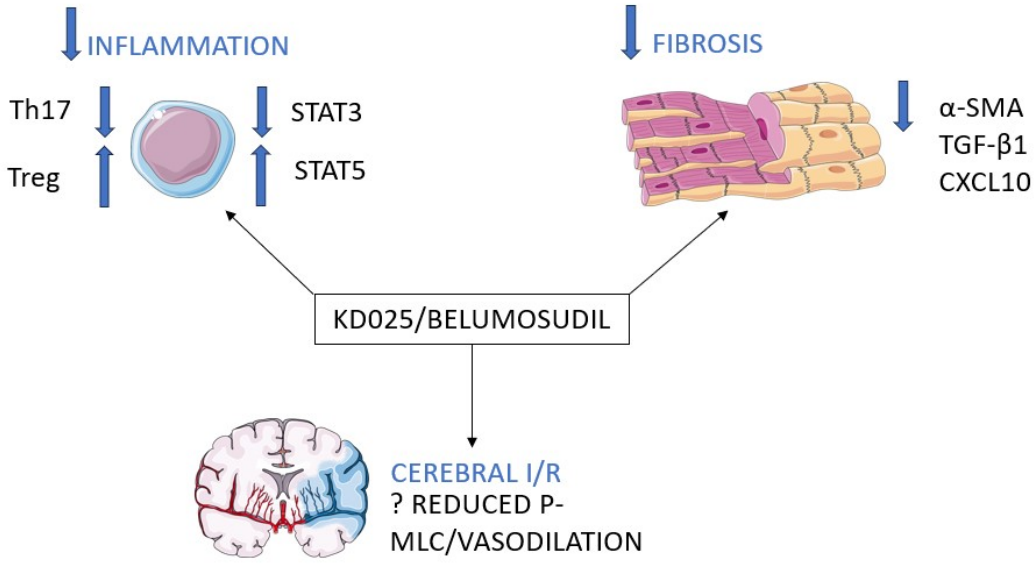

It is important to clarify the reasons for choosing to investigate the selective ROCK2i, KD025. Although GVHD and fibrosis are both chronic processes, the drug has been proven as effective in animal models of cerebral ischaemia (Lee et al., 2014). Its preferable side-effect profile and clinical safety rating, also make it worthy of investigation in further acute myocardial I/R experiments. The next set of experiments were planned to further

establish an optimal in vivo dose of KD025 in a closed chest model (dose-response). These studies were also used to try to ascertain a non-lethal dose of Fasudil, for comparison, and to establish whether doses <10mg/kg would be effective.

5.2: DOSE RESPONSE STUDIES OF FASUDIL AND KD025 (SELECTIVE ROCK2 INHIBITOR) IN A CLOSED CHEST RAT MODEL

i. Objectives

1. To establish an appropriate non-lethal dose of Fasudil (ROCK1/2 inhibitor) and optimal dose range for KD025 (selective ROCK2 inhibitor) for further in vivo I/R experiments
2. To record the haemodynamic responses in a closed chest rat model for the above ROCKi

ii. Methods

The in vivo experiments described in this section were performed by Dr David He. Experiments were designed and analysed by Dr Lucie Pearce.

Animals

Animals were handled according to section 3.1. Adult male Sprague-Dawley (SD) rats were selected for these experiments (250-350g). Induction anaesthesia was performed and maintained with 100mg/kg phenobarbital, after which animals were intubated and ventilated with room air and oxygen.

In vivo closed chest model (blood pressure dose-response)

After anaesthesia, intubation and ventilation, male SD rats (250-350g) were administered increasing doses of either Fasudil (1-10mg/kg) or KD025 (220mg/kg) or an escalating matched volume of DMSO control (0.2-2mls/kg) (Table 11). Increasing doses of ROCKi or DMSO control were administered via the i.p route every 15-minutes and mean arterial blood pressure (MAP) were recorded at each interval. ROCKi doses were administered cumulatively to achieve the final doses specified and blood pressure was monitored for a total of 60-minutes. The chest was not opened during these experiments and ischaemia/reperfusion was not performed. Therefore, these experiments were solely haemodynamic studies. The dose -response experiments were conducted firstly, with maximum DMSO volume of 2mls/kg, to try to ascertain whether this volume of solvent was contributing to a drop in MAP (mmHg) in absence of I/R (Table 11). Moreover, it was important to deduce whether these drugs alone can cause a drop in MAP, or whether this was attributable to their combination with I/R, in chapter 4. Determining this would be important to avoid further mortality in upcoming studies.

Chemicals

10mg of KD025 was purchased from MedChem express and dissolved in 1ml 100% DMSO (stock solution of 10mg/ml). MedChem specifies the maximum solubility of KD025 in DMSO to be at a concentration of 250mg/ml and for Fasudil 90mg/ml. 10mg of Fasudil hydrochloride was purchased

from MedChem Express and dissolved in 2mls 100% DMSO to give an initial stock solution of 5mg/ml. Stock solutions were pipette measured and drawn up and administered using a fine bore insulin syringe (0.5ml).

Table 11 Protocol for drug administration during closed chest dose response experiments. The concentration of both ROCKi and cumulative stock volume added are demonstrated below for a 300g animal (n=3). Fasudil stock 5mg/ml, KD025 stock 10mg/ml. Table sub-rows define individual treatment groups. G1: Group 1, G2: Group 2, G3: Group 3

TIME (min)	DRUG	CUMULATIVE DOSE	CUMULATIVE VOLUME STOCK SOLUTION
15 minutes	G1: Fasudil	1mg/kg	60µL
Dose 1	G2:KD025	2mg/kg	60µL
	G3: DMSO	0.2ml/kg	60µL
30 minutes	G1: Fasudil	3mg/kg	180µL
Dose 2	G2:KD025	6mg/kg	180µL
	G3: DMSO	0.6ml/kg	180µL
45 minutes	G1Fasudil	10mg/kg	600µL
Dose 3	G2:KD025	20mg/kg	600µL
	G3: DMSO	2ml/kg	600µL

iii) Results

In absence of I/R, Fasudil at a cumulative dose of 10mg/kg in 2mls/kg of DMSO, reduced MAP to a minimum value of 61mmHg at 50 minutes (5 minutes post dose 3 of drug administration, (Figure 38). This was the lowest reading obtained during the experiment and this correlates with haemodynamic data from the Fasudil results in chapter 4 during I/R. Minimum MAP following cumulative additions of KD025 was slightly higher, although overall MAP range was similar between groups.

It was observed during these experiments that cumulative additions of DMSO (in absence of I/R) also appeared to reduce MAP throughout the course of the experiment, to the extent that MAP ranges between DMSO animals and animals receiving Fasudil were not significantly different (Figure 38). All animals survived this first set of closed chest experiments and there were no hypotensive crises observed.

In response to these DMSO observations, further blood pressure closed chest experiments were planned with a reduced volume of DMSO. To enable a smaller volume of DMSO to be used for a given drug concentration, higher stock concentrations of KD025 (50mg/ml), and Fasudil (10mg/400µL) were prepared (Table 12, n=4). The Results of these second set of experiments with low volume DMSO are shown in Figure 39. Two main observations can be derived from these later results 1) reducing the total volume of DMSO appears to improve the overall MAP range in the

control group and the KD025 group. However, reducing the DMSO volume appears to do little to mitigate the hypotensive effects of Fasudil.

Figure 38 Dose response curve (MAP, mmHg) in response to increasing doses of ROCKi or DMSO control (n=3) Each drug was administered to individual animals in the absence of ischaemia/reperfusion (closed chest model). Protocol for drug quantity defined by table 11.

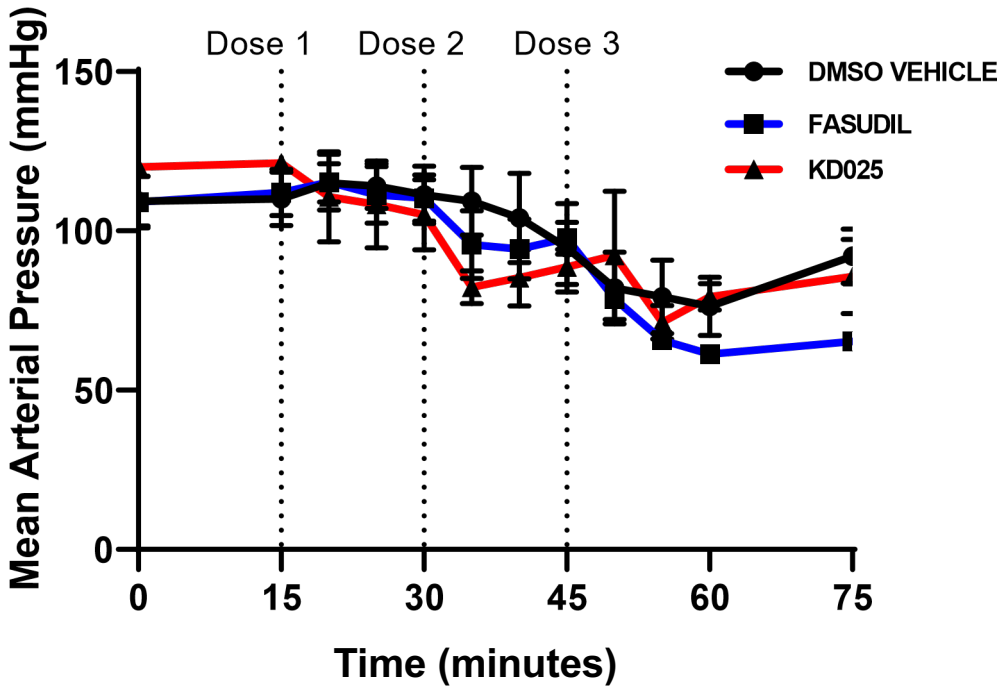

MAP (mmHg)	DMSO VEHICLE	FASUDIL	KD025	P VALUE DMSO VS FASUDIL	P VALUE DMSO VS KD025
MEAN ± SEM	100.0±4.1	93.1±5.8	95.9±4.8	0.54	0.80
MIN ± SEM	76.3±4.1	61.3±5.8	71.3±4.8	0.08	0.70
MAP RANGE ± SEM	38.7±4.1	54.0±5.8	50.0±4.8	0.08	0.21

Table 12 Protocol for drug administration during dose response experiments. The concentration of both ROCKi and cumulative stock volume are demonstrated below for a 300g animal (n=4). Fasudil stock 10mg/400µL, KD025 stock 50mg/ml. Maximum volume of DMSO 400µL/kg. G1: Group 1, G2: Group 2, G3: Group 3

TIME (min)	DRUG	CUMULATIVE DOSE	CUMULATIVE VOLUME STOCK SOLUTION
15 minutes	G1: Fasudil	1mg/kg	12µL
	G2:KD025	2mg/kg	12µL
	G3DMSO	40µL/kg	12µL
30 minutes	G1: Fasudil	3mg/kg	36µL
	G2:KD025	6mg/kg	36µL
	G3: DMSO	120µL/kg	36µL
45 minutes	G1: Fasudil	10mg/kg	120µL
	G2:KD025	20mg/kg	120µL
	G3DMSO	400µL/kg	120µL

Figure 39 Dose response curve (MAP, mmHg) in response to increasing doses of ROCKi or DMSO control (n=4) Each drug was administered to individual animals in the absence of ischaemia/reperfusion (closed chest model). Protocol for drug quantity defined by table 12 – utilising a smaller volume of DMSO.

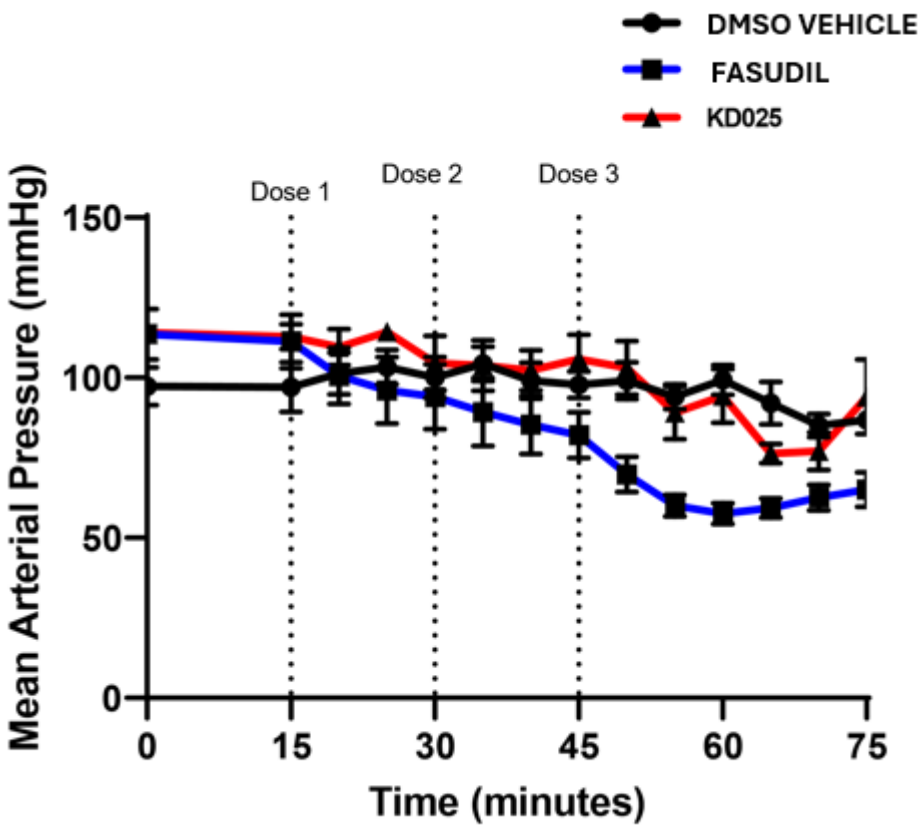

MAP (mmHg)	LOW VOLUME DMSO VEHICLE	FASUDIL	KD025	P VALUE DMSO VS FASUDIL	P VALUE DMSO VS KD025
MEAN ± SEM	96.9±1.5	81.8±5.2	100.0±3.3	0.01*	0.81
MIN ± SEM	85±1.5	57.5±5.2	76.3±3.3	<0.0001****	0.23
MAP RANGE ± SEM	19.2±1.5	56.0±5.2	38.0±3.3	<0.0001****	0.005**

Iv) Conclusions

In these closed chest experiments all drug doses evaluated were non-lethal, however Fasudil at a cumulative dose of 10mg/kg induced an unacceptable hypotensive effect in both sets of experiments, (irrespective of DMSO volume). In the second set of experiments, MAP range following the addition on KD025 was more acceptable, compared to the first set of closed chest experiments. For DMSO alone, a smaller MAP range was observed with the new lower volume (Figure 39) compared to the first set of experiments.

Following these optimisation studies, it was decided to further investigate Fasudil at a lower concentration of 3mg/kg, and KD025 20mg/kg in the next set of I/R experiments using low volume DMSO solvent (400μL/kg). If there were no significant haemodynamic effects with these doses of KD025, then KD025 at a high dose concentration of 100mg/kg would also be tested, consistent with previous literature (Lee et al., 2014).

5.3: THE SELECTIVE ROCK2 INHIBTIOR KD025 DOES NOT REDUCE INFARCT SIZE BUT DOES REDUCE MVO IN AN IN VIVO RAT MODEL OF ISCHAEMIA/REPERFUSION

i) Objectives

1. To investigate the effects of low dose Fasudil (3mg/kg) on IS% and MVO% in an in vivo rat model of ischaemia/reperfusion

2. To investigate the effects of the selective ROCK2 inhibitor KD025, on IS% and MVO% in an in vivo rat model of ischaemia/reperfusion

ii) Methods

All animal handling and in vivo protocols were as described in chapter 4 (section 4.2). Following the results of the above closed chest dose response experiments (5.1) further experiments were performed to investigate the effects of low dose Fasudil (3mg/kg) and the ROCK2 inhibitor KD025 (20100mg/kg) on IS% and MVO%. 3mg/kg of Fasudil or 2-100mg/kg of KD025 were administered 15-minutes prior to reperfusion via the I.P route in male SD rats (250-350g) undergoing ischaemia/reperfusion (Figure 32). The compound KD025 was purchased from MedChem Express and diluted in DMSO as per the manufacturer's recommendations. DMSO control was prepared to a

volume of 400μL/kg. For multiple group experiments, data was confirmed to be parametric using Shapiro-Wilk's test (GraphPad Prism©). Statistical significance was determined by a one-way ANOVA with post-hoc multiple comparisons test. Power calculations for ischaemia/reperfusion experiments were as described in section 4.2.

iii) Results

Figure 40 & Figure 41 A-D demonstrates the effects of Fasudil (3mg/kg) or KD025 (20-100mg/kg) on A) infarct size%, B) MVO% and C) IMH%. Figure 41 panel D demonstrates that there were no significant differences recorded in the area at risk (AAR%) between treatment groups compared to DMSO control ($p>0.05$). None of the drugs evaluated significantly reduced IS% (panel A) unlike Fasudil 10mg/kg. However, lower dose Fasudil 3mg/kg did significantly reduce MVO% and IMH% (panels B & C). No animals died after receiving Fasudil 3mg/kg, and this was well haemodynamically tolerated (Table 13). KD025 was well haemodynamically tolerated and did significantly reduce MVO% and IMH% compared to DMSO control (Table 11,Figure 41).

*Table 13:The effects of Fasudil (3mg/kg) or KD025 (20-100mg/kg) on infarct size%, MVO% and IMH%, *p<0.05, **p<0.01*

MEAN ±SEM	VEHICLE n=5	FASUDIL 3MG/KG n=6	KD025 20MG/KG n=6	KD025 100MG/KG n=8
IS% (AAR)	48.3±4.9	40.0±6.8	43.4±3.3	43.7±5.5
MVO% (AAR)	32.2±1.8	19.2±4.1*	22.0±1.7	21.8±2.5*
IMH% (AAR)	41.8±2.4	24.1±3.8**	29.8±3.0*	28.3±2.6*
AAR% (LV)	44.2±1.8	50.0±3.2	47.2±3.9	40.8±4.4

DUNNETT'S MULTIPLE COMPARISONS GROUP	ADJUSTED P VALUE IS%	ADJUSTED P VALUE MVO%	ADJUSTED P VALUE IMH%	ADJUSTED P VALUE AAR%
DMSO vehicle vs Fasudil 3mg/kg	0.60	0.01*	0.002**	0.66
DMSO vehicle vs KD025 20mg/kg	0.87	0.06	0.04*	0.90
DMSO Vehicle vs KD025 100mg/kg	0.87	0.04*	0.01*	0.86

Figure 40The effects of low dose Fasudil (3mg/kg) or KD025 (20-100mg/kg) on IS% (A), and MVO% (B), Vehicle n=5, Fasudil 3mg/kg n=6, KD025 20mg/kg n=6, KD025 100mg/kg n=8

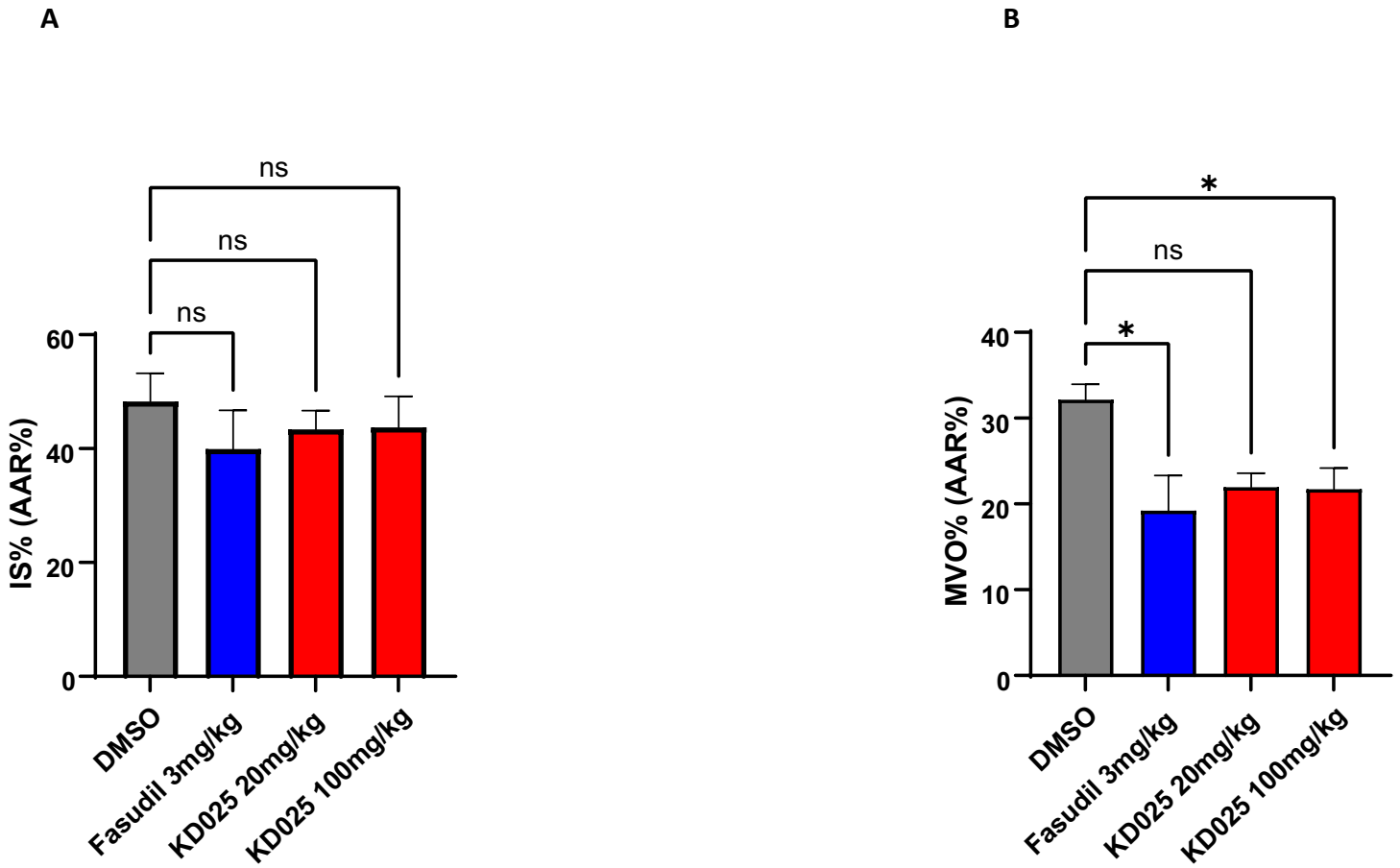

Figure 41. The effects of low dose Fasudil (3mg/kg) or KD025 (20-100mg/kg) IMH% c) or AAR% (D). Vehicle n=5, Fasudil 3mg/kg n=6, KD025 20mg/kg n=6, KD025 100mg/kg n=8

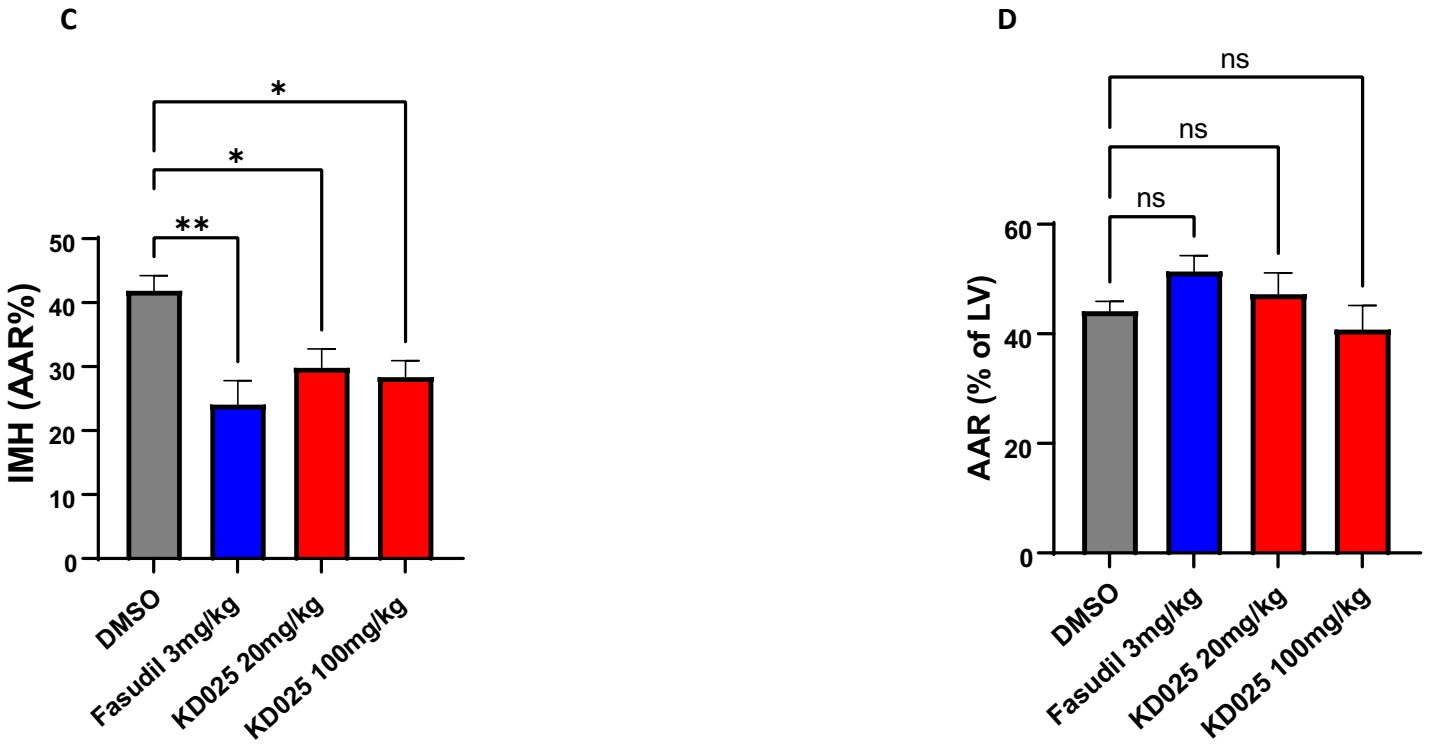

Table 14. MAP (mmHg) and HR (BPM) values throughout course of I/R experiments. MAP relates to the mean value across the entire experiment course of I/R from 0-180 minutes.

MAP (mmHg)	DMSO (n=5)	Fasudil 3mg/kg (n=6)	KD025 20mg/kg (n=6)	KD025 100mg/kg (n=8)
MEAN+/-SEM	84+/-2.3	78+/-3.6	88+/-2.3	92+/-2.9
MIN+/-SEM	70+/-11.1	62+/-4.1	76+/-4.5	80+/-4.5
MAP RANGE	33	54*	33	36

HR (BPM)	DMSO (n=5)	Fasudil 3mg/kg (n=6)	KD025 20mg/kg (n=6)	KD025 100mg/kg (n=8)
MEAN +/SEM	400+/-4.6	428+/-3.1	438+/-1.6	432+/-5.3
MIN +/-SEM	374+/-9	405+/-11	428+/-9	406+/-9
HR RANGE	67	55	21**	75

Table 14 demonstrates the effects of Fasudil and KD025 on mean arterial pressure (MAP) mmHg and HR (BPM) during the I/R experiments. Values were compared using a 2-way ANOVA with Dunnett's multiple comparisons test, to compare each drug with DMSO control. Whilst there were no significant differences identified between mean and minimum MAP values, there was a significant difference in MAP range identified between Fasudil 3mg/kg and DMSO control* ($p=0.02$), however other values were not significantly different ($p>0.05$). Baseline HR readings were significantly different between groups ($p=0.01$). HR range was significantly less in the KD025 20mg/kg group compared to DMSO control** ($p=0.007$), suggesting that this group maintained a more stable HR overall. The KD025 20mg/kg group had the lowest MAP range and was comparable to control (Table 14).

iv) Conclusion

When I/R experiments were repeated with a smaller volume of DMSO and lower doses of Fasudil, cardio protection was achieved with respect to MVO% and IMH%. None of the ROCKi evaluated matched the infarct limiting effects of Fasudil 10mg/kg. Given that all animals survived, Fasudil 3mg/kg and KD025 at all doses were better haemodynamically tolerated and may be even associated with positive chronotropic effects considering the haemodynamic results for KD025 20mg/kg. This dose of KD025, however, did have the most limited effects on cardio protection with statistical significance demonstrated only in the IMH% category (Figure 41).

V) Next experiments

It has previously been demonstrated that Fasudil can reduce the arterial vasospasm of aortic rings (Chapter 4), although the drug is of low potency. The vasoactive properties of selective ROCK2i's such as KD025 however, are unknown. In these in vivo experiments, KD025 has significantly reduced the vascular phenomenon of NRF and IMH%. However, it has not been established whether these effects are secondary to vasodilation or another vascular phenomenon.

Although such experiments would not directly prove a mechanism of action for the in vivo findings, further experiments using the aortic ring model of vasospasm were designed to test the vasoactive properties of ROCK2i.

5.4: KD025 (A SELECTIVE ROCK2i) DOES NOT EFFECTIVELY REDUCE ARTERIAL VASOCONSTRICTION OF RAT AORTIC RINGS

i) Objectives

1. To demonstrate that ROCK2 mRNA is expressed in rat aorta tunica media
2. To investigate the vasoactive effects of KD025 (selective ROCK2i) in rat aorta using a wire myography model

ii) Methods

RNAscope experiments

RNA scope experiments as described in chapter 3 were repeated according to protocol, with healthy rat aortic rings, to confirm the presence of ROCK2 mRNA expression within the tunica media. The purpose of this was to demonstrate that ROCK2 is present in aorta, as it was demonstrated to be present in coronary arteries, in whole heart sections (Figure 16). All methods including animal handling, were as described in chapter 3, however amendments were made to target retrieval and protease plus application steps, to adjust for the fragile nature of aortic ring tissue and to limit chemical destruction. Target retrieval was instead performed for 10-minutes, and protease plus was applied for 15 (and not 30) minutes. All other probes and fluorophores were applied as per chapter 3 protocol, and slides were visualised under confocal microscopy, as part of this qualitative analysis.

Aortic ring wire myography model

Animal handling and myography methods for this chapter are as described above in chapter 4.2 part ii). Healthy rat aortic rings were isolated and dissected as described previously. Rings were treated with 60mM KCL, 1μM PE and 10μM Ach as per protocol in Figure 22, Following a second 1μM PE constriction, aortic rings were treated with increasing concentrations of KD025 [10^{-9}-10^{-5}] (n=5), to investigate its vasoactive properties. Rings were treated every 4-minutes. As for in vivo studies, KD025 was dissolved in 100% DMSO as stock solution (purchased MedChem Express). However, rings were treated so that not > than 0.1% DMSO concentration was present in each 45ml water bath to avoid tissue toxicity (Galvao et al., 2014). Although KD025 was the main agent being investigated, for comparison of vasoactive properties, a second potent inhibitor of ROCK2i 'Chroman 1' was also prepared in DMSO solution and used in these aortic ring myography experiments in a separate treatment group. This second ROCK2i will be introduced in detail in the next chapter. It is included here, as these experiments were performed together.

Chroman 1 (purchased MedChem Express) is a ROCK1/2 inhibitor with an IC_{50} for ROCK2 of 1pM, and an IC_{50} for ROCK1 of 52pM. It is therefore more potent as a ROCK2 inhibitor than KD025, but less selective for ROCK2 (Chen et al., 2011). Aortic rings were treated with [10^{-12}-10^{-5}]M Chroman 1 every 4minutes, to observe for aortic ring relaxation. Relaxation was calculated as previously by the formula detailed in Figure 23. n=2 aortic

rings in the Chroman 1 group were treated down to minimum concentrations of 10^{-12} due to the high potency of the drug. A remaining n=5 aortic rings were treated from concentrations of [10^{-9}-10^{-5}] M (total n=7 rings). A 3rd group of aortic rings were treated with matched concentration DMSO control for respective drug doses [0.01-0.1%] (n=5) (Table 15). A DMSO control group is required, as this compound has previously been demonstrated to have weak vasodilatory properties, at concentrations of > 0.1% in a study by (Kaneda et al., 2016).

Table 15 Protocol for aortic ring experiments demonstrating the concentrations of each ROCK inhibitor investigated (n=5 DMSO, KD025, n=7 Chroman 1)

	WB1	WB2	WB3
DRUG	DMSO CONTROL	KD025	CHROMAN 1
REPORTED IC_{50} ROCK2	N/A	102nM	1pM
[CONC RANGE] M	0.01-0.1%	10^{-9}-10^{-5}	10^{-12}-10^{-5}

Statistical methods

Guidelines from the following vascular standards statement were adhered to when expressing results for statistical analysis (Wenceslau et al., 2021). Vasodilator responses are expressed as dose response curves, where X is increasing Log concentration of vasodilator dose, and Y is % relaxation. If data passed Log normality testing, non-logistic regression analysis was performed with a 4-parameter curve fit generated by GraphPad Prism©

Software and the $LogEC_{50}$ (concentration at which aortic rings were dilated to 50% of maximum) was automatically calculated. Statistical power was determined by the following formula: - [sample size = 2 SD^2 $(Z^{\alpha/2} + Z^{\beta})^2/d^2$], where SD = standard deviation, D= main effect size, and Z values which correspond to a type 1 error of 5% and 0.80 power. These experiments were powered to 0.80, which required n=5 animal aortas per experiment, based on data from previous pilot experiments in our lab (A Jamieson, 2018).

iv) Results

Figure 42 RNAscope image of rat aorta clearly demonstrating ROCK2 mRNA (purple) within the tunica media and ROCK1 mRNA (green) within the endothelial and elastic lamina layers. DAPI – (turquoise).

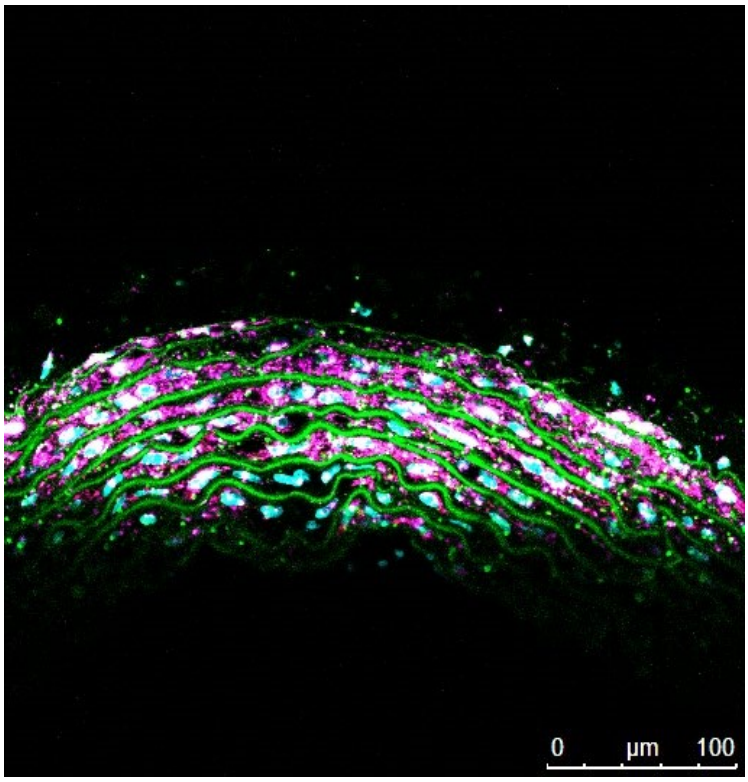

Figure 43 A) KD025 [10-9-10-5]M does not induce vasodilation of endothelial intact aortic rings (n=5). B) Chroman 1 [10-12-10-5]M induced dose dependent vasodilation of rat aortic rings to a maximum relaxation of 107% (n=7). Dose response curves have been 1) log transformed and 2) transformed for (Y=Y-K), where K is mean matched values for a DMSO control group.

A

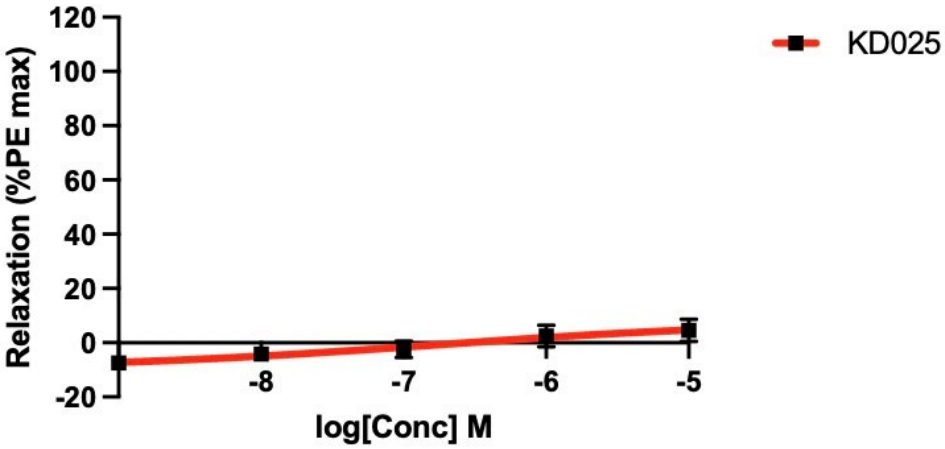

B

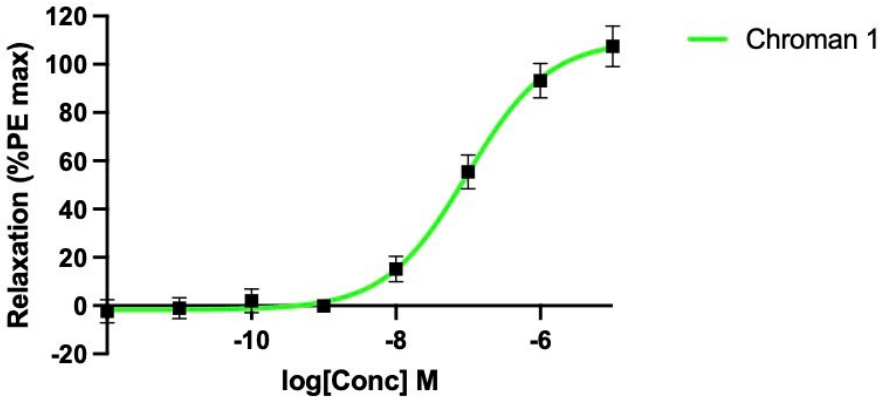

Table 16% Relaxation values for KD025 and Chroman 1 treated aortic rings (n=5, n=7). Table represents data log transformed and transformed for (Y=YK) where K is matched mean DMSO control group values.

LOG [CONC] M	MEAN RELXATION (%) KD025 ± SEM n=5	MEAN RELAXATION (%) Chroman 1 ± SEM n=7
10[-12] n=2		-2.3±4.8
10[-11] n=2		-1.0±4.4
10[-10] n=2		2.0±4.9
10[-9]	-7.5±0.3	-0.14±2.7
10[-8]	-4.3±1.4	15.1±5.3
10[-7]	-2.6±3.1	55.4±7.0
10[-6]	2.5±4.0	93.2±7.1
10[-5]	4.5±4.2	107.4±8.4
Best fit $LogEC_{50}$	n/a	-7.0, R^2=0.93
Emax (%)	4.5	107.4

v) Conclusion

Despite rat aorta clearly expressing ROCK2 mRNA, the most selective ROCK2 inhibitor examined, KD025, did not induce relaxation of aortic rings at concentrations [10^{-9}-10^{-5}'] M. The less selective, but more potent, ROCK2 inhibitor, Chroman 1 did induce dose dependent vasodilation of aortic rings with an estimated LogEC50 of -7.0; a value comparable to that of Ach. Chroman 1 has demonstrated a potency greater than Fasudil ex vivo, and therefore will be considered in the next set of in vivo experiments.

5.5 CHAPTER DISCUSSION

i) The selective ROCK2i, KD025 reduces MVO% and IMH% in vivo, but does not reduce myocardial infarction size

Replacing Fasudil (ROCK1/2 inhibitor) with a more selective ROCK2 inhibitor (KD025), did not improve myocardial infarction size following I/R, however, it did improve MVO% and IMH%. These findings are not entirely in keeping with the previously reported results from Lee et al (Lee et al., 2014) who investigated KD025 in cerebral I/R, here, KD025 reduced cerebral infarction size (Lee et al., 2014). If KD025 had successfully inhibited ROCK2 (not proven by this work) then it might be reasonable to propose that, ROCK1 is the most important isoform in myocardial infarction, with respect to IS%. There is some literature to support this suggestion, which implicates the ROCK1 isoform in the cell death cycle (Shi & Wei, 2007), particularly with respect to the regulation of phosphatase and tensin homolog (PTEN) and p-AKT, (AKT being an integral part of the RISK pro survival pathway (Rossello et al., 2017). The fact that Fasudil (ROCK1/2i) at 10mg/kg reduces infarct size, here, and in numerous other pre-clinical studies, is in keeping with this (Huang et al., 2018b). However, Fasudil at a dose of 3mg/kg did not reduce infarct size, as compared to the 10mg/kg dose observed in chapter 4, however, it did have a significant effect in reducing MVO% and IMH% in these experiments.

It is not possible to deduce from these results whether that is because MVO% and IMH% are an early marker of cardioprotection (detectable

before IS% becomes significant) or whether they are two distinct pathological processes, - one being cardiomyocyte related, and the other a purely vascular phenomenon. It has already been proven in studies of cardioprotection, that pro-survival pathways can be induced in I/R studies of cardiomyocytes alone (Rossello et al., 2017), however there is less literature on I/R studies of cell survival pathways in the isolated vasculature. One of the main reasons why these experiments can be more challenging, is that arterial vessels are felt to have much greater resilience to hypoxia than cardiomyocytes and are likely to demonstrate functional damage far earlier than apoptosis or pyroptosis (Hausenloy, Chilian, et al., 2019). This does support the rationale for performing the ex vivo functional vascular experiments; however, it might be useful in future work to extend these to include models of hypoxia/reoxygenation in isolated vasculature and measure cell death. In absence of this, I/R is simulated via vasoconstrictors such as PE and endothelin 1.

If two separate mechanisms are at work and IS% and MVO% outcomes can exist independently of one another, then the ability of KD025 to reduce MVO% and IMH%, would need to be explained. It is not suspected that any anti-fibrotic process has occurred in this model of acute myocardial infarction, as this is a chronic process (Q. Liu et al., 2022). Moreover, KD025 may have induced anti-inflammatory effects (which are known to be involved in the phenomenon of NRF, e.g., neutrophils/platelets (Heusch, 2019)) however it is well acknowledged that most of the inflammation occurring in acute MI occurs in a second phase of I/R injury (Hausenloy & Yellon, 2010),

(Shah et al., 2022). Nevertheless, it is possible that ROCK2i with KD025 has reduced inflammation via early neutrophil responses, and cytokine signalling which has mitigated the NRF. The latter of which has been proven in other disease pathologies (Cutler et al., 2021). Another possible explanation for a reduction in MVO and IMH, is that KD025 improves endothelial barrier function permeability. This was not examined in these experiments, nor has it been examined in the heart, however KD025 does improve vascular barrier function in the lungs (Lee et al., 2020).

As a suggestion to explain why these results do not match those observed by Lee et al in the brain (Lee et al., 2014), it is possible that KD025 has not demonstrated further cardioprotective effect for pharmacological reasons. Notably, PK studies were not performed separately here as part of this study. Therefore, it cannot be said with certainty that 20-100mg/kg of KD025 reached a therapeutic concentration in the plasma and myocardial tissue. However, in the work by Yoon et al (Yoon et al., 2020), 2mg/kg iv of KD025 was still detectable in the blood plasma of rats after 240 minutes, whereas these experiments were terminated at 180 minutes. Therefore, based on these former PK results, the drug should have still been present and at a higher concentration, given that the doses used in this study were higher and administered I.P. It would be expected that an intravenous drug would be eliminated much sooner via the iv route than via the i.p route (Bøtker et al., 2018). What is not known, is whether the drug was at a sub-therapeutic concentration in the latter stages of reperfusion. Future formal PK studies would be able to establish this.

ii) KD025 does not reduce arterial vasoconstriction of rat aortic rings nor demonstrate vasoactive potential

As all ROCKi are felt to inhibit smooth muscle contraction via RhoA/MYPT1/MLC signalling, it is surprising that KD025 at concentrations [10^{9}-10^{-5}] did not display vasoactive properties (Liao et al., 2007), (Loirand, 2015). Whereas there are lots of previous studies examining Fasudil in vascular reactivity, there are few other studies dedicated to the vasoactive abilities of ROCK2 inhibitors. This might indicate that the literature hypothesis, that both ROCK isoforms are similar in function, is incorrect. This may have represented a much earlier school of thought, which has been cast into question since the development of newer genetic KO models (Liao et al., 2007). The observations that KD025 did not vasodilate rat aortic rings, in an otherwise working model (as evidenced by the ROCK2i Chroman 1 as will be introduced in chapter 6) supports the clinical findings of the ROCKstar trial that some patients suffered hyper, and not hypotension, as a side-effect. In this work (especially for Fasudil) aortic ring response to ROCKi has closely correlated with the in vivo blood pressure responses following challenge with the drug.

One explanation for the above results, could be potential off-target effects of KD025 which are gaining more interest in the literature. Given its now wide clinical application, Park et al (Park & Chun, 2020) have recently attempted to identify downstream (non-ROCK pathway related) genetic targets of KD025. Genetic analysis via bioinformatics, has revealed

involvement of KD025 in stimulating both inflammatory and adipogenesis related pathways, which are distinct from ROCK signalling (Park & Chun, 2020). It is unclear at present which of these potential pathways might contribute to hypertension, which is a side effect not induced by other ROCKi. From an experimental perspective, ROCK2i was not confirmed here. However, whilst confirming ROCK activity is reduced by measuring changes to phosphorylation of MYPT1 would confirm ROCK inhibition had occurred, it would be extremely challenging to demonstrate that solely ROCK2 inhibition had occurred. Discrimination between ROCK1 and ROCK2 activity requires genetic KO models (Loirand, 2015). It was therefore decided to prioritise these techniques in future work as an alternative to measuring ROCK2 specific activity. Chroman 1 has clearly induced vasodilation, potentially via also inhibiting ROCK1 inhibition at the doses tested, or alternatively via other kinases. These Chroman 1 results will further be considered in the next chapter. It may also be the case, that the balance of ROCK1 and ROCK2 selectivity, is a key driver in vascular function. These results might indicate that moving away from ROCK1 selective compounds reduces vasoactive potential. It would be useful in this respect to test a highly selective ROCK1 inhibitor.

To summarise, the findings that KD025 does not reduce IS% but may reduce MVO% and IMH%, could generate many further hypotheses as discussed above. In the interest of clarity, it was decided to focus future experiments dedicated to the null hypothesis that the ROCK2 isoform is more important than ROCK1 in cardioprotection. Further in vivo work was first planned with the more potent ROCK2i, Chroman 1 (as this has

demonstrated vascular activity ex vivo at the doses tested) to be followed by a genetic ROCK2 KO model.

CHAPTER 6: THE EFFECTS OF THE POTENT ROCK2 INHIBITOR CHROMAN 1 ON ENDOTHELIN-1 INDUCED VASOCONSTRICTION AND CARDIO PROTECTION IN VIVO

6.1 : BACKGROUND

i) Introduction to the highly potent ROCK2i, Chroman 1

The previous chapter discussed how there has been an evolution towards selective ROCK2 inhibition in pharmacology, to improve therapeutic outcomes and reduce the side effects associated with ROCK1 inhibition (Shah & Savjani, 2016). In this regard, the clinical safety profile of KD025 has been discussed (Cutler et al., 2021), as have the many clinical trials of ROCK2i, involving multiple specialities including neurology, haematology, respiratory medicine, dermatology and rheumatology (Cutler et al., 2021), (Fu et al., 2023), (Zanin Zhorov et al., 2017), (Lee et al., 2014). Notably however, less ROCK2 research has taken place in cardiology and any prior cardiovascular research has largely been undertaken at a pre-clinical level (Q. Liu et al., 2022). In addition to the introduction of KD025, (a compound which is predominantly manufactured for its anti-fibrotic and anti-inflammatory effects) (Fu et al., 2023) other selective ROCK2 inhibitors have been synthesized to improve potency and increase downstream specificity for ROCK2 over other kinases including protein kinase A (PKA) (Shah & Savjani, 2016).

There are three regions where ROCK inhibitors can be manipulated to alter their potency and selectivity (Pan et al., 2019). Selectivity to ROCK2 from

molecular docking studies, is thought to be related to additional hydrogen bonding and hydrophobic regions within the molecule (Shah & Savjani, 2016). Newer ROCK2 inhibitors are being refashioned continuously, and there are many selective compounds on the market which have been synthesised even during this research (Fu et al., 2023).

One potent selective ROCK2 inhibitor is Chroman 1 (Yen Ting Chen 2011), which was first synthesised in 2011 from chroman-3-amides, formerly described by Chen et al (Chen et al., 2008) (Figure 44). Chroman 1 is therefore more potent than KD025 (IC_{50} of Chroman 1 for ROCK2 is 1pM and ROCK1 52pM). Chroman 1 also has activity against myotonic dystrophy kinase-related Cdc42-binding kinase (MRCKα) (IC_{50} of 150nM) which has similar downstream targets to ROCK (Zhao & Manser, 2015). MRCK enables the inhibition of MLCP in vascular smooth muscle and so acts in parallel to ROCK to enable vascular smooth muscle cell contraction (Zhao & Manser, 2015).

The efficacy of Chroman 1 was revisited in 2021 by Chen et al, when they performed further screening of multiple ROCK inhibitors to search for a therapeutic agent to prevent in vitro human stem cell death (Chen et al., 2021). The study, which was published in Nature methods, again noted the increased potency of Chroman 1 for ROCK2, and the investigators proposed that the drug should be trialled in place of another common and less potent ROCKi, Y27632 (ROCK1/2 inhibitor) which was, at the time, mainstay in stem cell research (Chen et al., 2021). The 2021 paper found that stem cell survival was greatly improved following treatment with

Chroman 1, as compared to Y-27632 and Fasudil (ROCK1/2 inhibitors). Interestingly, although Chroman 1 is known to be active in the picomolar concentration range, the investigators reported an approximate EC_{50} effect of the drug at log concentrations of 10^{-8} (mol) (Figure 45). This is interesting, as the same investigators performed a kinase 'hot spot' assay to determine that the IC_{50} of Chroman 1 for ROCK2 and ROCK1 was 1pM (10-^{12}) and 52pM (10^{-11}) respectively. The authors propose that Chroman 1 improves cellular survival via reducing myosin related cellular apoptotic contraction and cell blebbing (Chen et al., 2021). Whilst it useful to reduce vascular contractility in the right circumstances, it is less desirable to reduce cardiomyocyte contractility in the setting of myocardial infarction, as this could potentially lead to a decline in left ventricular function.

Given the promising vasodilatory effects that were observed in the previous experiments, and the reported increased potency of the drug, it was decided to proceed with further experiments, both ex vivo and in vivo, with Chroman 1 to ascertain whether this would improve IS% outcomes (in addition to MVO% and IMH%). Before these experiments, it is important that the vasodilatory properties of Chroman 1 are again considered. As prior experiments on the vascular myography apparatus had used phenylephrine (PE) as a standard vasoconstrictor, it was newly considered, that this may not be the best activator of the ROCK pathway, compared to other vasoconstrictors such as endothelin 1 (Kawarazaki & Fujita, 2021). Further literature was next explored below to further review the agonist activators of ROCK in VSMC.

Figure 44 The molecular structure of Chroman 1 a chroman-3-amide derivative. Reproduced from the original paper of Chen et al in 2011 (Yen Ting Chen 2011)

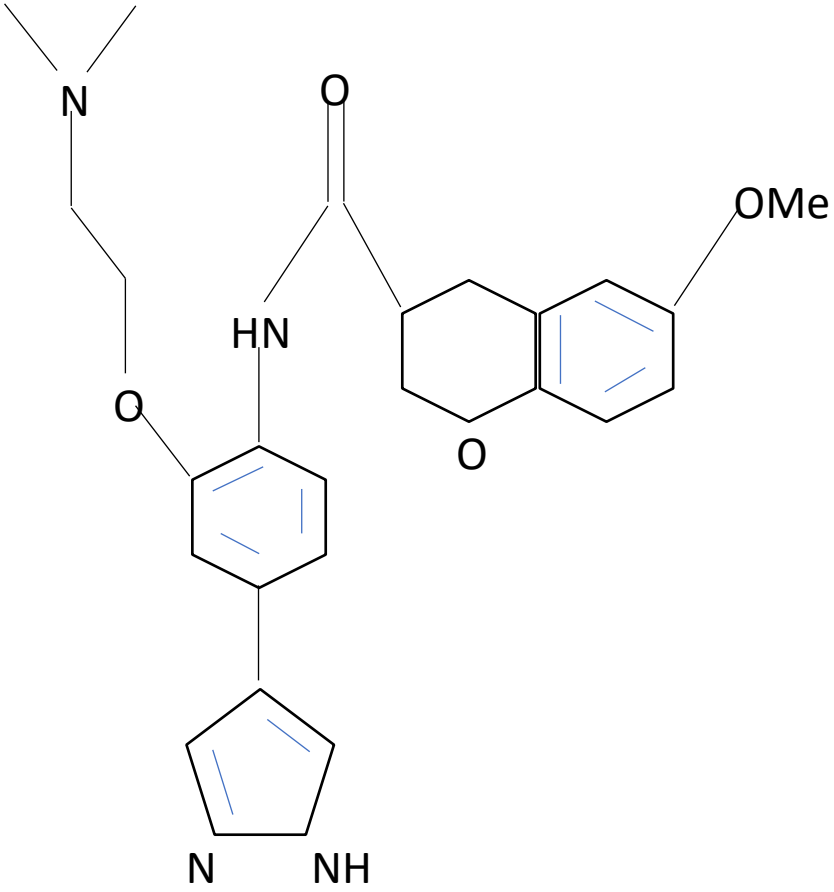

Figure 45–Chroman 1 demonstrated a greater potency for cell survival of human pluripotent stem cells, compared to other ROCK inhibitors. Illustration from Chen et al (Chen et al., 2021) (permission from Publishers has been granted).

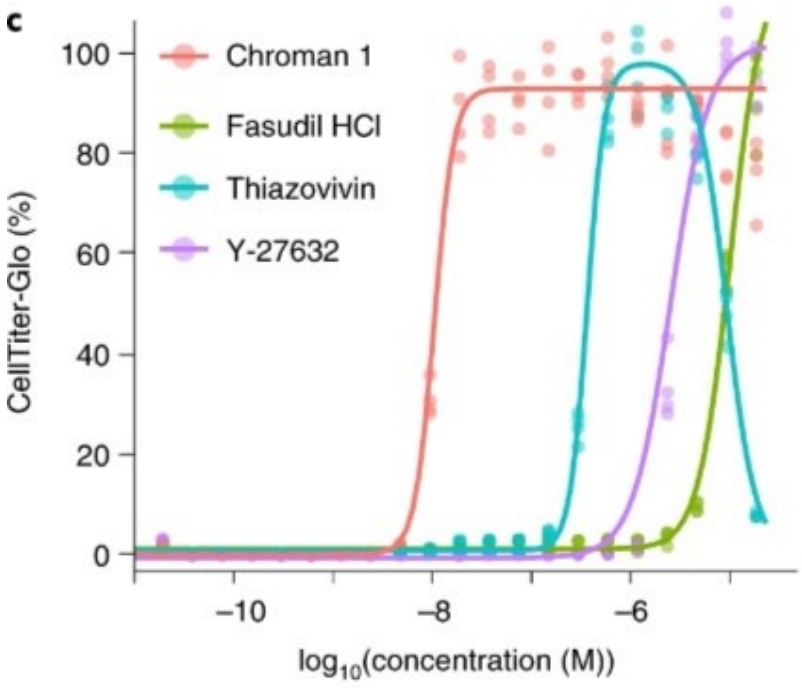

ii)ET-1/RhoA/ROCK mediated vasospasm

As an alternative to ex vivo hypoxia/reoxygenation, the functional vascular damage induced by myocardial infarction, has been simulated by inducing vasoconstriction with phenylephrine in a standard vascular myography model (chapters 4&5). Aside from the obvious limitation that this model utilises i.e. a conduit vessel and not the microvasculature; using PE as a vasoconstrictor may move further away from the physiological contractile responses seen in vivo during myocardial infarction and no reflow (Tona et al., 2023). For example, as has been discussed in chapter 1, it is known that other vasoconstrictors such as endothelin-1 (ET-1) more closely resemble

substances released by the injured vasculature during I/R, and ET-1 has been directly linked to causing coronary no re-flow (Tona et al., 2023), Moreover, ET-1 is released directly by damaged endothelium, whereas PE is part of a more general neurohormonal response governing vascular smooth muscle cell contraction (Niccoli et al., 2016). It is necessary then to consider agonist VSMC contraction in more detail. Chapter one has broadly considered this but has not explained specifically the selectivity of various vasoconstrictor agonists, concerning the ROCK pathway. Kawarzaki et al, describe ET-1 as being a direct activator of ROCK via RhoA (Gα12/13), whereas PE as a derivative of NE, may have more affinity for the alternate Gαq/11 Ca2+ dependent pathway of VSMC contraction (Kawarazaki & Fujita, 2021) (fig. 46).

Original research into agonist-induced VSMC by Gohla et al in 2000, discovered that both calcium dependent and sensitisation pathways are required for ET-1 mediated contraction (Gohla et al., 2000). However, when the G12/13 receptor (RhoA activator) was silenced in VSMC, ET-1 did not induce contraction in 90% of cells (Gohla et al., 2000). This would indicate that ET-1 mediated contraction (although utilising both pathways) enables most induced contraction via ROCK. Since this original research, further investigations have suggested that the two main pathways of VSMC contraction are perhaps not as distinct as initially thought. Discovery of the molecule cytosolic protein inhibitor 17 (CPI-17) (Figure 46) has demonstrated that the two pathways are intricately related and converge via phosphorylation of this molecule to enable inhibition of MLCP and

contraction (Ito et al., 2022) (Figure 46). It is therefore not possible without genetic models, to fully separate

ROCK mediated contraction from calcium dependent contraction. Tsai et al, 2022 agree that ET-1 stimulates ROCK specific contraction via RhoA in the coronary circulation and microvasculature (Tsai et al., 2017). Revisiting this study from chapter 1, in a TAC mouse model of myocardial pressure overload, ET-1, induced dose dependent contraction of coronary arterioles (Tsai et al., 2017). In healthy vessels, this process was not reduced by treatment with the ROCK inhibitor, H-1152, (IC_{50} for ROCK2 of 20nm). Vessels were however, treated with a H-1152 dose of 10nm which may have been sub-therapeutic (Tsai et al., 2017). H-1152 did reduce the additional ET-1 related vasoconstriction, seen in the TAC mice (Tsai et al., 2017). Therefore, this study suggested that ET-1 mediated RhoA activation and calcium sensitisation was present in disease pathology, but not healthy vasculature (Tsai et al., 2017).

To summarise - both important literature reviews and independent studies document an ET-1/RhoA/ROCK mediated pathway of arterial VSMC activation (Ivey et al., 2008; Tsai et al., 2017), and therefore ET-1 may be a more robust agonist to investigate in further models of arterial vasoconstriction. It was therefore decided to investigate the ability of ROCK2 inhibitors to reduce ET1 mediated contraction.

Figure 46The G12/13 RhoA/ROCK pathway (right) is activated by the agonists ET-1, ATII and TXA2. Conversely, the G-protein Gq11 calcium dependent pathway (left) is activated by most agonists including NE (left). Fasudil inhibits both pathways directly as it is also a ca Ca2+ channel blocker. Image inspired by from (Kawarazaki & Fujita, 2021), (Gohla et al., 2000).

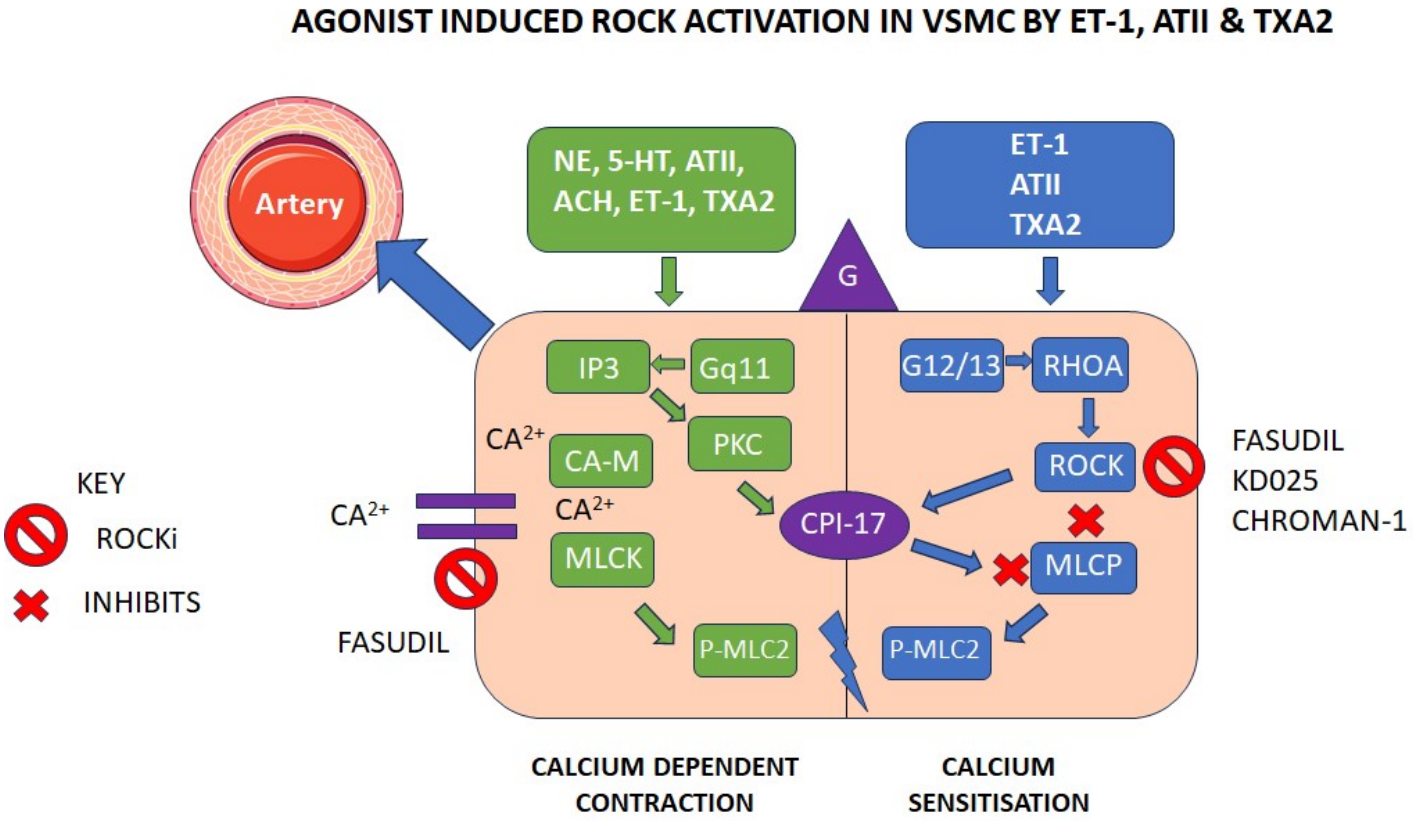

6.2: THE POTENT ROCK2 INHIBITOR CHROMAN 1 REDUCES ET-1 INDUCED VASOCONSTRICTION OF AORTIC RINGS

i) Objectives

1. To demonstrate that endothelin-1 (ET-1) is a potent vasoconstrictor of rat aortic rings

2. To demonstrate that the ROCK2 inhibitor Chroman 1, can attenuate ET1 induced vasoconstriction of rat aortic rings

ii) Methods

The aortic ring myography apparatus and buffers were set up as previously detailed in chapter 4. Animal handling protocols were followed as previously described, and male SD rats (250-350g) were selected for the experiments. Rats underwent terminal anaesthesia with phenobarbital as described in chapter 4, and the chest was opened and the aorta carefully removed from surrounding tissue, taking care not to damage the endothelium. For these set of experiments a slightly different protocol was applied compared to previous concentration, relaxation protocols which will now be described.

Testing different vasoconstrictors (n=5)

In the first set of experiments two known activators of ROCK (namely Endothelin-1 (ET-1) and angiotensin II (AT-II)), were prepared for

comparison against the previously used vasoconstrictor, phenylephrine (PE) (αadrenoreceptor agonist). ET-1 was purchased from Hello Bio© as a powder containing 500µg of peptide. ET-1 is fully soluble in saline buffer according to the manufacturer's instructions. AT-II was also purchased from Hello Bio© as a vial containing 100µg of powder and is also soluble in saline buffer. PE was used and prepared as previously described in chapter 4. Following aortic ring preparation, the rings were pre-constricted with 60mM KCL and allowed to reach their maximum contraction over 40-mimutes (protocol Figure 47) before KCL washout. Rings were allowed to equilibrate after washout and until baseline force level was achieved (mN).

Next, either PE, ATII or ET-1 at concentrations Log [10^{-9}-10^{-7}]M were added to each water bath in step wise increments every 6-minutes. ET-1 was tested to 10^{-7} in line with previous literature (Grisk et al., 2012) and due to the large quantity of ET-1 that this would require, higher doses were not utilised. These initial experiments were performed to confirm that these concentrations of the vasoconstrictors were adequate to reach a peak contraction, that was >70% KCL contraction. Concentration, contraction curves were then plotted, and contractile responses were compared between vasoconstrictors. Statistics and power calculations were applied as described in chapter 4, and as per vascular physiology best practice guidelines (Wenceslau et al., 2021).

Testing of ET-1 in ROCK2 inhibitor pre-treated aortic rings (n=5)

If constriction of aortic rings was observed following treatment with increasing concentrations of ET-1, a further set of experiments were planned to ascertain whether this vasospasm could be attenuated using ROCK inhibitors, including the potent ROCK2 inhibitor Chroman 1. The ROCK inhibitors Chroman 1, and Fasudil (ROCK1/2i) for comparison, were both prepared in 100% DMSO as a stock solution, alongside DMSO control vehicle. Ach was prepared as previously described to confirm the presence of endothelial function in the aortic rings. Stock solutions of ROCK inhibitors were prepared so that the concentration of DMSO in each individual water bath did not exceed 0.1%. Following KCL washout and stabilisation, aortic rings were pre-treated for 30minutes with either Chroman 1[10^{-7}], or Fasudil [10^{-5}] ($LogEC_{50}$ – parameter calculated from previous experiments) or matched concentration of DMSO vehicle (fig.49). As KD025 did not demonstrate vasodilatory properties previously, it was not possible to evaluate this drug in these experiments. Following 30-minutes of ROCKi treatment, aortic rings were treated with increasing concentrations log [10^{-7}-10^{-9}]M of ET-1 administered every 6 minutes (Grisk et al., 2012) (protocol shown **Error! Reference source not found.**).

Figure 47Experimental protocol for VMSC agonist treated aortic rings. Vessels are treated with 60mM KCL to achieve maximum contraction. KCL is washed out, and dose response contraction experiments are commenced with varying vasoconstrictors.

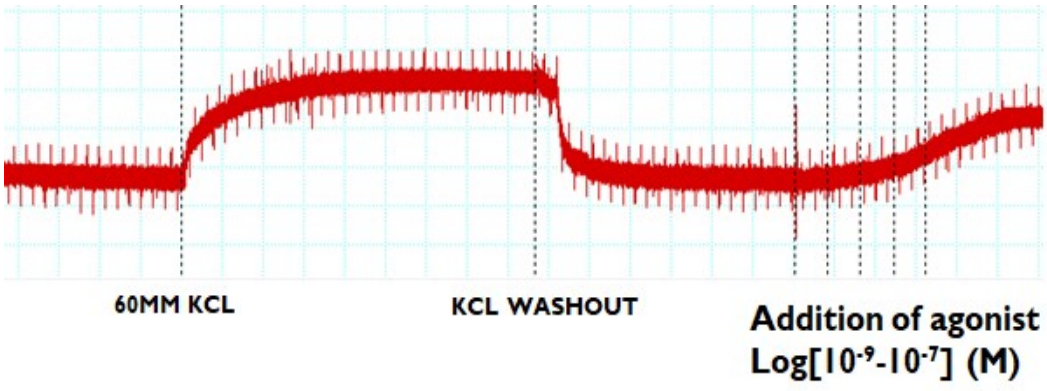

Figure 48Experimental protocol for VSMC agonist treated aortic rings with ROCKi pre-treatment. Vessels were first treated with 60mM KCL and washed out. To enable endothelial assessment, vessels were pre-constricted with 1μM PE and then treated with 10μM Ach to confirm endothelial function. PE and Ach were then thoroughly washed out and the rings were allowed to stabilise. Vessels were pre-treated with ROCKi or DMSO control for 30-minutes before ET-1 dose response experiments were performed every 6-minutes.

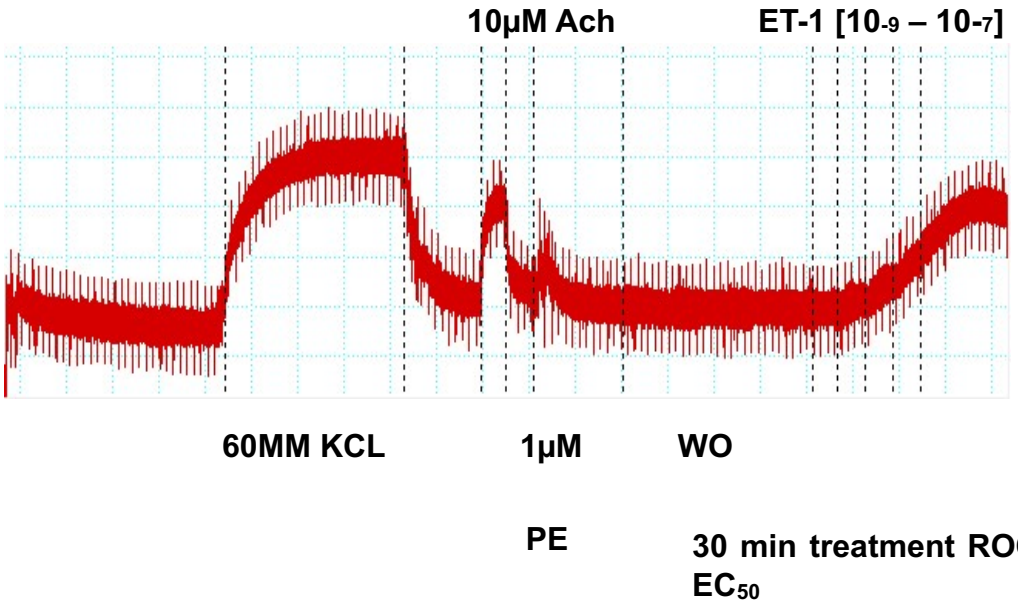

iii) Results

The 3 vasoconstrictor agents were investigated as described in the methods section and Figure 47. It was apparent that each agent produced a different dose response profile. AT-II produced a biphasic response (Figure 49) and reached a peak contraction at concentrations of approximately Log[-8]M. At greater concentrations of ATII, the contractile responses of the aortic rings were seen to diminish. ET-1 and PE followed a more typical dose-response pattern, however the Emax value of either curve was not reached at these concentrations. Given this difference in concentration curves for each vasoconstrictor, a 2-way ANOVA with mixed effects model was applied to log transformed data as an alternative to a non-linear regression model. This is an acceptable statistical method to use in vascular science (Wenceslau et al., 2021). Figure 49 demonstrates that the vasoconstrictor ET-1, induced the greatest contractile response (%KCL) compared to the more typically used PE, ($p<0.0001$).

Aortic rings were pre-treated with either ROCKi or DMSO control, prior to the addition of increasing concentrations of ET-1 Log [10^{-9}-10^{-7}]M (Figure 50). Following analysis with two-way ANOVA and mixed effects model, both ROCKi investigated, Fasudil and Chroman 1, attenuated ET-1 mediated contraction. However, these effects were greatest in the Chroman 1 treated aortic rings, suggesting that this was a stronger inhibitor of ET-1 induced vasoconstriction.

*Figure 49 Dose response curves for different vasoconstrictor agents in rat aortic rings (n=5). Original data was log transformed and transformed a second time for Y=Y-K, where K was mean contraction for an NaCL control group (n=5). *p=0.013 ET-1 vs PE, ****p<0.0001 ET-1 vs PE*

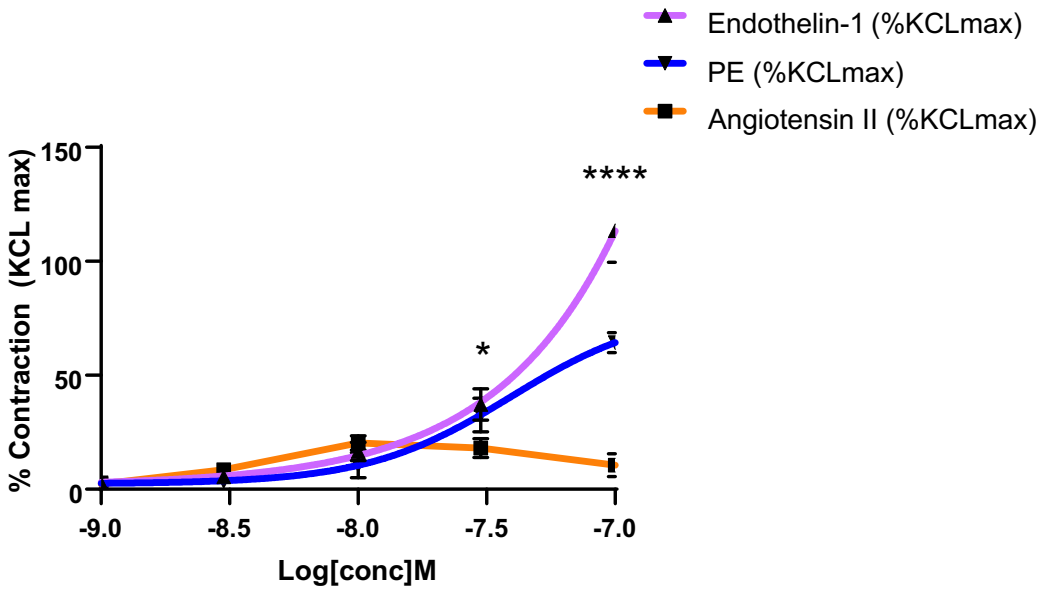

LOG [CONC] (M)	MEAN CONTRACTION ATII±SEM (%)	MEAN CONTRACTION PE±SEM (%)	MEAN CONTRACTION ET-1±SEM (%)
10-9	2.3±0.2	2.8±0.3	2.5±0.4
10-8.5	8.6±1.0	3.5±0.9	5.5±1.6
10-8	20.3±3.1	10.6±5.5	16.6±4.0
10-7.5	18.1±4.2	32.6±7.5	37.2±6.9
10-7	10.6±5.0	64.4±4.5	113.4±13.9

*Figure 50 Dose response curves for ROCKi vs DMSO control treated aortic rings prior to the addition of increasing concentrations of the vasoconstrictor ET-1 (n=5). *p=0.02 Fasudil vs control, **p=0.009 Fasudil vs control, ****p<0.0001 Fasudil vs control. ~~~~p<0.0001 Chroman 1 vs control (n=5).*

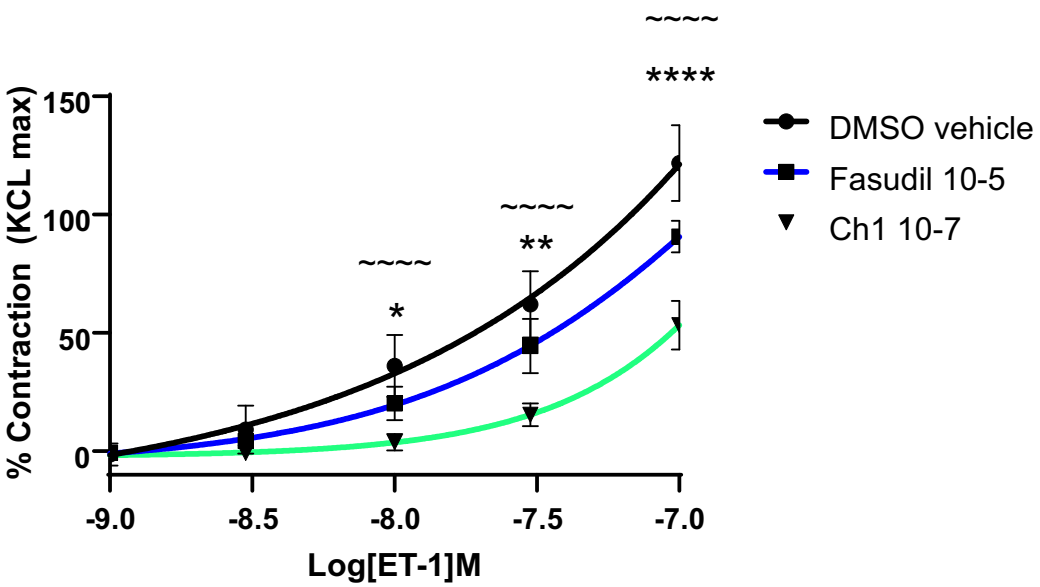

LOG [CONC] (M)	MEAN CONTRACTION DMSO VEHICLE±SEM (%)	MEAN CONTRACTION FASUDIL±SEM (%)	MEAN CONTRACTION CHROMAN 1± SEM (%)
10-9	-1.4±2.1	-0.5±0.3	-1.6±0.4
10-8.5	9.1±4.6	4.4±0.8	-0.7±0.5
10-8	36.1±5.8	20.2±3.5	3.8±1.6
10-7.5	62.1±7.0	44.4±5.8	15.4±2.1
10-7	121.8±8.0	90.7±3.4	53.2±4.6

iv) Conclusions

In a study of rat aortic rings, the peptide hormone ET-1 was demonstrated to induce significantly greater vasoconstriction compared to the previously used PE in pilot studies at the dose range tested. Despite ET-1 being a stronger vasoconstrictor of aortic rings, Chroman 1 (ROCK2i) was able to significantly attenuate this response. As ET-1 is implicated in the pathology of vascular injury during myocardial infarction and ROCK activation (Tona et al., 2023) Chroman 1 would therefore be a promising agent to test in further in vivo studies of MVO.

v) Next experiments

Chroman 1 has effectively demonstrated vasoactive potential in two studies of rat aortic rings, as described in chapters 5&6. This is likely via inhibition of a ROCK mediated VSMC agonist pathway, which leads to the active form of MLCP being expressed (Figure 46). However, it is not known whether ROCK2 inhibitors also reduce myocardial contractility. It is hypothesised that any drug that induces changes in myosin/actin binding and cytoskeleton organisation, may have the potential to affect this (Bers, 2002). This is undesirable in studies of acute cardioprotection, as a reduction in myocardial contractility would lead to a potential reduction in left ventricular ejection fraction. Further studies were planned to explore this, and to investigate the effects on LVEF% when rats were treated with the ROCK2i in vivo. Following the aortic ring model findings (which suggest that Chroman 1 might also acutely lower blood pressure) the next study was also a pilot study of haemodynamic effects of the drug in vivo, in absence of I/R.

6.3: THE HIGHLY POTENT ROCK2i CHROMAN 1 DOES NOT REDUCE LEFT VENTRICULAR SYSTOLIC FUNCTION IN VIVO (ECHOCARDIOGRAPHY STUDY)

i) Objectives

1. To perform closed chest in vivo experiments to investigate the haemodynamic effects of Chroman 1 in vivo and to establish a nonlethal dose range
2. To investigate the effects of Chroman 1 on left ventricular ejection fraction (LVEF%) using echocardiography

In these sets of experiments, intubation and anaesthesia was performed by Ms Liyana Yusof. All other aspects of the study including drug administration and echocardiography were performed independently by Dr Lucie Pearce.

ii) Methods

Haemodynamic studies

Male Sprague Dawley rats (250-350g) were handled and anaesthetised as per former protocol for the in vivo work in chapter 4&5. Experiments ran from 0-60 minutes and were undertaken in a closed- chest rat model. Chroman 1 was purchased from MedChem Express as in chapter 5 and was prepared in an original stock solution of DMSO to a concentration of

0.75mg/ml (high potency). Starting at 15 minutes, and then every 15 minutes, animals were administered either increasing doses of Chroman 1 stock solution (0300µg/kg) or a matched volume of DMSO control (Table 17). After the final cumulative dose was administered at 45-minutes, the experiment ran for a further 15 minutes to record final haemodynamic status. Heart rate (BPM), blood pressure (mmHg) and LVEF% were measured and recorded at baseline and at 15-minute intervals until the end of the experiment. The rationale for dose selection in the µg/kg range was due to the high potency of Chroman 1 for ROCK2 and ROCK1. There have been no other doses of Chroman 1 used in vivo for comparison. Given that Chroman 1 causes aortic ring vasodilation, it would seem reasonable to suggest that a drop in systemic blood pressure might indicate drug activity. As was the case for Fasudil, it is not desirable therapeutically to cause a MAP (mmHg) drop below an average of 70mmHg, this is based on commonly used clinical cardiological parameters and clinical opinion (Niccoli et al., 2019).

M-mode Echocardiography

In addition to blood pressure and heart rate, left ventricular ejection fraction (LVEF%) was measured at baseline and every 15 minutes throughout the experiment using M-mode echocardiography. After anaesthesia, the animal's chest was prepared so that the ECHO probe could image the thorax. Both parasternal long axis (PLAX) and parasternal short axis (PSAX) views were obtained to measure for each view: - left ventricular intraventricular septal diameter (IVS), left ventricular end diastolic volume (EDD), left ventricular end

systolic diameter (ESD) and the left ventricular posterior wall diameter (PWD) (Figure 51). The results of both PLAX and PSAX views were averaged to provide a final LVEF% from automated 2D calculation.

Table 17Protocol for Chroman 1 dose response experiments. A stock solution of 750µg/ml was prepared for Chroman 1 in 100% DMSO. A matched volume of either Chroman 1 stock or 100% DMSO was added every 15minutes to provide the cumulative doses described below for a 300g animal. Chroman 1 was added in cumulative dose increments of 30µg/kg, 100µg/kg, and 300µg/kg. Stock solution was pipette measured and administered using a fine bore insulin syringe (n=5).

TIME (min)	DRUG	CUMULATIVE DOSE	CUMULATIVE VOLUME STOCK SOLUTION
0	G1: Chroman 1 G2: DMSO	0 0	0 0
15	G1: Chroman 1 G2: DMSO	30µg/kg 40µL/kg	12µL 12µL
30	G1: Chroman 1 G2: DMSO	100µg/kg 133µL/kg	40µL 40µL
45	G1: Chroman 1 G2: DMSO	300µg/kg 400µL/kg	120µL 120µL

Figure 51Original echocardiography images demonstrating the calculation of LVEF% for in vivo closed chest experiments, A: Echocardiography PLAX view is demonstrated with a cross section through the left ventricle from which an M-mode trace is generated (B). LVEDD – left ventricular end diastolic diameter, IVSd – intraventricular septum diameter in diastole, PWDd – posterior wall diameter in diastole. Echocardiographic images were obtained every 15-minutes (n=5).

A

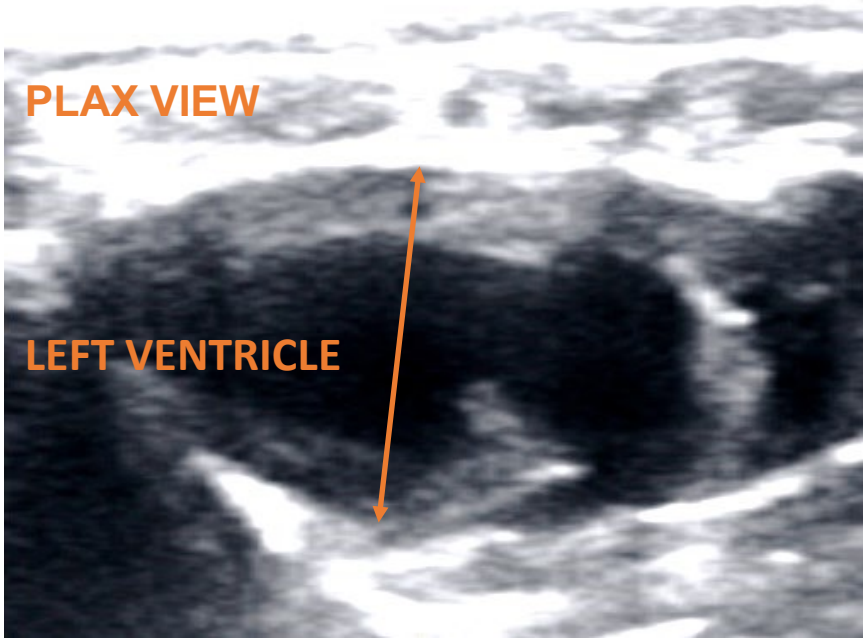

B

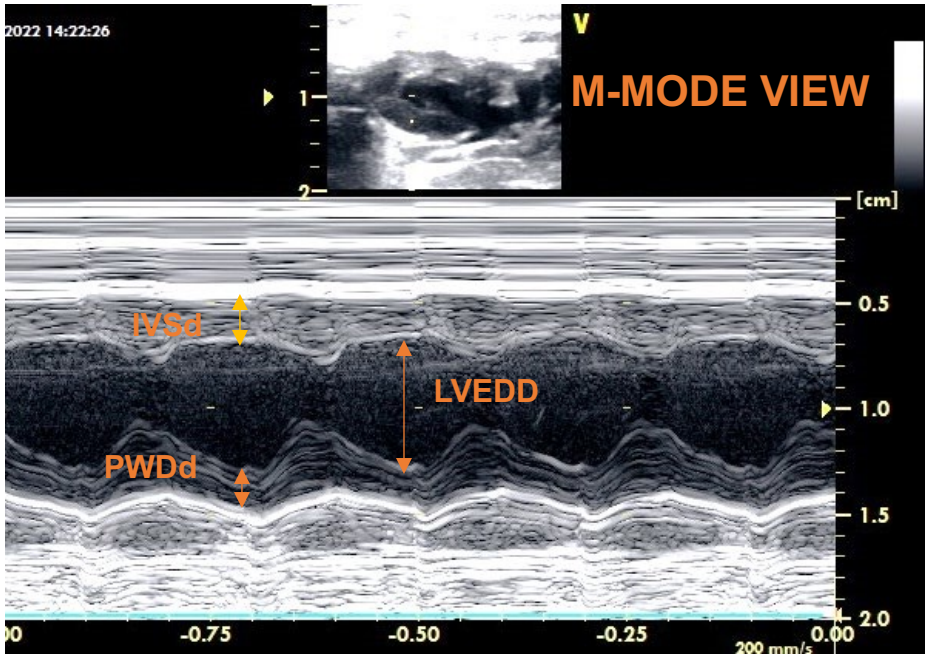

iii) Results

Haemodynamic studies

Figure 52 demonstrates that addition of 3 cumulative doses of Chroman 1, did not have a significant effect on blood pressure or heart rate over a 60-minute period (Table 18).

LVEF%

Similarly, Table 18 demonstrates that 3 cumulative doses of chroman 1 did not significantly reduce LVEF% in the time studied, compared to matched volume DMSO controls.

Conclusions

In this closed chest model in vivo study, the potent ROCK2i Chroman 1, did not significantly reduce LVEF%, blood pressure or heart rate, at doses between 0-300μg/kg, in the absence of ischaemia/reperfusion. This data suggested that this dose range was reasonable to test in vivo, in further I/R experiments, which will be described in the next section.

Figure 52 Addition of Chroman 1 cumulative doses (30-300µg/kg) over time in a closed chest model (n=5). Following analysis with 2-way ANOVA and multiple comparisons test, no significant differences in MAP (mmHg) were observed between the treatment group and DMSO control (n=5).

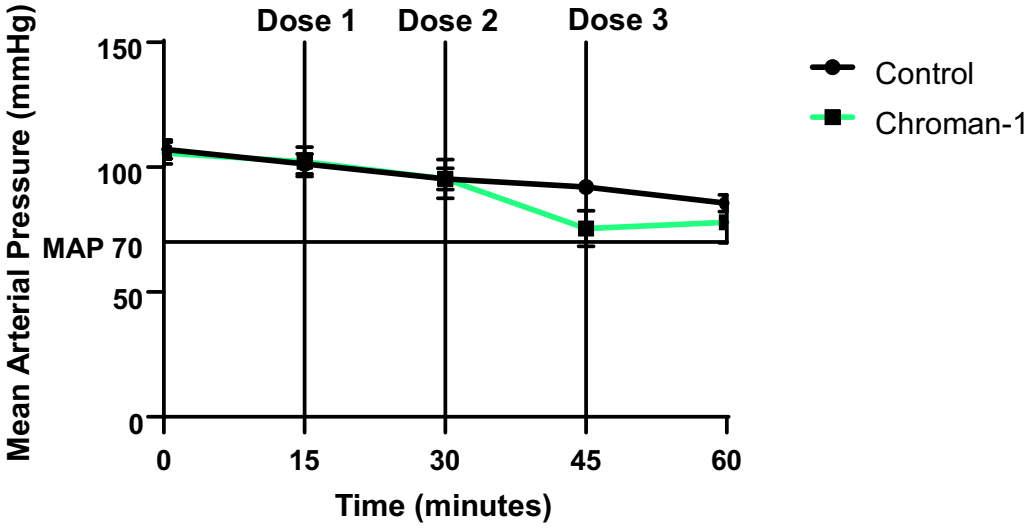

TIME (MINUTES)	MEAN MAP DMSO CONTROL (MMHG) ±SEM	MEAN MAP CHROMAN 1 (MMHG) ±SEM	P VALUE
0	107.2±3.7	105.7±4.4	0.99
15	101.3±4.0	102.2±5.8	>0.99
30	95.3±4.3	95.3±7.7	>0.99
45	92.1±2.8	75.4±7.1	0.33
60	85.6±3.4	77.98.2	0.94

Table 18: Heart rate and LVEF% response respectively to Chroman 1 (30-100µg/kg) in a closed chest model (n=5). There were no significant differences observed between the treatment groups and the DMSO control groups.

TIME (MINUTES)	MEAN HR DMSO VEHICLE (BPM) ±SEM	MEAN HR CHROMAN 1 (BPM) ±SEM	P VALUE
0	371.6±8.6	359.4±19.1	0.98
15	383.0±6.1	360.8±13.1	0.82
30	383.8±10.5	366.4±11.4	0.93
45	395.0±21.9	366.2±11.6	0.61
60	376.4±12.6	371.2±22.1	0.99

TIME (MINUTES)	MEAN LVEF% DMSO VEHICLE (MMHG) ±SEM	MEAN LVEF% CHROMAN 1 (MMHG) ±SEM	P VALUE
0	81.4±2.4	82.6±2.4	0.99
15	82.4±2.6	82.8±2.5	>0.99
30	85.6±2.0	78.8±1.6	0.45
45	84.6±2.9	79.0±3.4	0.65
60	81.0±4.1	76.6±4.4	0.83

6.4: THE HIGHLY POTENT ROCK2 INHIBITOR CHROMAN 1 DOES NOT ATTENUATE IS%, OR MVO% IN VIVO DURING ISCHAEMIA REPERFUSION

i) Objectives

1. To investigate the effects of Chroman 1 on a primary outcome measure of IS% during in vivo ischaemia/reperfusion

2. To investigate the effects of Chroman 1 on secondary outcome measures of MVO% and IMH% during in vivo ischaemia/reperfusion experiments

A new in vivo, randomised, blinded control study was planned to investigate the effects of Chroman 1 as detailed in the above objectives.

Experiments were designed by Dr Lucie Pearce, who also undertook the randomisation procedure. In vivo surgery was conducted by Dr David He, who was blinded to the treatment groups and performed a blinded analysis of heart sections using Image J© software. Dr Lucie Pearce performed final statistical analysis of the data.

ii) Methods

In vivo ischaemia/reperfusion

Animals were handled according to section 3.1. Adult male Sprague-Dawley (SD) rats were selected for these experiments (250-350g). Induction anaesthesia was performed and maintained with 100mg/kg phenobarbital, after which animals were intubated and ventilated with room air and oxygen.

Under anaesthesia, surgical thoracotomy was performed, and the left anterior descending coronary artery (LAD) was identified within the pericardium. This was ligated for 30 minutes, and myocardial ischaemia was confirmed by the presence of left anterior ST-elevation. After 30 minutes of ischaemia, the LAD ligature was released, and the vessel was re-perfused for a period of 180 minutes. 15-minutes prior to the onset of reperfusion, Chroman 1 (at doses 30-500μg/kg) was injected via the I.P route. The haemodynamic status and blood pH of the animals was monitored continuously and recorded via right carotid cannulation.

In accordance with previous chapters, 4% Thioflavin S dye was administered at the end of reperfusion, into the systemic circulation, to allow further assessment of MVO%. Finally, the LAD vessel was re-occluded with the ligature, and Evans blue dye injected into the systemic circulation, to demonstrate the area at risk (AAR%). For analysis of the in vivo work, cardiac tissue was prepared into 2mm sections and stained with tetrazolium (TTC) to measure infarct size as a % of the AAR. Under UV light, regions not perfused by the Thioflavin S dye were quantified (%) and recorded as regions of NRF/MVO (Figure 33, chapter 4). %IS, %MVO and %IMH were all estimated for each section using the electronic

software program, Image J©. %IMH was estimated visually following TTC staining from necrotic regions of myocardium and again quantified using Image J software© (fig.33, chapter 4) (Kumar et al., 2011).

Statistics

Statistical power was determined by the following formula: - [sample size = 2 SD^2 $(Z^{\alpha/2} + Z^{\beta})^2/d^2$], where SD = standard deviation, D= main effect size, and Z values which correspond to a type 1 error of 5% and 0.80 power. These experiments were powered to 0.80, which required n=5 animals per experiment, based on data from previous in vivo ischaemia/reperfusion experiments in our lab (Rossello et al., 2017). Data was normality tested and then analysed with a one-way analysis of variance (ANOVA) for multiple groups.

Drugs and stock solutions

10mg of Chroman 1 powder was purchased from MedChem Express as for the previous experiments. For the I/R experiments two main stock solutions of Chroman 1 were dissolved in 100% DMSO 1) concentration 75μg/ml and 2) concentration of 750μg/ml. For doses of Chroman 1 of 10μg/kg and 30μg/kg, stock solution 1 was used at volumes of 40μL and 120μL respectively (for a 300g animal). Stock solution was measured using a pipette and drawn up from an Eppendorf tube using a fine bore insulin syringe before I.P administration.

For doses of Chroman 1 of 100μg/kg and 500μg/kg, stock solution 2 was used at volumes of 40μL and 200μL respectively, for a 300g animal. For the control animals, matched volumes of 100% DMSO were used in the same manner.

iii) Results

A range of doses of Chroman 1 (10-500μg/kg) were investigated for both the primary and secondary outcomes and according to the doses tested in the previous section of this chapter. Unfortunately, Chroman 1 at any dose tested, did not significantly reduce IS%, MVO% or IMH% compared to DMSO controls, following a period of myocardial I/R (Figure 53-A-C, table 21,22). Figure 54A demonstrates that there were no significant differences observed in the AAR% between groups.

Figure 54B demonstrates the MVO% results which have been further adjusted for IS%. Despite this adjustment there were no significant differences in MVO% found, between treatment groups and controls. Of note, animals in the 500μg/kg cohort (n=4) did become critically hypotensive to a minimum MAP value of 52mmHg (Table 19), however all 4 animals survived. For this reason, this dose was deemed not suitable to continue with greater than n=4. There was no significant hypotension observed for other doses of Chroman 1, suggesting that these results were consistent with previous closed chest haemodynamic studies. For the 100μg/kg cohort, there was an early signal that IS% was increasing in the treatment group, and it was not felt that proceeding to n=5 for this dose would be beneficial. Two groups were therefore underpowered for safety reasons.

Table 19: Blood pressure and HR responses following addition of Chroman 1 500µg/kg to n=4 animals. Chroman 1 500µg/kg was the only dose that had not previously been tested in closed chest haemodynamic studies. Chroman 1 induced significant hypotension in animals undergoing I/R.

MAP (mmHg)	DMSO VEHICLE (n=15)	Chroman 1 500µg/kg (n=4)	P VALUE
MEAN ± SEM	104.4±5.0	71.9±6.3	0.02
MIN ± SEM	85.7±5.0	52.3±6.3	0.01
MAP RANGE ± SEM	54.6±5.0	70.8±6.3	0.79

iv) Conclusion

In an in vivo randomised, blinded control study of myocardial ischaemia/reperfusion, the ROCK inhibitor Chroman 1 at any dose tested, did not reduce either the primary outcome (IS%) or the secondary outcomes (MVO% and IMH%). This remained the case when MVO% was adjusted for IS% and not AAR%. The dose group 500µg/kg tested n=4 only, due to animals becoming unacceptably hypotensive with a MAP around 50mmHg. Doses above 500µg/kg were not haemodynamically safe, in this study. The chapter discussion will next address a move away from investigating Chroman 1 and different ROCK inhibitors, to a murine ROCK2(+/-) KO model.

Figure 53The effects of chroman 1 (10-500µg/kg) on A) IS%, B) – MVO%, C) – IMH, vehicle (n=15), chroman 1 10µg/kg (n=8), chroman 1 30µg/kg (n=10), chroman 1 100µg/kg (n=4), chroman 1 500µg/kg (n=4)

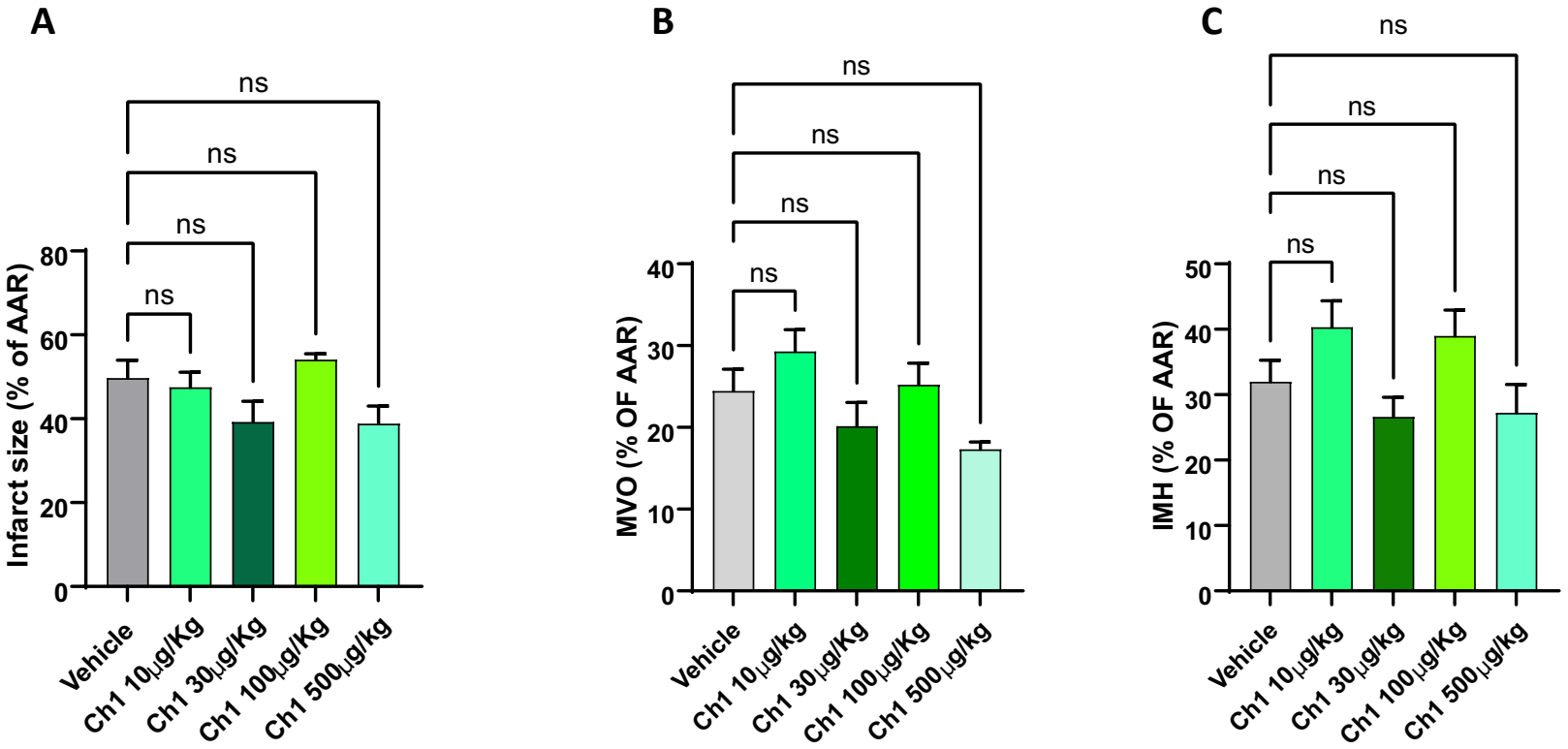

Figure 54: A) AAR% between treatment groups for the myocardial I/R model, B) MVO% from figure B, readjusted for IS%, vehicle (n=15), chroman 1 10µg/kg (n=8), chroman 1 30µg/kg (n=10), chroman 1 100µg/kg (n=4), chroman 1 500µg/kg (n=4)

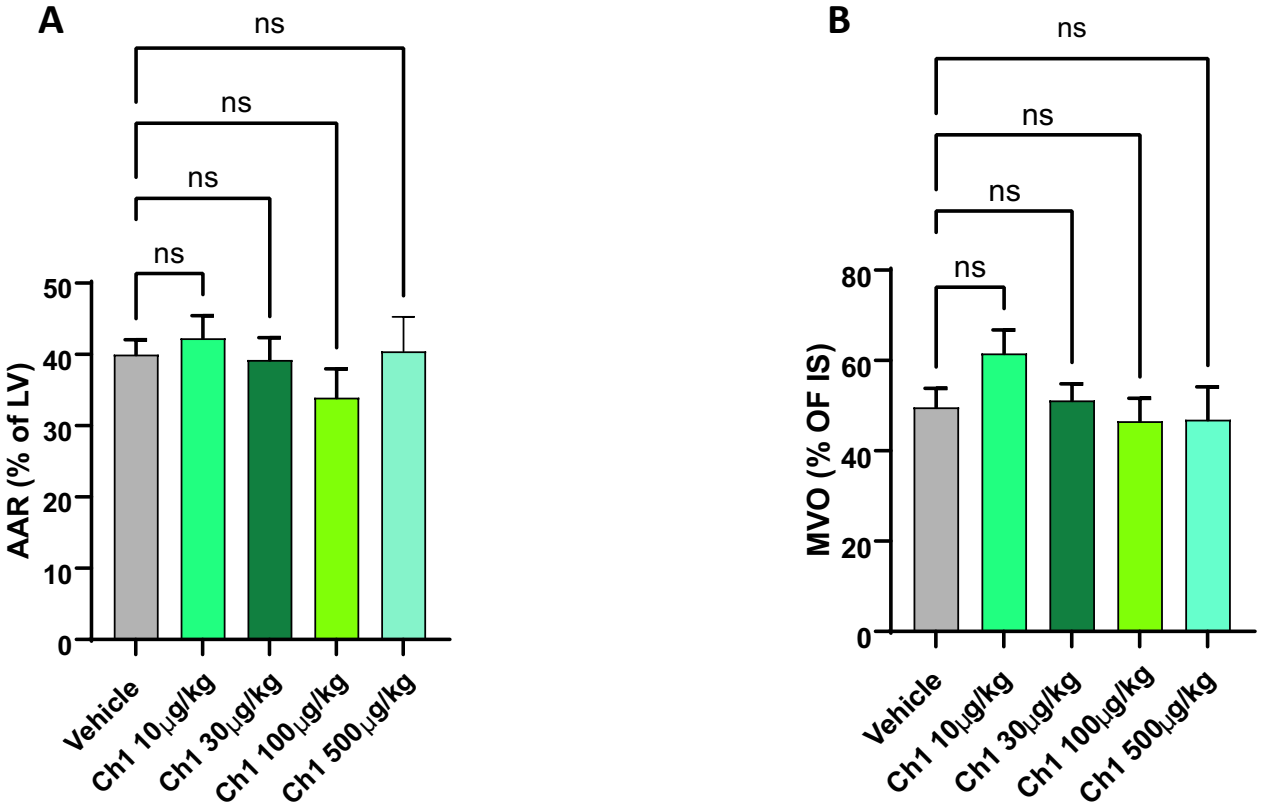

Table 20 Mean values ± SEM for effects of Chroman 1 (10-500µg/kg) on IS%, MVO%, IMH% and AAR%

MEAN ±SEM	DMSO VEHICLE n=15	CHROMAN 1 10µg/KG n=8	CHROMAN 1 30µg/KG n=10	CHROMAN 1 100µg/KG n=4	CHROMAN 1 500µg/kg n=4
IS% (AAR)	49.7±4.3	47.5±3.6	39.3±4.9	54.1±1.3	38.9±4.2
MVO% (AAR)	24.4±2.7	29.3±2.7	20.1±3.0	25.2±2.7	17.3±4.2
IMH% (AAR)	32.0±3.3	40.3±4.0	26.6±3.0	39.0±4.0	27.2±4.4
AAR% (LV)	40.0±2.1	42.3±3.2	39.2±3.1	33.9±4.1	40.5±4.8
MVO% (IS)	49.6±4.2	61.5±5.2	51.2±3.7	46.6±5.0	46.9±7.2

Table 21 Multiple comparisons results between Chroman 1 and control groups following one-way ANOVA & Dunnett's test

	P VALUE IS%	P VALUE MVO%	P VALUE IMH%	P VALUE AAR%	P VALUE MVO (IS%)
Vehicle vs Chroman 1 10μg/kg	0.97	0.87	0.28	0.95	0.12
Vehicle vs Chroman 1-30μg/kg	0.10	0.40	0.34	0.99	0.99
Vehicle vs Chroman 1-100μg/kg	0.96	0.99	0.57	0.63	>0.99
Vehicle vs Chroman 1 500μg/kg	0.49	0.60	0.94	>0.99	>0.99

.

6.5: CHAPTER DISCUSSION

i) Chroman 1 (ROCKi) attenuates ET-1 mediated vasoconstriction of aortic rings

The justification for testing Chroman 1 (ROCK2i) pre-treated aortic rings with a second vasoconstrictor (ET-1) was to try to mimic the conditions of I/R more closely (during which ET-1 is released from damaged endothelium) (Tsai et al., 2017). It must be re-iterated that as the aorta is a conduit vessel, the results of these experiments may not correlate with the physiological responses of the coronary circulation. Moreover, the model was used as a more general model of vasospasm, and to ascertain which of the ROCK inhibitors are vasodilators. That said, the previous chapters have demonstrated that ROCK2 mRNA is expressed in both the aorta and the coronary circulation (chapter 3&5).

Before considering the response to pre-treatment with ROCK inhibitors, the contractile responses to different vasoconstrictors must be reviewed. ET-1 is a known activator of ROCK (Kawarazaki & Fujita, 2021). In the above experiments, ET-1 induced the greatest contractile response of all the vasoconstrictors investigated. It is likely that ET-1 binds to ETA receptors in rat thoracic aorta (Ivey et al., 2008). A biphasic contractile response of aortic rings was observed after addition of AT-II (Figure 49). This has been reported by other investigators and may possibly be caused by autosensitisation of AT-II type I receptors on VSMC, or binding to AT-II type II receptors, which induces a depressor response at higher

concentrations (Scheuer & Perrone, 1993), (Haulica et al., 2003). The maximum contractile response of ATII however, was much lower compared to that observed for ET-1 and PE (Figure 49). ET-1 was therefore used in further vascular ring studies of the ROCK2 inhibitor Chroman 1.

To the author's knowledge, there are no other studies that have tested the vasoactive properties of the ROCK2i, Chroman 1. Several other studies have explored ROCK induced vascular contraction in response to ET-1 with other ROCK inhibitors. One such study by Tsai et al, has already been addressed in the background section (Tsai et al., 2017). Another study compared the responses of ET-1 induced vasoconstriction in both rat coronary arteries and renal resistance vessels, and following pre-treatment with the ROCKi, SAR407899 (Grisk et al., 2012). SAR407899 (an ATP competitive pan-ROCK inhibitor) was noted to reduce ET-1 mediated constriction in renal resistance vessels, but not in coronary arteries (Grisk et al., 2012). This suggests that ROCK mediated VSMC contraction as stimulated by ET-1, may vary in vessel type and size.

In support of the results from chapter 3 of this thesis, the same study found a much greater abundance of ROCK2 mRNA in human small thymic arteries (obtained from consenting patients during CABG surgery). It was noted that ROCK1 was not present altogether in some human vessels tested (Grisk et al., 2012). This paper was published in 2012, which pre-dated many of the newer selective ROCK2 inhibitors,

and thus SAR407899 was selected for use at that time. One final important point from this paper, is the acknowledgement that ET-1 is more ROCK specific than other α-adrenoreceptor agonists (Grisk et al., 2012).

In these thesis experiments, Chroman 1 was able to successfully reduce ET1 mediated contraction of rat thoracic aorta, to a greater degree than another well-known vasodilator, Fasudil (Figure 50). It is not apparent from these experiments, what mechanism is responsible for the enhanced vasodilatory capabilities of Chroman 1, but possibilities include either greater ROCK1, ROCK2 or MRCKα inhibition compared to Fasudil. A greater potency of the drug may be one explanation, however Chen et al also noted when they originally designed this drug, that Chroman 1 showed affinity for MRCK (Chen et al., 2008). To explain the difficulty in discriminating between these kinases, it is necessary to describe the downstream actions of MRCK in more detail (Figure 55). Before this, it is important to state that there are also no MRCK specific phospho-antibodies available, which would allow for measuring MRCK activity via this method (Zhao & Manser, 2015).

MRCK like ROCK, is also a G-protein activated kinase, but it resides downstream of a molecule called CDC42 rather than RhoA (Wilkinson et al., 2005). There are three forms of MRCK including α, β and γ (Ruscetta et al., 2023) which regulate cell motility within the cytoskeleton, and smooth muscle migration. They also like ROCK, have implications in cancer cell replication (Zhao & Manser, 2015). A former study investigating MRCK expression in different tissues, using Western blot

analyses, suggested that the kinase is expressed in the heart, but to a lesser degree than the brain or the lungs (Leung et al., 1998). This study did not further examine expression within different cell types in the heart. MRCK is known to inhibit MLCP in the same way as ROCK (via phosphorylation of MYPT1 at T696/T853), and therefore 'releases the break' on the inhibition of P-MLC2 to induce smooth muscle contraction (Zhao & Manser, 2015). ROCK and MRCK therefore have common downstream substrates (Zhao & Manser, 2015) (Figure 55). Unlike ROCK, there are not many studies in the literature that have examined the contractile effects of MRCK in smooth muscle.

In a prominent literature review from 2020, only one preclinical study is identified as investigating the contractile role of the CDC42/MRCK pathway in canine tracheal smooth muscle (Li et al., 2020). No studies are identified as having been conducted in vascular smooth muscle (Li et al., 2020). Some authors have attributed this lack of specific research to the difficulty in producing a selective MRCK inhibitor which does not also inhibit ROCK (Ruscetta et al., 2023). Two known inhibitors of MRCK include Chelerythrine and the new compound BDP5290 (Zhao & Manser, 2015). BDP5290 has recently been investigated in the heart in the study of atrial fibrillation (AF) where it was found that inhibiting MRCK in mice induced AF, by reducing MLC2 phosphorylation and contractility. MRCK inhibitors were, therefore, not therapeutic, and moreover were detrimental (Perike et al., 2023). This study did not explore the role of MRCK in vascular smooth muscle.

Figure 55: VSMC agonist pathways and the role of MRCK: The G-protein coupled kinases, ROCK and MRCK, share the common substrates of MLCP (MYPT1) and MLC2, involved in cellular and VSMC contraction. Original artwork inspired by (Kawarazaki & Fujita, 2021)

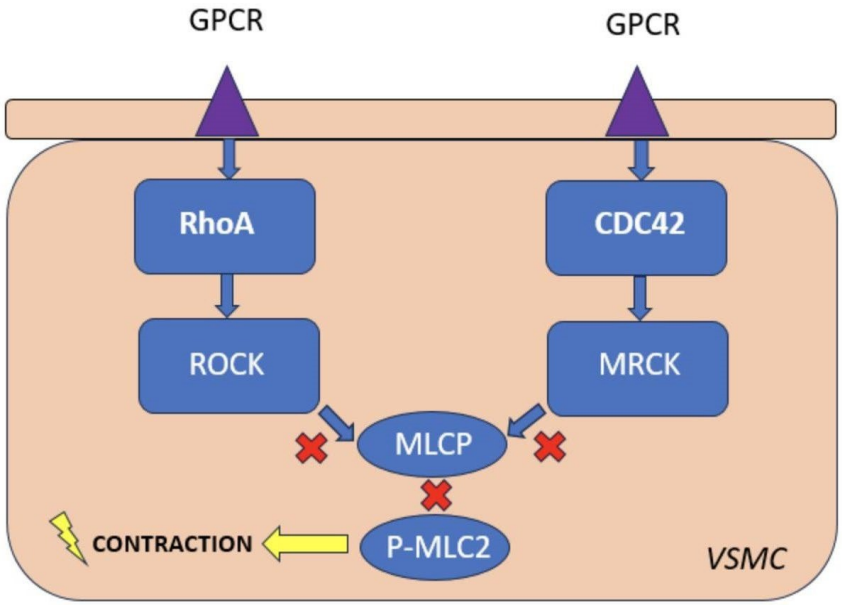

In summary, it is extremely difficult to discriminate between the actions of MRCK and ROCK (as is the case for ROCK1 and ROCK2) without KO studies. It might be possible in further studies to use an MRCK inhibitor such as BDP5290 in vascular tissue and to observe whether this induces vasodilation, however this does not directly prove that MRCK inhibition has occurred in these experiments to explain the vasoactive properties of Chroman 1. Moreover, this is less relevant to the original hypothesis - that ROCK2 is the most important isoform in vasodilation and cardioprotection. This should therefore be considered in future experiments, but not necessarily as a focus of this thesis. A more general validation of the ROCK inhibitors tested, using either P-MYPT1 or P-MLC2 would be useful in future experiments.

ii) Chroman 1 is a potent vasodilator, but it does not reduce LVEF% in vivo

The experiments performed in section 6.3, were performed predominantly to assess the haemodynamic effects of Chroman 1 in vivo and to ensure that a range of non-lethal doses were established. However, it was decided to concurrently measure the LVEF% of animals receiving the drug, to ensure that no further negative inotropic effects were observed via a reduction in either myocardial contractility or systolic function (LVEF%) (Niccoli et al., 2019). Inotropic support was required in a previous clinical study of Fasudil during myocardial infarction (Kikuchi et al., 2019) and it is unclear whether this was secondary to an acute reduction in blood pressure causing a hypotensive crisis or another mechanism of myocardial compromise. Direct inhibitors of cardiac

myosin (i.e., the drug Mavacamten) do reduce LVEF% acutely, and so it was to be established whether a ROCKi mediated reduction in MLC-P, might also induce similar effects in the myocardium.

It has already been discussed that Chroman 1 reduces the VSMC contractility of aortic rings by either potently inhibiting ROCK1/2, or the ROCK like kinase, MRCK. ROCK reduces VSMC contractility by reducing P-MLC2 mediated actin/myosin contraction via inhibition of MLCP (Shimokawa et al., 2016). Whether or not similar ROCK contractile pathways exist in the myocardium and cardiomyocytes, has been speculated by Shimokawa et al, and identified as an area which requires further research (Shimokawa et al., 2016). It is important here to state that the key mechanisms governing cardiomyocyte contraction (involuntary) and VSMC contraction (voluntary) are distinct (Dirksen et al., 2022). Cardiomyocyte contraction is initiated by a group of specialised cells known as pacemaker cells. These trigger cardiac excitation via the influx of calcium ions through an electrical 'action potential.' Free calcium in the cell binds to the Troponin C complex, which moves from its previous actin binding site, and allows actin to bind to myosin (Bers, 2002). Actin/myosin binding subsequently stimulates cardiac muscle contraction (Dirksen et al., 2022). Cardiomyocyte contraction cycles are longer than those experienced by vascular smooth muscle, and notably cardiomyocytes do not fatigue in the same way as other skeletal muscles (Ito et al., 2022). A review by Ito et al from Nature publications (2022), has described the uncertainty concerning the role of the MLCP/MLC axis in cardiac muscle contraction (Ito et al., 2022). It is generally felt that

MLCK and MLC are not primary targets of Ca^{2+} in cardiac muscle. As described above, troponin C is the primary effector of actin/myosin mediated contraction in cardiomyocytes (Bers, 2002). The Ito et al, paper states that just 40% of MLC is phosphorylated at any one time in cardiac muscle, and this does not fluctuate during the cardiac cycle (Ito et al., 2022). This contrasts with regulation of contraction in VSMC, where fluctuating amounts of P-MLC determine the extent of contraction (Gohla et al., 2000). However, Ito et al also describe a possible role for cardiac muscle specific MLCP in calcium sensitization (Figure 56). It is hypothesised that calcium sensitisation via the ROCK pathway in cardiac muscle, can increase isovolumetric force of contraction, however it is not the main determinant.

The authors conclude that the most important regulatory subunit of MLCP in cardiac muscle is ‘MYPT2’ (rather than MYPT1 isoform expressed in VSMC). It is stated that the kinases which phosphorylate MYPT2 however, are largely unknown. The original research providing information on MYPT2 isoforms was derived from genetic animal models of MYPT2 overexpression, where such modifications resulted in calcium desensitisation and reduced contractility (Mizutani et al., 2010). The earlier review by Shimokawa et al (Shimokawa et al., 2016) highlights another preclinical study which demonstrated that MLCK and P-MLC2 were implicated in rat papillary muscle contraction (induced by the αadrenoreceptor agonist, PE) (Grimm et al., 2005). However, whilst an MLCK inhibitor (calcium dependent pathway) abolished this contraction entirely, the ROCK inhibitor Y-27632 only reduced PE mediated

myocardial contraction by 16% (Grimm et al., 2005). Therefore, the ROCK pathway of calcium sensitisation appeared to contribute less significantly, in this study. For reasons discussed in the introduction, it is possible that this was due to the choice of PE as an agonist, being less G12/13/RhoA/ROCK selective (Grimm et al., 2005). In another study from 2009, Vlasbolm et al (Vlasblom et al., 2009) linked ventricular cardiomyocyte contraction to ROCK signalling.

When neonatal ventricular cardiomyocytes had contraction arrested with the compound BDM (a calcium contraction uncoupler) there was an observed reduction in RhoA and ROCK signalling leading to disorganisation and loss of actin filaments (Vlasblom et al., 2009). Therefore, some evidence may suggest that ROCK mediates cardiomyocyte contractility in addition to its well-known role in VSMC calcium sensitisation. It follows then, that a reduction in LVEF% might be a theoretical risk following ROCK inhibition during myocardial infarction (Grimm et al., 2005), (Vlasblom et al., 2009), (Niccoli et al., 2019), (Shimokawa et al., 2016) despite these drugs otherwise being linked to cardioprotection(Huang et al., 2018b). The results of the experiments in section 6.3, do not suggest that Chroman 1 reduced LV systolic function at the doses examined and between 0-60 minutes. Notably, this model was in absence of ischaemia/reperfusion. LVEF% as an echocardiographic parameter was selected over Db/DT as this was felt to be more clinically translatable. Considering other studies which have reviewed LVEF% as an outcome measure following ROCK inhibition with

Fasudil, it is difficult to discriminate between the effects of I/R and the effects of the drug on systolic function.

Figure 56 Key differences between cardiomyocyte contraction and VSMC contraction and the potential differing role of ROCK. Original artwork inspired by Ito et al(Ito et al., 2022)

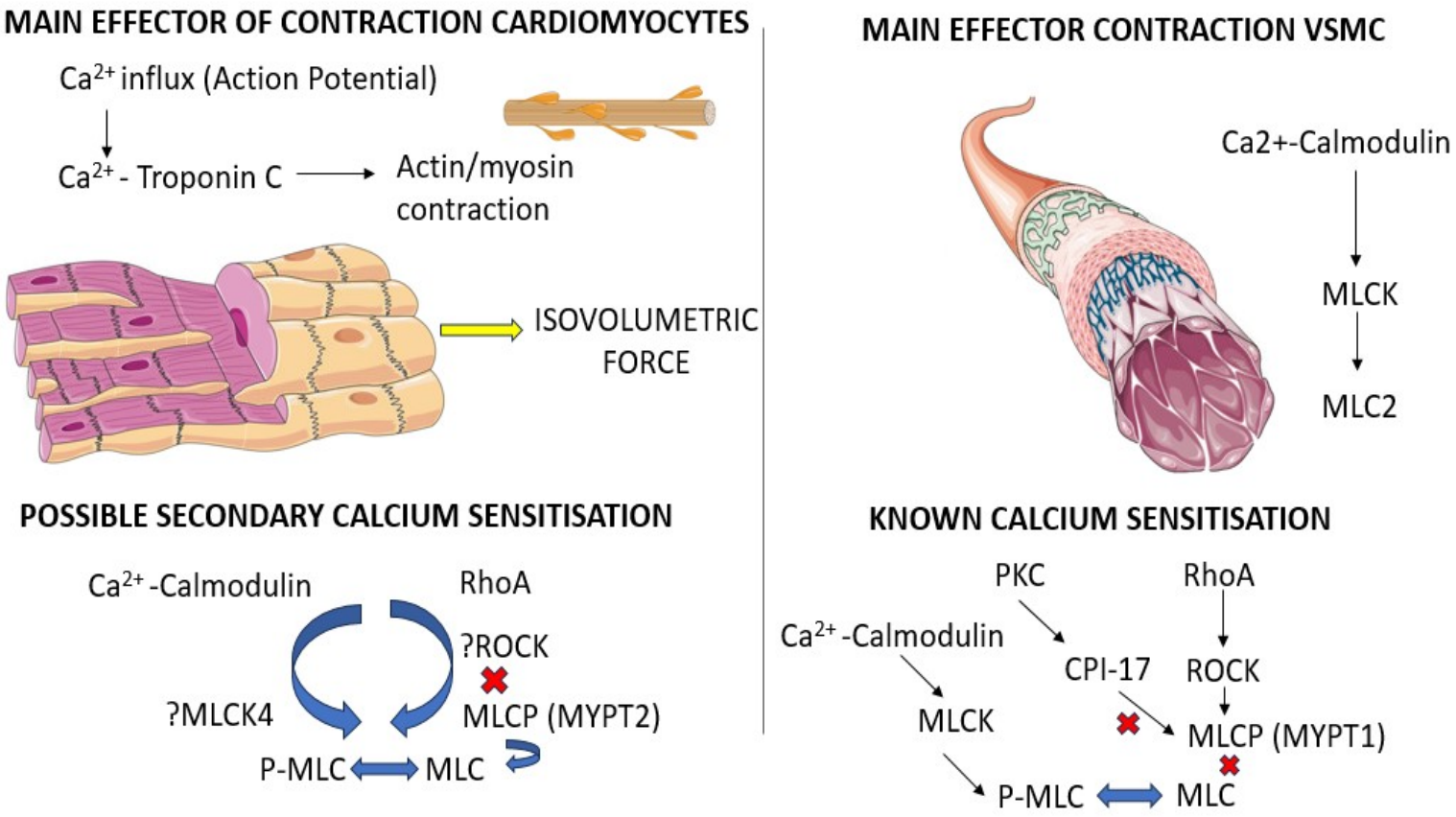

Shibata et al performed a study of myocardial I/R in pigs receiving Fasudil, which was found to reduce infarct size (Shibata et al., 2008). It was noted that ischaemia alone reduced left ventricular fractional shortening (FS%) but this was not significantly worsened by Fasudil (Shibata et al., 2008). Similarly, Miyahara et al performed LAD infarction of male Wistar rats and did not find any statistical differences in LVEF% between animals which had received Fasudil 10mg/kg and those which had received vehicle. The authors had originally hypothesised that Fasudil or Fasudil in combination with ventricular offloading, might improve LVEF% through reducing ventricular preload, rather than compromise this (Miyahara et al., 2022). It is important to state here that a reduction in LVEDP and preload is desirable, and distinct from a direct reduction in myocardial contractility.

It can be concluded that the findings from section 6.3 are in support of the literature discussed, which argues that ROCK inhibition does not influence myocardial contractility directly, nor to the same extent as VSMC contractility (Ito et al., 2022), (Mizutani et al., 2010). This is not proven directly in these experiments but could be investigated in future works by inducing contraction of isolated cardiomyocytes and measuring P-MLC2 both with and without Chroman 1 pre-treatment. As a further consideration, contractility has been assessed as global LVEF% and not using another method, Db/DT and therefore may not have detected earlier changes in myocardial contractility and LVEDP. Nevertheless, both the haemodynamic profile and the echocardiographic results indicated that Chroman 1 was appropriate to consider for further studies of myocardial I/R (primary outcome) and these results will be discussed in the next section.

iii) The highly potent ROCK2 inhibitor Chroman 1 does not attenuate IS%, or MVO% in vivo during ischaemia/reperfusion

The final set of experiments in this chapter, 6.4, examined the effects of Chroman 1 in an in vivo model of ischaemia/reperfusion to see if this would induce cardioprotection in the same way as Fasudil 10mg/kg. The reason for pursuing chroman 1 above other agents was to try to find a pharmacotherapy that would attenuate all three outcomes without causing negative inotropy. It was hoped that this would be achievable due to the high potency of Chroman 1 for ROCK2 (Chen et al., 2021) with the drug also demonstrating vasodilatory potential in response to endothelin-1 in section 6.2.

Unfortunately, Chroman 1 did not attenuate IS%, MVO% or IMH% at any dose tested. Firstly, it must be stated that the experiments have not proved that ROCK inhibition took place in vivo, nor that the drug Chroman 1 effectively reached the target tissue at these doses. It is therefore one possibility that the drug was not effective for pharmacokinetic reasons. The solution to this would be to look to perform PK studies in vivo for the drug – in absence of any other in vivo data from elsewhere. Moreover, the half-life of Chroman 1 and its derivatives is not directly stated in the landmark paper which reported on their synthesis (Yen Ting Chen 2011). Assuming for the sake of argument that Chroman 1 did reach the target tissue at these doses, one other potential explanation might be that the drug has inhibited P-AKT, a molecule which is part of the RISK pathway (Rossello et al., 2017) and an important part of cardioprotection. Several

papers describing the Chroman-3-amides do refer to possible affinity for the drug for AKT (Chen et al., 2008), (Yen Ting Chen 2011). This is out of keeping however with the recent experiments performed by Chen et al in vitro, which proved that Chroman 1 dramatically improved cell survival and reduced cell death (Chen et al., 2021). AKT was also not identified as a target for the drug in the extensive screening which was performed as part of this most recent study (Chen et al., 2021). Overall, it is surprising that Chroman 1 has not demonstrated any potential as a cardioprotective drug, especially considering its key role in the new CEPT cocktail (Chen et al., 2021). This discrepancy seems to favour a pharmacological explanation (discussed above) as to why cardioprotection has not occurred.

One further point to address is the robustness of the Thioflavin S model as a measure of MVO%, considering control values between the three in vivo I/R studies (Figure 57). It was noted that there was some variation across the three studies with mean DMSO control value for MVO% being 18% (Fasudil 10mg/kg), 32% (Fasudil 3mg/kg, KD025) and 24% (Chroman 1) respectively. However, when this was formally analysed using a 2-way ANOVA, there was no significant difference found between studies for control values of MVO% ($p=0.25$). It does follow however, that for smaller mean control values (such as in study 3 compared to study 2) it would require a greater n number to potentially demonstrate a statistically significant outcome. An n=10 for 30μg/g of Chroman 1 is reputable and therefore should have been adequately powered to demonstrate an effect. Arguably chroman 1 500μg/kg was not powered

highly enough to demonstrate this (n=4) however experiments were aborted due to animal hypotension.

Figure 57. An analysis of the control values for IS%, MVO% and IMH% for each in vivo study. Study 1 (n=6), study 2 (n=5), study 3 (n=15). 2-way ANOVA with multiple comparisons did not demonstrate any significant differences between studies.

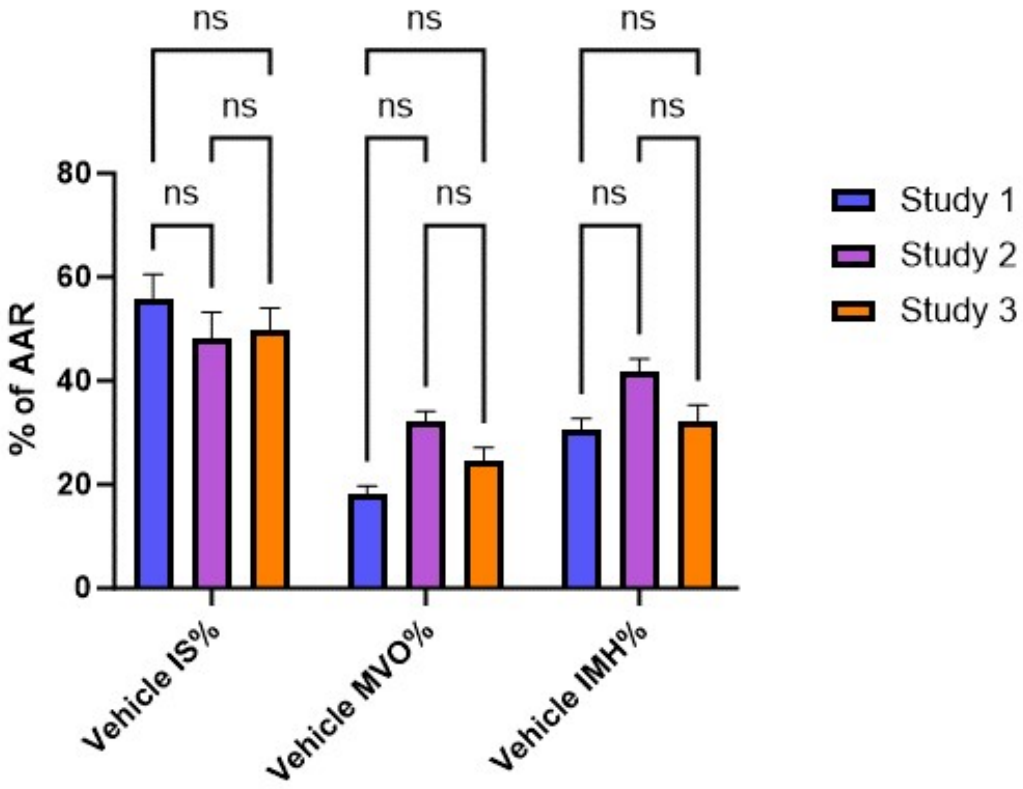

iv) Next experiments

In essence, increasing the potency of ROCK2 (and likely ROCK1) inhibition with Chroman 1, did not lead to increased cardioprotection. Increasing the potency of ROCK2 inhibition was at the expense of ROCK2 selectivity for Chroman 1 (compared to KD025 which was >200

fold more selective for ROCK2). Chroman 1 has only a selectivity index of approximately x50 fold (Chen et al., 2021) Considering KD025, MVO% outcomes were better with greater ROCK2 selectivity. However, conversely, Fasudil demonstrated the greatest cardioprotective effects of all drugs and this is the least selective and the least potent for ROCK.

Chapter 6 has raised some interesting questions and generated multiple additional research hypotheses including those concerning the role of MRCK in vasodilation and of myosin light chain phosphatases in cardiac myocyte specific contraction. However, it was decided to plan further experiments to try to prove the original hypothesis that selective ROCK2 inhibition is beneficial in cardioprotection with an initial primary outcome of IS%. As it has not been possible to prove this definitively with pharmacological inhibition, the next chapter will discuss myocardial ischaemia/reperfusion in a heterozygous ROCK2(+/-) KO model.

CHAPTER 7: THE EFFECTS OF A HETEROZYGOUS ROCK2 (+/-) MURINE KNOCK OUT MODEL ON INFARCTION SIZE FOLLOWING MYOCARDIAL ISCHAEMIA/REPERFUSION

7.1 BACKGROUND

i) Previous ROCK2 knock out models in the heart

Genetic models of RhoA deletion (and its downstream effectors such as ROCK) have been studied since 2003, by groups such as Thumkeo et al (Thumkeo et al., 2013),(Hartmann et al., 2015),(Thumkeo et al., 2003). Both mice with homozygous deletions of ROCK1 or ROCK2, and combination deletions such as (ROCK1+/- & ROCK2-/-) or (ROCK2+/-& ROCK1-/-) all die before birth, thus demonstrating the integral role of ROCK in the formation of the cytoskeleton (Thumkeo et al., 2013). Homozygous deletions also limit vascular development in-utero (Kamijo et al., 2011). In original work by Thumkeo et al (Thumkeo et al., 2003), 90% of ROCK2 (-/-) animals did not survive to birth, however those that did survive, were of normal phenotype. Some animals were noted to have early growth retardation; however, they later matched the body weight of their littermates (Thumkeo et al., 2003). Surviving animals with global ROCK1 deletion are born with their eyelids open (Thumkeo et al., 2013).

Most literature sources agree that ROCK2 homozygous deletion is un-survivable from an embryonic developmental perspective, unless it is induced after birth as in certain models (Thumkeo et al., 2013), (Shi et al., 2019). Or unless it is performed as part of conditional, knock-out model e.g. cardiomyocyte specific (Sunamura et al., 2018). The

heterozygous deletion (ROCK1+/-) or (ROCK2+/-) produces a milder phenotype, and offspring are both developmentally normal and fertile (Thumkeo et al., 2013), (Hartmann et al., 2015). There are very few studies which have assessed ROCK1 or ROCK2 deletions in in vivo models of myocardial ischaemia/reperfusion (Rikitake et al., 2005). This is possibly because prior attention has been focused on ROCK deletion to mitigate cardiac fibrosis or hypertrophy (Hartmann et al., 2015), (Shi et al., 2019). Rikitake et al, produced a whole body murine ROCK1 (+/-) model to study the effects of the genotype on myocardial fibrosis in mice, undergoing LAD infarction (Rikitake et al., 2005). There are no published outcomes regarding infarct size from the study, however the mutation was found to reduce the development of post ischaemic perivascular myocardial fibrosis (Rikitake et al., 2005). In the same study, ROCK1 (+/) mice did not demonstrate reduced hypertrophy, in response to the eNOS inhibitor (LNAME) (Rikitake et al., 2005). At baseline, ROCK1 (+/-) animals had comparable systolic blood pressure and LV mass compared to those of the wildtype animals, which is consistent with previous findings that haplosufficient mice display a normal cardiac phenotype (Rikitake et al., 2005), (Hartmann et al., 2015).

Several other models of conditional homozygous and heterozygous ROCK1/2 deletion have demonstrated a reduction in cardiac fibrosis (Shi et al., 2019), (Sunamura et al., 2018), (Shimizu et al., 2017). One such pathology leading to myocardial fibrosis, is pulmonary hypertension (Sunamura et al., 2018). Whilst this is less relevant here, it is important to note that cardiomyocyte specific ROCK2 deletion models have been

well utilised to demonstrate that ROCK2 (-/-) deletion is beneficial in pulmonary hypertension (Shi et al., 2019). Sunamura et al developed a cardiomyocyte specific ROCK2 (-/-) model to demonstrate that knockdown mitigates pulmonary hypertension associated fibrosis, by reducing the levels of reactive oxygen species (ROS) involved in adverse remodelling (Sunamura et al., 2018). ROS are also a known source of myocardial damage in ischaemia/reperfusion injury (Yellon & Hausenloy, 2007), suggesting that this mutation may also be beneficial in acute myocardial protection.

Similarly, VSMC specific ROCK1/2 knockout models have been studied in the context of pulmonary hypertension (Shimizu et al., 2013). Both myocardial infarction and pulmonary hypertension are driven by hypoxia and inflammation, although pulmonary hypertension is a chronic process (Shimizu et al., 2013), (Yellon & Hausenloy, 2007). In a study by Shimizu et al, mice with VSMC specific ROCK2 (+/-) deletion, demonstrated reduced levels of the inflammatory cytokines, interferon-gamma (IFN-γ) and tumour necrosis factor alpha (TNF-α) in response to chronic hypoxia (Shimizu et al., 2013). However, animals had comparable resting blood pressure, heart rate and left ventricular end diastolic pressure (LVEDP) in the presence of normoxia, indicating that this phenotype did not alter baseline physiology in absence of disease (Shimizu et al., 2013). Sladojevic et al, developed a platelet specific ROCK2 (-/-) murine model and investigated the effects of this on cerebral infarction size, in an embolic clot model of I/R (Sladojevic et al., 2017). ROCK2 (-/-plat) deletion significantly increased intrinsic bleeding time, and reduced

cerebral injury following I/R, however only when the embolic clot had originated from the ROCK2 (-/-plat) mice. When clots from other wildtype animals were implanted into ROCK2 (-/-plat) animals, cerebral injury was not attenuated. The author's concluded that platelet specific ROCK2 (-/-) deletion alters clot formation but does not infer protection from clot propagation (Sladojevic et al., 2017).

More recently, ROCK2 (+/-) murine models have been explored in research of insulin resistance and obesity (Soliman et al., 2015). Soliman et al, bred ROCK2 (+/-) mice to investigate the changes in insulin resistance, when mutant animals' vs wildtype were fed with high fat diet. It was noted that ROCK2 (+/-) deficient animals performed better in glucose tolerance tests and did not develop obesity induced left ventricular systolic dysfunction, as observed in other wildtype animals (Soliman et al., 2015). This has suggested a potential role for ROCK2 in the development of obesity and insulin resistance.

Another new concept in ROCK2 genetic research, has been the development of ROCK isoform specific 'kinase dead' (KD) mutations (Shi & Wei, 2022), where ROCK 1 or 2 is inactivated as a functioning molecule, but protein levels remain unchanged. This is felt to be a potential solution to overcompensation of one isoform for another, in homozygous deletion models e.g. increased levels of ROCK1 protein observed in ROCK2 (-/-) deletion (Shi et al., 2019; Shi & Wei, 2022). Unfortunately, homozygous (KD) animals for both ROCK1 and ROCK2 do not survive to birth, as is the case for homozygous full KO animals (Shi & Wei, 2022). ROCK2 (+/KD) (heterozygous kinase dead) mice do

display reduced levels of phosphorylated myosin light chain kinase (as would be expected given reduced ROCK activity) and can be used in experimental studies (Shi & Wei, 2022). Wei et al, used such mice in a second study investigating the role of ROCK2 in obesity (Wei et al., 2020). ROCK2 (+/KD) mice were noted to be leaner and displayed increased thermogenesis compared to wildtype animals (Wei et al., 2020). It has long been speculated that the phenotype observed from various ROCK deletions are species dependent, therefore the above study findings are perhaps not absolute.

ii) Scope of this work

Whilst the above literature demonstrates a previous interest in genetic ROCK2 KO models in the heart and vasculature (especially concerning myocardial fibrosis) there is a lack of investigations using such models in studies of acute myocardial ischaemia/reperfusion. It was therefore decided to investigate a ROCK2 (+/-) murine model to address the main hypothesis, that the ROCK2 isoform has a significant role in myocardial protection.

7.2 HETEROZYGOUS ROCK2 (+/-) KO DOES NOT REDUCE INFARCT SIZE IN MICE FOLLOWING MYOCARDIAL ISCHAEMIA/REPERFUSION

i) Objectives

1. To breed and maintain a colony of genetic ROCK2 (+/-) KO mice for use in further myocardial I/R experiments

2. To ascertain whether ROCK2 (+/-) KO reduces infarct size % following myocardial I/R

ii) Methods

In this chapter, PCR and Western blotting techniques were performed independently by Dr Lucie Pearce. In vivo ischaemia/reperfusion experiments were designed by Dr Lucie Pearce and performed by Dr David He, who was blinded to the KO groups. Dr David He analysed the Image J© slices and Dr Lucie Pearce analysed the results. With thanks to Dr Pelin Golforoush for her expertise and teaching of PCR techniques and to Dr Sapna Arjun for teaching of Western Blotting techniques.

ROCK2 KO Mice (+/-)

Mouse ROCK2 (+/-) embryos were kindly provided by the Centre for Cell Signalling at the John Vane Science Centre, Queen Mary's University of London, and were from the strain C57B6/J OlaHsd (Harlan). This strain was a targeted whole body ROCK2 deletion (heterozygous) of mild severity. ROCK2 KO homozygous animals do not survive to birth,

however heterozygous animals do survive and are fertile (Thumkeo et al., 2013). Animals from the original strain were produced by Sandra Kuemper et al (Kümper et al., 2016) in their original work investigating the role of ROCK isoforms in tumorigenesis, however this study used further conditional models. n=5 original pups underwent genotyping of ear clippings at 6 weeks as below. Genotyping revealed 3 HET animals and 2 wildtype (WT). Breeding was continued as WT vs HET to produce a combination of WT and HET (haplosufficient) animals.

PCR Protocol

PCR was performed to confirm the presence of ROCK2 (+/-) mutant DNA. Ear clippings were obtained from pups at 6-weeks of age and samples were genotyped using DNAPCR. Prior to this, primers specific to the ROCK2 deletion (heterozygous) were obtained from Sigma laboratories as:

RK350 (F) 5' gatagcactgacgtgtcccac 3'

RK351 (Rev) 5' gtcaggctacagtacgttgcc 3'

RK11766(Rev) 5' ggctccacacatgcctttaccc 3'

Primers were diluted to a concentration of 1:10 for upcoming PCR experiments. Ear clippings were first lysed using 200µL of Viagen© Direct PCR reagent (containing 0.2- 0.4 mg/ml Proteinase K from Sigma©). Samples were heated to 60 degrees Celsius overnight, and then to 85 degrees Celsius for a further 45-minutes the following day, to extract DNA from the samples. Next ‘PCR mix’ was created using GoTaq© DNA

polymerase (Promega) in combination with the primers as above, and distilled water. Next lysed DNA samples were spun down using the centrifuge, and 1μL of this lysed DNA mix was added to each PCR tube. 19μL of PCR mix was added so that the total volume of each tube was 20μL. Tubes were transferred to the PCR machine to undergo denaturation, annealing and elongation steps (Table 22).

Table 22: PCR protocol for ROCK2 samples

TIME (minutes)	TEMPERATURE
3	95^0c
30	95^0c
30	59^0c
30	72^0c
5	72^0c

Whilst PCR samples were being incubated, a 1% agarose gel was prepared using 100mls of 1x Tris-acetate-EDTA (TAE) buffer, 1g of agarose and 10μL of DNA loading dye (Thermofisher). A small PCR tank was located and filled with further 1x TAE buffer in preparation for gel loading. Gel mixture was poured into the PCR tank and allowed to set for 45-minutes with a lane comb in-situ. When the PCR sample programme was complete, samples were allowed to cool and removed from the PCR machine. When the gel was set and cooled, the lane comb was removed and to the pre-prepared gel, 5μL of protein ladder was loaded, in addition to 10μL of each PCR mix sample. To enable gel electrophoresis, the PCR

tank was connected to the electrodes so that samples ran in the direction of the anode (red) at 100V for one hour. After this DNA separation process was complete, the gel was carefully removed, and PCR bands were visualised under UV light to identify mutant DNA (Figure 58). The number of mutant and wildtype animals were carefully recorded.

Figure 58: PCR bands visible under UV light. Mutant bands for heterozygous animals were expected at 354bp, and for wildtype animals 314 bp. The experiment below demonstrates that animals 42 and 44 were WT animals, and animal 43 was a heterozygous (ROCK2+/-) animal.

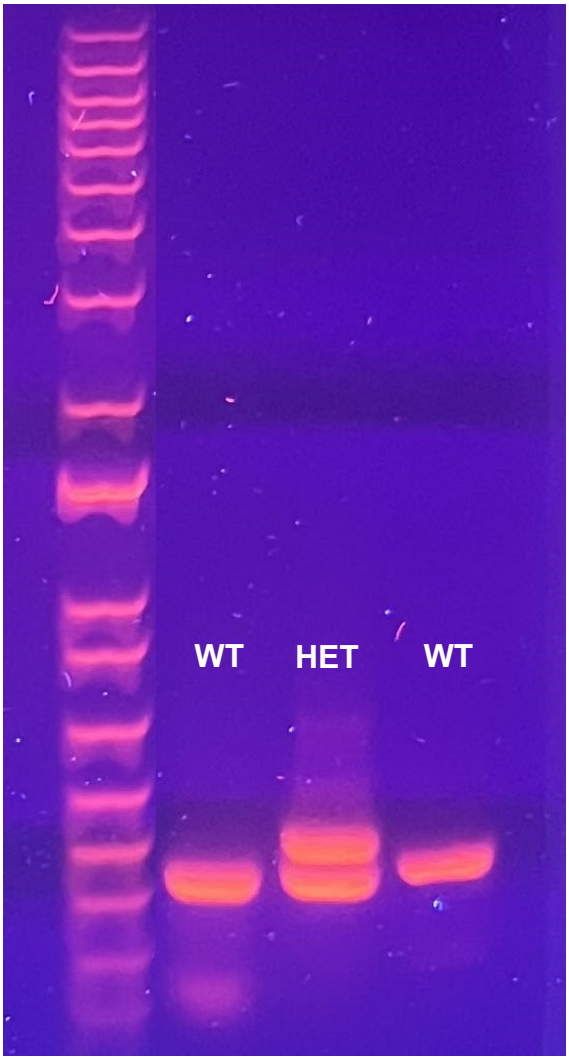

Western Blotting (n=3 per group)

In addition to confirming the presence of mutant DNA, it was also important to confirm the phenotype and demonstrate a reduction in ROCK2 protein in murine hearts. Animals were kept and handled according to section 3.1. ROCK2 (+/+) (WT) or ROCK2 (+/-) (HET) mice weighing (25-50g) were selected and anaesthesia was undertaken with 100 mg/kg sodium pentobarbitone via intraperitoneal injection. A thoracotomy was performed to remove the heart under full surgical sedation, (confirmed by absence pedal reflexes) and this was flushed thoroughly with a syringe of H_20 to remove erythrocytes and blood components. *n=6 total* animals were sacrificed for these Western blot experiments. Whole hearts were snap frozen in liquid nitrogen and stored at -80^0C until the day of tissue lysis.

Tissue Lysis

100mls of tissue lysis buffer [Tris pH 6.8 100mM; NaCl 300mM; IGEPAL 0.5%; H_20] was prepared to pH 7.4 and stored at 4^0C. Mouse hearts were removed from the -80^0C freezer and frozen tissue was quickly weighed without allowing the sample to thaw. EDTA, protease and phosphatase cocktail were added to tissue lysis buffer to a concentration of 1:100. Frozen tissue was submerged in lysis buffer, in a homogenization tube to a volume of 10mls lysis buffer per 1g of tissue. Remaining lysis buffer was kept on ice throughout. Tissue was then

homogenized using a Potter-Elvehjem grinder approximately 20 times, until there was a confluent solution. Homogenized hearts were next sonicated on ice for 5 seconds (Vibracell sonicator) and then centrifuged at 10,000 RPM for 10 minutes. Supernatant was removed in preparation for BCA assay of protein quantification.

BCA Assay (protein quantification)

Next a BCA assay was performed to define the protein concentration (µg/µL) of each sample. A 96 well plate was selected and labelled according to sample number, and to set BCA standards of known protein concentration (Table 23). To complete the assay, BCA reagent was prepared in $CuS0_4$ solution to a ratio of 50:1, to form the base solution of the assay. 200µL of this assay solution was added to each well, before addition of either control (10µL H_20), sample lysate (1µL + 9µL H_20) or standards of known concentration (10µL). Once all reagents were added to the 96-well plate, this was transferred to a shaker oven at 37^0C for 30-minutes. After 30-minutes samples were removed and visualised using the Odyssey scanner, which reads the absorbance value of each sample (nm). The results of the known standards (1-7) in absorbance (nm) were used to generate an equation of the line using Graph Pad Prism. This could then be used to interpolate unknown protein concentrations in each tissue sample for given absorbance values. R^2 was analysed for each prism generated equation to determine the goodness of fit for the line equation.

For each sample, the volume required to achieve a protein amount of 20µg was calculated (between 10-12µL). Each sample was then diluted in lysis buffer to a final volume of 20µL to use for each lane during electrophoresis. Prior to electrophoresis, samples were denatured in LDS sample buffer (NuPage©) containing the reducing agent β-mercaptoethanol, for 30-minutes at 80^0C. After this step samples were allowed to cool and either returned to the -80 freezer or used immediately for electrophoresis (below).

Gel electrophoresis

To perform gel electrophoresis, first appropriate reagents were selected. As the ROCK1 and ROCK2 proteins of interest had a molecular weight of 160kDa (large proteins) a 4-12% gradient Bis-tris gel was selected (Invitrogen ©). Due to the Bis-tris constituents of the gel, MOPS SDS running buffer (x10) prepared from NuPage© was diluted down to a 1X concentration in 1 litre of distilled H_20.

Table 23. Description of assay volume used for BCA assay of protein quantification

SAMPLE	PROTEIN CONCENTRATION	ASSAY VOLUME
CONTROL	0	1µL lysis buffer + 9µL H_20
TISSUE LYSATE (X6)	X	1µL tissue lysate + 9µL H_20
STANDARD 1	0	10µL H_20
STANDARD 2	1.25µg/well	10µL standard
STANDARD 3	2.5µg/well	10µL standard
STANDARD 4	5.0µg/well	10µL standard
STANDARD 5	7.5µg/well	10µL standard
STANDARD 6	10.0µg/well	10µL standard
STANDARD 7	15.0µg/well	10µL standard
STANDARD 8	20.0µg/well	10µL standard

Each tissue sample containing 20µg of protein in 20µL was then loaded to respective lanes of the gradient gel. The first lane contained 7.5µL of protein ladder (PageRuler Plus, ThermoFIsher©), to enable molecular weight identification. Once protein samples were loaded, the electrophoresis tank was filled with running buffer as above, and samples were connected to a voltage of 90V for the first 30-minutes, followed by 160V for 1hr 15 minutes (to improve protein band resolution). Gels were

inspected during the running process to ensure that samples did not run off the edge of the gel in the given time frame. At the end of the running period, gels were removed from the electrophoresis tank and prepared for protein transfer.

Protein transfer

To enable protein transfer, first 10X transfer buffer was prepared (Glycine 144g, Tris base 30g, SDS 10g, distilled H20 1L) and diluted down in 20% methanol to make 1X transfer buffer. Gels were carefully removed from their casing material using a chisel and placed carefully on pre-prepared nitrocellulose membrane paper (taking care for the gel not to tear). Gel and membrane soaked in transfer buffer, were loaded into cassettes to form a sandwich, between filter paper and two sponges. The nitrocellulose membrane was orientated towards the positive anode (red,+) and the cassette was inserted into a BioRad © transfer system containing an ice pack. The container was filled with transfer buffer, and a stirrer and connected to a power supply. Cassettes were run at 100V for 90-minutes and the system was placed in an additional tray of ice to prevent overheating.

Antibody application

Cassettes were removed from the transfer container and the membrane was placed into an opaque container filed with 10mls of red Ponceau stain (ThermoFisher), to visualise protein bands. The membrane was incubated for 30 seconds and then Ponceau stain was washed off with distilled water. Next the membrane was incubated in 10mls blocking solution (5% BSA) for 1-hour to remove background staining. Following blocking steps, rabbit primary ROCK2 antibody was applied at a concentration of 1:1000 in 10mls of 5% BSA (AB125025). Mouse beta-actin at a concentration of 1:1000 was applied to the membrane as a housekeeping control (AB8226). The above process was repeated using a separate gel and membrane for ROCK1 antibody, 1:1000 (AB134181). Membranes were allowed to incubate overnight at 4^0C with gentle agitation. Each container was labelled carefully as either ROCK1, or ROCK2.

The following morning, primary antibody solution was rinsed off with 0.1% TBS-tween for 15 minutes, on a total of 3 occasions. 0.1% TBS-tween was produced by adding 1ml of Tween 20 to 1L of pre-prepared TBS (10X TBS 100mls, 900mls distilled H_20). 10X TBS was produced as (24g tris base, 80g NaCl, 1L distilled water) adjusted with HCL to a final pH of 7.6. Each container was next treated with fluorescent secondary antibodies (IRdye 680LT at 1:20000) and (IRdye 800CW at 1:15,000) in 5% BSA. Samples were allowed to incubate for 1 hour with gentle agitation. At the

end of this period each membrane was rinsed with TBS-Tween for 15-miutes on 3 separate occasions. At the end of washing, samples were visualised using the Odyssey scanner to analyse red and green channels. ROCK1/2 bands (visualised separately) were expected to be seen as green at a molecular weight of 160kDa, whereas Beta-actin was expected to be red, and observed at a molecular weight of 42kDa. Protein bands were quantified using a standard protocol from Image-studio lite v5.5 (LICOR software©). Bands were carefully demarcated, and the amount of fluorescent pigment was converted into arbitrary units of protein for quantification (Figure 59). Amount of protein between KO and WT groups for both ROCK1 and ROCK2 membranes were normalised for Beta-actin controls.

Figure 59. Western Blotting quantification process using Image-studio lite©. Fluorescent bands are converted to units of protein (AU). Shown below for ROCK2, 160kDa.

Myocardial ischaemia/reperfusion (n=6)

Animal breeding, and handling were as described in the methods section 1 and 3 (tissue preparation for Western Blot analyses). 12 mice in total (6

WT animals and 6 ROCK2 (+/-) KO animals) were identified by PCR and selected for myocardial ischaemia/reperfusion experiments at between 2-4 months old. This selection of animals contained both male and female mice. Mice were anaesthetised for in vivo studies with 100mg/kg of pentobarbitone and intubated and ventilated with room air and oxygen. For in vivo work in our lab, mice do not undergo carotid cannulation due to the risk of tissue damage and body fluid loss that this can cause in mice of this size. Therefore, MAP readings were not taken in this study. Under anaesthesia, surgical thoracotomy was performed, and the left anterior descending coronary artery (LAD) was identified within the pericardium. This was ligated for 40 minutes, and myocardial ischaemia was confirmed by the presence of anterior ST-elevation. After 40 minutes of ischaemia, the LAD ligature was released, and the vessel was re-perfused for a period of 120 minutes. A shorter period of reperfusion was selected for these experiments as studies of MVO% were not performed in this model. As IS% was the primary outcome, this was prioritised as a parameter in the first instance. Moreover, periods of 180-minutes required for reperfusion to demonstrate MVO, have been associated with high mortality in mice in our lab. As per chapter 4, the LAD vessel was re-occluded with the ligature, and Evans blue dye injected into the systemic circulation, to demonstrate the area at risk (AAR %). Cardiac tissue was prepared into 2mm sections and stained with tetrazolium (TTC) to measure infarct size as a % of the AAR (Figure 33). In vivo power calculations were as specified in chapter 4.

iii) Results

Western Blotting (n=3)

On visual inspection of Western blots, using the Odyssey fluorescent scanner, there appeared to be less ROCK2 protein present in ROCK2 (+/-) KO animals compared to wildtype (WT) and compared to ROCK1 bands (Figure 60). This was suggestive of successful ROCK2 heterozygous (HET) knockdown. Following normalisation and quantification methods, ROCK2 levels in HET animals were found to be approximately 30% of the WT, whilst ROCK1 levels between groups, remained unchanged (Figure 61).

Figure 60: A Western blot is shown below for ROCK1, ROCK2 and beta-actin in KO ROCK2 (+/-) animals (lanes 1-3) and in WT ROCK2(+/+) animals (lanes 4-6). On visual inspection there appears to be less ROCK2 in lanes 1-3 compared to ROCK1 and compared to ROCK2 in lanes 4-6.

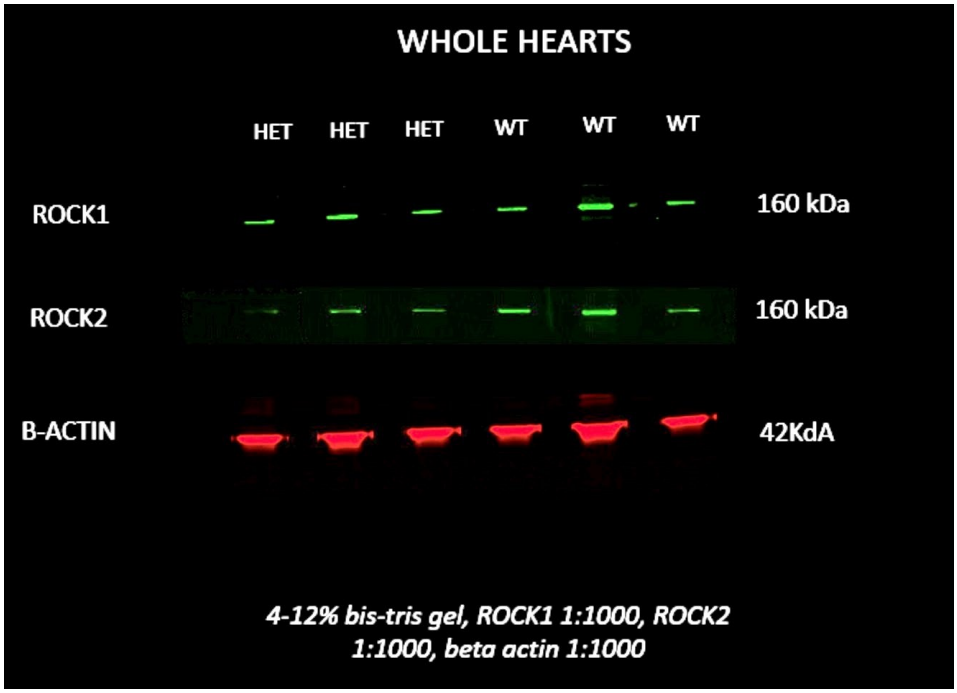

Figure 61. Protein expression levels for ROCK1 and ROCK2 in KO animals as a % of the WT. ROCK2 levels in KO animals were approximately 30% of ROCK2 levels in WT animals (n=3). ROCK1 levels, however appeared unchanged.

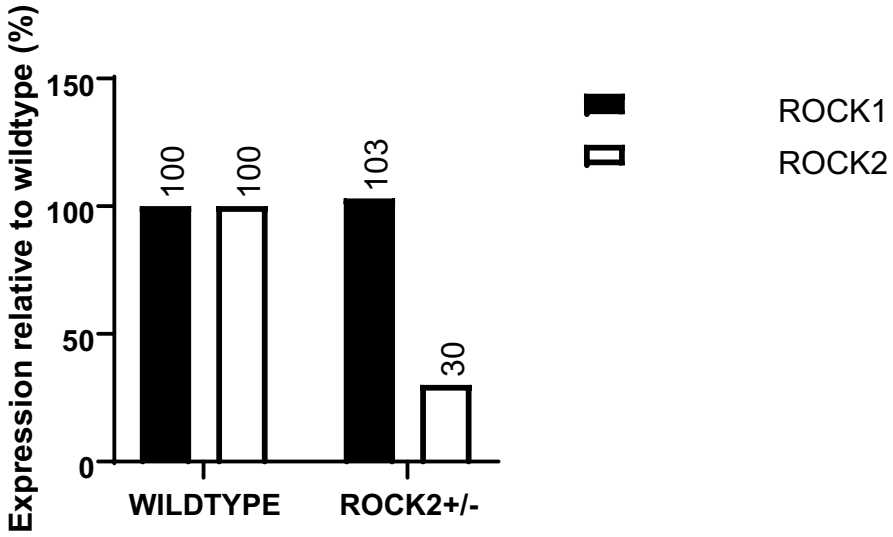

Myocardial Ischaemia/reperfusion in vivo experiments (n=6)

Following 40 minutes of myocardial ischaemia and 120 minutes of reperfusion, all animals survived until the end of the experiment. 66.7 % of all ROCK2 (+/) animals were female, compared to 33.3% male (p=0.56, Chi Squared). The weight of the ROCK2 (+/-) KO animals was significantly less compared to WT animals; however, it is possible that this was confounded by more female mice in the KO group. All female animals weighed significantly less, compared to all male animals (p=0.006, not shown). There were no statistically significant differences observed in either group for IS% or AAR% following ischaemia/reperfusion experiments (Figure 62). In these analyses %

proportions for animal gender were compared with a Chi-squared test and IS% and AAR% parameters were compared using a student's t test.

Figure 62. Ischaemia/reperfusion experiments in ROCK2 (+/-) mice vs control (n=6). Following 40/120 minutes ischaemia/reperfusion no significant differences in IS (%) were observed between groups (p=0.70).

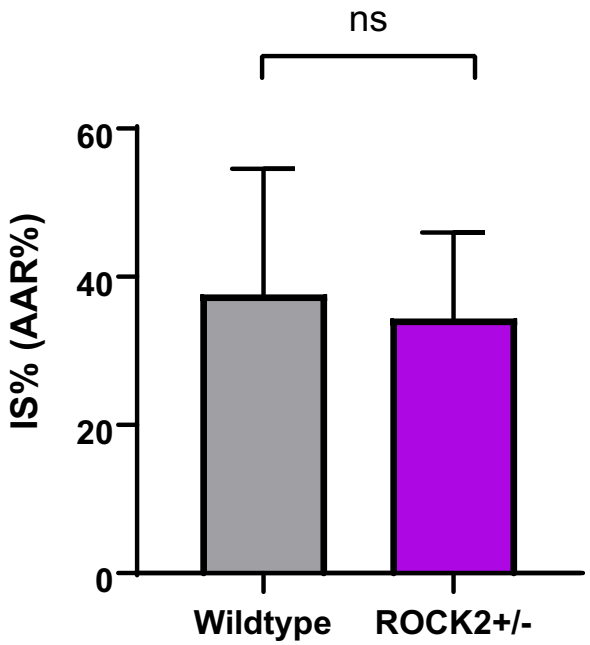

*Table 24: Differences in weight and I/R outcome measures for WT vs ROCK2+/- KO animals (n=6). *p<0.05*

CATEGORY	WILDTYPE RESULT ± SEM (n=6)	ROCK2 (+/-) KO RESULT± SEM (n=6)	P VALUE
FEMALE (%) n=7 MALE (%) n=5	3(50) 3(50)	4(66.7) 2(33.3)	0.56
MEAN WEIGHT (g)	37.4± 2.4	28.8±2.0	0.02*
MEAN IS (% AAR)	37.6±-6.6	34.4±4.5	0.70

MEAN AAR (% of LV)	41.1±3.4	49.1±2.3	0.08

iv) Conclusions

In this set of myocardial ischaemia/reperfusion experiments, haplosufficient ROCK2 deletion, ROCK2 (+/-) was not associated with cardioprotection in vivo.

7.3: CHAPTER DISCUSSION

i) Protein Expression

In ROCK2 (+/-) animals, Western blot analyses suggested that ROCK2 protein levels were approximately 30% of the wildtype, whilst ROCK1 protein levels appeared unchanged. In theory, a heterozygous ROCK2 (+/-) animal should contain 50% of ROCK2 protein levels compared to the wildtype. Given the known lethality of the ROCK2 (-/-) mutation (Thumkeo et al., 2003), it is unlikely that homozygous animals were included in this study without observing associated increased mortality. Animals were bred HET vs WT so that theoretically, the homozygous mutation should not occur. Moreover, these results are comparable to the protein levels seen in a murine ROCK2 (+/-) heterozygous model utilised by Soliman et al (Soliman et al., 2015), where normalised ROCK2 levels were just under <50% of the WT and ROCK1 levels were unchanged. Reports of ROCK1 overcompensation in genetic models relates to the study by Shi et al (Shi et al., 2019) investigating the role of ROCK in myocardial fibrosis, which examined multiple ROCK deletion models. The investigators initially produced an inducible cardiomyocyte specific (ROCK1-/, ROCK2-/-) double KO model, which was associated with globally reduced ROCK activity (p-MLC). Of note, this double deletion model could not be achieved by conditional breeding due to excess lethality and therefore required a tamoxifen induction method after birth (Shi et al., 2019). A cardiomyocyte specific single ROCK2 KO however,

ROCK2 (-/-) demonstrated increased levels of p-MLC which was attributed by the authors to increased ROCK1 activity (Shi et al., 2019). This phenomenon seems to be reported less in heterozygous models (Shi & Wei, 2022), (Shi et al., 2019).

The results in this chapter have investigated protein expression levels, but not changes in ROCK activity (p-MYPT1, p-MLC), which would be an interesting experiment to perform in the future. Also, in agreement with the results of this chapter, Baba et al examined changes to ROCK1/2 protein levels following partial ROCK2 deletion (+/-) in the kidney. ROCK2 levels were found to be 40% of the wildtype, with no significant observed changes to ROCK1 (Baba et al., 2016). Unlike cardiac models, this study did not find any benefit from ROCK2 reduction in the development of renal fibrosis following ureteric obstruction. This might suggest that the anti-fibrotic actions of ROCK2 deletion are organ dependent (Baba et al., 2016). Finally, a difference of 20% in protein levels (between 50% and 30%) could be explained by semi-quantifiable Western blot analysis, and a total n number of 3. There is some subjectivity in analysing and tracing protein bands using Micro-lite software©, which could account for some degree of error. Fully quantifiable systems (like the program Halo used in RNAscope analysis) can auto-detect regions of interest without user dependence. With a greater n number, the results for HET mice may have demonstrated a ROCK2 level closer to 50%.

ii) Myocardial Ischaemia/reperfusion

To the best of the author's knowledge this is the only study investigating ROCK2 (+/-) deletion in a murine model of myocardial ischaemia/reperfusion, in the published literature (MEDLINE indexed). There is a lack overall, of ROCK2 research in acute cardioprotection, despite ongoing developments in cerebral ischaemia/reperfusion and other anti-inflammatory conditions such as GVHD (Lee et al., 2014), (Cutler et al., 2021) .There are therefore no direct results to compare this study to, however the results have suggested that ROCK2 as an isoform is perhaps not an important target in acute myocardial infarction. Before considering the implications of this, it is important to state that this deletion was heterozygous, hence at best, a 50% reduction in the desired treatment effect would be observed, compared to a homozygous model. Another option to address this question, would be to repeat these experiments in a cardiomyocyte specific ROCK (2-/-) model and to see if this improved IS% outcomes. This would require an assessment of ROCK1 and ROCK2 activity to rule out increased ROCK1 levels in a homozygous model (Shi et al., 2019). As an alternate suggestion it would be interesting to investigate diabetic or hypertensive hearts undergoing I/R in either of the above ROCK2 deletion models, as there is evidence that knock down of ROCK2 is more beneficial in such chronic pathologies compared to otherwise healthy animals (Soliman et al., 2020), (Shimizu et al., 2017). The reasons why ROCK2 heterozygous deletion has not proven cardioprotective, will next be considered as part of a wider, final

thesis discussion in the next chapter. This section will aim to summarise the previous chapter discussions and determine whether the original thesis hypotheses have been proven and explained.

CHAPTER 8: FINAL DISCUSSION & FUTHER WORK

8.1: FINAL DISCUSSION & LIMITATIONS OF RESULTS

As each chapter has been summarised and discussed with relevant literature at the end of each section, the aim of this summary discussion is to address each hypothesis individually, re-summarise the main conclusions, and to address the limitations of the work. There will then be statement of suggestions for future investigations.

HYPOTHESIS #1: ROCK2 is differentially expressed in rat myocardium and coronary circulation

Chapter 3 has demonstrated via two distinct methods (immunohistochemistry and RNAscope) that both ROCK2 protein and ROCK2 mRNA are localised to rat coronary vasculature (VSMC) and myocardium (fig.16). Respective markers of VSMC used to identify coronary vessels were α-SMA (IHC) and TGLN (RNAscope). It has been discussed that these results are in keeping with those of large genetic tissue and ScRNA-Seq/SnRNA-Seq databases, although the proportion of ROCK2 in cardiac tissues may be species dependent (Julian & Olson, 2014), (Hu et al., 2018). In the results from this thesis, when RNAscope was quantified with the AI autorecognition programme, Halo©, there was a greater proportion of ROCK2 mRNA observed in myocardium compared to ROCK1 (Figure 17). When co-expression analysis of VSMC were performed, the ROCK2:ROCK1 ratio appeared to normalise, although large quantities of ROCK2 mRNA were clearly visible in larger

arterial vessels upon visual inspection (Figure 16). Measurement using Halo© of arterial wall thickness, and amount of VSMC mRNA, enabled the potential range of coronary circulation vessels included, to be estimated, (4-45μm, Figure 22) It is suggested, that the analysis included some smaller arterial vessels and microvasculature (Figure 18). In chapter 7, a second estimation of ROCK1 and ROCK2 protein levels was made in wildtype mice (the littermates of ROCK2 +/- KO animals) via Western Blotting in whole hearts. In these results the proportions of ROCK1 and ROCK2 protein levels were similar (Figure 61). The RNAscope technique may have had two strengths over the other techniques used, considering firstly, that experimental number and repetitions were higher (n=4, 5 fields of view) in the RNAscope analysis. Secondly, RNAscope as a technique has a higher degree of sensitivity than other methods such as IHC and Western blotting, and this is documented as reaching near 100% (Atout et al., 2022). However, it is important to clarify that RNAscope and Western blotting are measuring different things; mRNA vs protein, and so the quantitative results are not directly comparable.

<u>CONCLUSION #1: ROCK2 mRNA is expressed in both rat myocardium and coronary vasculature in greater quantity than ROCK1</u>

HYPOTHESIS #2: ROCK agonists such as ET-1 will induce vasoconstriction

of rat aortic rings

Chapters 4,5 &6 utilised a vascular wire myography model to investigate the functional changes of rat aortic rings subject to vasoactive substances. The basic model demonstrated that PE induces vasoconstriction of rat aortic rings which can be relieved by addition of the commonly used vasodilator acetyl choline (endothelial dependent vasodilation) (Figure 22). In chapter 6, a new model of aortic ring vasoconstriction was developed to try to more closely mimic vasospasm during myocardial infarction, by using the peptide hormone endothelin-1 (Tona et al., 2023). This model was also considered to be more relevant to the overall hypothesis, as ET-1 is a proven and specific activator of the RhoA/ROCK pathway (g-protein coupled) (Tsai et al., 2017) compared to PE. In chapter 6 experiments, ET-1 induced a greater contractile response than the other two vasoconstrictors PE and AT-II (Figure 49). It was therefore used in the next set of experiments examining the effects of ROCK2 inhibition in aortic rings. One strength of the aortic ring myography model is that functional information is gained, and results are readily reproducible. It is important to state here, however, that the aorta is not a suitable physiological surrogate, from which to draw conclusions about the actions of vasoconstrictors in the coronary circulation (Goodwill et al., 2017).

Ideally, these experiments would have been performed in coronary arteries and microvasculature, however the investigation was limited by the selection of apparatus which was readily available. These findings that ET-1 causes vasoconstriction of aortic rings are not novel, but allow a conclusion to be drawn:

#CONCLUSION 2: ET-1 (known ROCK activator) is a potent vasoconstrictor of rat aortic rings

HYPOTHESIS #3: ROCK2 inhibitors will alleviate agonist mediated arterial vasoconstriction (e.g. PE, ET-1)

The last paragraph has concluded that the peptide hormone ET-1 was found to be a powerful vasoconstrictor of rat aortic rings. This vascular wire myography model was further used to investigate the potential of ROCK2 inhibitors in mitigating ET-1 (ROCK induced) arterial vasospasm. Fasudil (a non-selective ROCK1/2 inhibitor) has been used previously in clinical studies of vasospasm, such as that observed following subarachnoid haemorrhage in the brain (Satoh et al., 2014). As the vasodilatory actions of Fasudil are well known to be non-kinase specific (Porras-González et al., 2014), it is not possible to deduce whether the vasodilation observed in the literature in response to this well-known drug, is secondary to ROCK 1 or 2 inhibition, PKC inhibition, or even calcium channel blockade (Shimokawa & Rashid, 2007).

In this thesis, Fasudil was proven to be vasoactive and relieved PE induced contraction, although the drug's actions were not very potent compared to another well-known NO donor, sodium nitroprusside (Figure 28). Large quantities of Fasudil were required to reach the maximum

efficacy of the drug (Figure 28, Figure 29), which occurred around the $10^{-2.5}$ or 10mM range. This may limit further clinical translation, as larger dose requirements of the drug may increase the potential for off-target side-effects such as systemic hypotension (Liao et al., 2007).

This was the rationale to further explore other ROCK inhibitors with firstly, greater selectivity for ROCK2. Other in vitro studies have demonstrated that ROCK2 as an isoform is closely linked to VSMC contraction (Wang et al., 2009). At the time of designing this research, the most ROCK2 selective inhibitor was KD025, (200x fold selectivity for ROCK2 over ROCK1). It must be kept in mind that ROCK2 selectivity as advertised by some manufacturers does not always relate to selectivity over ROCK1, but instead refers to other kinases e.g. PKC. However, in the case of KD025, this drug is highly selective for ROCK2 over ROCK1 (Shah & Savjani, 2016). Moreover, KD025 is a clinically safe drug as evidenced by the recent large-scale clinical trial “ROCKstar” (Cutler et al., 2021). In the trial, KD025 was investigated as an anti-inflammatory drug and an anti-fibrotic therapy however, and not as a vasodilator. Since these thesis experiments were conducted, a newer more selective ROCK2 compound called GV101 has been synthesised with a selectivity ratio for ROCK2 of approximately 4000 (Zanin-Zhorov et al., 2023). The drug has been used to mitigate liver fibrosis in mice and upregulate p-AKT (Zanin-Zhorov et al., 2023). This agent may also be useful to investigate in future experiments.

In chapter 5, KD025 (selective ROCK2 inhibitor) soluble in DMSO, was investigated in the aortic ring myography model following PE induced

contraction. Unfortunately, the compound appeared to be mostly non-vasoactive in rat aorta (Figure 43), despite the same vessels demonstrating adequate vasodilatory responses to acetyl choline (as part of the basic model) and to Chroman 1 (another more potent, but less selective ROCK2 inhibitor), and it also being demonstrated that rat aorta expresses ROCK2 mRNA. In these experiments therefore, greater selectivity for ROCK2>ROCK1 inhibition did not appear to translate to increased vasodilatory potential. This has not been firmly proven however, as the assay did not prove that pharmacological ROCK2 inhibition took place. In practice, this is extremely difficult, as the downstream targets of ROCK2 (p-MYPT1, p-MLC2) are shared with ROCK1. Many traditional authors also believe that the functions of ROCK1 and ROCK2 cannot ever be truly separated (Hartmann et al., 2015). A definitive answer as to whether arterial vasodilation is ROCK isoform specific, would be gained from a VSMC conditional (ROCK1-/-) KO model and the investigation of these murine aortic ring's vs wildtype. In future work these experiments might be prioritised, to enable a firm conclusion to be reached, however this would require the acquisition of a different apparatus such as small vessel wire myography, suitable for mouse aortic rings which are of smaller diameter to rat vessels. Another alternative would be to perform in vitro studies of ET-1 mediated contraction on VSMC from KO mice (VSMC ROCK1-/-) and to investigate these responses in comparison to WT VSMCs.

It is true to say that measuring changes to total ROCK activity (via the phosphorylation of MYPT1/P-MLC2) would have been useful in the

KD025 ex vivo experiments, as if ROCK activity had decreased overall, then this is less suggestive of a problem with the reagent. This should, therefore, also be considered in future studies. Against KD025 not reaching the target tissue, the same stock reagent had been used in vivo and demonstrated therapeutic effects (Figure 40). Given the reported IC_{50} of KD025 for ROCK2 (105nM), concentrations of [10^{-9}-10-^{5}]M ex vivo should have been sufficient to investigate the compound. One possibility is that KD025 precipitated out of solution in a large water bath of 45mls. This is a draw-back of this myography setup which requires rings to be submerged in a large volume of buffer.

In the same sets of aortic rings, Chroman 1 (potent ROCK2 inhibitor) did demonstrate significant potential as a vasodilator, both in PE constricted aortic rings and those constricted with the more potent, ET-1. Due to the increased potency of Chroman 1 (with IC_{50} in the picomolar range), it is highly likely that the drug inhibited both ROCK1 and ROCK2 at the concentrations of the drug tested. The approximate selectivity index for Chroman 1 is around 50x fold and so it is less selective compared to KD025 (Chen et al., 2021). The Chroman 1 results may also indicate that ROCK1 is more important for vasodilatory response than ROCK2, however this would require a highly selective ROCK1 inhibitor to firmly prove this. Moreover, the chapter discussion could not exclude that Chroman 1 had not inhibited MRCK, which is another ROCK like kinase.

MRCK is activated by shared G protein coupled receptors and the upstream molecule CDC42 (as opposed to RhoA) (Zhao & Manser,

2015). It is not widely known whether MRCK is a vasodilator of aortic rings on review of the present literature. A prominent paper which has investigated the potential role of MRCK in atrial fibrillation, has noted that this kinase is relatively understudied compared to its ROCK like counterparts (Perike et al., 2023). It would be interesting in future studies to treat aortic rings with an MRCK inhibitor, e.g. BDP5290 (Perike et al., 2023) and observe whether this does induce vasodilation to account for the Chroman 1 effects. If MRCKi did not induce vasodilation, then this would still leave both ROCK1 and ROCK2 isoforms as potential instigators of Chroman 1 mediated vasodilation, therefore these experiments are only partially helpful to the hypothesis, and a KO model is preferential to prove this.

#CONCLUSION 3: These results suggest that increasing the selectivity of inhibitors for ROCK2 (over ROCK1) reduces vasoactive potential, however this cannot be firmly concluded from these experiments.

HYPOTHESIS #4: As vasospasm is a known feature of myocardial I/R injury and no reflow, selective ROCK2 inhibitors will be cardioprotective with respect to i) Infarct size% and ii) MVO%

Pilot experiments - Fasudil outcomes (ROCK1/2 inhibitor)

In vivo studies of myocardial ischaemia/reperfusion were undertaken to measure IS% outcomes using TTC staining (traditional method) and to

measure MVO% using Thioflavin S dye with analysis under UV light. The latter method was originally introduced by Robert Kloner in the 1980's in the investigation of ischaemic NRF (Kloner et al., 1974), and this remains a well-recognised method of MVO% assessment in animal studies in the modern day (Dai et al., 2022), (Kumar et al., 2011). Fasudil is well proven to be cardioprotective with respect to IS% at doses of 10mg/kg (Huang et al., 2018a), and so these experiments were conducted to demonstrate a functioning in vivo model and to affirm what is already known in the literature with regards to ROCK1/2 inhibition. Mechanisms of action for Fasudil (ROCK1/2i) induced cardioprotection, have previously been proposed as 1) the drug inducing a potential BCL/caspase mediated reduction in apoptosis and augmenting NO levels as a downstream consequence of the RISK pathway, and 2) AKT phosphorylation and activation (Huang et al., 2011), (Zhang et al., 2014). In keeping with this, adding Wortmannin (a RISK pathway inhibitor) to hearts treated with Fasudil during ischaemia/reperfusion, mitigates the protective effects of the drug with regards to IS% (Wu et al., 2014). Much less literature has considered the effects of Fasudil on MVO% in vivo, compared to IS%. One previous study has examined the effects of hydroxyfasudil (the active metabolite of Fasudil) on the area of MVO% in pigs undergoing myocardial I/R (Zhao et al., 2009). Hydroxyfasudil was found to reduce the area of no reflow % (as measured by Thioflavin S dye) in the treatment group. This study protocol also differed from the experiments in this thesis, in that the ischaemia time was 3-hours (Zhao et al., 2009).

In support of prior discussion in this thesis, Zhao et al also describe the phenomenon of MVO/NRF% as multi-factorial and a likely combination of small vessel vasospasm, platelet aggregation, immune cell complexes, capillary rupture and myocardial oedema (Zhao et al., 2009), (Reffelmann & Kloner, 2002). However, they also conclude that the K_{ATP} channel may be implicated in the protection that hydroxyfasudil provides to the microvasculature. Furthermore, when hearts were treated with Glibenclamide (a K_{ATP} channel blocker), both the reduction in NRF%, mediated by hydroxyfasudil and conditioning, were lost (Zhao et al., 2009). The K_{ATP} channel has long been suggested as having a fundamental role in ischaemia/reperfusion injury and ischaemic preconditioning (Oldenburg et al., 2002), (Yellon et al., 2023), and it is thought to reside on the inner mitochondrial membrane. In the context of ischaemic preconditioning, early opening of K_{ATP} channels, results in generation of ROS species which can provide myocardial protection to a controlled degree. Note, this is a distinct concept to the description of I/R injury which involves uncontrolled, and harmful amounts of ROS, which contribute to I/R injury (Heusch, 2015), (Yellon et al., 2023).

Moreover, other drugs such as Nicorandil, are known to act as openers of the K_{ATP} channel, and these have been associated with myocardial protection in both humans and animals (Pearce et al., 2023). Although, this thesis has not proven a direct mechanism for the actions of Fasudil in vivo, to explain a reduction in either IS% or NRF%, one possible explanation is an increase in activity of the RISK pathway, via AKT

phosphorylation and subsequent opening of K_{ATP} channels (Huang et al., 2018a), (Zhang et al., 2014). It can be argued that this work has demonstrated indirectly, a possible mechanism of L-NAME independent vasodilation exerted by Fasudil (albeit in aorta and these limitations are already discussed above). However, these findings are not novel, and Fasudil is known to have vasodilatory actions and can relieve coronary vasospasm elsewhere (Masumoto et al., 2002).

In this thesis, a moderate correlation was demonstrated between IS% outcomes and NRF% outcomes (Figure 35). One major difficulty in interpreting the MVO% results in vivo, is that it is not known to what extent the results relate to changes in infarct size, and to what degree these two outcomes are mutually exclusive (Kloner et al., 2018). Furthermore, the mechanisms described above with regards to ROCKi related cardioprotection (reduction in apoptosis, phosphorylation of AKT, & opening of K_{ATP} channels) have often been proven in myocardial tissue or cardiomyocytes, and not in vascular tissue alone (Huang et al., 2018a), (Zhang et al., 2014).

Proving that there has been an increase in the activity of the RISK pathway in coronary artery tissue following ROCK inhibitor treatment in I/R, may contribute to the argument, that the NRF% can be considered as a separate treatment target to IS% in myocardial protection. As it is difficult to isolate the microvasculature in in vivo studies, this would require investigations using microvascular cells and models of hypoxia/reoxygenation to mimic I/R. In the literature, translational work has favoured investigating the physiological functions of vascular tissue,

in the presence of vasoconstrictors which are highly active during I/R e.g. ET-1 (Tsai et al., 2017). This is because blood vessels are resilient to ischaemia and are far more likely to demonstrate alterations to vasoreactivity before apoptosis occurs (Heusch, 2016). However, in future studies, both types of experiments would be useful, to try to prove that MVO and NRF% are a separate target to IS% i.e. there is independent RISK pathway activity (or an unknown equivalent) in the vasculature to be attenuated. Both Robert Kloner and Gerd Heusch, (who have previously studied MVO and NRF extensively), believe that IS% and MVO% are distinct measurable variables, however, Heusch et al do not feel that targeting improvements in MVO% alone (without a reduction in IS%) is a useful endeavour, and that state that these parameters should be considered in combination as a primary outcome in cardioprotection (Heusch, 2016), (Heusch, 2019), (Kloner et al., 2018).

Regarding the third measured outcome, intramyocardial haemorrhage (IMH), the results from this thesis demonstrated that Fasudil, at 10mg/kg and 3mg/kg, significantly reduced IMH% in vivo (Figure 41). Chapter 1 has discussed that IMH is closely related to myocardial necrosis and capillary rupture and is associated with a worsening prognosis compared to MVO alone (Konijnenberg et al., 2020) (Berry & Ibanez, 2022). Further work is required to investigate this phenomenon at a vascular level (Bonfig, Soukup, Shah, Davidson, et al., 2022), (Carrick et al., 2016). One possibility behind the mechanism of IMH% is capillary rupture and damage to the endothelial glycocalyx and basement membrane (Davidson, Andreadou, Garcia-Dorado, et al., 2019) following

ischaemia/reperfusion. ROCK inhibitors have been shown to improve endothelial membrane permeability in other organs e.g. lungs during sepsis (Lee et al., 2020), therefore it is possible (however not proven) that a similar mechanism could have occurred here. To the best of the author's knowledge there is not any other literature that has explored the effects of ROCKi on intramyocardial haemorrhage despite ample interest in Fasudil in myocardial protection.

At the juncture of the Fasudil findings, one possibility for continued study would have been to further investigate Fasudil dependent mechanisms with regards to MVO% and IMH%. However, this was not pursued, as for other reasons, Fasudil was deemed to be a clinically undesirable drug. In these experiments, rats suffered severe haemodynamic effects at Fasudil doses 10mg/kg (required to mitigate IS% in addition to other outcomes) leading to the death of an animal and another becoming critically unwell. Attentions therefore turned to the use of ROCK2 inhibitors in cardioprotection, to try to address the main hypothesis.

ROCK2 inhibition in cardioprotection – IS% (primary outcome)

Two measures of selective ROCK2 inhibition were examined in this thesis i) Selective ROCK2 inhibition with KD025 (a drug which is currently licenced in clinical practice) and ii) ROCK2 (+/-) partial deletion in a murine model. The author feels that although Chroman 1 is a potent ROCK2 inhibitor, it is much less selective for ROCK2>ROCK1 and

therefore the neutral results are difficult to interpret with respect to this hypothesis.

Following the addition of KD025 prior to myocardial reperfusion, the primary aim of reducing IS% was not achieved for any dose of the drug. These findings are supported by the ROCK2 (+/-) KO mouse model, where there were also no observed reductions in IS% following I/R. These results might suggest that the ROCK2 isoform is less important in myocardial protection and cell death following ischaemia/reperfusion. Moreover, Fasudil, a ROCK1/2 inhibitor, was the only agent to improve IS% outcomes and so perhaps it is the ROCK1 isoform that is most important in cardioprotection. Some investigators have stated that the ROCK1 isoform is able to mediate cell death such as apoptosis, and caspase mediated activation of the PTEN molecule (which has deleterious effects on the RISK pathway and p-AKT) (Chang et al., 2006). This would seem to suggest that at least an element of ROCK1 inhibition is required to inhibit these processes, increase p-AKT activity, and therefore reduce infarct size following myocardial infarction (Yellon et al., 2023), (Rossello & Yellon, 2018). The Chroman 1 results are not consistent with this however, and these will be further discussed below.

The limitations of not conducting formal PK studies for KD025 and Chroman 1 have been considered in the individual chapters. KD025, has however, been validated as a ROCK2 inhibitor previously by Lee et al (Lee et al., 2014) in their studies of brain tissue at similar doses

(100mg/kg). Chapter 7 has considered the reasons why Chroman 1 (with increased potency for ROCK2 and ROCK1) was not cardioprotective with regards to any outcome. This is difficult to explain and raises the possibility of a pharmacological issue. Significant blood pressure effects of the drug were noted at doses >500μg/kg however which does suggest that there was some drug activity at this dose. It is possible that although the selectivity window is small, the balance of selectivity for ROCK2>ROCK1 is not in favour of cardioprotection. To try to be as definitive as possible, the murine ROCK (2+/-) model was developed as the best way of addressing this main hypothesis. ROCK2 heterozygous KO was confirmed via Western Blotting which demonstrated reduced amounts of ROCK2 protein, and no changes to ROCK1 protein levels. Following I/R experiments ROCK (2+/-) partial deletion was not associated with cardioprotection as assessed by IS% alone (Figure 62) in mice. Although the KO model is the most robust model to draw a conclusion from, all the results are consistent in that ROCK2 inhibition was not cardioprotective, when considering IS% outcomes. Therefore: -

#CONCLUSION 4: Selectivity for ROCK2 inhibition is not associated with a reduction in IS% and cardioprotection (primary outcome).

It can be further speculated (but is not proven here) that ROCK1 is the most important isoform in acute myocardial infarction. It would be useful to investigate a ROCK1 specific inhibitor in future studies of myocardial I/R or alternatively, cardiomyocyte specific KO models.

ROCK2 inhibition in cardioprotection – MVO% (secondary outcome)

As the KO model did not extend to MVO% for technical reasons, it is more difficult to be more definitive about the role of ROCK2 in MVO. One ROCK2 inhibitor, KD025, demonstrated some improvements in MVO% and IMH% in vivo (Figure 40, Figure 41).

As KD025 was not vasoactive in the aortic ring experiments, assuming ROCK2i has taken place, it could be an alternate mechanism of NRF that KD025 has attenuated, rather than vasoconstriction of arterial vessels. This comes with the caveat that simply because KD025 was not vasoactive in the aorta, this does not prove that it does not have vasoactive potential in the coronary circulation. As has been demonstrated in other studies, where different vessel types had different responses to ROCK inhibitors (Grisk et al., 2012). Moreover, KD025 has demonstrated some vasoactive properties in mesenteric arteries challenged with ET-1 (Björling et al., 2018). In these small resistance vessels, this response may be associated with advancing age (Björling et al., 2018).

One possible explanation for KD025 reducing MVO% and IMH% is T-cell and cytokine mediated inflammation (as in the well-known case of GVHD (Cutler et al., 2021), or an improvement in endothelial membrane permeability resulting in preserved vascular architecture as in previous pulmonary studies (Lee et al., 2020). Further studies which could be performed to confirm the above, include measuring cytokines such as IL-17 (Mora-Ruíz et al., 2019)) during I/R, and markers of endothelial

membrane function such as VE cadherins, in I/R hearts treated with KD025. ROCK2 inhibition was notably associated with a reduction in IL-17 in the ROCKstar trial (Cutler et al., 2021) and so this is already a known target for the drug. As an alternate explanation, KD025 has previously been shown to have favourable off-target drug effects in other studies of thermogenesis and obesity (Tran & Chun, 2021). Following analysis of a large bioinformatics database which has profiled the downstream targets of KD025 (including those independent of ROCK signalling) Park et al demonstrated that KD025 also modulates expression of STC1 (stanniocalcin1) and the cytokine CXCL8 (Park & Chun, 2020). The former has previously inhibited vascular leakage in pulmonary fibrosis (Ohkouchi et al., 2015), and the latter is known to be associated with inflammation in myocardial infarction (Frangogiannis, 2004). KD025 remains a useful drug to continue to investigate, given that it is licenced in the UK already, and has passed safety outcome clinical trials (Cutler et al., 2021). Regarding these safety trials and ROCKstar findings (Cutler et al., 2021), the potential mild side effects following oral therapy with KD025, have already been described in chapter 5. Moreover, this clinical use is for refractory GVHD, therefore some degree of drug side-effects is accepted, in the same way as chemotherapy side effects are accepted in patients undergoing cancer treatment, i.e. weighing the risk vs benefit.

Refractory GVHD is both a debilitating and life-threatening disease (Cutler et al., 2021). It is appreciated therefore, that the balance of side

effects vs clinical outcomes may be different in younger patients with myocardial infarction, especially as STEMI outcomes are optimal following PPCI, and some patients may have few co-morbidities or those which are modifiable (Niccoli et al., 2019). The balance of risk regarding disease modifying therapies and potential side effects would therefore be different in this patient cohort compared to the end stage GVHD population.

Related to this, it is known that KD025 is not suitable for those of childbearing age (men or women) due to its potential teratogenic side effects (Cutler et al., 2021), this must be considered as a limitation when considering the drug for alternate medical uses such as in acute myocardial infarction. Another important consideration/limitation is the possibility of any kinase inhibitor in humans to modulate the risk of cancer- and the expression of cancer-causing oncogenes. In fact, ROCKi is broadly associated with beneficial outcomes in oncology, given that ROCK has a role in tumour cell migration, proliferation and metastases (Kim et al., 2021). ROCK2 over-expression has been associated with worsening prognosis in bladder cancer, medullary thyroid cancer and colon cancer (de Sousa et al., 2020). Over-expression of ROCK1 is a poor prognostic marker in breast cancer according to the same extensive review by (de Sousa et al., 2020).

Whilst ROCKi look to suppress tumour proliferation, one possible cause for concern, is the over expression of either isoform which may occur because of prolonged therapeutic treatment and modifications to mRNA expression. Therefore, it is not so much the exact levels of ROCK1 and

ROCK2 but the balance of these levels and homeostasis, which if disturbed, could cause unwelcome changes to the cell cycle (Kim et al., 2021). The new 'ROCK inhibitory peptides' which deactivate ROCK without initiating full kinase inhibition may be one solution to this dilemma (Abbasgholizadeh et al., 2019). The long term follow up results of patients in the ROCKstar trial are currently awaited (Cutler et al., 2021). Conversely, short term treatment with such agents in the catheter lab as a one-off treatment, may be less of a concern and may not lead to post translational genetic modifications. Increasing the potency of ROCK2 inhibition with Chroman 1 failed to confer a benefit in MVO% or IMH%, much like for IS%. The reasons why this may not have occurred have been considered above.

In summary, it is not clear whether KD025 has improved MVO% outcomes because of ROCK inhibition, or another non-canonical pathway and this should be investigated in the future. As stated previously, it is not possible to be definitive about the exact role of the ROCK2 isoform in MVO from these results, although ROCK 1/2, may be implicated in NRF based on the previous positive Fasudil outcomes.

One possible explanation for some of the discrepancies between MVO% outcomes for KD025 and Chroman 1, as discussed in the relevant chapter of this thesis, may be the differences in specificity for ROCK1 and 2 between Chroman 1 and KD025. KD025 has a greater specificity and selectivity for ROCK2 compared to Chroman 1, whereas Chroman 1 is a more potent inhibitor of ROCK2 (but less selective). From these results, therefore it could be further hypothesised that it is the ROCK2 specificity

that is more important for MVO% outcomes. Whether this is due to microvasculature vasodilation or improvement in barrier function, it is not possible to deduce from these results.

Therefore:

#CONCLUSION 5: It is not possible to conclude whether ROCK2 is an important isoform in MVO% and IMH%.

8.2 SUGGESTIONS FOR FUTHER WORK

This thesis has evoked two principal areas of further research questions, which are both topics for future investigations. The first topic concerns MVO% as a treatment target in relation to IS%, and whether there is evidence for an independent protection pathway i.e. RISK pathway in the vasculature which Fasudil and KD025 can protect independently of the myocardium. This would not just be of academic interest to establish, as it is well discussed that improving MVO% improves patient prognosis post-STEMI independently to infarct size (de Waha et al., 2017). These experiments have been suggested already in the discussion above, and entail the measuring of p-AKT in vascular tissue treated with ROCKi, prior to myocardial I/R.

The second main research area concerns the continuing pursuit of ROCK signalling and isoform specific function, in a setting of acute myocardial protection, which was the overall hypothesis of this thesis. This is a complex area of research, and for many years it was argued that ROCK1 and ROCK2 were too homologous to demonstrate any functional

differences in downstream activity (Noma et al., 2006). This was recently questioned with the new findings of KD025 in the ROCKstar trial and the clinical use of KD025 in GVHD as an anti-inflammatory agent, (demonstrating distinct actions to other non-selective ROCK1/2 inhibitors). However, it is newly emerging, that KD025 may have many off-target functions which do not utilise the ROCK pathway (Park & Chun, 2020), suggesting that its novel anti-inflammatory effects may not be isoform specific. Further studies could be planned to investigate other selective ROCK2 inhibitors, such as the newly described drug, GV01, in liver fibrosis by (Zanin-Zhorov et al., 2023) with ~4000 selectivity for ROCK2. However, this can never fully eliminate the actions of other kinases to answer the research question definitively. It is the opinion of the author that these questions can only be answered using genetic KO models, one of which has been considered in this work to try to best address the hypothesis. More specifically, a conditional vascular ROCK1-/- KO could be used to confirm the newly generated hypothesis, that ROCK1 that is the more important isoform in arterial vasodilation. To further investigate and consolidate these in vivo results, a cardiomyocyte specific ROCK2-/- model could be used to confirm that ROCK2 is not a target in acute myocardial protection. This has the advantage of a double KO model, but without the lethality.

In the case of KD025, further investigations into the mechanism behind MVO% and IMH% protection may involve the examination of other off-target molecules such as STC1 which has been discussed above, as important in mediating vascular integrity (Ohkouchi et al., 2015). Other

ROCK inhibitor studies could also be conducted in different models of disease such as diabetes or hypertension. The author would favour these as more suitable models to use to continue to pursue the protective effects of selective ROCK2 inhibitors, as there is a large body of evidence that ROCK2 signalling, and expression is most enhanced and distinct in models of chronic disease (Björling et al., 2018), (Cutler et al., 2021), (Shimizu et al., 2013). (Soliman et al., 2020), (Tsai et al., 2017).

Given its observed actions in the aortic ring experiments, Chroman 1 may also warrant further pursuit as an anti-hypertensive, and this could be studied in the current model using aortas from hypertensive rats.

8.3 FINAL COMMENTS

This thesis has highlighted, that whilst investigations have been conducted into ROCK signalling for 40-years, this remains a fast-moving field. The subdivision of ROCK2 selectivity is slowly gaining traction in other specialties such as haematology and neurology, and some large-scale clinical trials are expected within the next few years. Indeed, the ROCKstar trial was published, and KD025 came into clinical practice, during this thesis. However, none of these trials planned, at present, relate to the heart.

Although Fasudil has been well investigated in cardioprotection, the role of ROCK2 in acute myocardial protection has, prior to this work, been unexplored. For these reasons, this work has produced a broad overview

of newer ROCK inhibitors in cardioprotection, rather than investigate a specific ROCK2 signalling pathway. At present the results of these investigations are neutral with regards to ROCK2 (considering IS%). It is therefore hoped with the aforementioned areas of continued research, that the benefits of selective ROCK2 inhibition can be translated to myocardial and vascular protection in the future; be this in a more chronic model of cardiovascular disease.

REFERENCES

A Jamieson, S. A., R Bell, D Yellon. (2018). The role of sodium-glucose co-transporters (SGLT's) in endothelial funcon in diabetes and elevated glucose [Journal Arcle]. *Unpublished*.

Abbasgholizadeh, R., Zhang, H., Cra, J. W., Jr., Bryan, R. M., Jr., Bark, S. J., Briggs, J. M., Fox, R. O., Agarkov, A., Zimmer, W. E., Gilbertson, S. R., & Schwartz, R. J. (2019). Discovery of vascular Rho kinase (ROCK) inhibitory pepdes. *Exp Biol Med (Maywood)*, *244*(11), 940-951. https://doi.org/10.1177/1535370219849581

Abbate, A., Wohlford, G. F., Del Buono, M. G., Chiabrando, J. G., Markley, R., Turlington, J., Kadariya, D., Trankle, C. R., Biondi-Zoccai, G., Lipinski, M. J., & Van Tassell, B. W. (2022). Interleukin-1 blockade with anakinra and heart failure following ST-segment elevaon myocardial infarcon: results from a pooled analysis of the VCUART clinical trials. *Eur Heart J Cardiovasc Pharmacother*, *8*(5), 503-510. https://doi.org/10.1093/ehjcvp/pvab075

ABCAM. *IHC-P protocol V3*. https://www.abcam.com/ps/pdf/protocols/ihc_p.pdf

Abedi, F., Omidkhoda, N., Arasteh, O., Ghavami, V., & Hosseinzadeh, H. (2023). The Therapeuc Role of Rho Kinase Inhibitor, Fasudil, on Pulmonary Hypertension; a Systemac Review and Meta-Analysis. *Drug Res (Stuttg)*, *73*(1), 5-16. https://doi.org/10.1055/a-1879-3111

Adlbrecht, C., Andreas, M., Redwan, B., Distelmaier, K., Mascherbauer, J., Kaider, A., Wolzt, M., Tilea, I. A., Neunteufl, T., Delle-Karth, G., Maurer, G., & Lang, I. M. (2012). Systemic endothelin receptor blockade in ST-segment elevaon acute coronary syndrome protects the microvasculature: a randomised pilot study. *EuroIntervention*, *7*(12), 1386-1395. https://doi.org/10.4244/eijv7i12a218

Aguiar, M. O. D., Tavares, B. G., Tsutsui, J. M., Fava, A. M., Borges, B. C., Oliveira, M. T., Jr., Soeiro, A., Nicolau, J. C., Ribeiro, H. B., Chiang, H. P., Sbano, J. C. N., Goldsweig, A., Rochite, C. E., Lopes, B. B. C., Ramirez, J. A. F., Kalil Filho, R., Porter, T. R., & Mathias, W., Jr. (2020). Sonothrombolysis Improves Myocardial Dynamics and Microvascular Obstrucon Prevenng Le Ventricular Remodeling in Paents With ST Elevaon Myocardial Infarcon. *Circ Cardiovasc Imaging*, *13*(4), e009536. https://doi.org/10.1161/circimaging.119.009536

Ali, F., & Ilyas, A. (2022). Belumosudil with ROCK-2 inhibion: chemical and therapeuc development to FDA approval for the treatment of chronic gra-versus-host disease. *Curr Res Transl Med*, *70*(3), 103343. https://doi.org/10.1016/j.retram.2022.103343 Alvarez-Santos, M. D., Alvarez-Gonzalez, M., Estrada-Soto, S., & Bazan-Perkins, B. (2020). Regulaon of Myosin Light-Chain Phosphatase Acvity to Generate Airway Smooth Muscle Hypercontraclity. *Front Physiol*, *11*, 701. https://doi.org/10.3389/fphys.2020.00701

Andreadou, I., Cabrera-Fuentes, H. A., Devaux, Y., Frangogiannis, N. G., Frantz, S., Guzik, T., Liehn, E. A., Gomes, C. P. C., Schulz, R., & Hausenloy, D. J. (2019). Immune cells as targets for cardioprotecon: new players and novel therapeuc opportunies. *Cardiovasc Res*, *115*(7), 1117-1130. https://doi.org/10.1093/cvr/cvz050

Atout, S., Shurrab, S., & Loveridge, C. (2022). Evaluaon of the Suitability of RNAscope as a Technique to Measure Gene Expression in Clinical Diagnoscs: A Systemac Review. *Mol Diagn Ther*, *26*(1), 19-37. https://doi.org/10.1007/s40291-021-00570-2

Avolio, E., Campagnolo, P., Katare, R., & Madeddu, P. (2023). The role of cardiac pericytes in health and disease: therapeuc targets for myocardial infarcon. *Nat Rev Cardiol*. https://doi.org/10.1038/s41569-023-00913-y

Baba, I., Egi, Y., & Suzuki, K. (2016). Paral deleon of the ROCK2 protein fails to reduce renal fibrosis in a unilateral ureteral obstrucon model in mice. *Mol Med Rep*, *13*(1), 231-236. https://doi.org/10.3892/mmr.2015.4569

Basalay, M. V., Mastskaya, S., Mrochek, A., Ackland, G. L., Del Arroyo, A. G., Sanchez, J., Sjoquist, P. O., Pernow, J., Gourine, A. V., & Gourine, A. (2016). Glucagon-like pepde1 (GLP-1) mediates cardioprotecon by remote ischaemic condioning. *Cardiovasc Res*, *112*(3), 669-676. https://doi.org/10.1093/cvr/cvw216

Bell, R. M., & Yellon, D. M. (2003). Atorvastan, administered at the onset of reperfusion, and independent of lipid lowering, protects the myocardium by up-regulang a prosurvival pathway. *J Am Coll Cardiol*, *41*(3), 508-515. https://doi.org/10.1016/s07351097(02)02816-4

Bentzon, J. F., Otsuka, F., Virmani, R., & Falk, E. (2014). Mechanisms of plaque formaon and rupture. *Circ Res*, *114*(12), 1852-1866. https://doi.org/10.1161/CIRCRESAHA.114.302721

Berry, C., & Ibanez, B. (2022). Intramyocardial Hemorrhage: The Final Froner for Prevenng Heart Failure Post-Myocardial Infarcon. *J Am Coll Cardiol*, *79*(1), 49-51. https://doi.org/10.1016/j.jacc.2021.11.002

Bers, D. M. (2002). Cardiac excitaon-contracon coupling. *Nature*, *415*(6868), 198-205. https://doi.org/10.1038/415198a

Bhar-Amato, J., Davies, W., & Agarwal, S. (2017). Ventricular Arrhythmia aer Acute Myocardial Infarcon: 'The Perfect Storm'. *Arrhythm Electrophysiol Rev*, *6*(3), 134-139. https://doi.org/10.15420/aer.2017.24.1

Bio, A. (2022). RNAscope™ Mulplex Fluorescent Reagent Kit v2 . . In. https://acdbio.com/sites/default/files/UM%20323100%20Mulplex%20Fluorescent%20v2_RevB.pdf.

Björling, K., Joseph, P. D., Egebjerg, K., Salomonsson, M., Hansen, J. L., Ludvigsen, T. P., & Jensen, L. J. (2018). Role of age, Rho-kinase 2 expression, and G protein-mediated signaling in the myogenic response in mouse small mesenteric arteries. *Physiol Rep*, *6*(17), e13863. https://doi.org/10.14814/phy2.13863

Bochaton, T., Lassus, J., Paccalet, A., Derimay, F., Rioufol, G., Prieur, C., Bonnefoy-Cudraz, E., Crola Da Silva, C., Bernelin, H., Amaz, C., Espanet, S., de Bourguignon, C., Dufay, N., Carer, R., Croisille, P., Ovize, M., & Mewton, N. (2021). Associaon of myocardial hemorrhage and persistent microvascular obstrucon with circulang inflammatory biomarkers in STEMI paents. *PLoS One*, *16*(1), e0245684. https://doi.org/10.1371/journal.pone.0245684

Bolli, R. (1990). Mechanism of myocardial "stunning". *Circulation*, *82*(3), 723-738. https://doi.org/10.1161/01.CIR.82.3.723

Bonanno, G., Coppo, S., Modregger, P., Pellegrin, M., Stuber, A., Stampanoni, M., Mazzolai, L., Stuber, M., & van Heeswijk, R. B. (2015). Ultra-high-resoluon 3D imaging of atherosclerosis in mice with synchrotron differenal phase contrast: a proof of concept study. *Sci Rep*, *5*, 11980. https://doi.org/10.1038/srep11980

Bonaventura, A., Vecchié, A., Abbate, A., & Montecucco, F. (2020). Neutrophil Extracellular Traps and Cardiovascular Diseases: An Update. *Cells*, *9*(1). https://doi.org/10.3390/cells9010231

Bonfig, N. L., Soukup, C. R., Shah, A. A., Davidson, S. J., Stanberry, L. I., Okeson, B. K., & Traverse, J. H. (2022). Circadian dependence of microvascular obstrucon during STsegment elevaon myocardial infarcon. *Int J Cardiol*, *366*, 25-29. https://doi.org/10.1016/j.ijcard.2022.07.012

Bonfig, N. L., Soukup, C. R., Shah, A. A., Olet, S., Davidson, S. J., Schmidt, C. W., Peterson, R., Henry, T. D., & Traverse, J. H. (2022). Increasing myocardial edema is associated with

greater microvascular obstrucon in ST-segment elevaon myocardial infarcon. *Am J Physiol Heart Circ Physiol*, *323*(4), H818-H824. https://doi.org/10.1152/ajpheart.00347.2022

Borlo, A., Jerosch-Herold, M., Liu, D., Viliani, D., Bracco, A., Alkhalil, M., De Maria, G. L., Channon, K. M., Banning, A. P., Choudhury, R. P., Neubauer, S., Kharbanda, R. K., & Dall'Armellina, E. (2019). Acute Microvascular Impairment Post-Reperfused STEMI Is Reversible and Has Addional Clinical Predicve Value. *JACC: Cardiovascular Imaging*. https://doi.org/10.1016/j.jcmg.2018.10.028

Bøtker, H. E., Hausenloy, D., Andreadou, I., Antonucci, S., Boengler, K., Davidson, S. M., Deshwal, S., Devaux, Y., Di Lisa, F., Di Sante, M., Efentakis, P., Femminò, S., GarcíaDorado, D., Giricz, Z., Ibanez, B., Iliodromis, E., Kaludercic, N., Kleinbongard, P., Neuhäuser, M., . . . Heusch, G. (2018). Praccal guidelines for rigor and reproducibility in preclinical and clinical studies on cardioprotecon. *Basic Res Cardiol*, *113*(5), 39. https://doi.org/10.1007/s00395-018-0696-8

Brandt, M. M., Cheng, C., Merkus, D., Duncker, D. J., & Sorop, O. (2021). Mechanobiology of Microvascular Funcon and Structure in Health and Disease: Focus on the Coronary Circulaon. *Front Physiol*, *12*, 771960. https://doi.org/10.3389/fphys.2021.771960

Broch, K., Anstensrud, A. K., Woxholt, S., Sharma, K., Tøllefsen, I. M., Bendz, B., Aakhus, S., Ueland, T., Amundsen, B. H., Damås, J. K., Berg, E. S., Bjørkelund, E., Bendz, C., Hopp, E., Kleveland, O., Stensæth, K. H., Opdahl, A., Kløw, N. E., Seljeflot, I., . . . Gullestad, L. (2021). Randomized Trial of Interleukin-6 Receptor Inhibion in Paents With Acute ST-Segment Elevaon Myocardial Infarcon. *J Am Coll Cardiol*, *77*(15), 1845-1855. https://doi.org/10.1016/j.jacc.2021.02.049

Calò, L. A., Pagnin, E., Davis, P. A., Sartori, M., Semplicini, A., & Pessina, A. C. (2005). Rho kinase inhibion and vascular protecon: support from studies in Barter and Gitelman syndrome. *Arterioscler Thromb Vasc Biol*, *25*(4), e34; author reply e34-35. https://doi.org/10.1161/01.Atv.0000153089.74997.02

Carrick, D., Haig, C., Ahmed, N., McEntegart, M., Petrie, M. C., Eteiba, H., Hood, S., Watkins, S., Lindsay, M. M., Davie, A., Mahrous, A., Mordi, I., Rauhalammi, S., Satar, N., Welsh, P., Radjenovic, A., Ford, I., Oldroyd, K. G., & Berry, C. (2016). Myocardial Hemorrhage Aer Acute Reperfused ST-Segment-Elevaon Myocardial Infarcon: Relaon to Microvascular Obstrucon and Prognosc Significance. *Circ Cardiovasc Imaging*, *9*(1), e004148. https://doi.org/10.1161/circimaging.115.004148

Carrick, D., Oldroyd, K. G., McEntegart, M., Haig, C., Petrie, M. C., Eteiba, H., Hood, S., Owens, C., Watkins, S., Layland, J., Lindsay, M., Peat, E., Rae, A., Behan, M., Sood, A., Hillis, W. S., Mordi, I., Mahrous, A., Ahmed, N., . . . Berry, C. (2014). A randomized trial of deferred stenng versus immediate stenng to prevent no- or slow-reflow in acute ST-segment elevaon myocardial infarcon (DEFER-STEMI). *J Am Coll Cardiol*, *63*(20), 2088-2098. https://doi.org/10.1016/j.jacc.2014.02.530

Chaffin, M., Papangeli, I., Simonson, B., Akkad, A. D., Hill, M. C., Arduini, A., Fleming, S. J., Melanson, M., Hayat, S., Kost-Alimova, M., Atwa, O., Ye, J., Bedi, K. C., Jr., Nahrendorf, M., Kaushik, V. K., Stegmann, C. M., Margulies, K. B., Tucker, N. R., & Ellinor, P. T. (2022). Single-nucleus profiling of human dilated and hypertrophic cardiomyopathy. *Nature*, *608*(7921), 174-180. https://doi.org/10.1038/s41586-022-04817-8

Chang, J., Xie, M., Shah, V. R., Schneider, M. D., Entman, M. L., Wei, L., & Schwartz, R. J. (2006). Acvaon of Rho-associated coiled-coil protein kinase 1 (ROCK-1) by caspase-3 cleavage plays an essenal role in cardiac myocyte apoptosis. *Proc Natl Acad Sci U S A*, *103*(39), 14495-14500. https://doi.org/10.1073/pnas.0601911103

Chen, Y., Su, F., Han, J., Jiao, P., & Guo, W. (2018). Expression of Rho Kinase and Its Mechanism in the Le Atrial Appendage in Paents with Atrial Fibrillaon. *Heart Surg Forum*, *21*(1), E044-e048. https://doi.org/10.1532/hsf.1851

Chen, Y., Tristan, C. A., Chen, L., Jovanovic, V. M., Malley, C., Chu, P. H., Ryu, S., Deng, T., Ormanoglu, P., Tao, D., Fang, Y., Slamecka, J., Hong, H., LeClair, C. A., Michael, S., Ausn, C. P., Simeonov, A., & Singeç, I. (2021). A versale polypharmacology plaorm promotes cytoprotecon and viability of human pluripotent and differenated cells. *Nat Methods*, *18*(5), 528-541. https://doi.org/10.1038/s41592-021-01126-2

Chen, Y. T., Bannister, T. D., Weiser, A., Griffin, E., Lin, L., Ruiz, C., Cameron, M. D., Schürer, S., Ducket, D., Schröter, T., LoGrasso, P., & Feng, Y. (2008). Chroman-3-amides as potent Rho kinase inhibitors. *Bioorg Med Chem Lett*, *18*(24), 6406-6409. https://doi.org/10.1016/j.bmcl.2008.10.080

Chen, Y. T., Vojkovsky, T., Fang, X., Pocas, J. R., Grant, W., Handy, A. M. W., Schröter, T., LoGrasso, P., Bannister, T. D., & Feng, Y. (2011). Asymmetric synthesis of potent chroman-based Rho kinase (ROCK-II) inhibitors [10.1039/C0MD00194E]. *MedChemComm*, *2*(1), 73-75. https://doi.org/10.1039/C0MD00194E

Chouchani, E. T., Pell, V. R., Gaude, E., Aksenjevic, D., Sundier, S. Y., Robb, E. L., Logan, A., Nadtochiy, S. M., Ord, E. N. J., Smith, A. C., Eyassu, F., Shirley, R., Hu, C. H., Dare, A. J., James, A. M., Roga, S., Hartley, R. C., Eaton, S., Costa, A. S. H., . . . Murphy, M. P. (2014). Ischaemic accumulaon of succinate controls reperfusion injury through mitochondrial ROS. *Nature*, *515*(7527), 431-435. https://doi.org/10.1038/nature13909

Coffey, S., & Adamson, P. D. (2021). Microvascular obstrucon: me to bust the clot hypothesis? *Heart*. https://doi.org/10.1136/heartjnl-2020-318324

Cohen, M. V., & Downey, J. M. (2017). The impact of irreproducibility and compeng protecon from P2Y(12) antagonists on the discovery of cardioprotecve intervenons. *Basic Res Cardiol*, *112*(6), 64. https://doi.org/10.1007/s00395-0170653-y

Collet, J. P., Thiele, H., Barbato, E., Barthélémy, O., Bauersachs, J., Bhat, D. L., Dendale, P., Dorobantu, M., Edvardsen, T., Folliguet, T., Gale, C. P., Gilard, M., Jobs, A., Jüni, P., Lambrinou, E., Lewis, B. S., Mehilli, J., Meliga, E., Merkely, B., . . . Sions, G. C. M. (2021). 2020 ESC Guidelines for the management of acute coronary syndromes in paents presenng without persistent ST-segment elevaon. *Eur Heart J*, *42*(14), 1289-1367. https://doi.org/10.1093/eurheartj/ehaa575

Comità, S., Femmino, S., Thairi, C., Alloa, G., Boengler, K., Pagliaro, P., & Penna, C. (2021). Regulaon of STAT3 and its role in cardioprotecon by condioning: focus on nongenomic roles targeng mitochondrial funcon. *Basic Res Cardiol*, *116*(1), 56. https://doi.org/10.1007/s00395-021-00898-0

Cung, T. T., Morel, O., Cayla, G., Rioufol, G., Garcia-Dorado, D., Angoulvant, D., BonnefoyCudraz, E., Guérin, P., Elbaz, M., Delarche, N., Coste, P., Vanzeto, G., Metge, M., Aupet, J. F., Jouve, B., Motreff, P., Tron, C., Labeque, J. N., Steg, P. G., . . . Ovize, M. (2015). Cyclosporine before PCI in Paents with Acute Myocardial Infarcon. *N Engl J Med*, *373*(11), 1021-1031. https://doi.org/10.1056/NEJMoa1505489

Cutler, C., Lee, S. J., Arai, S., Rota, M., Zoghi, B., Lazaryan, A., Ramakrishnan, A., DeFilipp, Z., Salhotra, A., Chai-Ho, W., Mehta, R., Wang, T., Arora, M., Pusic, I., Saad, A., Shah, N. N., Abhyankar, S., Bachier, C., Galvin, J., . . . Pavlec, S. (2021). Belumosudil for chronic gra-versus-host disease aer 2 or more prior lines of therapy: the ROCKstar Study. *Blood*, *138*(22), 2278-2289. https://doi.org/10.1182/blood.2021012021

Dai, W., Amoedo, N. D., Perry, J., Le Grand, B., Boucard, A., Carreno, J., Zhao, L., Brown, D. A., Rossignol, R., & Kloner, R. A. (2022). Effects of OP2113 on Myocardial Infarct Size and

No Reflow in a Rat Myocardial Ischemia/Reperfusion Model. *Cardiovasc Drugs Ther*, *36*(2), 217-227. https://doi.org/10.1007/s10557-020-07113-7

Davidson, S. M., Adameová, A., Barile, L., Cabrera-Fuentes, H. A., Lazou, A., Pagliaro, P., Stensløkken, K.-O., Garcia-Dorado, D., & Acon, t. E.-C. C. (2020). Mitochondrial and mitochondrial-independent pathways of myocardial cell death during ischaemia and reperfusion injury. *Journal of Cellular and Molecular Medicine*, *24*(7), 3795-3806. https://doi.org/https://doi.org/10.1111/jcmm.15127

Davidson, S. M., Adameová, A., Barile, L., Cabrera-Fuentes, H. A., Lazou, A., Pagliaro, P., Stensløkken, K. O., & Garcia-Dorado, D. (2020). Mitochondrial and mitochondrialindependent pathways of myocardial cell death during ischaemia and reperfusion injury. *J Cell Mol Med*, *24*(7), 3795-3806. https://doi.org/10.1111/jcmm.15127

Davidson, S. M., Andreadou, I., Barile, L., Birnbaum, Y., Cabrera-Fuentes, H. A., Cohen, M. V., Downey, J. M., Girao, H., Pagliaro, P., Penna, C., Pernow, J., Preissner, K. T., & Ferdinandy, P. (2019). Circulang blood cells and extracellular vesicles in acute cardioprotecon. *Cardiovasc Res*, *115*(7), 1156-1166. https://doi.org/10.1093/cvr/cvy314

Davidson, S. M., Andreadou, I., Garcia-Dorado, D., & Hausenloy, D. J. (2019). Shining the spotlight on cardioprotecon: beyond the cardiomyocyte. *Cardiovasc Res*, *115*(7), 1115-1116. https://doi.org/10.1093/cvr/cvz072

Davidson, S. M., Ferdinandy, P., Andreadou, I., Botker, H. E., Heusch, G., Ibanez, B., Ovize, M., Schulz, R., Yellon, D. M., Hausenloy, D. J., Garcia-Dorado, D., & Acon, C. C. (2019). Multarget Strategies to Reduce Myocardial Ischemia/Reperfusion Injury: JACC Review Topic of the Week. *J Am Coll Cardiol*, *73*(1), 89-99. https://doi.org/10.1016/j.jacc.2018.09.086

De Marco, C., Charron, T., & Rousseau, G. (2022). Adenosine in Acute Myocardial InfarconAssociated Reperfusion Injury: Does it Sll Have a Role? *Front Pharmacol*, *13*, 856747. https://doi.org/10.3389/fphar.2022.856747

De Maria, G. L., Alkhalil, M., Wolfrum, M., Fahrni, G., Borlo, A., Gaughran, L., Dawkins, S., Langrish, J. P., Lucking, A. J., Choudhury, R. P., Porto, I., Crea, F., Dall'Armellina, E., Channon, K. M., Kharbanda, R. K., & Banning, A. P. (2019). Index of Microcirculatory Resistance as a Tool to Characterize Microvascular Obstrucon and to Predict Infarct Size Regression in Paents With STEMI Undergoing Primary PCI. *JACC Cardiovasc Imaging*, *12*(5), 837-848. https://doi.org/10.1016/j.jcmg.2018.02.018 de Sousa, G. R., Vieira, G. M., das Chagas, P. F., Pezuk, J. A., & Brassesco, M. S. (2020). Should we keep rocking? Portraits from targeng Rho kinases in cancer. *Pharmacol Res*, *160*, 105093. https://doi.org/10.1016/j.phrs.2020.105093 de Waha, S., Patel, M. R., Granger, C. B., Ohman, E. M., Maehara, A., Eitel, I., Ben-Yehuda, O., Jenkins, P., Thiele, H., & Stone, G. W. (2017). Relaonship between microvascular obstrucon and adverse events following primary percutaneous coronary intervenon for ST-segment elevaon myocardial infarcon: an individual paent data pooled analysis from seven randomized trials. *Eur Heart J*, *38*(47), 3502-3510. https://doi.org/10.1093/eurheartj/ehx414

Defert, O., & Boland, S. (2017). Rho kinase inhibitors: a patent review (2014 - 2016). *Expert Opin Ther Pat*, *27*(4), 507-515. https://doi.org/10.1080/13543776.2017.1272579

Dirksen, R. T., Eisner, D. A., Ríos, E., & Sipido, K. R. (2022). Excitaon-contracon coupling in cardiac, skeletal, and smooth muscle. *J Gen Physiol*, *154*(9). https://doi.org/10.1085/jgp.202213244

Do e, Z., Fukumoto, Y., Sugimura, K., Miura, Y., Tatebe, S., Yamamoto, S., Aoki, T., Nochioka, K., Nergui, S., Yaoita, N., Satoh, K., Kondo, M., Nakano, M., Wakayama, Y., Fukuda, K., Nihei, T., Kikuchi, Y., Takahashi, J., & Shimokawa, H. (2013). Rho-kinase acvaon in

paents with heart failure. *Circ J*, *77*(10), 2542-2550. https://doi.org/10.1253/circj.cj13-0397

Dogan, A., Dogdu, O., Ozdogru, I., Yarlioglues, M., Kalay, N., Inanc, M. T., Ardic, I., Celik, A., Kaynar, L., Kurnaz, F., Eryol, N. K., & Kaya, M. G. (2013). Cardiac effects of chronic gra-versus-host disease aer stem cell transplantaon. *Tex Heart Inst J*, *40*(4), 428434.

Dong, L. Y., Qiu, X. X., Zhuang, Y., & Xue, S. (2019). Y-27632, a Rho-kinase inhibitor, atenuates myocardial ischemia-reperfusion injury in rats. *Int J Mol Med*, *43*(4), 1911-1919. https://doi.org/10.3892/ijmm.2019.4097

Durante, A., Laricchia, A., Benede, G., Esposito, A., Margonato, A., Rimoldi, O., De Cobelli, F., Colombo, A., & Camici, P. G. (2017). Idenficaon of High-Risk Paents Aer STSegment-Elevaon Myocardial Infarcon: Comparison Between Angiographic and Magnec Resonance Parameters. *Circ Cardiovasc Imaging*, *10*(6), e005841. https://doi.org/10.1161/CIRCIMAGING.116.005841

Elliot, A. D. (2020). Confocal Microscopy: Principles and Modern Pracces. *Curr Protoc Cytom*, *92*(1), e68. https://doi.org/10.1002/cpcy.68

Falk, E. (2006). Pathogenesis of atherosclerosis. *J Am Coll Cardiol*, *47*(8 Suppl), C7-12. https://doi.org/10.1016/j.jacc.2005.09.068

Fanaroff, A. C., Garcia, S., & Giri, J. (2021). Myocardial Infarcon During the COVID-19 Pandemic. *JAMA*, *326*(19), 1916-1918. https://doi.org/10.1001/jama.2021.19608

Feng, C., Liu, Y., Wang, L., Niu, D., & Han, B. (2019). Effects of Early Intracoronary Administraon of Nicorandil During Percutaneous Coronary Intervenon in Paents With Acute Myocardial Infarcon. *Heart Lung Circ*, *28*(6), 858-865. https://doi.org/10.1016/j.hlc.2018.05.097

Feng, Y., LoGrasso, P. V., Defert, O., & Li, R. (2016). Rho Kinase (ROCK) Inhibitors and Their Therapeuc Potenal. *J Med Chem*, *59*(6), 2269-2300. https://doi.org/10.1021/acs.jmedchem.5b00683

Flynn, R., Paz, K., Du, J., Reichenbach, D. K., Taylor, P. A., Panoskaltsis-Mortari, A., Vulic, A., Luznik, L., MacDonald, K. K., Hill, G. R., Nyuydzefe, M. S., Weiss, J. M., Chen, W., Trzeciak, A., Serody, J. S., Aguilar, E. G., Murphy, W. J., Maillard, I., Munn, D., . . . Blazar, B. R. (2016). Targeted Rho-associated kinase 2 inhibion suppresses murine and human chronic GVHD through a Stat3-dependent mechanism. *Blood*, *127*(17), 2144-2154. https://doi.org/10.1182/blood-2015-10-678706

Francis, R., Chong, J., Ramlall, M., Bucciarelli-Ducci, C., Clayton, T., Dodd, M., Engstrøm, T., Evans, R., Ferreira, V. M., Fontana, M., Greenwood, J. P., Kharbanda, R. K., Kim, W. Y., Kotecha, T., Lønborg, J. T., Mathur, A., Møller, U. K., Moon, J., Perkins, A., . . . Hausenloy, D. J. (2021). Effect of remote ischaemic condioning on infarct size and remodelling in ST-segment elevaon myocardial infarcon paents: the CONDI-2/ERIC-PPCI CMR substudy. *Basic Res Cardiol*, *116*(1), 59. https://doi.org/10.1007/s00395-021-00896-2

Frangogiannis, N. G. (2004). Chemokines in the ischemic myocardium: from inflammaon to fibrosis. *Inflamm Res*, *53*(11), 585-595. https://doi.org/10.1007/s00011-004-1298-5

Frangogiannis, N. G. (2015). Pathophysiology of Myocardial Infarcon. In *Comprehensive Physiology* (pp. 1841-1875). https://doi.org/https://doi.org/10.1002/cphy.c150006

Freund, A., Schock, S., Sermaier, T., de Waha-Thiele, S., Eitel, I., Lurz, P., Thiele, H., & Desch, S. (2019). Thrombus aspiraon in paents with ST-elevaon myocardial infarcon presenng late aer symptom onset: long-term clinical outcome of a randomized trial. *Clin Res Cardiol*, *108*(11), 1208-1214. https://doi.org/10.1007/s00392-019-01452-8

Fu, S., Wen, Y., Peng, B., Tang, M., Shi, M., Liu, J., Yang, Y., Si, W., Guo, Y., Li, X., Yan, T., Kang, J., Pei, H., & Chen, L. (2023). Discovery of indoline-based derivaves as effecve ROCK2

inhibitors for the potenal new treatment of idiopathic pulmonary fibrosis. *Bioorg Chem*, *137*, 106539. https://doi.org/10.1016/j.bioorg.2023.106539

Galvao, J., Davis, B., Tilley, M., Normando, E., Duchen, M. R., & Cordeiro, M. F. (2014). Unexpected low-dose toxicity of the universal solvent DMSO. *Faseb j*, *28*(3), 1317-1330. https://doi.org/10.1096/.13-235440

Gambardella, A., Guisot, N. E. S., Bunyard, P. R., & Offer, E. (2022). Effects of RXC007, a highly potent and selecve ROCK2 inhibitor, in ex-vivo and in vivo models of pulmonary fibrosis. *European Respiratory Journal*, *60*(suppl 66), 3033. https://doi.org/10.1183/13993003.congress-2022.3033

Gao, J., Min, F., Wang, S., Lv, H., Liang, H., Cai, B., Jia, X., Gao, Q., & Yu, Y. (2022). Effect of RhoKinase and Autophagy on Remote Ischemic Condioning-Induced Cardioprotecon in Rat Myocardial Ischemia/Reperfusion Injury Model. *Cardiovasc Ther*, *2022*, 6806427. https://doi.org/10.1155/2022/6806427

Gao, X. M., Su, Y., Moore, S., Han, L. P., Kiriazis, H., Lu, Q., Zhao, W. B., Ruze, A., Fang, B. B., Duan, M. J., & Du, X. J. (2019). Relaxin migates microvascular damage and inflammaon following cardiac ischemia-reperfusion. *Basic Res Cardiol*, *114*(4), 30. https://doi.org/10.1007/s00395-019-0739-9

García-Méndez, R. C., Almeida-Guerrez, E., Serrano-Cuevas, L., Sánchez-Díaz, J. S., Rosas-Peralta, M., Ortega-Ramirez, J. A., Palomo-Villada, J. A., Isordia-Salas, I., AlonsoBravo, R. M., & Borrayo-Sanchez, G. (2018). Reducon of No Reflow with a Loading Dose of Atorvastan before Primary Angioplasty in Paents with Acute ST Myocardial Infarcon. *Arch Med Res*, *49*(8), 620-629. https://doi.org/10.1016/j.arcmed.2018.10.006

García Del Blanco, B., Otaegui, I., Rodríguez-Palomares, J. F., Bayés-Genis, A., FernándezNofrerías, E., Vilalta Del Olmo, V., Carrillo, X., Ibáñez, B., Worner, F., Casanova, J., Pueo, E., González-Juanatey, J. R., López-Pais, J., Bardají, A., Bonet, G., Fuertes, M., Rodríguez-Sinovas, A., Ruiz-Meana, M., Inserte, J., . . . García-Dorado, D. (2021). Effect of COMBinAon therapy with remote ischemic condioning and exenade on the Myocardial Infarct size: a two-by-two factorial randomized trial (COMBAT-MI). *Basic Res Cardiol*, *116*(1), 4. https://doi.org/10.1007/s00395-021-00842-2

Garcia, R., Boule, C., Sirol, M., Logeart, D., Monnot, C., Ardidie-Robouant, C., Caligiuri, G., Mercadier, J. J., & Germain, S. (2019). VEGF-A plasma levels are associated with microvascular obstrucon in paents with ST-segment elevaon myocardial infarcon. *Int J Cardiol*, *291*, 19-24. https://doi.org/10.1016/j.ijcard.2019.02.067

Giannini, F., Candilio, L., Mitomo, S., Ruparelia, N., Chieffo, A., Balde, L., Poncelli, F., Lab, A., & Colombo, A. (2018). A Praccal Approach to the Management of Complicaons During Percutaneous Coronary Intervenon. *JACC Cardiovasc Interv*, *11*(18), 1797-1810. https://doi.org/10.1016/j.jcin.2018.05.052

Goel, A., Zhang, Y., Anderson, L., & Rahimian, R. (2007). Gender difference in rat aorta vasodilaon aer acute exposure to high glucose: involvement of protein kinase C beta and superoxide but not of Rho kinase. *Cardiovasc Res*, *76*(2), 351-360. https://doi.org/10.1016/j.cardiores.2007.06.029

Gohla, A., Schultz, G., & Offermanns, S. (2000). Role for G(12)/G(13) in agonist-induced vascular smooth muscle cell contracon. *Circ Res*, *87*(3), 221-227. https://doi.org/10.1161/01.res.87.3.221

Golino, P., Maroko, P. R., & Carew, T. E. (1987). Efficacy of platelet depleon in counteracng the detrimental effect of acute hypercholesterolemia on infarct size and the no-reflow phenomenon in rabbits undergoing coronary artery occlusion-reperfusion. *Circulation*, *76*(1), 173-180. https://doi.org/10.1161/01.cir.76.1.173

Gong, G. Q., Bilanges, B., Allsop, B., Masson, G. R., Roberton, V., Askwith, T., Oxenford, S., Madsen, R. R., Conduit, S. E., Bellini, D., Fitzek, M., Collier, M., Najam, O., He, Z., Wahab, B., McLaughlin, S. H., Chan, A. W. E., Feierberg, I., Madin, A., . . . Vanhaesebroeck, B. (2023). A small-molecule PI3Kalpha acvator for cardioprotecon and neuroregeneraon. *Nature*, *618*(7963), 159-168. https://doi.org/10.1038/s41586-023-05972-2

Goodwill, A. G., Dick, G. M., Kiel, A. M., & Tune, J. D. (2017). Regulaon of Coronary Blood Flow. *Compr Physiol*, *7*(2), 321-382. https://doi.org/10.1002/cphy.c160016

Grimm, M., Haas, P., Willipinski-Stapelfeldt, B., Zimmermann, W. H., Rau, T., Pantel, K., Weyand, M., & Eschenhagen, T. (2005). Key role of myosin light chain (MLC) kinasemediated MLC2a phosphorylaon in the alpha 1-adrenergic posive inotropic effect in human atrium. *Cardiovasc Res*, *65*(1), 211-220. https://doi.org/10.1016/j.cardiores.2004.09.019

Grisk, O., Schlüter, T., Reimer, N., Zimmermann, U., Katsari, E., Pletenburg, O., Löhn, M., Wollert, H. G., & Reg, R. (2012). The Rho kinase inhibitor SAR407899 potently inhibits endothelin-1-induced constricon of renal resistance arteries. *J Hypertens*, *30*(5), 980-989. https://doi.org/10.1097/HJH.0b013e328351d459

Grothaus, J. S., Ares, G., Yuan, C., Wood, D. R., & Hunter, C. J. (2018). Rho kinase inhibion maintains intesnal and vascular barrier funcon by upregulaon of occludin in experimental necrozing enterocolis. *Am J Physiol Gastrointest Liver Physiol*, *315*(4), G514-g528. https://doi.org/10.1152/ajpgi.00357.2017

Group, R. C. (2022). Baricinib in paents admited to hospital with COVID-19 (RECOVERY): a randomised, controlled, open-label, plaorm trial and updated meta-analysis. *Lancet*, *400*(10349), 359-368. https://doi.org/10.1016/S0140-6736(22)01109-6

Gumkowska-Sroka, O., Kotyla, K., Mojs, E., Palka, K., & Kotyla, P. (2023). Novel Therapeuc Strategies in the Treatment of Systemic Sclerosis. *Pharmaceuticals (Basel)*, *16*(8). https://doi.org/10.3390/ph16081066

Haesen, S., Cöl, Ü., Schurgers, W., Evens, L., Verboven, M., Driesen, R. B., Bronckaers, A., Lambrichts, I., Deluyker, D., & Bito, V. (2020). Glycolaldehyde-modified proteins cause adverse funconal and structural aorc remodeling leading to cardiac pressure overload. *Sci Rep*, *10*(1), 12220. https://doi.org/10.1038/s41598-020-68974-4

Hamid, S. A., Bower, H. S., & Baxter, G. F. (2007). Rho kinase acvaon plays a major role as a mediator of irreversible injury in reperfused myocardium. *Am J Physiol Heart Circ Physiol*, *292*(6), H2598-2606. https://doi.org/10.1152/ajpheart.01393.2006

Hartmann, D. A., Berthiaume, A. A., Grant, R. I., Harrill, S. A., Koski, T., Tieu, T., McDowell, K. P., Faino, A. V., Kelly, A. L., & Shih, A. Y. (2021). Brain capillary pericytes exert a substanal but slow influence on blood flow. *Nat Neurosci*, *24*(5), 633-645. https://doi.org/10.1038/s41593-020-00793-2

Hartmann, S., Ridley, A. J., & Lutz, S. (2015). The Funcon of Rho-Associated Kinases ROCK1 and ROCK2 in the Pathogenesis of Cardiovascular Disease. *Front Pharmacol*, *6*, 276. https://doi.org/10.3389/fphar.2015.00276

Haulica, I., Bild, W., Mihaila, C. N., Ionita, T., Boisteanu, C. P., & Neagu, B. (2003). Biphasic effects of angiotensin (1-7) and its interacons with angiotensin II in rat aorta. *J Renin Angiotensin Aldosterone Syst*, *4*(2), 124-128. https://doi.org/10.3317/jraas.2003.013

Hausenloy, D. J., & Bøtker, H. E. (2019). Why did remote ischaemic condioning not improve clinical outcomes in acute myocardial infarcon in the CONDI-2/ERIC-PPCI trial? *Cardiovascular Research*, *115*(14), e161-e163. https://doi.org/10.1093/cvr/cvz242

Hausenloy, D. J., Chilian, W., Crea, F., Davidson, S. M., Ferdinandy, P., Garcia-Dorado, D., van Royen, N., Schulz, R., & Heusch, G. (2019). The coronary circulaon in acute

myocardial ischaemia/reperfusion injury: a target for cardioprotecon. *Cardiovasc Res*, *115*(7), 1143-1155. https://doi.org/10.1093/cvr/cvy286

Hausenloy, D. J., Kharbanda, R. K., Møller, U. K., Ramlall, M., Aarøe, J., Butler, R., Bulluck, H., Clayton, T., Dana, A., Dodd, M., Engstrom, T., Evans, R., Lassen, J. F., Christensen, E. F., Garcia-Ruiz, J. M., Gorog, D. A., Hjort, J., Houghton, R. F., Ibanez, B., . . . Bøtker, H. E. (2019). Effect of remote ischaemic condioning on clinical outcomes in paents with acute myocardial infarcon (CONDI-2/ERIC-PPCI): a single-blind randomised controlled trial. *Lancet*, *394*(10207), 1415-1424. https://doi.org/10.1016/s01406736(19)32039-2

Hausenloy, D. J., & Yellon, D. M. (2010). The second window of precondioning (SWOP) where are we now? *Cardiovasc Drugs Ther*, *24*(3), 235-254. https://doi.org/10.1007/s10557-010-6237-9

Hausenloy, D. J., & Yellon, D. M. (2013). Myocardial ischemia-reperfusion injury: a neglected therapeuc target. *J Clin Invest*, *123*(1), 92-100. https://doi.org/10.1172/JCI62874

Hausenloy, D. J., & Yellon, D. M. (2016). Ischaemic condioning and reperfusion injury. *Nat Rev Cardiol*, *13*(4), 193-209. https://doi.org/10.1038/nrcardio.2016.5

He, Z., Davidson, S. M., & Yellon, D. M. (2020). The importance of clinically relevant background therapy in cardioprotecve studies. *Basic Res Cardiol*, *115*(6), 69. https://doi.org/10.1007/s00395-020-00830-y

Heusch, G. (2015). Molecular basis of cardioprotecon: signal transducon in ischemic pre-, post-, and remote condioning. *Circ Res*, *116*(4), 674-699. https://doi.org/10.1161/CIRCRESAHA.116.305348

Heusch, G. (2016). The Coronary Circulaon as a Target of Cardioprotecon. 1643-1658. https://doi.org/10.1161/CIRCRESAHA.116.308640

Heusch, G. (2019). Coronary microvascular obstrucon: the new froner in cardioprotecon. *Basic Res Cardiol*, *114*(6), 45. https://doi.org/10.1007/s00395-019-0756-8

Heusch, G. (2020). Myocardial ischaemia-reperfusion injury and cardioprotecon in perspecve. *Nat Rev Cardiol*, *17*(12), 773-789. https://doi.org/10.1038/s41569-0200403-y

Heusch, G. (2021). Myocardial stunning and hibernaon revisited. *Nat Rev Cardiol*, *18*(7), 522-536. https://doi.org/10.1038/s41569-021-00506-7

Heusch, G., Boengler, K., & Schulz, R. (2008). Cardioprotecon: nitric oxide, protein kinases, and mitochondria. *Circulation*, *118*(19), 1915-1919. https://doi.org/10.1161/circulaonaha.108.805242

Heusch, G., & Gersh, B. J. (2020). Is Cardioprotecon Salvageable? *Circulation*, *141*(6), 415417. https://doi.org/10.1161/CIRCULATIONAHA.119.044176

Hidaka, H., Inagaki, M., Kawamoto, S., & Sasaki, Y. (1984). Isoquinolinesulfonamides, novel and potent inhibitors of cyclic nucleode dependent protein kinase and protein kinase C. *Biochemistry*, *23*(21), 5036-5041. https://doi.org/10.1021/bi00316a032

Hjortbak, M. V., Olesen, K. K. W., Seefeldt, J. M., Lassen, T. R., Jensen, R. V., Perkins, A., Dodd, M., Clayton, T., Yellon, D., Hausenloy, D. J., & Bøtker, H. E. (2021). Translaon of experimental cardioprotecve capability of P2Y(12) inhibitors into clinical outcome in paents with ST-elevaon myocardial infarcon. *Basic Res Cardiol*, *116*(1), 36. https://doi.org/10.1007/s00395-021-00870-y

Hosseini, S. H., Talasaz, A. H., Alidoos, M., Tajdini, M., Van Tassell, B. W., Etesamifard, N., Kakavand, H., Jalali, A., Aghakouchakzadeh, M., Gheyma, A., Sadeghian, M., & Jenab, Y. (2022). Preprocedural Colchicine in Paents With Acute ST-elevaon Myocardial Infarcon Undergoing Percutaneous Coronary Intervenon: A Randomized Controlled Trial (PodCAST-PCI). *J Cardiovasc Pharmacol*, *80*(4), 592-599. https://doi.org/10.1097/c.0000000000001317

Hsiao, S. T., Spencer, T., Boldock, L., Prosseda, S. D., Xanthis, I., Tovar-Lopez, F. J., Van Beusekom, H. M., Khamis, R. Y., Foin, N., Bowden, N., Hussain, A., Rothman, A., Ridger, V., Halliday, I., Perrault, C., Gunn, J., & Evans, P. C. (2016). Endothelial repair in stented arteries is accelerated by inhibion of Rho-associated protein kinase. *Cardiovasc Res*, *112*(3), 689-701. https://doi.org/10.1093/cvr/cvw210

Hu, P., Liu, J., Zhao, J., Wilkins, B. J., Lupino, K., Wu, H., & Pei, L. (2018). Single-nucleus transcriptomic survey of cell diversity and funconal maturaon in postnatal mammalian hearts. *Genes Dev*, *32*(19-20), 1344-1357. https://doi.org/10.1101/gad.316802.118

Huang, X. N., Fu, J., & Wang, W. Z. (2011). The effects of fasudil on the permeability of the rat blood-brain barrier and blood-spinal cord barrier following experimental autoimmune encephalomyelis. *J Neuroimmunol*, *239*(1-2), 61-67. https://doi.org/10.1016/j.jneuroim.2011.08.015

Huang, Y. Y., Wu, J. M., Su, T., Zhang, S. Y., & Lin, X. J. (2018a). Fasudil, a Rho-Kinase Inhibitor, Exerts Cardioprotecve Funcon in Animal Models of Myocardial Ischemia/Reperfusion Injury: A Meta-Analysis and Review of Preclinical Evidence and Possible Mechanisms [Systemac Review]. *Front Pharmacol*, *9*(1083), 1083. https://doi.org/10.3389/fphar.2018.01083

Huang, Y. Y., Wu, J. M., Su, T., Zhang, S. Y., & Lin, X. J. (2018b). Fasudil, a Rho-Kinase Inhibitor, Exerts Cardioprotecve Funcon in Animal Models of Myocardial Ischemia/Reperfusion Injury: A Meta-Analysis and Review of Preclinical Evidence and Possible Mechanisms. *Front Pharmacol*, *9*, 1083. https://doi.org/10.3389/fphar.2018.01083

Hubert, A., Seitz, A., Pereyra, V. M., Bekeredjian, R., Sechtem, U., & Ong, P. (2020). Coronary Artery Spasm: The Interplay Between Endothelial Dysfuncon and Vascular Smooth Muscle Cell Hyperreacvity. *Eur Cardiol*, *15*, e12. https://doi.org/10.15420/ecr.2019.20

Ibanez, B., Macaya, C., Sánchez-Brunete, V., Pizarro, G., Fernández-Friera, L., Mateos, A., Fernández-Orz, A., García-Ruiz, J. M., García-Álvarez, A., Iñiguez, A., JiménezBorreguero, J., López-Romero, P., Fernández-Jiménez, R., Goicolea, J., Ruiz-Mateos, B., Bastante, T., Arias, M., Iglesias-Vázquez, J. A., Rodriguez, M. D., . . . Fuster, V. (2013). Effect of early metoprolol on infarct size in ST-segment-elevaon myocardial infarcon paents undergoing primary percutaneous coronary intervenon: the Effect of Metoprolol in Cardioprotecon During an Acute Myocardial Infarcon (METOCARD-CNIC) trial. *Circulation*, *128*(14), 1495-1503. https://doi.org/10.1161/circulaonaha.113.003653

Ito, M., Okamoto, R., Ito, H., Zhe, Y., & Dohi, K. (2022). Regulaon of myosin light-chain phosphorylaon and its roles in cardiovascular physiology and pathophysiology. *Hypertens Res*, *45*(1), 40-52. https://doi.org/10.1038/s41440-021-00733-y

Ivey, M. E., Osman, N., & Litle, P. J. (2008). Endothelin-1 signalling in vascular smooth muscle: pathways controlling cellular funcons associated with atherosclerosis. *Atherosclerosis*, *199*(2), 237-247. https://doi.org/10.1016/j.atherosclerosis.2008.03.006

Jennings, R. B., Sommers, H. M., Smyth, G. A., Flack, H. A., & Linn, H. (1960). Myocardial necrosis induced by temporary occlusion of a coronary artery in the dog. *Arch Pathol*, *70*, 68-78. https://www.ncbi.nlm.nih.gov/pubmed/14407094

Jiang, Z. H., Zhang, T. T., & Zhang, J. F. (2013). Protecve effects of fasudil hydrochloride postcondioning on acute myocardial ischemia/reperfusion injury in rats. *Cardiol J*, *20*(2), 197-202. https://doi.org/10.5603/cj.2013.0034

Johnson, N. P., Gould, K. L., & De Bruyne, B. (2021). Autoregulaon of Coronary Blood Supply in Response to Demand: JACC Review Topic of the Week. *J Am Coll Cardiol*, *77*(18), 2335-2345. https://doi.org/10.1016/j.jacc.2021.03.293

Jolly, S. S., Cairns, J. A., Yusuf, S., Meeks, B., Pogue, J., Rokoss, M. J., Kedev, S., Thabane, L., Stankovic, G., Moreno, R., Gershlick, A., Chowdhary, S., Lavi, S., Niemelä, K., Steg, P. G., Bernat, I., Xu, Y., Cantor, W. J., Overgaard, C. B., . . . Džavík, V. (2015). Randomized Trial of Primary PCI with or without Roune Manual Thrombectomy. *New England Journal of Medicine*, *372*(15), 1389-1398. https://doi.org/10.1056/NEJMoa1415098

Julian, L., & Olson, M. F. (2014). Rho-associated coiled-coil containing kinases (ROCK): structure, regulaon, and funcons. *Small GTPases*, *5*, e29846. https://doi.org/10.4161/sgtp.29846

Kakavand, H., Saadatagah, S., Naderian, M., Aghakouchakzadeh, M., Jalali, A., Sadri, F., Amoli, A. I., Hosseini, S. H., Jenab, Y., Pourhosseini, H., Salarifar, M., & Talasaz, A. H. (2023). Evaluang the role of intravenous pentoxifylline administraon on primary percutaneous coronary intervenon success rate in paents with ST-elevaon myocardial infarcon (PENTOS-PCI). *Naunyn Schmiedebergs Arch Pharmacol*, *396*(3), 557-565. https://doi.org/10.1007/s00210-022-02368-3

Kamijo, H., Matsumura, Y., Thumkeo, D., Koike, S., Masu, M., Shimizu, Y., Ishizaki, T., & Narumiya, S. (2011). Impaired vascular remodeling in the yolk sac of embryos deficient in ROCK-I and ROCK-II. *Genes Cells*, *16*(10), 1012-1021. https://doi.org/10.1111/j.1365-2443.2011.01546.x

Kaneda, T., Sasaki, N., Urakawa, N., & Shimizu, K. (2016). Endothelium-Dependent and Independent Vasodilator Effects of Dimethyl Sulfoxide in Rat Aorta. *Pharmacology*, *97*(3-4), 171-176. https://doi.org/10.1159/000443894

Kanwar, S. S., Stone, G. W., Singh, M., Virmani, R., Olin, J., Akasaka, T., & Narula, J. (2016). Acute coronary syndromes without coronary plaque rupture. *Nat Rev Cardiol*, *13*(5), 257-265. https://doi.org/10.1038/nrcardio.2016.19

Kaul, S., Methner, C., Cao, Z., & Mishra, A. (2023). Mechanisms of the "No-Reflow" Phenomenon Aer Acute Myocardial Infarcon: Potenal Role of Pericytes. *JACC Basic Transl Sci*, *8*(2), 204-220. https://doi.org/10.1016/j.jacbts.2022.06.008

Kaul, S., Methner, C., Cao, Z., & Mishra, A. (2023). Mechanisms of the “No-Reflow” Phenomenon Aer Acute Myocardial Infarcon: Potenal Role of Pericytes. *JACC: Basic to Translational Science*, *8*(2), 204-220. https://doi.org/https://doi.org/10.1016/j.jacbts.2022.06.008

Kawarazaki, W., & Fujita, T. (2021). Role of Rho in Salt-Sensive Hypertension. *Int J Mol Sci*, *22*(6). https://doi.org/10.3390/ijms22062958

Kelbæk, H., Høfsten, D. E., Køber, L., Helqvist, S., Kløvgaard, L., Holmvang, L., Jørgensen, E., Pedersen, F., Saunamäki, K., De Backer, O., Bang, L. E., Kofoed, K. F., Lønborg, J., Ahtarovski, K., Vejlstrup, N., Bøtker, H. E., Terkelsen, C. J., Chrisansen, E. H., Ravkilde, J., . . . Engstrøm, T. (2016). Deferred versus convenonal stent implantaon in paents with ST-segment elevaon myocardial infarcon (DANAMI 3-DEFER): an open-label, randomised controlled trial. *Lancet*, *387*(10034), 2199-2206. https://doi.org/10.1016/s0140-6736(16)30072-1

Khab, S. A., Ma, L., Dang, H., Forgues, M., Chung, J. Y., Ylaya, K., Hewit, S. M., Chaisaingmongkol, J., Rucchirawat, M., & Wang, X. W. (2022). Single-cell biology uncovers apoptoc cell death and its spaal organizaon as a potenal modifier of

tumor diversity in HCC. *Hepatology*, *76*(3), 599-611. https://doi.org/10.1002/hep.32345

Kikuchi, Y., Takahashi, J., Hao, K., Sato, K., Sugisawa, J., Tsuchiya, S., Suda, A., Shindo, T., Ikeda, S., Shiroto, T., Matsumoto, Y., Miyata, S., Sakata, Y., & Shimokawa, H. (2019). Usefulness of intracoronary administraon of fasudil, a selecve Rho-kinase inhibitor, for PCI-related refractory myocardial ischemia. *Int J Cardiol*, *297*, 8-13. https://doi.org/10.1016/j.ijcard.2019.09.057

Kim, B. G., Cho, S. W., Seo, J., Kim, G. S., Jin, M. N., Lee, H. Y., Byun, Y. S., & Kim, B. O. (2022). Effect of direct stenng on microvascular dysfuncon during percutaneous coronary intervenon in acute myocardial infarcon: a randomized pilot study. *J Int Med Res*, *50*(9), 3000605221127888. https://doi.org/10.1177/03000605221127888

Kim, S., Kim, S. A., Han, J., & Kim, I. S. (2021). Rho-Kinase as a Target for Cancer Therapy and Its Immunotherapeuc Potenal. *Int J Mol Sci*, *22*(23). https://doi.org/10.3390/ijms222312916

Kirma, C., Izgi, A., Dundar, C., Tanalp, A. C., Oduncu, V., Aung, S. M., Sonmez, K., Mutlu, B., Ozdemir, N., & Erentug, V. (2008). Clinical and procedural predictors of no-reflow phenomenon aer primary percutaneous coronary intervenons: experience at a single center. *Circ J*, *72*(5), 716-721. https://doi.org/10.1253/circj.72.716

Kleinbongard, P., Andreadou, I., & Vilahur, G. (2021). The platelet paradox of injury versus protecon in myocardial infarcon-has it been overlooked? *Basic Res Cardiol*, *116*(1), 37. https://doi.org/10.1007/s00395-021-00876-6

Kleinbongard, P., & Heusch, G. (2022). A fresh look at coronary microembolizaon. *Nat Rev Cardiol*, *19*(4), 265-280. https://doi.org/10.1038/s41569-021-00632-2

Kleinbongard, P., Lieder, H. R., Skyschally, A., & Heusch, G. (2023). No robust reducon of infarct size and no-reflow by metoprolol pretreatment in adult Göngen minipigs. *Basic Res Cardiol*, *118*(1), 23. https://doi.org/10.1007/s00395-023-00993-4

Kloner, R. A. (1993). Does reperfusion injury exist in humans? *J Am Coll Cardiol*, *21*(2), 537545. https://doi.org/10.1016/0735-1097(93)90700-b

Kloner, R. A., Brown, D. A., Csete, M., Dai, W., Downey, J. M., Gotlieb, R. A., Hale, S. L., & Shi, J. (2017). New and revisited approaches to preserving the reperfused myocardium. *Nat Rev Cardiol*, *14*(11), 679-693. https://doi.org/10.1038/nrcardio.2017.102

Kloner, R. A., Ganote, C. E., & Jennings, R. B. (1974). The "no-reflow" phenomenon aer temporary coronary occlusion in the dog. *J Clin Invest*, *54*(6), 1496-1508. https://doi.org/10.1172/jci107898

Kloner, R. A., King, K. S., & Harrington, M. G. (2018). No-reflow phenomenon in the heart and brain. *Am J Physiol Heart Circ Physiol*, *315*(3), H550-H562. https://doi.org/10.1152/ajpheart.00183.2018

Knipe, R. S., Probst, C. K., Lagares, D., Franklin, A., Spinney, J. J., Brazee, P. L., Grasberger, P., Zhang, L., Black, K. E., Sakai, N., Shea, B. S., Liao, J. K., Medoff, B. D., & Tager, A. M. (2018). The Rho Kinase Isoforms ROCK1 and ROCK2 Each Contribute to the Development of Experimental Pulmonary Fibrosis. *Am J Respir Cell Mol Biol*, *58*(4), 471-481. https://doi.org/10.1165/rcmb.2017-0075OC

Knipe, R. S., Tager, A. M., & Liao, J. K. (2015). The Rho kinases: crical mediators of mulple profibroc processes and raonal targets for new therapies for pulmonary fibrosis. *Pharmacol Rev*, *67*(1), 103-117. https://doi.org/10.1124/pr.114.009381

Koch, J. C., Tatenhorst, L., Roser, A. E., Saal, K. A., Tönges, L., & Lingor, P. (2018). ROCK inhibion in models of neurodegeneraon and its potenal for clinical translaon. *Pharmacol Ther*, *189*, 1-21. https://doi.org/10.1016/j.pharmthera.2018.03.008

Konijnenberg, L. S. F., Damman, P., Duncker, D. J., Kloner, R. A., Nijveldt, R., van Geuns, R. M., Berry, C., Riksen, N. P., Escaned, J., & van Royen, N. (2020). Pathophysiology and

diagnosis of coronary microvascular dysfuncon in ST-elevaon myocardial infarcon. *Cardiovasc Res*, *116*(4), 787-805. https://doi.org/10.1093/cvr/cvz301

Konijnenberg, L. S. F., Luiken, T. T. J., Velen, A., Uthman, L., Kuster, C. T. A., Rodwell, L., de Waard, G. A., Kea-Te Lindert, M., Akiva, A., Thijssen, D. H. J., Nijveldt, R., & van Royen, N. (2023). Imanib atenuates reperfusion injury in a rat model of acute myocardial infarcon. *Basic Res Cardiol*, *118*(1), 2. https://doi.org/10.1007/s00395-022-00974-z

Koshinuma, S., Miyamae, M., Kaneda, K., Kotani, J., & Figueredo, V. M. (2014). Combinaon of necroptosis and apoptosis inhibion enhances cardioprotecon against myocardial ischemia-reperfusion injury. *J Anesth*, *28*(2), 235-241. https://doi.org/10.1007/s00540-013-1716-3

Krijnen, P. A., Nijmeijer, R., Meijer, C. J., Visser, C. A., Hack, C. E., & Niessen, H. W. (2002). Apoptosis in myocardial ischaemia and infarcon. *J Clin Pathol*, *55*(11), 801-811. https://doi.org/10.1136/jcp.55.11.801

Kumar, A., Green, J. D., Sykes, J. M., Ephrat, P., Carson, J. J., Mitchell, A. J., Wisenberg, G., & Friedrich, M. G. (2011). Detecon and quanficaon of myocardial reperfusion hemorrhage using T2*-weighted CMR. *JACC Cardiovasc Imaging*, *4*(12), 1274-1283. https://doi.org/10.1016/j.jcmg.2011.08.016

Kümper, S., Mardakheh, F. K., McCarthy, A., Yeo, M., Stamp, G. W., Paul, A., Worboys, J., Sadok, A., Jørgensen, C., Guichard, S., & Marshall, C. J. (2016). Rho-associated kinase (ROCK) funcon is essenal for cell cycle progression, senescence and tumorigenesis. *Elife*, *5*, e12994. https://doi.org/10.7554/eLife.12203

Kurtul, A., Yarlioglues, M., Celik, I. E., Duran, M., Elcik, D., Kilic, A., Oksuz, F., & Murat, S. N. (2015). Associaon of lymphocyte-to-monocyte rao with the no-reflow phenomenon in paents who underwent a primary percutaneous coronary intervenon for ST-elevaon myocardial infarcon. *Coron Artery Dis*, *26*(8), 706-712. https://doi.org/10.1097/mca.0000000000000301

Laboratories, V. (2022). Immunohistochemistry resource guide. In. https://vectorlabs.com/resources/brochures/.

Labs, I. (2022). A Guide for RNAscope®Data Analysis, A wealth of gene expression informaon from ssue context. In *https://www.indicalab.com/wpcontent/uploads/2018/04/MK_51_103_RNAScope_data_analysis_guide_RevB.pdf*.

Lacerda, L., Somers, S., Opie, L. H., & Lecour, S. (2009). Ischaemic postcondioning protects against reperfusion injury via the SAFE pathway. *Cardiovasc Res*, *84*(2), 201-208. https://doi.org/10.1093/cvr/cvp274

Lecour, S. (2009). Acvaon of the protecve Survivor Acvang Factor Enhancement (SAFE) pathway against reperfusion injury: Does it go beyond the RISK pathway? *Journal of Molecular and Cellular Cardiology*, *47*(1), 32-40. https://doi.org/https://doi.org/10.1016/j.yjmcc.2009.03.019

Lee, J. H., Zheng, Y., von Bornstadt, D., Wei, Y., Balcioglu, A., Daneshmand, A., Yalcin, N., Yu, E., Herisson, F., Atalay, Y. B., Kim, M. H., Ahn, Y. J., Balkaya, M., Sweetnam, P., Schueller, O., Poyurovsky, M. V., Kim, H. H., Lo, E. H., Furie, K. L., & Ayata, C. (2014). Selecve ROCK2 Inhibion In Focal Cerebral Ischemia. *Ann Clin Transl Neurol*, *1*(1), 2-14. https://doi.org/10.1002/acn3.19

Lee, J. Y., Stevens, R. P., Kash, M., Zhou, C., Koloteva, A., Renema, P., Paudel, S. S., & Stevens, T. (2020). KD025 Shis Pulmonary Endothelial Cell Bioenergecs and Decreases Baseline Lung Permeability. *Am J Respir Cell Mol Biol*, *63*(4), 519-530. https://doi.org/10.1165/rcmb.2019-0435OC

Leung, T., Chen, X. Q., Tan, I., Manser, E., & Lim, L. (1998). Myotonic dystrophy kinase-related Cdc42-binding kinase acts as a Cdc42 effector in promong cytoskeletal reorganizaon. *Mol Cell Biol*, *18*(1), 130-140. https://doi.org/10.1128/mcb.18.1.130

Li, B., Wang, R., Wang, Y., Sef, C. G., & Hennenberg, M. (2020). Regulaon of smooth muscle contracon by monomeric non-RhoA GTPases. *Br J Pharmacol*, *177*(17), 3865-3877. https://doi.org/10.1111/bph.15172

Li, X., Wu, X., Li, H., Chen, H., Wang, Y., Li, W., Ding, X., & Hong, X. (2016). Increased Rho kinase acvity predicts worse cardiovascular outcome in ST-segment elevaon myocardial infarcon paents. *Cardiol J*, *23*(4), 456-464. https://doi.org/10.5603/CJ.a2016.0031

Li, Y., Wang, C., Li, T., Ma, L., Fan, F., Jin, Y., & Shen, J. (2019). The whole transcriptome and proteome changes in the early stage of myocardial infarcon. *Cell Death Discov*, *5*, 73. https://doi.org/10.1038/s41420-019-0152-z

Liao, J. K., Seto, M., & Noma, K. (2007). Rho kinase (ROCK) inhibitors. *J Cardiovasc Pharmacol*, *50*(1), 17-24. https://doi.org/10.1097/FJC.0b013e318070d1bd

Liao, Y. C., Liu, P. Y., Lin, H. F., Lin, W. Y., Liao, J. K., & Juo, S. H. (2015). Two funconal polymorphisms of ROCK2 enhance arterial sffening through inhibing its acvity and expression. *J Mol Cell Cardiol*, *79*, 180-186. https://doi.org/10.1016/j.yjmcc.2014.11.023

Lie, J. T. (1993). The reasons why clinical cardiologists disregard reperfusion arrhythmias. *Cardiovasc Res*, *27*(11), 1906. https://doi.org/10.1093/cvr/27.11.1906

Liu, H., Pan, Z., Ma, X., Cui, J., Gao, J., Miao, Q., Zhu, Z., Chen, X., & Su, S. (2022). ROCK inhibitor fasudil reduces the expression of inflammatory factors in LPS-induced rat pulmonary microvascular endothelial cells via ROS/NF-κB pathway. *BMC Pharmacol Toxicol*, *23*(1), 24. https://doi.org/10.1186/s40360-022-00565-7

Liu, Q., Li, H. Y., Wang, S. J., Huang, S. Q., Yue, Y., Maihemu, A., Zhang, Y., Huang, L., Luo, L., Feng, K. N., & Wu, Z. K. (2022). Belumosudil, ROCK2-specific inhibitor, alleviates cardiac fibrosis by inhibing cardiac fibroblasts acvaon. *Am J Physiol Heart Circ Physiol*, *323*(1), H235-h247. https://doi.org/10.1152/ajpheart.00014.2022

Liu, W., Gao, J., Yi, X., Li, Y., & Zeng, Y. (2020). Absorpon, ssue disposion, and excreon of fasudil hydrochloride, a RHO kinase inhibitor, in rats and dogs. *Biopharm Drug Dispos*, *41*(4-5), 206-220. https://doi.org/10.1002/bdd.2231

Liu, X., Yu, X., Zack, D. J., Zhu, H., & Qian, J. (2008). TiGER: a database for ssue-specific gene expression and regulaon. *BMC Bioinformatics*, *9*, 271. https://doi.org/10.1186/1471-2105-9-271

Lodrini, A. M., & Goumans, M. J. (2021). Cardiomyocytes Cellular Phenotypes Aer Myocardial Infarcon. *Front Cardiovasc Med*, *8*, 750510. https://doi.org/10.3389/fcvm.2021.750510

Loirand, G. (2015). Rho Kinases in Health and Disease: From Basic Science to Translaonal Research. *Pharmacol Rev*, *67*(4), 1074-1095. https://doi.org/10.1124/pr.115.010595

Loirand, G., Guerin, P., & Pacaud, P. (2006). Rho kinases in cardiovascular physiology and pathophysiology. *Circ Res*, *98*(3), 322-334. https://doi.org/10.1161/01.RES.0000201960.04223.3c

Lønborg, J., Engstrøm, T., Ahtarovski, K. A., Nepper-Christensen, L., Helqvist, S., Vejlstrup, N., Kyhl, K., Schoos, M. M., Ghotbi, A., Göransson, C., Bertelsen, L., Holmvang, L., Pedersen, F., Jørgensen, E., Saunamäki, K., Clemmensen, P., De Backer, O., Kløvgaard, L., Høfsten, D. E., . . . Kelbæk, H. (2017). Myocardial Damage in Paents With Deferred Stenng Aer STEMI: A DANAMI-3-DEFER Substudy. *J Am Coll Cardiol*, *69*(23), 2794-2804. https://doi.org/10.1016/j.jacc.2017.03.601

Lorenz, R., Wu, J., Herberg, F. W., Taylor, S. S., & Engh, R. A. (2021). Drugging the Undruggable: How Isoquinolines and PKA Iniated the Era of Designed Protein Kinase Inhibitor Therapeucs. *Biochemistry*, *60*(46), 3470-3484. https://doi.org/10.1021/acs.biochem.1c00359

Lu, D., & Thum, T. (2019). RNA-based diagnosc and therapeuc strategies for cardiovascular disease. *Nat Rev Cardiol*, *16*(11), 661-674. https://doi.org/10.1038/s41569-0190218-x

Lukhna, K., Hausenloy, D. J., Ali, A. S., Bajaber, A., Calver, A., Mutyaba, A., Mohamed, A. A., Kiggundu, B., Chishala, C., Variava, E., Elmakki, E. A., Ogola, E., Hamid, E., Okello, E., Gaafar, I., Mwazo, K., Makotoko, M., Naidoo, M., Abdelhameed, M. E., . . . Yellon, D. M. (2023). Remote Ischaemic Condioning in STEMI Paents in Sub-Saharan AFRICA: Raonale and Study Design for the RIC-AFRICA Trial. *Cardiovasc Drugs Ther*, *37*(2), 299-305. https://doi.org/10.1007/s10557-021-07283-y

Ma, M., Wang, L., Diao, K. Y., Liang, S. C., Zhu, Y., Wang, H., Wang, M., Zhang, L., Yang, Z. G., & He, Y. (2022). A randomized controlled clinical trial of prolonged balloon inflaon during stent deployment strategy in primary percutaneous coronary intervenon for ST-segment elevaon myocardial infarcon: a pilot study. *BMC Cardiovasc Disord*, *22*(1), 30. https://doi.org/10.1186/s12872-022-02477-0

Masumoto, A., Mohri, M., Shimokawa, H., Urakami, L., Usui, M., & Takeshita, A. (2002). Suppression of coronary artery spasm by the Rho-kinase inhibitor fasudil in paents with vasospasc angina. *Circulation*, *105*(13), 1545-1547. https://doi.org/10.1161/hc1002.105938

Matoba, K., Takeda, Y., Nagai, Y., Sekiguchi, K., Yokota, T., Utsunomiya, K., & Nishimura, R. (2020). The Physiology, Pathology, and Therapeuc Intervenons for ROCK Isoforms in Diabec Kidney Disease. *Front Pharmacol*, *11*, 585633. https://doi.org/10.3389/fphar.2020.585633

Matsumoto, A., Manthey, H. D., Marsh, S. A., Fasset, R. G., de Haan, J. B., Rolfe, B. E., & Coombes, J. S. (2013). Effects of exercise training and RhoA/ROCK inhibion on plaque in ApoE-/- mice. *Int J Cardiol*, *167*(4), 1282-1288. https://doi.org/10.1016/j.ijcard.2012.03.172

Matsumoto, Y., Uwatoku, T., Oi, K., Abe, K., Hatori, T., Morishige, K., Eto, Y., Fukumoto, Y., Nakamura, K., Shibata, Y., Matsuda, T., Takeshita, A., & Shimokawa, H. (2004). Longterm inhibion of Rho-kinase suppresses neoinmal formaon aer stent implantaon in porcine coronary arteries: involvement of mulple mechanisms. *Arterioscler Thromb Vasc Biol*, *24*(1), 181-186. https://doi.org/10.1161/01.ATV.0000105053.46994.5B

Maznyczka, A. M., Carrick, D., Oldroyd, K. G., James-Rae, G., McCartney, P., Greenwood, J. P., Good, R., McEntegart, M., Eteiba, H., Lindsay, M. M., Coton, J. M., Petrie, M. C., & Berry, C. (2021). Thermodiluon-derived temperature recovery me: a novel predictor of microvascular reperfusion and prognosis aer myocardial infarcon. *EuroIntervention*, *17*(3), 220-228. https://doi.org/10.4244/eij-d-19-00904

Maznyczka, A. M., Oldroyd, K. G., Greenwood, J. P., McCartney, P. J., Coton, J., Lindsay, M., McEntegart, M., Rocchiccioli, J. P., Good, R., Robertson, K., Eteiba, H., Watkins, S., Shaukat, A., Petrie, C. J., Murphy, A., Petrie, M. C., & Berry, C. (2020). Comparave Significance of Invasive Measures of Microvascular Injury in Acute Myocardial Infarcon. *Circ Cardiovasc Interv*, *13*(5), e008505. https://doi.org/10.1161/CIRCINTERVENTIONS.119.008505

McCartney, P. J., Maznyczka, A. M., Eteiba, H., McEntegart, M., Oldroyd, K. G., Greenwood, J. P., Maredia, N., Schmit, M., McCann, G. P., Fairbairn, T., McAlindon, E., Tait, C., Welsh, P., Satar, N., Orchard, V., Corcoran, D., Ford, T. J., Radjenovic, A., Ford, I., . . .

Invesgators, T. T. (2020). Low-Dose Alteplase During Primary Percutaneous Coronary Intervenon According to Ischemic Time. *J Am Coll Cardiol*, *75*(12), 1406-1421. https://doi.org/10.1016/j.jacc.2020.01.041

Methner, C., Cao, Z., Mishra, A., & Kaul, S. (2021). Mechanism and potenal treatment of the "no reflow" phenomenon aer acute myocardial infarcon: role of pericytes and GPR39. *Am J Physiol Heart Circ Physiol*, *321*(6), H1030-h1041. https://doi.org/10.1152/ajpheart.00312.2021

Miranda, A. M. A., Janbandhu, V., Maatz, H., Kanemaru, K., Cranley, J., Teichmann, S. A., Hübner, N., Schneider, M. D., Harvey, R. P., & Noseda, M. (2023). Single-cell transcriptomics for the assessment of cardiac disease. *Nat Rev Cardiol*, *20*(5), 289-308. https://doi.org/10.1038/s41569-022-00805-7

Miyahara, S., Jenke, A., Yazdanyar, M., Kistner, J., Immohr, M. B., Sugimura, Y., Aubin, H., Kamiya, H., Okita, Y., Lichtenberg, A., & Akhyari, P. (2022). The combinaon approach with Rhokinase inhibion and mechanical circulatory support in myocardial ischemia-reperfusion injury: Rho-kinase inhibion and ventricular unloading. *Asian Cardiovasc Thorac Ann*, *30*(8), 894-905. https://doi.org/10.1177/02184923221114457

Mizutani, H., Okamoto, R., Moriki, N., Konishi, K., Taniguchi, M., Fujita, S., Dohi, K., Onishi, K., Suzuki, N., Satoh, S., Makino, N., Itoh, T., Hartshorne, D. J., & Ito, M. (2010). Overexpression of myosin phosphatase reduces Ca(2+) sensivity of contracon and impairs cardiac funcon. *Circ J*, *74*(1), 120-128. https://doi.org/10.1253/circj.cj-090462

Mora-Ruíz, M. D., Blanco-Favela, F., Chávez Rueda, A. K., Legorreta-Haquet, M. V., & ChávezSánchez, L. (2019). Role of interleukin-17 in acute myocardial infarcon. *Mol Immunol*, *107*, 71-78. https://doi.org/10.1016/j.molimm.2019.01.008

Nagai, Y., Matoba, K., Kawanami, D., Takeda, Y., Akamine, T., Ishizawa, S., Kanazawa, Y., Yokota, T., Utsunomiya, K., & Nishimura, R. (2019). ROCK2 regulates TGF-β-induced expression of CTGF and profibroc genes via NF-κB and cytoskeleton dynamics in mesangial cells. *Am J Physiol Renal Physiol*, *317*(4), F839-f851. https://doi.org/10.1152/ajprenal.00596.2018

Naghshtabrizi, N., Sajedi, M., Naghshtabrizi, B., Mozayanimonfared, A., Ali Seif Rabiei, M., & Kanonisabet, A. (2020). Randomized trial of intracoronary adenosine as adjuncve therapy for prevenon of the no-reflow phenomenon. *Coron Artery Dis*, *31*(6), 527-529. https://doi.org/10.1097/mca.0000000000000863

Nakagawa, O., Fujisawa, K., Ishizaki, T., Saito, Y., Nakao, K., & Narumiya, S. (1996). ROCK-I and ROCK-II, two isoforms of Rho-associated coiled-coil forming protein serine/threonine kinase in mice. *FEBS Lett*, *392*(2), 189-193. https://doi.org/10.1016/00145793(96)00811-3

Nazir, S. A., McCann, G. P., Greenwood, J. P., Kunadian, V., Khan, J. N., Mahmoud, I. Z., Blackman, D. J., Been, M., Abrams, K. R., Shipley, L., Wilcox, R., Adgey, A. A., & Gershlick, A. H. (2016). Strategies to atenuate micro-vascular obstrucon during PPCI: the randomized reperfusion facilitated by local adjuncve therapy in STelevaon myocardial infarcon trial. *Eur Heart J*, *37*(24), 1910-1919. https://doi.org/10.1093/eurheartj/ehw136

Nepper-Christensen, L., Kelbæk, H., Ahtarovski, K. A., Høfsten, D. E., Holmvang, L., Pedersen, F., Tilsted, H. H., Aarøe, J., Jensen, S. E., Raungaard, B., Terkelsen, C. J., Køber, L., Engstrøm, T., & Lønborg, J. (2022). Angiographic outcome in paents treated with deferred stenng aer ST-segment elevaon myocardial infarcon-results from DANAMI-3-DEFER. *Eur Heart J Acute Cardiovasc Care*, *11*(10), 742-748. https://doi.org/10.1093/ehjacc/zuac098

Newby, L. K. (2019). Inflammaon as a Treatment Target aer Acute Myocardial Infarcon. *N*

Engl J Med, *381*(26), 2562-2563. https://doi.org/10.1056/NEJMe1914378

Niccoli, G., Giubilato, S., Russo, E., Spaziani, C., Leo, A., Porto, I., Leone, A. M., Burzota, F., Riondino, S., Pulcinelli, F., Biasucci, L. M., & Crea, F. (2008). Plasma levels of thromboxane A2 on admission are associated with no-reflow aer primary percutaneous coronary intervenon. *Eur Heart J*, *29*(15), 1843-1850. https://doi.org/10.1093/eurheartj/ehn325

Niccoli, G., Montone, R. A., Ibanez, B., Thiele, H., Crea, F., Heusch, G., Bulluck, H., Hausenloy, D. J., Berry, C., Sermaier, T., Camici, P. G., & Eitel, I. (2019). Opmized Treatment of ST-Elevaon Myocardial Infarcon. *Circ Res*, *125*(2), 245-258. https://doi.org/10.1161/circresaha.119.315344

Niccoli, G., Rigaeri, S., De Vita, M. R., Valgimigli, M., Corvo, P., Fabbiocchi, F., Romagnoli, E., De Caterina, A. R., La Torre, G., Lo Schiavo, P., Taranno, F., Ferrari, R., Tomai, F., Olivares, P., Cosenno, N., D'Amario, D., Leone, A. M., Porto, I., Burzota, F., . . . Crea, F. (2013). Open-label, randomized, placebo-controlled evaluaon of intracoronary adenosine or nitroprusside aer thrombus aspiraon during primary percutaneous coronary intervenon for the prevenon of microvascular obstrucon in acute myocardial infarcon: the REOPEN-AMI study (Intracoronary Nitroprusside Versus Adenosine in Acute Myocardial Infarcon). *JACC Cardiovasc Interv*, *6*(6), 580-589. https://doi.org/10.1016/j.jcin.2013.02.009

Niccoli, G., Scalone, G., Lerman, A., & Crea, F. (2016). Coronary microvascular obstrucon in acute myocardial infarcon. *Eur Heart J*, *37*(13), 1024-1033. https://doi.org/10.1093/eurheartj/ehv484

Noma, K., Oyama, N., & Liao, J. K. (2006). Physiological role of ROCKs in the cardiovascular system. *Am J Physiol Cell Physiol*, *290*(3), C661-668. https://doi.org/10.1152/ajpcell.00459.2005

O'Farrell, F. M., Mastskaya, S., Hammond-Haley, M., Freitas, F., Wah, W. R., & Atwell, D. (2017). Capillary pericytes mediate coronary no-reflow aer myocardial ischaemia. *Elife*, *6*. https://doi.org/10.7554/eLife.29280

Ocaranza, M. P., Gabrielli, L., Mora, I., Garcia, L., McNab, P., Godoy, I., Braun, S., Córdova, S., Castro, P., Novoa, U., Chiong, M., Lavandero, S., & Jalil, J. E. (2011). Markedly increased Rho-kinase acvity in circulang leukocytes in paents with chronic heart failure. *Am Heart J*, *161*(5), 931-937. https://doi.org/10.1016/j.ahj.2011.01.024

Ohkouchi, S., Ono, M., Kobayashi, M., Hirano, T., Tojo, Y., Hisata, S., Ichinose, M., Irokawa, T., Ogawa, H., & Kurosawa, H. (2015). Myriad Funcons of Stanniocalcin-1 (STC1) Cover Mulple Therapeuc Targets in the Complicated Pathogenesis of Idiopathic Pulmonary Fibrosis (IPF). *Clin Med Insights Circ Respir Pulm Med*, *9*(Suppl 1), 91-96. https://doi.org/10.4137/ccrpm.S23285

Oldenburg, O., Cohen, M. V., Yellon, D. M., & Downey, J. M. (2002). Mitochondrial K(ATP) channels: role in cardioprotecon. *Cardiovasc Res*, *55*(3), 429-437. https://doi.org/10.1016/s0008-6363(02)00439-x

Otsuka, T., Ibuki, C., Suzuki, T., Ishii, K., Yoshida, H., Kodani, E., Kusama, Y., Atarashi, H., Kishida, H., Takano, T., & Mizuno, K. (2008). Administraon of the Rho-kinase inhibitor, fasudil, following nitroglycerin addionally dilates the site of coronary spasm in paents with vasospasc angina. *Coron Artery Dis*, *19*(2), 105-110. https://doi.org/10.1097/MCA.0b013e3282f3420c

Paik, D. T., Cho, S., Tian, L., Chang, H. Y., & Wu, J. C. (2020). Single-cell RNA sequencing in cardiovascular development, disease and medicine. *Nat Rev Cardiol*, *17*(8), 457-473. https://doi.org/10.1038/s41569-020-0359-y

Palasubramaniam, J., Wang, X., & Peter, K. (2019). Myocardial Infarcon-From Atherosclerosis to Thrombosis. *Arterioscler Thromb Vasc Biol*, *39*(8), e176-e185. https://doi.org/10.1161/ATVBAHA.119.312578

Pan, J., Yin, Y., Zhao, L., & Feng, Y. (2019). Discovery of (S)-6-methoxy-chroman-3-carboxylic acid (4-pyridin-4-yl-phenyl)-amide as potent and isoform selecve ROCK2 inhibitors. *Bioorg Med Chem*, *27*(7), 1382-1390. https://doi.org/10.1016/j.bmc.2019.02.047

Park, J., & Chun, K. H. (2020). Idenficaon of novel funcons of the ROCK2-specific inhibitor KD025 by bioinformacs analysis. *Gene*, *737*, 144474. https://doi.org/10.1016/j.gene.2020.144474

Pearce, L., Carr, R. D., Yellon, D. M., & Davidson, S. M. (2023). Nicorandil - an Effecve Multarget Drug for Cardioprotecon? *Cardiovasc Drugs Ther*, *37*(1), 5-8. https://doi.org/10.1007/s10557-022-07397-x

Pearce, L., Davidson, S. M., & Yellon, D. M. (2021). Does remote ischaemic condioning reduce inflammaon? A focus on innate immunity and cytokine response. *Basic Res Cardiol*, *116*(1), 12. https://doi.org/10.1007/s00395-021-00852-0

Pearson, J. T., Jenkins, M. J., Edgley, A. J., Sonobe, T., Joshi, M., Waddingham, M. T., Fujii, Y., Schwenke, D. O., Tsuchimochi, H., Yoshimoto, M., Umetani, K., Kelly, D. J., & Shirai, M. (2013). Acute Rho-kinase inhibion improves coronary dysfuncon in vivo, in the early diabec microcirculaon. *Cardiovasc Diabetol*, *12*, 111. https://doi.org/10.1186/1475-2840-12-111

Pelliccia, F., Greco, C., Tanzilli, G., Viceconte, N., Schiari, M., & Gaudio, C. (2021). Long-term outcome of paents with ST-segment elevaon myocardial infarcon treated with low-dose intracoronary thrombolysis during primary percutaneous coronary intervenon: the 5-year results of the DISSOLUTION Trial. *J Thromb Thrombolysis*, *51*(1), 212-216. https://doi.org/10.1007/s11239-020-02157-w

Perera, D., Clayton, T., O'Kane, P. D., Greenwood, J. P., Weerackody, R., Ryan, M., Morgan, H. P., Dodd, M., Evans, R., Canter, R., Arnold, S., Dixon, L. J., Edwards, R. J., De Silva, K., Sprat, J. C., Conway, D., Coton, J., McEntegart, M., Chiribiri, A., . . . Petrie, M. C. (2022). Percutaneous Revascularizaon for Ischemic Le Ventricular Dysfuncon. *N Engl J Med*, *387*(15), 1351-1360. https://doi.org/10.1056/NEJMoa2206606

Perera, D., Ryan, M., Morgan, H. P., Greenwood, J. P., Petrie, M. C., Dodd, M., Weerackody, R., O'Kane, P. D., Masci, P. G., Nazir, M. S., Papachrisdis, A., Chahal, N., Khatar, R., Ezad, S. M., Kapetanakis, S., Dixon, L. J., De Silva, K., McDiarmid, A. K., Marber, M. S., . . . Chiribiri, A. (2023). Viability and Outcomes With Revascularizaon or Medical Therapy in Ischemic Ventricular Dysfuncon: A Prespecified Secondary Analysis of the REVIVED-BCIS2 Trial. *JAMA Cardiol*, *8*(12), 1154-1161. https://doi.org/10.1001/jamacardio.2023.3803

Perike, S., Gonzalez-Gonzalez, F. J., Abu-Taha, I., Damen, F. W., Han, L. M., Lizama, K. S., Aboonabi, A., Capote, A. E., Aguilar-Sanchez, Y., Levin, B., Han, Z., Sridhar, A., Grand, J., Marn, J., Akar, J. G., Warren, C. M., Solaro, R. J., Ong, S. G., Darbar, D., . . . McCauley, M. D. (2023). PPP1R12C Promotes Atrial Hypocontraclity in Atrial Fibrillaon. *Circ Res*, *133*(9), 758-771. https://doi.org/10.1161/circresaha.123.322516

Perry, W. H. (1983). Methotrexate and teratogenesis. *Arch Dermatol*, *119*(11), 874-875.

Porras-González, C., González-Rodríguez, P., Calderón-Sánchez, E., López-Barneo, J., & Ureña, J. (2014). Low-dose combinaon of Rho kinase and L-type Ca(2+) channel antagonists for selecve inhibion of depolarizaon-induced sustained arterial contracon. *Eur J Pharmacol*, *732*, 130-138. https://doi.org/10.1016/j.ejphar.2014.02.046

Prabhu, S. D., & Frangogiannis, N. G. (2016). The Biological Basis for Cardiac Repair Aer Myocardial Infarcon: From Inflammaon to Fibrosis. *Circ Res*, *119*(1), 91-112. https://doi.org/10.1161/circresaha.116.303577

Przepiorka, D., Le, R. Q., Ionan, A., Li, R. J., Wang, Y. H., Gudi, R., Mitra, S., Vallejo, J., Okusanya, O. O., Ma, L., Yang, Y., Patel, P., Mezaache, D., Shah, R., Banerjee, A., McLamore, S., Maung, A. N., Goldberg, K. B., Pazdur, R., . . . De Claro, R. A. (2022). FDA Approval Summary: Belumosudil for Adult and Pediatric Paents 12 Years and Older with Chronic GvHD aer Two or More Prior Lines of Systemic Therapy. *Clin Cancer Res*, *28*(12), 2488-2492. https://doi.org/10.1158/1078-0432.Ccr-21-4176

Qian, G., A, X., Jiang, X., Jiang, Z., Li, T., Dong, W., Guo, J., & Chen, Y. (2023). Early Trimetazidine Therapy in Paents Undergoing Primary Percutaneous Coronary Intervenon for ST Segment Elevaon Myocardial Infarcon Reduces Myocardial Infarcon Size. *Cardiovasc Drugs Ther*, *37*(3), 497-506. https://doi.org/10.1007/s10557-021-07259y

Qian, G., Zhang, Y., Dong, W., Jiang, Z. C., Li, T., Cheng, L. Q., Zou, Y. T., Jiang, X. S., Zhou, H., A, X., Li, P., Chen, M. L., Su, X., Tian, J. W., Shi, B., Li, Z. Z., Wu, Y. Q., Li, Y. J., & Chen, Y. D. (2022). Effects of Nicorandil Administraon on Infarct Size in Paents With STSegment-Elevaon Myocardial Infarcon Undergoing Primary Percutaneous Coronary Intervenon: The CHANGE Trial. *J Am Heart Assoc*, *11*(18), e026232. https://doi.org/10.1161/jaha.122.026232

Rada, B. (2019). Neutrophil Extracellular Traps. *Methods Mol Biol*, *1982*, 517-528. https://doi.org/10.1007/978-1-4939-9424-3_31

Rauf, A., Shah, M., Yellon, D. M., & Davidson, S. M. (2019). Role of Caspase 1 in Ischemia/Reperfusion Injury of the Myocardium. *J Cardiovasc Pharmacol*, *74*(3), 194-200. https://doi.org/10.1097/c.0000000000000694

Redfors, B., Mohebi, R., Giusno, G., Chen, S., Selker, H. P., Thiele, H., Patel, M. R., Udelson, J. E., Ohman, E. M., Eitel, I., Granger, C. B., Maehara, A., Ali, Z. A., Ben-Yehuda, O., & Stone, G. W. (2021). Time Delay, Infarct Size, and Microvascular Obstrucon Aer Primary Percutaneous Coronary Intervenon for ST-Segment-Elevaon Myocardial Infarcon. *Circ Cardiovasc Interv*, *14*(2), e009879. https://doi.org/10.1161/CIRCINTERVENTIONS.120.009879

Reffelmann, T., & Kloner, R. A. (2002). The "no-reflow" phenomenon: basic science and clinical correlates. *Heart*, *87*(2), 162-168. https://doi.org/10.1136/heart.87.2.162

Reffelmann, T., & Kloner, R. A. (2006). The no-reflow phenomenon: A basic mechanism of myocardial ischemia and reperfusion. *Basic Res Cardiol*, *101*(5), 359-372. https://doi.org/10.1007/s00395-006-0615-2

Reynolds, H. R., Merz, C. N. B., Berry, C., Samuel, R., Saw, J., Smilowitz, N. R., Souza, A. C. d. A. H. d., Sykes, R., Taque, V. R., & Wei, J. (2022). Coronary Arterial Funcon and Disease in Women With No Obstrucve Coronary Arteries. *Circulation Research*, *130*(4), 529-551. https://doi.org/doi:10.1161/CIRCRESAHA.121.319892

Rezkalla, S. H., Stankowski, R. V., Hanna, J., & Kloner, R. A. (2017). Management of No-Reflow Phenomenon in the Catheterizaon Laboratory. *JACC Cardiovasc Interv*, *10*(3), 215-223. https://doi.org/10.1016/j.jcin.2016.11.059

Riento, K., & Ridley, A. J. (2003). Rocks: mulfunconal kinases in cell behaviour. *Nat Rev Mol Cell Biol*, *4*(6), 446-456. https://doi.org/10.1038/nrm1128

Rikitake, Y., & Liao, J. K. (2005). Rho GTPases, stans, and nitric oxide. *Circ Res*, *97*(12), 12321235. https://doi.org/10.1161/01.Res.0000196564.18314.23

Rikitake, Y., Oyama, N., Wang, C. Y., Noma, K., Satoh, M., Kim, H. H., & Liao, J. K. (2005). Decreased perivascular fibrosis but not cardiac hypertrophy in ROCK1+/-

haploinsufficient mice. *Circulation*, *112*(19), 2959-2965. https://doi.org/10.1161/circulaonaha.105.584623

Rossello, X., Riquelme, J. A., He, Z., Taferner, S., Vanhaesebroeck, B., Davidson, S. M., & Yellon, D. M. (2017). The role of PI3Kα isoform in cardioprotecon. *Basic Res Cardiol*, *112*(6), 66. https://doi.org/10.1007/s00395-017-0657-7

Rossello, X., & Yellon, D. M. (2018). The RISK pathway and beyond. *Basic Res Cardiol*, *113*(1), 2. https://doi.org/10.1007/s00395-017-0662-x

Rusceta, V. M., Seaton, T. J., Shakeel, A., Vasconcelos, S. N. S., Viirre, R. D., Adler, M. J., & Olson, M. F. (2023). Opportunies and Challenges for the Development of MRCK Kinases Inhibitors as Potenal Cancer Chemotherapeucs. *Cells*, *12*(4). https://doi.org/10.3390/cells12040534

Russo, M., Montone, R. A., D'Amario, D., Camilli, M., Canonico, F., Santamaria, C., Iannaccone, G., Pedicino, D., Pidone, C., Galli, M., Trani, C., Severino, A., Liuzzo, G., Niccoli, G., & Crea, F. (2021). Role of perilipin 2 in microvascular obstrucon in paents with STelevaon myocardial infarcon. *Eur Heart J Acute Cardiovasc Care*, *10*(6), 633-642. https://doi.org/10.1093/ehjacc/zuaa004

Sadeghian, M., Mousavi, S. H., Aamaraee, Z., & Shafiee, A. (2022). Administraon of intracoronary adenosine before stenng for the prevenon of no-reflow in paents with ST-elevaon myocardial infarcon. *Scand Cardiovasc J*, *56*(1), 23-27. https://doi.org/10.1080/14017431.2022.2035807

Santos, G. L., Hartmann, S., Zimmermann, W. H., Ridley, A., & Lutz, S. (2019). Inhibion of Rho-associated kinases suppresses cardiac myofibroblast funcon in engineered connecve and heart muscle ssues. *J Mol Cell Cardiol*, *134*, 13-28. https://doi.org/10.1016/j.yjmcc.2019.06.015

Sata, M., & Nagai, R. (2002). Phosphadylinositol 3-kinase: a key regulator of vascular tone? *Circ Res*, *91*(4), 273-275. https://doi.org/10.1161/01.res.0000031956.29928.62

Satoh, S., Ikegaki, I., Kawasaki, K., Asano, T., & Shibuya, M. (2014). Pleiotropic effects of the rho-kinase inhibitor fasudil aer subarachnoid hemorrhage: a review of preclinical and clinical studies. *Curr Vasc Pharmacol*, *12*(5), 758-765. https://doi.org/10.2174/15701611126661406131158 13

Scarsini, R., Terentes-Printzios, D., Shanmuganathan, M., Kotronias, R. A., Borlo, A., Marin, F., Langrish, J., Lucking, A., Ribichini, F., Kharbanda, R., Ferreira, V. M., Channon, K. M., De Maria, G. L., & Banning, A. P. (2022). Pressure-controlled intermitent coronary sinus occlusion improves the vasodilatory microvascular capacity and reduces myocardial injury in paents with STEMI. *Catheter Cardiovasc Interv*, *99*(2), 329-339. https://doi.org/10.1002/ccd.29793

Scheuer, D. A., & Perrone, M. H. (1993). Angiotensin type 2 receptors mediate depressor phase of biphasic pressure response to angiotensin. *Am J Physiol*, *264*(5 Pt 2), R917-923. https://doi.org/10.1152/ajpregu.1993.264.5.R917

Selker, H. P., Beshansky, J. R., Sheehan, P. R., Massaro, J. M., Griffith, J. L., D'Agosno, R. B., Ruthazer, R., Atkins, J. M., Sayah, A. J., Levy, M. K., Richards, M. E., Aufderheide, T. P., Braude, D. A., Pirrallo, R. G., Doyle, D. D., Frascone, R. J., Kosiak, D. J., Leaming, J. M., Van Gelder, C. M., . . . Udelson, J. E. (2012). Out-of-hospital administraon of intravenous glucose-insulin-potassium in paents with suspected acute coronary syndromes: the IMMEDIATE randomized controlled trial. *JAMA*, *307*(18), 1925-1933. https://doi.org/10.1001/jama.2012.426

Selker, H. P., Udelson, J. E., Massaro, J. M., Ruthazer, R., D'Agosno, R. B., Griffith, J. L., Sheehan, P. R., Desvigne-Nickens, P., Rosenberg, Y., Tian, X., Vickery, E. M., Atkins, J. M., Aufderheide, T. P., Sayah, A. J., Pirrallo, R. G., Levy, M. K., Richards, M. E., Braude, D. A., Doyle, D. D., . . . Beshansky, J. R. (2014). One-year outcomes of out-of-hospital

administraon of intravenous glucose, insulin, and potassium (GIK) in paents with suspected acute coronary syndromes (from the IMMEDIATE [Immediate Myocardial Metabolic Enhancement During Inial Assessment and Treatment in Emergency Care] Trial). *Am J Cardiol*, *113*(10), 1599-1605. https://doi.org/10.1016/j.amjcard.2014.02.010

Seo, J., Nam, Y. W., Kim, S., Oh, D. B., & Song, J. (2021). Necroptosis molecular mechanisms: Recent findings regarding novel necroptosis regulators. *Exp Mol Med*, *53*(6), 1007-1017. https://doi.org/10.1038/s12276-021-00634-7

Sezer, M., Royen, N. v., Umman, B., Bugra, Z., Bulluck, H., Hausenloy, D. J., & Umman, S. (2018). Coronary Microvascular Injury in Reperfused Acute Myocardial Infarcon: A View From an Integrave Perspecve. *Journal of the American Heart Association*, *7*(21), e009949. https://doi.org/doi:10.1161/JAHA.118.009949

Shah, M., He, Z., Rauf, A., Beikoghli Kalkhoran, S., Heiestad, C. M., Stenslokken, K. O., Parish, C. R., Soehnlein, O., Arjun, S., Davidson, S. M., & Yellon, D. (2022). Extracellular histones are a target in myocardial ischaemia-reperfusion injury. *Cardiovasc Res*, *118*(4), 1115-1125. https://doi.org/10.1093/cvr/cvab139

Shah, S., & Savjani, J. (2016). A review on ROCK-II inhibitors: From molecular modelling to synthesis. *Bioorg Med Chem Lett*, *26*(10), 2383-2391. https://doi.org/10.1016/j.bmcl.2016.03.113

Shaw, R. L., Norton, C. E., & Segal, S. S. (2021). Apoptosis in resistance arteries induced by hydrogen peroxide: greater resilience of endothelium versus smooth muscle. *Am J Physiol Heart Circ Physiol*, *320*(4), H1625-h1633. https://doi.org/10.1152/ajpheart.00956.2020

Shi, J., Surma, M., Yang, Y., & Wei, L. (2019). Disrupon of both ROCK1 and ROCK2 genes in cardiomyocytes promotes autophagy and reduces cardiac fibrosis during aging. *Faseb j*, *33*(6), 7348-7362. https://doi.org/10.1096/.201802510R

Shi, J., & Wei, L. (2007). Rho kinase in the regulaon of cell death and survival. *Arch Immunol Ther Exp (Warsz)*, *55*(2), 61-75. https://doi.org/10.1007/s00005-007-0009-7

Shi, J., & Wei, L. (2022). Rho Kinases in Embryonic Development and Stem Cell Research. *Arch Immunol Ther Exp (Warsz)*, *70*(1), 4. https://doi.org/10.1007/s00005-022-00642-z

Shi, J., Zhang, L., & Wei, L. (2011). Rho-kinase in development and heart failure: insights from genec models. *Pediatr Cardiol*, *32*(3), 297-304. https://doi.org/10.1007/s00246011-9920-0

Shibata, I., Yoshitomi, O., Use, T., Ureshino, H., Cho, S., Maekawa, T., Hara, T., & Sumikawa, K. (2008). Administraon of the Rho-kinase inhibitor fasudil before ischemia or just aer reperfusion, but not 30 min aer reperfusion, protects the stunned myocardium in swine. *Cardiovasc Drugs Ther*, *22*(4), 293-298. https://doi.org/10.1007/s10557-008-6106-y

Shibuya, M., Hirai, S., Seto, M., Satoh, S., & Ohtomo, E. (2005). Effects of fasudil in acute ischemic stroke: results of a prospecve placebo-controlled double-blind trial. *J Neurol Sci*, *238*(1-2), 31-39. https://doi.org/10.1016/j.jns.2005.06.003

Shibuya, M., Suzuki, Y., Sugita, K., Saito, I., Sasaki, T., Takakura, K., Okamoto, S., Kikuchi, H., Takemae, T., & Hidaka, H. (1990). Dose escalaon trial of a novel calcium antagonist, AT877, in paents with aneurysmal subarachnoid haemorrhage. *Acta Neurochir (Wien)*, *107*(1-2), 11-15. https://doi.org/10.1007/bf01402606

Shimizu, T., Fukumoto, Y., Tanaka, S., Satoh, K., Ikeda, S., & Shimokawa, H. (2013). Crucial role of ROCK2 in vascular smooth muscle cells for hypoxia-induced pulmonary hypertension in mice. *Arterioscler Thromb Vasc Biol*, *33*(12), 2780-2791. https://doi.org/10.1161/atvbaha.113.301357

Shimizu, T., Narang, N., Chen, P., Yu, B., Knapp, M., Janardanan, J., Blair, J., & Liao, J. K. (2017). Fibroblast deleon of ROCK2 atenuates cardiac hypertrophy, fibrosis, and diastolic dysfuncon. *JCI Insight*, *2*(13). https://doi.org/10.1172/jci.insight.93187

Shimokawa, H., Hiramori, K., Iinuma, H., Hosoda, S., Kishida, H., Osada, H., Katagiri, T., Yamauchi, K., Yui, Y., Minamino, T., Nakashima, M., & Kato, K. (2002). An-anginal effect of fasudil, a Rho-kinase inhibitor, in paents with stable effort angina: a mulcenter study. *J Cardiovasc Pharmacol*, *40*(5), 751-761. https://doi.org/10.1097/00005344-200211000-00013

Shimokawa, H., & Rashid, M. (2007). Development of Rho-kinase inhibitors for cardiovascular medicine. *Trends Pharmacol Sci*, *28*(6), 296-302. https://doi.org/10.1016/j.ps.2007.04.006

Shimokawa, H., Sunamura, S., & Satoh, K. (2016). RhoA/Rho-Kinase in the Cardiovascular System. *Circ Res*, *118*(2), 352-366. https://doi.org/10.1161/CIRCRESAHA.115.306532

Sladojevic, N., Oh, G. T., Kim, H. H., Beaulieu, L. M., Falet, H., Kaminski, K., Freedman, J. E., & Liao, J. K. (2017). Decreased thromboembolic stroke but not atherosclerosis or vascular remodelling in mice with ROCK2-deficient platelets. *Cardiovasc Res*, *113*(11), 1307-1317. https://doi.org/10.1093/cvr/cvx071

Soliman, H., Nyamandi, V., Garcia-Pano, M., Varela, J. N., Bankar, G., Lin, G., Jia, Z., & MacLeod, K. M. (2015). Paral deleon of ROCK2 protects mice from high-fat dietinduced cardiac insulin resistance and contracle dysfuncon. *Am J Physiol Heart Circ Physiol*, *309*(1), H70-81. https://doi.org/10.1152/ajpheart.00664.2014

Soliman, H., Nyamandi, V., Hove-Madsen, L., & MacLeod, K. M. (2020). ROCK2 as a novel target for diabec cardiomyopathy. *Int J Cardiol*, *299*, 206. https://doi.org/10.1016/j.ijcard.2019.10.017

Søndergaard, F. T., Beske, R. P., Frydland, M., Møller, J. E., Helgestad, O. K. L., Jensen, L. O., Holmvang, L., Goetze, J. P., Engstrøm, T., & Hassager, C. (2023). Soluble ST2 in plasma is associated with post-procedural no-or-slow reflow aer primary percutaneous coronary intervenon in ST-elevaon myocardial infarcon. *Eur Heart J Acute Cardiovasc Care*, *12*(1), 48-52. https://doi.org/10.1093/ehjacc/zuac146

Soylu, K., Ataş, A. E., Yenerçağ, M., Akçay, M., Şeker, O., Aksan, G., Gülel, O., & Şahin, M. (2018). Effect of roune postdilataon on final coronary blood flow in primary percutaneous coronary intervenon paents without angiographic stent expansion problems. *J Investig Med*, *66*(8), 1096-1101. https://doi.org/10.1136/jim-2018000725

Stähli, B. E., Klingenberg, R., Heg, D., Branca, M., Manka, R., Kapos, I., Müggler, O., Denegri, A., Kesterke, R., Berger, F., Stehli, J., Candreva, A., von Eckardstein, A., Carballo, D., Hamm, C., Landmesser, U., Mach, F., Mocce, T., Jung, C., . . . Ruschitzka, F. (2022). Mammalian Target of Rapamycin Inhibion in Paents With ST-Segment Elevaon Myocardial Infarcon. *J Am Coll Cardiol*, *80*(19), 1802-1814. https://doi.org/10.1016/j.jacc.2022.08.747

Stajic, Z., Milicevic, D., Kafedzic, S., Aleksic, A., Cerovic, M., Tasic, M., Andjelkovic Apostolovic, M., Ignjatovic, A., Zornic, N., Obradovic, G., Jovanovic, V., Jagic, N., Neskovic, A. N., & Davidovic, G. (2022). Predicng no-reflow phenomenon prior to primary percutaneous coronary intervenon using a novel probability risk score derived from clinical and angiographic parameters. *Eur Rev Med Pharmacol Sci*, *26*(3), 759-770. https://doi.org/10.26355/eurrev_202202_27984

Sermaier, T., Thiele, H., & Eitel, I. (2017). Coronary Microvascular Obstrucon: Key Factor in the Prognosis of ST-Segment-Elevaon Myocardial Infarcon. *Circ Cardiovasc Imaging*, *10*(6), e006568. https://doi.org/10.1161/CIRCIMAGING.117.006568

Stoess, C., Leszczynska, A., Kui, L., & Feldstein, A. E. (2023). Pyroptosis and gasderminsEmerging insights and therapeuc opportunies in metabolic dysfuncon-associated steatohepas. *Front Cell Dev Biol*, *11*, 1218807. https://doi.org/10.3389/fcell.2023.1218807

Su, Q., Lv, X., Sun, Y., Ye, Z., Kong, B., & Qin, Z. (2018). Role of TLR4/MyD88/NF-κB signaling pathway in coronary microembolizaon-induced myocardial injury prevented and treated with nicorandil. *Biomed Pharmacother*, *106*, 776-784. https://doi.org/10.1016/j.biopha.2018.07.014

Su, Q., Lv, X., Ye, Z., Sun, Y., Kong, B., Qin, Z., & Li, L. (2019). The mechanism of miR-142-3p in coronary microembolizaon-induced myocardiac injury via regulang target gene IRAK-1. *Cell Death Dis*, *10*(2), 61. https://doi.org/10.1038/s41419-019-1341-7

Sun, W., Lu, H., Dong, S., Li, R., Chu, Y., Wang, N., Zhao, Y., Zhang, Y., Wang, L., Sun, L., & Lu, D. (2021). Beclin1 controls caspase-4 inflammsome acvaon and pyroptosis in mouse myocardial reperfusion-induced microvascular injury. *Cell Commun Signal*, *19*(1), 107. https://doi.org/10.1186/s12964-021-00786-z

Sunamura, S., Satoh, K., Kurosawa, R., Ohtsuki, T., Kikuchi, N., Elias-Al-Mamun, M., Shimizu, T., Ikeda, S., Suzuki, K., Satoh, T., Omura, J., Nogi, M., Numano, K., Siddique, M. A. H., Miyata, S., Miura, M., & Shimokawa, H. (2018). Different roles of myocardial ROCK1 and ROCK2 in cardiac dysfuncon and postcapillary pulmonary hypertension in mice. *Proc Natl Acad Sci U S A*, *115*(30), E7129-e7138. https://doi.org/10.1073/pnas.1721298115

Taggart, P., & Yellon, D. M. (2002). Precondioning and arrhythmias. *Circulation*, *106*(24), 2999-3001. https://doi.org/10.1161/01.cir.0000041803.03687.7a

Tanaka, K., Minami, H., Kota, M., Kuwamura, K., & Kohmura, E. (2005). Treatment of cerebral vasospasm with intra-arterial fasudil hydrochloride. *Neurosurgery*, *56*(2), 214-223; discussion 214-223. https://doi.org/10.1227/01.neu.0000147975.24556.bc

Tardif, J. C., Kouz, S., Waters, D. D., Bertrand, O. F., Diaz, R., Maggioni, A. P., Pinto, F. J., Ibrahim, R., Gamra, H., Kiwan, G. S., Berry, C., Lopez-Sendon, J., Ostadal, P., Koenig, W., Angoulvant, D., Gregoire, J. C., Lavoie, M. A., Dube, M. P., Rhainds, D., . . . Roubille, F. (2019). Efficacy and Safety of Low-Dose Colchicine aer Myocardial Infarcon. *N Engl J Med*, *381*(26), 2497-2505. https://doi.org/10.1056/NEJMoa1912388

Thumkeo, D., Keel, J., Ishizaki, T., Hirose, M., Nonomura, K., Oshima, H., Oshima, M., Taketo, M. M., & Narumiya, S. (2003). Targeted disrupon of the mouse rho-associated kinase 2 gene results in intrauterine growth retardaon and fetal death. *Mol Cell Biol*, *23*(14), 5043-5055. https://doi.org/10.1128/mcb.23.14.5043-5055.2003

Thumkeo, D., Watanabe, S., & Narumiya, S. (2013). Physiological roles of Rho and Rho effectors in mammals. *Eur J Cell Biol*, *92*(10-11), 303-315. https://doi.org/10.1016/j.ejcb.2013.09.002

Tiik, R. N., Erol, A., Cnar, M. G., Kubat, H., Ark, M., Ulker, S., & Büyükafşar, K. (2008). Nitric oxide does not downregulate Rho-kinase (ROCK-2) expression in rat coronary endothelial cells. *J Cardiovasc Pharmacol*, *51*(2), 140-147. https://doi.org/10.1097/FJC.0b013e31815e4089

Toldo, S., Mauro, A. G., Cuter, Z., & Abbate, A. (2018). Inflammasome, pyroptosis, and cytokines in myocardial ischemia-reperfusion injury. *Am J Physiol Heart Circ Physiol*, *315*(6), H1553-H1568. https://doi.org/10.1152/ajpheart.00158.2018

Tona, F., Vadori, M., Civieri, G., Masiero, G., Iop, L., Antonelli, G., Perazzolo Marra, M., Bianco, F., Cecere, A., Lorenzoni, G., Naumova, N., Bernava, G., Basso, D., Plebani, M., Cozzi, E., & Iliceto, S. (2023). Associaon of autoanbodies targeng endothelin type-A receptors with no-reflow in ST-elevaon myocardial infarcon. *Atherosclerosis*, 117179. https://doi.org/10.1016/j.atherosclerosis.2023.06.970

Touyz, R. M., Alves-Lopes, R., Rios, F. J., Camargo, L. L., Anagnostopoulou, A., Arner, A., & Montezano, A. C. (2018). Vascular smooth muscle contracon in hypertension. *Cardiovasc Res*, *114*(4), 529-539. https://doi.org/10.1093/cvr/cvy023

Tran, N. N. Q., & Chun, K. H. (2021). ROCK2-Specific Inhibitor KD025 Suppresses Adipocyte Differenaon by Inhibing Casein Kinase 2. *Molecules*, *26*(16). https://doi.org/10.3390/molecules26164747

Traverse, J. H., Swingen, C. M., Henry, T. D., Fox, J., Wang, Y. L., Chavez, I. J., Lips, D. L., Lesser, J. R., Pedersen, W. R., Burke, N. M., Pai, A., Lindberg, J. L., & Garberich, R. F. (2019). NHLBI-Sponsored Randomized Trial of Postcondioning During Primary Percutaneous Coronary Intervenon for ST-Elevaon Myocardial Infarcon. *Circ Res*, *124*(5), 769-778. https://doi.org/10.1161/circresaha.118.314060

Tsai, S. H., Lu, G., Xu, X., Ren, Y., Hein, T. W., & Kuo, L. (2017). Enhanced endothelin-1/Rhokinase signalling and coronary microvascular dysfuncon in hypertensive myocardial hypertrophy. *Cardiovasc Res*, *113*(11), 1329-1337. https://doi.org/10.1093/cvr/cvx103

Tucker, N. R., Chaffin, M., Fleming, S. J., Hall, A. W., Parsons, V. A., Bedi, K. C., Jr., Akkad, A. D., Herndon, C. N., Arduini, A., Papangeli, I., Roselli, C., Aguet, F., Choi, S. H., Ardlie, K. G., Babadi, M., Margulies, K. B., Stegmann, C. M., & Ellinor, P. T. (2020). Transcriponal and Cellular Diversity of the Human Heart. *Circulation*, *142*(5), 466-482. https://doi.org/10.1161/circulaonaha.119.045401

Uemura, M. T., Maki, T., Ihara, M., Lee, V. M. Y., & Trojanowski, J. Q. (2020). Brain Microvascular Pericytes in Vascular Cognive Impairment and Demena. *Front Aging Neurosci*, *12*, 80. https://doi.org/10.3389/fnagi.2020.00080 van Nieuw Amerongen, G. P., Beckers, C. M., Achekar, I. D., Zeeman, S., Musters, R. J., & van Hinsbergh, V. W. (2007). Involvement of Rho kinase in endothelial barrier maintenance. *Arterioscler Thromb Vasc Biol*, *27*(11), 2332-2339. https://doi.org/10.1161/atvbaha.107.152322

Vlasblom, R., Muller, A., Beckers, C. M., van Nieuw Amerongen, G. P., Zuidwijk, M. J., van Hardeveld, C., Paulus, W. J., & Simonides, W. S. (2009). RhoA-ROCK signaling is involved in contracon-mediated inhibion of SERCA2a expression in cardiomyocytes. *Pflugers Arch*, *458*(4), 785-793. https://doi.org/10.1007/s00424009-0659-x

Waddingham, M. T., Edgley, A. J., Astolfo, A., Inagaki, T., Fujii, Y., Du, C. K., Zhan, D. Y., Tsuchimochi, H., Yagi, N., Kelly, D. J., Shirai, M., & Pearson, J. T. (2015). Chronic Rhokinase inhibion improves le ventricular contracle dysfuncon in early type-1 diabetes by increasing myosin cross-bridge extension. *Cardiovasc Diabetol*, *14*, 92. https://doi.org/10.1186/s12933-015-0256-6

Wang, L., Xie, L., Wei, X., & Xie, Z. (2019). Beneficial effects of early administraon of recombinant human B-type natriurec pepde in ST-elevaon myocardial infarcon paents receiving percutaneous coronary intervenon treatment. *Singapore Med J*, *60*(12), 621-625. https://doi.org/10.11622/smedj.2019093

Wang, Y., Zheng, X. R., Riddick, N., Bryden, M., Baur, W., Zhang, X., & Surks, H. K. (2009). ROCK isoform regulaon of myosin phosphatase and contraclity in vascular smooth muscle cells. *Circ Res*, *104*(4), 531-540. https://doi.org/10.1161/circresaha.108.188524

Wei, L., Surma, M., Yang, Y., Tersey, S., & Shi, J. (2020). ROCK2 inhibion enhances the thermogenic program in white and brown fat ssue in mice. *Faseb j*, *34*(1), 474-493. https://doi.org/10.1096/.201901174RR

Wenceslau, C. F., McCarthy, C. G., Earley, S., England, S. K., Filosa, J. A., Goulopoulou, S., Guterman, D. D., Isakson, B. E., Kanagy, N. L., Marnez-Lemus, L. A., Sonkusare, S. K., Thakore, P., Trask, A. J., Wats, S. W., & Webb, R. C. (2021). Guidelines for the measurement of vascular funcon and structure in isolated arteries and veins. *Am J*

Physiol Heart Circ Physiol, *321*(1), H77-h111. https://doi.org/10.1152/ajpheart.01021.2020

Wetschureck, N., & Offermanns, S. (2002). Rho/Rho-kinase mediated signaling in physiology and pathophysiology. *J Mol Med (Berl)*, *80*(10), 629-638. https://doi.org/10.1007/s00109-002-0370-2

Wilder, C. D. E., Pavlaki, N., Dursun, T., Gyimah, P., Caldwell-Dunn, E., Ranieri, A., Lewis, H. R., & Curs, M. J. (2018). Facilitaon of ischaemia-induced ventricular fibrillaon by catecholamines is mediated by beta1 and beta2 agonism in the rat heart in vitro. *Br J Pharmacol*, *175*(10), 1669-1690. https://doi.org/10.1111/bph.14176

Wilkinson, S., Paterson, H. F., & Marshall, C. J. (2005). Cdc42-MRCK and Rho-ROCK signalling cooperate in myosin phosphorylaon and cell invasion. *Nat Cell Biol*, *7*(3), 255-261. https://doi.org/10.1038/ncb1230

Wu, K. C., Zerhouni, E. A., Judd, R. M., Lugo-Olivieri, C. H., Barouch, L. A., Schulman, S. P., Blumenthal, R. S., & Lima, J. A. (1998). Prognosc significance of microvascular obstrucon by magnec resonance imaging in paents with acute myocardial infarcon. *Circulation*, *97*(8), 765-772. https://doi.org/10.1161/01.cir.97.8.765

Wu, N., Li, W., Shu, W., Lv, Y., & Jia, D. (2014). Inhibion of Rho-kinase by fasudil restores the cardioprotecon of ischemic postcondioninng in hypercholesterolemic rat heart. *Mol Med Rep*, *10*(5), 2517-2524. https://doi.org/10.3892/mmr.2014.2566

Yada, T., Shimokawa, H., Hiramatsu, O., Kajita, T., Shigeto, F., Tanaka, E., Shinozaki, Y., Mori, H., Kiyooka, T., Katsura, M., Ohkuma, S., Goto, M., Ogasawara, Y., & Kajiya, F. (2005). Beneficial effect of hydroxyfasudil, a specific Rho-kinase inhibitor, on ischemia/reperfusion injury in canine coronary microcirculaon in vivo. *J Am Coll Cardiol*, *45*(4), 599-607. https://doi.org/10.1016/j.jacc.2004.10.053

Yellon, D. M., Baxter, G. F., Garcia-Dorado, D., Heusch, G., & Sumeray, M. S. (1998). Ischaemic precondioning: present posion and future direcons. *Cardiovasc Res*, *37*(1), 21-33. https://doi.org/10.1016/s0008-6363(97)00214-9

Yellon, D. M., Beikoghli Kalkhoran, S., & Davidson, S. M. (2023). The RISK pathway leading to mitochondria and cardioprotecon: how everything started. *Basic Res Cardiol*, *118*(1), 22. https://doi.org/10.1007/s00395-023-00992-5

Yellon, D. M., & Hausenloy, D. J. (2007). Myocardial reperfusion injury. *N Engl J Med*, *357*(11), 1121-1135. https://doi.org/10.1056/NEJMra071667

Yen Ting Chen , T. V., Xingang Fang , Jennifer R. Pocas , Wayne Grant , Amiee M. W. Handy , Thomas Schröter , Philip LoGrasso , Thomas D. Bannister * and Yangbo Feng *. (2011). Asymmetric synthesis of potent chroman-based Rho kinase (ROCK-II) inhibitors.
MedChemComm(2), 73-75. https://pubs.rsc.org/en/content/arclehtml/2011/md/c0md00194e

Yoon, J. H., Nguyen, T. T., Duong, V. A., Chun, K. H., & Maeng, H. J. (2020). Determinaon of KD025 (SLx-2119), a Selecve ROCK2 Inhibitor, in Rat Plasma by High-Performance Liquid Chromatography-Tandem Mass Spectrometry and its Pharmacokinec Applicaon. *Molecules*, *25*(6). https://doi.org/10.3390/molecules25061369

Yuan, T. Y., Chen, D., Chen, Y. C., Zhang, H. F., Niu, Z. R., Jiao, X. Z., Xie, P., Fang, L. H., & Du, G. H. (2019). A novel hypertensive crisis rat model established by excessive norepinephrine infusion and the potenal therapeuc effects of Rho-kinase inhibitors on it. *Biomed Pharmacother*, *109*, 1867-1875. https://doi.org/10.1016/j.biopha.2018.11.061

Zanin-Zhorov, A., Chen, W., More, J., Nyuydzefe, M. S., Zhorov, I., Munshi, R., Ghosh, M., Serdjebi, C., MacDonald, K., Blazar, B. R., Palmer, M., & Waksal, S. D. (2023). Selecvity

maters: selecve ROCK2 inhibitor ameliorates established liver fibrosis via targeng inflammaon, fibrosis, and metabolism. *Commun Biol*, *6*(1), 1176. https://doi.org/10.1038/s42003-023-05552-0

Zanin-Zhorov, A., Weiss, J. M., Trzeciak, A., Chen, W., Zhang, J., Nyuydzefe, M. S., Arencibia, C., Polimera, S., Schueller, O., Fuentes-Duculan, J., Bonifacio, K. M., Kunjravia, N., Cueto, I., Soung, J., Fleischmann, R. M., Kivitz, A., Lebwohl, M., Nunez, M., Woodson, J., . . . Waksal, S. D. (2017). Cung Edge: Selecve Oral ROCK2 Inhibitor Reduces Clinical Scores in Paents with Psoriasis Vulgaris and Normalizes Skin Pathology via Concurrent Regulaon of IL-17 and IL-10. *J Immunol*, *198*(10), 3809-3814. https://doi.org/10.4049/jimmunol.1602142

Zdanyte, M., Borst, O., & Münzer, P. (2023). NET-(works) in arterial and venous thromboocclusive diseases. *Front Cardiovasc Med*, *10*, 1155512. https://doi.org/10.3389/fcvm.2023.1155512

Zhang, J., Chen, Z., Ma, M., & He, Y. (2022). Soluble ST2 in coronary artery disease: Clinical biomarkers and treatment guidance. *Front Cardiovasc Med*, *9*, 924461. https://doi.org/10.3389/fcvm.2022.924461

Zhang, J., Liu, X. B., Cheng, C., Xu, D. L., Lu, Q. H., & Ji, X. P. (2014). Rho-kinase inhibion is involved in the acvaon of PI3-kinase/Akt during ischemic-precondioning-induced cardiomyocyte apoptosis. *Int J Clin Exp Med*, *7*(11), 4107-4114.

Zhang, Y. S., Tang, L. J., Tu, H., Wang, S. J., Liu, B., Zhang, X. J., Li, N. S., Luo, X. J., & Peng, J. (2018). Fasudil ameliorates the ischemia/reperfusion oxidave injury in rat hearts through suppression of myosin regulatory light chain/NADPH oxidase 2 pathway. *Eur J Pharmacol*, *822*, 1-12. https://doi.org/10.1016/j.ejphar.2018.01.007

Zhao, J. L., Yang, Y. J., Pei, W. D., Sun, Y. H., You, S. J., & Gao, R. L. (2009). Remote pericondioning reduces myocardial no-reflow by the acvaon of K ATP channel via inhibion of Rho-kinase. *Int J Cardiol*, *133*(2), 179-184. https://doi.org/10.1016/j.ijcard.2007.12.024

Zhao, X., Han, J., Zhou, L., Zhao, J., Huang, M., Wang, Y., Kou, J., Kou, Y., & Jin, J. (2023). High mobility group box 1 derived mainly from platelet microparcles exacerbates microvascular obstrucon in no reflow. *Thromb Res*, *222*, 49-62. https://doi.org/10.1016/j.thromres.2022.12.003

Zhao, Z., & Manser, E. (2015). Myotonic dystrophy kinase-related Cdc42-binding kinases (MRCK), the ROCK-like effectors of Cdc42 and Rac1. *Small GTPases*, *6*(2), 81-88. https://doi.org/10.1080/21541248.2014.1000699

Zhou, F. T., & Ma, K. (2020). Fasudil protects against isoproterenol-induced myocardial infarcon in mice via inhibing Rho/ROCK signaling pathway. *Eur Rev Med Pharmacol Sci*, *24*(10), 5659-5667. https://doi.org/10.26355/eurrev_202005_21357

Ziegler, M., Wang, X., & Peter, K. (2019). Platelets in cardiac ischaemia/reperfusion injury: a promising therapeuc target. *Cardiovasc Res*, *115*(7), 1178-1188. https://doi.org/10.1093/cvr/cvz070

Zuurbier, C. J., Abbate, A., Cabrera-Fuentes, H. A., Cohen, M. V., Collino, M., De Kleijn, D. P. V., Downey, J. M., Pagliaro, P., Preissner, K. T., Takahashi, M., & Davidson, S. M. (2019). Innate immunity as a target for acute cardioprotecon. *Cardiovasc Res*, *115*(7), 11311142. https://doi.org/10.1093/cvr/cvy304

Balta, S., Celik, T., Ozturk, C., Kaya, M. G., Aparci, M., Yildirim, A. O., Demir, M., Kilic, S., Aydin, İ., & Iyisoy, A. (2016). The relation between monocyte to HDL ratio and no-reflow phenomenon in the patients with acute ST-segment elevation myocardial infarction. *Am J Emerg Med*, *34*(8), 1542-1547. https://doi.org/10.1016/j.ajem.2016.05.031

Broch, K., Anstensrud, A. K., Woxholt, S., Sharma, K., Tøllefsen, I. M., Bendz, B., Aakhus, S., Ueland, T., Amundsen, B. H., Damås, J. K., Berg, E. S., Bjørkelund, E., Bendz, C., Hopp, E., Kleveland, O., Stensæth, K. H., Opdahl, A., Kløw, N. E., Seljeflot, I., . . . Gullestad, L. (2021). Randomized Trial of Interleukin-6 Receptor Inhibition in Patients With Acute ST-Segment Elevation Myocardial Infarction. *J Am Coll Cardiol*, *77*(15), 1845-1855. https://doi.org/10.1016/j.jacc.2021.02.049

Cutler, C., Lee, S. J., Arai, S., Rotta, M., Zoghi, B., Lazaryan, A., Ramakrishnan, A., DeFilipp, Z., Salhotra, A., Chai-Ho, W., Mehta, R., Wang, T., Arora, M., Pusic, I., Saad, A., Shah, N. N., Abhyankar, S., Bachier, C., Galvin, J., . . . Pavletic, S. (2021). Belumosudil for chronic graft-versus-host disease after 2 or more prior lines of therapy: the ROCKstar Study. *Blood*, *138*(22), 2278-2289. https://doi.org/10.1182/blood.2021012021

Davidson, S. M., Ferdinandy, P., Andreadou, I., Botker, H. E., Heusch, G., Ibanez, B., Ovize, M., Schulz, R., Yellon, D. M., Hausenloy, D. J., Garcia-Dorado, D., & Action, C. C. (2019). Multitarget Strategies to Reduce Myocardial Ischemia/Reperfusion Injury: JACC Review Topic of the Week. *J Am Coll Cardiol*, *73*(1), 89-99. https://doi.org/10.1016/j.jacc.2018.09.086

de Waha, S., Patel, M. R., Granger, C. B., Ohman, E. M., Maehara, A., Eitel, I., Ben-Yehuda, O., Jenkins, P., Thiele, H., & Stone, G. W. (2017). Relationship between microvascular obstruction and adverse events following primary percutaneous coronary intervention for ST-segment elevation myocardial infarction: an individual patient data pooled analysis from seven randomized trials. *Eur Heart J*, *38*(47), 3502-3510. https://doi.org/10.1093/eurheartj/ehx414

Dong, M., Mu, N., Ren, F., Sun, X., & Yang, J. (2015). ASSA14-01-02 Circulating Platelet-Leukocyte Aggregates: a Sensitive Marker of No-reflow in Acute Myocardial Infarction Patients. *Heart*, *101*(Suppl 1), A1-A1. https://doi.org/10.1136/heartjnl-2014-307109.2

Dutta, P., & Nahrendorf, M. (2015). Monocytes in myocardial infarction. *Arterioscler Thromb Vasc Biol*, *35*(5), 1066-1070. https://doi.org/10.1161/atvbaha.114.304652

Furman, M. I., Barnard, M. R., Krueger, L. A., Fox, M. L., Shilale, E. A., Lessard, D. M., Marchese, P., Frelinger, A. L., 3rd, Goldberg, R. J., & Michelson, A. D. (2001). Circulating monocyte-platelet aggregates are an early marker of acute myocardial infarction. *J Am Coll Cardiol*, *38*(4), 1002-1006. https://doi.org/10.1016/s0735-1097(01)01485-1

Gong, G. Q., Bilanges, B., Allsop, B., Masson, G. R., Roberton, V., Askwith, T., Oxenford, S., Madsen, R. R., Conduit, S. E., Bellini, D., Fitzek, M., Collier, M., Najam, O., He, Z., Wahab, B., McLaughlin, S. H., Chan, A. W. E., Feierberg, I., Madin, A., . . . Vanhaesebroeck, B. (2023). A small-molecule PI3Kalpha activator for cardioprotection and neuroregeneration. *Nature*, *618*(7963), 159-168. https://doi.org/10.1038/s41586-023-05972-2

Hubert, A., Seitz, A., Pereyra, V. M., Bekeredjian, R., Sechtem, U., & Ong, P. (2020). Coronary Artery Spasm: The Interplay Between Endothelial Dysfunction and

Vascular Smooth Muscle Cell Hyperreactivity. *Eur Cardiol*, *15*, e12. https://doi.org/10.15420/ecr.2019.20

Kloner, R. A., Ganote, C. E., & Jennings, R. B. (1974). The "no-reflow" phenomenon after temporary coronary occlusion in the dog. *J Clin Invest*, *54*(6), 1496-1508. https://doi.org/10.1172/JCI107898

Lee, J. Y., Stevens, R. P., Kash, M., Zhou, C., Koloteva, A., Renema, P., Paudel, S. S., & Stevens, T. (2020). KD025 Shifts Pulmonary Endothelial Cell Bioenergetics and Decreases Baseline Lung Permeability. *Am J Respir Cell Mol Biol*, *63*(4), 519-530. https://doi.org/10.1165/rcmb.2019-0435OC

Mavroudis, C. A., Majumder, B., Lowdell, M., & Rakhit, R. D. (2011). 27 Platelet monocyte aggregates are determinants of microvascular dysfunction during percutaneous coronary intervention for stable angina and non-ST segment elevation myocardial infarction. *Heart*, *97*(Suppl 1), A20-A20. https://doi.org/10.1136/heartjnl-2011-300198.27

Nazir, S. A., McCann, G. P., Greenwood, J. P., Kunadian, V., Khan, J. N., Mahmoud, I. Z., Blackman, D. J., Been, M., Abrams, K. R., Shipley, L., Wilcox, R., Adgey, A. A., & Gershlick, A. H. (2016). Strategies to attenuate micro-vascular obstruction during P-PCI: the randomized reperfusion facilitated by local adjunctive therapy in ST-elevation myocardial infarction trial. *Eur Heart J*, *37*(24), 1910-1919. https://doi.org/10.1093/eurheartj/ehw136

Niccoli, G., Scalone, G., Lerman, A., & Crea, F. (2016). Coronary microvascular obstruction in acute myocardial infarction. *Eur Heart J*, *37*(13), 1024-1033. https://doi.org/10.1093/eurheartj/ehv484

Paik, D. T., Cho, S., Tian, L., Chang, H. Y., & Wu, J. C. (2020). Single-cell RNA sequencing in cardiovascular development, disease and medicine. *Nat Rev Cardiol*, *17*(8), 457-473. https://doi.org/10.1038/s41569-020-0359-y

Peet, C., Ivetic, A., Bromage, D. I., & Shah, A. M. (2020). Cardiac monocytes and macrophages after myocardial infarction. *Cardiovasc Res*, *116*(6), 1101-1112. https://doi.org/10.1093/cvr/cvz336

Prabhu, S. D., & Frangogiannis, N. G. (2016). The Biological Basis for Cardiac Repair After Myocardial Infarction: From Inflammation to Fibrosis. *Circ Res*, *119*(1), 91-112. https://doi.org/10.1161/circresaha.116.303577

Qian, G., Zhang, Y., Dong, W., Jiang, Z. C., Li, T., Cheng, L. Q., Zou, Y. T., Jiang, X. S., Zhou, H., A, X., Li, P., Chen, M. L., Su, X., Tian, J. W., Shi, B., Li, Z. Z., Wu, Y. Q., Li, Y. J., & Chen, Y. D. (2022). Effects of Nicorandil Administration on Infarct Size in Patients With ST-Segment-Elevation Myocardial Infarction Undergoing Primary Percutaneous Coronary Intervention: The CHANGE Trial. *J Am Heart Assoc*, *11*(18), e026232. https://doi.org/10.1161/jaha.122.026232

Rezkalla, S. H., Stankowski, R. V., Hanna, J., & Kloner, R. A. (2017). Management of No-Reflow Phenomenon in the Catheterization Laboratory. *JACC Cardiovasc Interv*, *10*(3), 215-223. https://doi.org/10.1016/j.jcin.2016.11.059

Rolling, C. C., Barrett, T. J., & Berger, J. S. (2023). Platelet-monocyte aggregates: molecular mediators of thromboinflammation. *Front Cardiovasc Med*, *10*, 960398. https://doi.org/10.3389/fcvm.2023.960398

Shah, S., & Savjani, J. (2016). A review on ROCK-II inhibitors: From molecular modelling to synthesis. *Bioorg Med Chem Lett*, *26*(10), 2383-2391. https://doi.org/10.1016/j.bmcl.2016.03.113

Shimokawa, H., Sunamura, S., & Satoh, K. (2016). RhoA/Rho-Kinase in the Cardiovascular System. *Circ Res*, *118*(2), 352-366. https://doi.org/10.1161/CIRCRESAHA.115.306532

Tsai, S. H., Lu, G., Xu, X., Ren, Y., Hein, T. W., & Kuo, L. (2017). Enhanced endothelin-1/Rho-kinase signalling and coronary microvascular dysfunction in hypertensive myocardial hypertrophy. *Cardiovasc Res*, *113*(11), 1329-1337. https://doi.org/10.1093/cvr/cvx103

Wang, Z., Ren, L., Liu, N., Lei, L., Ye, H., & Peng, J. (2016). Association of monocyte count on admission with angiographic no-reflow after primary percutaneous coronary intervention in patients with ST-segment elevation myocardial infarction. *Kardiol Pol*, *74*(10), 1160-1166. https://doi.org/10.5603/KP.a2016.0065

Yellon, D. M., Beikoghli Kalkhoran, S., & Davidson, S. M. (2023). The RISK pathway leading to mitochondria and cardioprotection: how everything started. *Basic Res Cardiol*, *118*(1), 22. https://doi.org/10.1007/s00395-023-00992-5

Zuurbier, C. J., Abbate, A., Cabrera-Fuentes, H. A., Cohen, M. V., Collino, M., De Kleijn, D. P. V., Downey, J. M., Pagliaro, P., Preissner, K. T., Takahashi, M., & Davidson, S. M. (2019). Innate immunity as a target for acute cardioprotection. *Cardiovasc Res*, *115*(7), 1131-1142. https://doi.org/10.1093/cvr/cvy304